ADAPTIVE BOUNDARY CONTROL USING BACKSTEPPING FOR 1D VARIABLE LENGTH STRING-MASS SYSTEM UNDER DISTURBANCES

by

Mateusz Szczesiak

B.E., Mechanical Engineering, The City College of New York, 2005

M.A., Physics, The City College of New York, 2007

M.S. Mechatronics Engineering, Istanbul Technical University, 2016

Submitted to the Institute for Graduate Studies in
Science and Engineering in partial fulfillment of
the requirements for the degree of
Doctor of Philosophy

Graduate Program in Mechanical Engineering

Boğaziçi University

2022

ACKNOWLEDGEMENTS

I wish to express my great thanks to all members of the examination committee: Prof. Günay Anlaş, Prof. Çetin Yılmaz, Prof. Hilmi Luş, and Assoc. Prof. Evren Samur for guiding me throughout the Ph.D. studies. I count myself lucky to have had your help and assistance. I would also like to convey my very great appreciation to Prof. Çağatay Başdoğan and Assoc. Prof. Zeki Yağız Bayraktaroğlu for joining the defense committee.

I'm deeply indebted to Assoc. Prof. Halil İ. Baştürk for his invaluable contributions and stewardship. This dissertation would not have been possible without his oversight and advice. Thank you.

Finally, my utmost love and gratitude to my wife İrem and my two sons, Kacper Pamir and Marcel Semih, for the unwavering support and encouragement they offered at every point on this journey.

ABSTRACT

ADAPTIVE BOUNDARY CONTROL USING BACKSTEPPING FOR 1D VARIABLE LENGTH STRING-MASS SYSTEM UNDER DISTURBANCES

In this thesis, an adaptive boundary control using delayed control methodology for a 1D wave equation is examined. The outlined problem is applied in the control of an ideal string-mass system with constant or time-varying length. The dynamics of the system, which constitutes the basis for the control problem, is first derived using the extended Hamilton‘s Principle. The resulting wave PDE is then transformed into two decoupled hyperbolic equations using the method of characteristics. The solution of the characteristic equation allows one to project the input signal at one boundary onto the dynamics describing the other boundary. Here, the input appears with an explicit delay. If the domain is characterized by a moving boundary, i.e., the length of the string is non-constant, the delay is time-varying. The problem then becomes that of control of a linear ODE with an input delay. Afterward, the transport PDE representation is used to re-express the delay in terms of a PDE‘s boundary value resulting in an ODE-PDE cascade system. The backstepping transformation then gives the control law and transforms the system into the target system characterized by favorable control properties. The only feedback required for the control is the boundary measurements. Thereafter, Lyapunov‘s theory is used in the stability analysis. Any unknown in-domain or boundary disturbances, as well as uncertain boundary parameters, are handled using the adaptive control strategies. The dynamics of the string-mass system and the performance of the derived controllers are illustrated using numerical simulations. This is followed by a case study where the deployment and control of an underwater sensor in the presence of the water waves are simulated.

ÖZET

BOZUKLUKLAR ALTINDA 1B DEĞİŞKEN UZUNLUKLU İP-KÜTLE SİSTEMİ İÇİN GERİ ADIMLAMALI KULLANARAK UYARLANABİLİR SINIR KONTROLÜ

Bu tezde, 1B dalga denklemi için gecikmeli kontrol metodolojisini kullanan uyarlanabilir bir sınır kontrolü incelenmiştir. Ana hatlarıyla verilen problem, sabit veya zamanla değişen uzunlukta ideal bir dizi kütle sisteminin kontrolünde uygulanmıştır. Kontrol probleminin temelini oluşturan sistemin dinamiği, ilk olarak genişletilmiş Hamilton Prensibi kullanılarak türetilmiştir. Elde edilen dalga kısmi diferansiyel denklem (KDD) daha sonra karakteristikler yöntemi kullanılarak iki ayrıştırılmış hiperbolik denkleme dönüştürülmüştür. Karakteristik denklemin çözümü, bir sınırdaki giriş sinyalinin diğer sınırı tanımlayan dinamiklere yansıtılmasına izin verir. Burada girdi, belirgin bir gecikmeyle görünür. Etki alanı hareketli bir sınırla karakterize edilirse, yani dizenin uzunluğu sabit değilse, gecikme zamana göre değişir. O zaman sorun, giriş gecikmeli doğrusal bir adi diferansiyel denklemin (ADD) kontrolü haline gelir. Daha sonra, taşıma KDD temsili, gecikmeyi bir ADD-KDD kademeli sistemi ile sonuçlanan bir KDD'nin sınır değeri cinsinden yeniden ifade etmek için kullanılır. Geri adımlamalı dönüşüm daha sonra kontrol yasasını verir ve sistemi uygun kontrol özellikleri ile karakterize edilen hedef sisteme dönüştürür. Kontrol için gerekli olan tek girdi sınır ölçümleridir. Daha sonra kararlılık analizinde Lyapunov'un teorisi kullanılır. Bilinmeyen herhangi bir etki alanı içi veya sınır bozucu etkinin yanı sıra belirsiz sınır parametreleri, uyarlamalı kontrol stratejileri kullanılarak işlenir. Dizi-kütle sisteminin dinamikleri ve türetilmiş kontrolcülerin performansı, sayısal simülasyonlar kullanılarak gösterilmektedir. Bunu, su dalgalarının varlığında bir sualtı sensörünün konuşlandırılması ve kontrolünün simüle edildiği bir vaka çalışması takip eder.

TABLE OF CONTENTS

LIST OF FIGURES

LIST OF TABLES

LIST OF SYMBOLS

a, b, ...	Constant parameters
$\hat{a}$	Parameter estimate
$\tilde{a}$	Parameter error
$\bar{a}$	Maximum of a, dimensioned variables
$\underline{a}$	Minimum of a
g	Gravitational constant, time-varying delay
l, l_c, L	Length of a string
m	Mass
t	Temporal variable
T	Period, time span
u	Control input
U	Intermediate control input
v, v_c	Velocity
V	Lyapunov function
W, Γ, Π	Backstepping States
x	Spatial variable
X	State
y	Displacement
z	Auxiliary domain variable
Z	Displacement of a transformed problem
$\mathbf{a}, \mathbf{b}$, ...	Vectors
$\mathbf{z}$	Disturbance vector
$\mathbf{A}, \mathbf{B}$, ...	Matrices
σ, ϱ, ζ	Integration, dummy variables
η, ξ	Riemann variables
λ	Eigenvalue, wavelength
ν, p, P	Disturbances

π	Propagation speed of the transport system
ρ	Linear mass density
ϕ	Delay function, potential function
ω	Angular frequency

LIST OF ACRONYMS/ABBREVIATIONS

1D	One dimensional
ARE	Algebraic Riccati equation
BBC	Bottom boundary condition
BC	Boundary condition
BD	Backward-difference
CD	Center-difference
CFL	Courant-Friedrichs-Lewy
DDE	Delay differential equation
DFSBC	Dynamic free surface boundary condition
FD	Forward-difference
FDM	Finite-difference method
HOT	Higher-order terms
IC	Initial condition
KFSBC	Kinematic free surface boundary condition
LTI	Linear time invariant
LTV	Linear time varying
ODE	Ordinary differential equation
PDE	Partial differential equation
PID	Proportional-integral-derivative
PLBC	Periodic lateral boundary condition
RMS	Root mean square
RDE	Riccati differential equation

1. INTRODUCTION[1]

1.1. Boundary Control Problem

The boundary control problem refers to control of a distributed parameter system through actuation at one of its boundaries. The partial differential equations (PDEs) and delay differential equations (DDEs) are examples of the distributed parameter systems, also known as infinite-dimensional systems. Here, the control of a mass at the end of an ideal string is the subject of this thesis. The in-domain system or the string is described by a hyperbolic PDE. The boundary condition (BC) is an ordinary differential equation (ODE) describing the dynamics of a mass. Thus, one end of the string is actuated, the input boundary, to stabilize the mass and the string itself, Figure 1.1. The backstepping method is used to derive the required control law. A general overview of the method, as it pertains to boundary control of PDEs, can be found in Krstic and Smyshlyaev (2008b). A more detailed review of the literature is given below.

1.2. Delay Control and Backstepping

One of the more recent developments in boundary control of the PDEs is the application of the backstepping method. First developed in Krstic *et al.* (1995), as an extension of the feedback linearization for adaptive and robust control of the ODEs, this technique is further expanded in Smyshlyaev and Krstic (2004) to include partial differential equations. When applied to a distributed systems, the technique utilizes the change of variables using Volterra transformation to bring the system to a new form, the target system. Nonlinear and other undesired terms are brought up by the transformation to the boundary where the application of the feedback control allows one to cancel out the troublesome terms.

[1]This chapter is a modified version of Szczesiak and Basturk (2020) and Szczesiak and Basturk (2021) and has been reproduced here with the permission of the copyright holder.

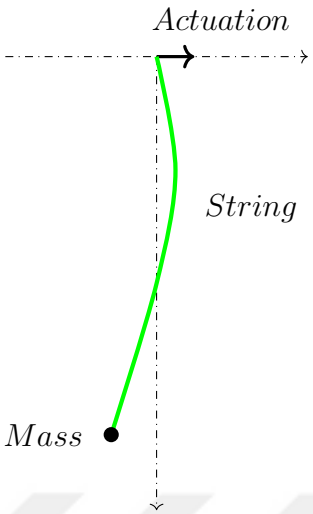

Figure 1.1. String-mass system.

The Lyapunov analysis is employed in proving the stability of the target system. Invertibility of the transformation ensures that the stability can then be extended to the states of the PDE. In Krstic and Smyshlyaev (2008a), backstepping for PDEs is used to represent a design for the linear time-invariant (LTI) - ODE system with input delay, ultimately recovering classical Smith predictor, Smith (1959).

The backstepping method has been successfully applied in the control of infinite-dimensional systems as well as ordinary differential equations with delays by Krstic and Smyshlyaev (2008a). Original work regarding stabilization of a wave PDE through adaptive boundary control and backstepping transformation can be found in Krstic (2009a). Here, a problem of an unstable wave equation with an unmatched parametric uncertainty is considered. In Smyshlyaev *et al.* (2010), authors examine wave equation with in-domain anti-damping, an internal destabilizing term. Both papers assume knowledge of the entire distributed state. In Bresch-Pietri and Krstic (2014b), an adaptive output-feedback controller is designed to control a wave PDE with uncertain, anti-damping parameter in the boundary dynamics. Furthermore, the design requires measurements at the two boundaries only. This approach is further expanded in Bresch-Pietri and Krstic (2014a), where the regulation problem for the stick-slip instability in drill strings is examined. Whereas Bresch-Pietri and Krstic (2014a) requires both boundary measurements, in Basturk (2017), an analogous problem is solved

where only surface measurements are required. Similarly, in Roman *et al.* (2019), which builds upon Smyshlyaev *et al.* (2010), only measurements at the controlled boundary are needed. All Bresch-Pietri and Krstic (2014a), Basturk (2017), and Roman *et al.* (2019) include uncertain and unstable boundary dynamics but have no in-domain disturbances. In Zhang *et al.* (2016) and Guo *et al.* (2017), authors discuss wave equation with time-dependent, harmonic disturbance in the uncontrolled boundary. In Guo and Guo (2013), the disturbance is collocated with the control. The harmonic disturbances here are characterized by unknown amplitudes but are of known frequencies. General time-dependent boundary disturbance, together with an unknown, internal, and nonlinear uncertainty, is studied in Zhou and Guo (2018). The above papers are characterized by known boundary measurements and known system parameters. In Basturk and Ayberk (2018), authors discuss an inhomogeneous wave equation where the unknown, in-domain disturbance is position-dependent but otherwise constant in time. Moreover, an unknown and constant disturbance is present in the boundary dynamics. Finally, the analysis utilizing reformulation of the problem as a stabilization of the LTI system that describes the boundary of the wave PDE and contains delayed input is given in Yilmaz and Basturk (2020) and Szczesiak and Basturk (2020). Whereas the first paper contains an unknown in-domain spatial disturbance, the second paper discusses an in-domain harmonic time disturbance and an unknown parameter in the dynamics of the BC. Again, only surface boundary measurements are required for the controller. Please note that Szczesiak and Basturk (2020) constitutes the basis of Chapter 3 of this document. Here, the problem is applied explicitly to a string-mass system resulting in a slightly different boundary ODE characterized by two unknown parameters.

Contrary to the aforementioned papers, the domain of a problem may no longer be constant in time, resulting in a boundary system with a time-varying input delay. When the delay is time-varying, the speed of propagation of the transport equation is no longer constant. While the predictor feedback for the LTI system with a time-varying input delay has been put forward in Nihtila (1991), the proof of the stability properties of the proposed control law has been explicitly given in Krstic (2010). Stability analysis

using a truncated predictor feedback, omitting infinite-dimensional distributed terms in the predictor-based feedback, is given in Zhou *et al.* (2012) for a bounded time-varying input delay and an open-loop system characterized by eigenvalues located on the imaginary axis. The detailed stability analysis for both linear Cai *et al.* (2017) and nonlinear systems with time-varying input delays can be found in Bekiaris-Liberis and Krstic (2013). This particular methodology is readily applicable in the boundary control of a wave equation on a domain with a moving boundary. In Izadi *et al.* (2015), backstepping has been applied in the control of a one-dimensional (1D) heat equation on a time-varying domain. Motivated by the control of stick-slip oscillations in oil-drilling, Cai and Krstic (2016) apply backstepping to a non-linear system under wave actuator dynamics with time and state-dependent moving boundaries. The boundary control of non-linear ODE/wave PDE cascade system with spatially-varying propagation speed is analyzed by Cai and Diagne (2020). In Diagne *et al.* (2016), the authors study the control of transport PDE/nonlinear ODE cascade system with state-dependent propagation speed.

1.3. Methods

The governing equations of motion describing the string-mass system are derived using the extended Hamilton‘s Principle and then normalized. Thereafter, the boundary actuation is utilized to stabilize a one-dimensional wave PDE with and without in-domain and boundary disturbances. For a constant domain problem with disturbances, Chapter 3, the problem is first reformulated using Riemman variables. The resulting two decoupled first order hyperbolic PDEs or transport PDEs are solved using the Laplace transforms or the method of characteristics. As a result, the in-domain disturbance of the wave PDE now appears in the bottom boundary ODE together with the delayed input. In doing so, the thesis closely follow the methods of disturbance cancellation for an LTI system with unknown parameters and input delay, found in Basturk and Krstic (2015), and applies it to a problem of controlling a boundary of wave PDE-ODE system describing the mass-string system.

The unknown disturbance itself is parameterized following the technique found in Nikiforov (2004). Here, the disturbance is modeled as an output of an exo-system after which the observer is designed. The delay compensation follows Krstic and Smyshlyaev (2008a) and Krstic (2009b) where the delay is expressed as a boundary output of a first order hyperbolic PDE. The delay compensation is achieved using predictor feedback based on the backstepping boundary control for the PDEs Krstic and Smyshlyaev (2008b). By applying Volterra operator, the PDE-ODE cascade system is transformed into a target system and the control law is derived. Next, the Lyapunov analysis is applied. Normalized Lyapunov tuning and resulting update laws for the unknown parameters are based on the approach found in Bresch-Pietri and Krstic (2009). Finally, the boundedness of the original states of the wave PDE is proven.

Boundary problem with a non-constant domain is the subject of Chapter 4 and Chapter 5. As before, the problem of Chapter 4 is first reformulated as the control of an uncertain, input delayed LTI system. When the problem is transformed, the input at the top boundary appears explicitly in the dynamics of the second boundary. This time, the input into the boundary ODE system in characterized by a non-constant time delay. This time-varying, input delayed LTI system is then stabilized using the predictor feedback design as in Bekiaris-Liberis and Krstic (2013). As before, Lyapunov analysis is used to prove the stability. Similar approach in pursued in Chapter 5. However, since the input delay is no longer linear, the dynamics of the bottom boundary is now described not by an LTI but by a linear time-varying (LTV) system. Once more, the technique outlined in the Bekiaris-Liberis and Krstic (2013) is followed. The derived transformation and the control are novel as they pertain to a control of an LTV system with input time-varying delay.

1.4. Contributions of the Thesis

The primary contributions of this thesis are in the application of the delay control methods, backstepping in particular, to a problem of controlling a distributed parameter system with uncertain boundary dynamics and disturbances. Furthermore, the

domain of the aforementioned system may not be constant due to a moving boundary. The analysis is applied to a practical problem of controlling a mass at the end of an ideal string under disturbances and with varying lengths.

Novelties, some of which are published or in the process of publication, are introduced in this thesis. Chapter 3 is a modified version of Szczesiak and Basturk (2020), and Chapter 4 is based on Szczesiak and Basturk (2021). Finally, and to the best knowledge of the author, the transformation and the controller derived in Chapter 5 for the LTV system have not been seen in the literature previously.

The following is a summary of the contributions made within the scope of this thesis:

- The delay control method of backstepping is employed in the control of systems with constant and time-varying delays, uncertain system parameters, and subject to unknown disturbances. The problem is complex and presents a challenge in the control field.
- Whereas most of the literature proves stability for the class of problems considered, the stability analysis for the boundary control employed in this thesis, Chapter 3 and Chapter 5, guarantees the convergence of the state in addition to establishing boundedness of the remaining variables.
- The stability and convergence are proven in the presence of delay with limited measurements. Boundary measurements are the only feedback required. No plant state observer is used in the analysis or in the control implementation.
- The backstepping transformation and the predictor-feedback law for the LTV system with time-varying actuator delay are given. The exponential stability using the derived target system is proven. This constitutes a contribution in the field of control of LTV systems with input delays.
- The control and the stability analyses presented for a string with a non-constant length apply to a wider class of problems described by hyperbolic PDEs and characterized by a domain with a moving boundary.
- It is shown that there exists a particular state transformation, incorporating

the delayed boundary states, which allows mapping of the problem‘s boundary condition into an LTI/LTV system characterized by an actuator delay.

- The performance of the derived controllers is tested on unstable systems. A comparison is made against delay-uncompensated control laws, Chapter 4 and Chapter 7.
- A simulated case study provides a practical application for the analysis presented in the thesis. The delay-compensated controllers are used to stabilize an underwater sensor under the influence of water wave disturbances.

1.5. Applications

The boundary control of a wave PDE has been employed as a model for many practical applications. Herein, the problem under consideration can be used as a model for the control of an underwater load suspended on a cable and exposed to harmonic wave disturbances. Likewise, positioning of a load suspended from a crane or a drone, and subjected to wind disturbances, is another practical application. Many papers cover this area. Among some of them, an overhead crane with flexible cable is considered in D'Andréa-Novel and Coron (2000). In Böhm *et al.* (2014), control of a hanging cable immersed in water is studied. In Sagert *et al.* (2013), Bresch-Pietri and Krstic (2014b), and Basturk (2017), authors examine the stabilization of the stick-slip phenomenon for drilling.

The boundary control of a wave PDE on a domain with a moving boundary has long been studied as it pertains to the dynamics of a string with a variable-length or a string in motion. First stated as the Spaghetti Problem in Carrier (1949), it has been reviewed comprehensively in Miranker (1960), Cooper (1993), and Terumichi *et al.* (1997). In Zhu *et al.* (2001), the control for a translating string with an arbitrarily prescribed length, utilizing the control volume viewpoint and based on the rate of change of energy, is derived. An axially moving string system for a crane is considered in Kim and Hong (2009). The control of a crane system in a two-dimensional space with output constraints is analyzed in He *et al.* (2017). A maritime application can be found

in Pham and Hong (2019) where the vibration control of a marine riser is examined. An axially moving belt system with high acceleration/deceleration is studied in Zhao *et al.* (2016). The vibration control in three dimensions of a string with a time-varying length and input quantization is given in Xing *et al.* (2020). Liu and coauthors utilize a boundary control for a flexible aerial refueling hose in the presence of boundary and distributed disturbances Liu *et al.* (2017). In Wang *et al.* (2018a), Wang *et al.* (2018b), and Wang *et al.* (2019), the control of axial vibrations in a mining elevator cable is analyzed. Finally, Chapter 7 takes a look at a more realistic form of harmonic disturbances, as per linear wave theory, that may affect an underwater operation.

1.6. Organization of the Thesis

This work is organized as follows: Chapter 2 provides derivation of the equations of motion. Afterwards, the next three chapters contain individual boundary control problems. Chapter 3 assumes a string of constant length under harmonic time disturbances. An adaptive controller is derived and the stability analysis is given. Chapter 4 extend the problem to a string whose length changes linearly. It is an adaptive problem with no disturbances. Finally, Chapter 5 considers the most general case where the velocity, at which the length of the string changes, follows a time-varying trajectory. Numerical analysis used in this work is reviewed in the chapter that follows. Chapter 7 provides a case study where an underwater sensor under the influence of the water waves is controlled during the deployment. Lastly, the work ends with the Conclusions chapter and various Appendices discussing finer details of the analysis.

1.7. Notation

Throughout this document the bar notation $\bar{(\cdot)}$ is used to denote two separate concepts. In Chapters 2 and 7, the bar notation denotes the dimensioned variables. Once the equations of motion are non-dimensionalized at the end of Chapter 2, the bar is dropped. Afterward, and throughout Chapters 3–6, the bar notation is used to denote the maxima, the maximum value of a given variable.

2. DERIVATION OF EQUATIONS OF MOTION

2.1. Introduction

Consider a mechanical system comprised of a cable and a suspended load. As the load is raised or lowered, the length of the cable will change. Furthermore, the cable and the load may be subject to damping forces and external disturbances due to water or air, currents, or periodic waves. Such a physical system may arise during loading and unloading of ships, construction crane operations, Figure 2.1, or underwater or aerial transports and positioning, Figure 2.2. In general, it is a difficult and complex problem. A mathematical model, only the essential features of which will be used in its description, is desired. These features include the 'wave" like nature of the string on a domain with a moving boundary, dynamics of the load, and the effect of external forces and disturbances. With that in mind, the following assumptions are made to simplify the problem at hand:

Assumption 2.1. The cable is modelled as an ideal string and no other material properties, besides its linear density, are used in the analysis.

Assumption 2.2. A one-dimensional problem is considered. Whereas the length of the string may change along the axial direction, the transverse vibrations in only one normal direction are analyzed.

Assumption 2.3. The load is considered as a point with a prescribed mass value.

Assumption 2.4. Velocity proportional viscous damping forces are considered along the transverse direction only.

Assumption 2.5. Transverse velocity $\bar{y}_{\bar{t}}(0,\bar{t})$ at the top boundary, $x = 0$, is used to actuate the string-mass system. The required control law $\bar{u}(\bar{t}) = \bar{y}_{\bar{t}}(0,\bar{t})$ will be derived in the following chapters but the nature of the velocity controller/physical apparatus required at the boundary $x = 0$ is not considered. No assumptions are made concerning the power of the actuator and the forces necessary to generate the required velocity input.

Figure 2.1. Construction crane operations, Rübig (2011).

Figure 2.2. Helicopter transport and positioning, Hasselmann (n.d.).

Assumption 2.6. The in-domain and the bottom boundary disturbances are considered both spatial and temporal in nature. The disturbances only act along the transverse direction.

Assumption 2.7. The length of the string changes as per the prescribed velocity profile.

The mathematical system will be defined in terms of the PDE associated with the string and the ODE describing the boundary condition, i.e., the dynamics of the mass. To that effect, the variational method, Goldstein *et al.* (2002), will be utilized to obtain the equations of motion from the basic principles. The upcoming derivation closely follows the one found in Zhu *et al.* (2001).

2.2. Equations of Motion

Consider a one dimensional ideal string of linear density ρ and length $L(\bar{t})$, together with mass m suspended at one end of the string as in Figure 2.3. An inertial reference frame anchored at $(\bar{x}, \bar{y}) = (0, 0)$ is assumed.

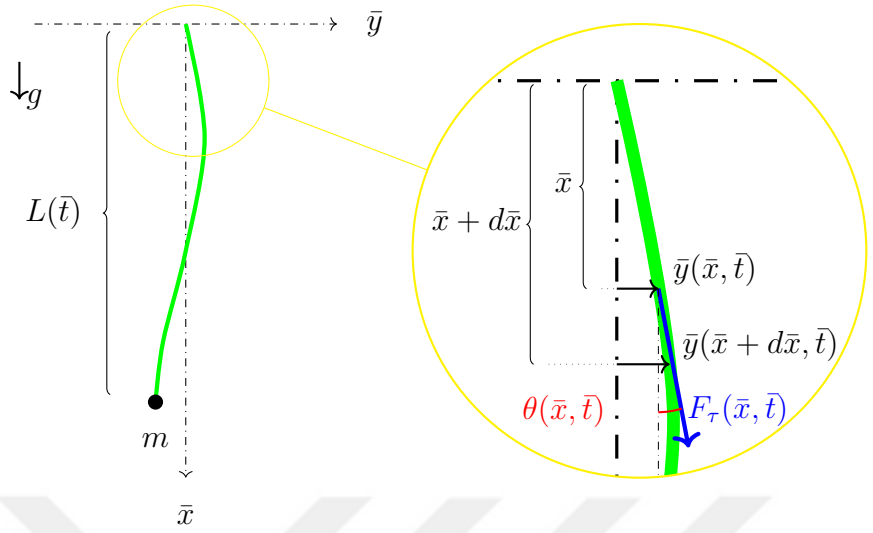

Figure 2.3. String diagram and string tension $F_\tau(\bar{x}, \bar{t})$.

The string is fed at $\bar{x} = 0$ at a rate $\bar{v}(\bar{t}) = \dot{L}(\bar{t})$. Both the string and the mass are subject to gravity, the damping forces, the in-domain, $\bar{p}(\bar{x}, \bar{t})$, and the boundary, $\bar{P}(\bar{x}, \bar{t})\big|_{L(\bar{t})}$, disturbance forces, Figure 2.4. The differential length of the string is

$$dL = \sqrt{d\bar{x}^2 + d\bar{y}^2}, \tag{2.1}$$

$$dL = d\bar{x}\sqrt{1 + \left(\frac{d\bar{y}}{d\bar{x}}\right)^2}. \tag{2.2}$$

The above expression can be further simplified by assuming small vibrations or $|\theta(\bar{x}, \bar{t})| \ll 1 \implies |\frac{d\bar{y}}{d\bar{x}}| \ll 1$. This warrants application of binomial approximation, $(1 + x)^\alpha \approx 1 + \alpha x$ for $|x| < 1$ and $|\alpha x| \ll 1$, to write

$$dL = d\bar{x}\Big(1 + \frac{1}{2}\left(\frac{d\bar{y}}{d\bar{x}}\right)^2\Big), \tag{2.3}$$

and

$$\delta L = dL - d\bar{x} = \frac{1}{2}\Big(\frac{d\bar{y}}{d\bar{x}}\Big)^2. \tag{2.4}$$

Differential of potential energy of the string due to tension $F_\tau(\bar{x}, \bar{t})$ is

$$dV_e = F_\tau \delta L. \tag{2.5}$$

The potential energy can then be written as an integral over the domain $\bar{x} \in [0, L(\bar{t})]$

$$V_e = \frac{1}{2}\int_0^{L(\bar{t})} F_\tau(\bar{x}, \bar{t})\bar{y}_{\bar{x}}^2 d\bar{x}, \tag{2.6}$$

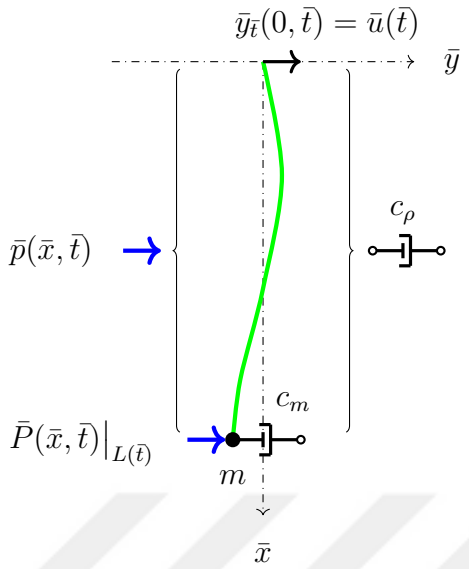

Figure 2.4. Actuation and non-potent forces acting on the mass-string system.

where, assuming negligible effects of buoyancy, tension in the string due to its own weight, weight of the mass m, and the acceleration $\dot{\bar{v}}(\bar{t})$, is

$$F_\tau(\bar{x},\bar{t}) = \Big(m + \rho\big(L(\bar{t}) - \bar{x}\big)\Big)\Big(g - \dot{\bar{v}}(\bar{t})\Big). \tag{2.7}$$

The kinetic energy of the string and the mass is composed of axial and transverse components as follows

$$\begin{aligned} T_e = &\frac{1}{2}m\bar{v}(\bar{t})^2 + \frac{1}{2}m\Big(\frac{D\bar{y}}{D\bar{t}}\big(\bar{x} = L(\bar{t}),\bar{t}\big)\Big)^2 \\ &+ \frac{1}{2}\rho L(\bar{t})\bar{v}(\bar{t})^2 + \frac{1}{2}\rho\int_0^{L(\bar{t})}\Big(\frac{D\bar{y}}{D\bar{t}}(\bar{x},\bar{t})\Big)^2 d\bar{x}, \end{aligned} \tag{2.8}$$

where the Material or Total derivative given by

$$\frac{D}{D\bar{t}} = \frac{\partial}{\partial\bar{t}} + \bar{v}(\bar{t})\frac{\partial}{\partial\bar{x}} \tag{2.9}$$

is utilized. Work associated with non-potent forces $\boldsymbol{f}_i$ acting on the system is

$$W_e = \sum_i \boldsymbol{f}_i^T \boldsymbol{r}_i, \tag{2.10}$$

or, in this particular case,

$$\begin{aligned} W_e = &\bar{P}(\bar{x},\bar{t})\ \bar{y}\Big|_{\bar{x}=L(\bar{t})} + \int_0^{L(\bar{t})}\bar{p}(\bar{x},\bar{t})d\bar{x}\ \bar{y} \\ &- c_m\frac{D\bar{y}}{D\bar{t}}\big(\bar{x} = L(\bar{t}),\bar{t}\big)\ \bar{y} - \int_0^{L(\bar{t})} c_\rho\frac{D\bar{y}}{D\bar{t}}(\bar{x},\bar{t})d\bar{x}\ \bar{y}, \end{aligned} \tag{2.11}$$

where c_ρ and c_m are coefficient associated with damping forces acting on the string and on the mass m (Please see Figure 2.4). Furthermore, note that no work associated with the control input is included here, see Assumption 2.5.

Applying the extended Hamilton's Principle allows one to write action, a characteristic of the dynamics associated with a physical system, as

$$S = \int_{\bar{t}_1}^{\bar{t}_2} (T_e - V_e + W_e) d\bar{t}. \tag{2.12}$$

Since the path taken by a system is the one which minimizes action S, take variation of action δS and set it equal to zero

$$\delta S = \int_{\bar{t}_1}^{\bar{t}_2} (\delta T_e - \delta V_e + \delta W_e) d\bar{t} = 0. \tag{2.13}$$

Starting with increment Δ, individual variations are evaluated as follows

$$\Delta V_e = V_e(\bar{y} + \Delta\bar{y}, \bar{y}_{\bar{x}} + \Delta\bar{y}_{\bar{x}}, \dot{\bar{y}} + \Delta\dot{\bar{y}}, \bar{t}) - V_e(\bar{y}, \bar{y}_{\bar{x}}, \dot{\bar{y}}, \bar{t}), \tag{2.14}$$

or

$$\begin{aligned} \Delta V_e = & V_e(\bar{y}, \bar{y}_{\bar{x}}, \dot{\bar{y}}, \bar{t}) + \frac{\partial V_e}{\partial \bar{y}}(...)\delta\bar{y} + \frac{\partial V_e}{\partial \bar{y}_{\bar{x}}}(...)\delta\bar{y}_{\bar{x}} + \frac{\partial V_e}{\partial \dot{\bar{y}}}(...)\delta\dot{\bar{y}} \\ & + HOT - V_e(...), \end{aligned} \tag{2.15}$$

where for clarity $\dot{\bar{y}} = \frac{D\bar{y}}{D\bar{t}}$ and $\bar{y}_{\bar{t}} = \frac{\partial\bar{y}}{\partial\bar{t}}$. The first variation of the potential energy δV_e, the liner part, is then represented by the first order derivative terms in the above expression, or

$$\delta V_e = \frac{\partial V_e}{\partial \bar{y}}(...)\delta\bar{y} + \frac{\partial V_e}{\partial \bar{y}_{\bar{x}}}(...)\delta\bar{y}_{\bar{x}} + \frac{\partial V_e}{\partial \dot{\bar{y}}}(...)\delta\dot{\bar{y}}. \tag{2.16}$$

Since the potential depends only on $\bar{y}_{\bar{x}}$ as in (2.6),

$$\delta V_e = \frac{\partial V_e}{\partial \bar{y}_{\bar{x}}}(...)\delta\bar{y}_{\bar{x}} = \int_0^{L(\bar{t})} F_\tau(\bar{x}, \bar{t})\bar{y}_{\bar{x}}\delta\bar{y}_{\bar{x}} d\bar{x}. \tag{2.17}$$

Using the integration by parts gives

$$\delta V_e = F_\tau(\bar{x}, \bar{t})\bar{y}_{\bar{x}}\delta\bar{y}\Big|_0^{L(\bar{t})} - \int_0^{L(\bar{t})} \left(F_\tau(\bar{x}, \bar{t})\bar{y}_{\bar{x}}\right)_{\bar{x}}\delta\bar{y} d\bar{x}. \tag{2.18}$$

Similarly, the kinetic energy variation δT_e is the linear part of the increment ΔT_e, or

$$\delta T_e = \frac{\partial T_e}{\partial \bar{y}}(...)\delta\bar{y} + \frac{\partial T_e}{\partial \bar{y}_{\bar{x}}}(...)\delta\bar{y}_{\bar{x}} + \frac{\partial T_e}{\partial \dot{\bar{y}}}(...)\delta\dot{\bar{y}}. \tag{2.19}$$

Since the kinetic energy depends only on $\dot{\bar{y}}$, please see (2.8), expression (2.19) becomes

$$\begin{aligned}\delta T_e &= \frac{\partial T_e}{\partial \dot{\bar{y}}}(...)\delta\dot{\bar{y}} \\ &= \frac{\partial}{\partial \dot{\bar{y}}}\left(\frac{1}{2}m\Big(\frac{D\bar{y}}{D\bar{t}}\big(\bar{x}=L(\bar{t}),\bar{t}\big)\Big)^2\right)\delta\dot{\bar{y}} + \frac{\partial}{\partial \dot{\bar{y}}}\left(\frac{1}{2}\rho\int_0^{L(\bar{t})}\Big(\frac{D\bar{y}}{D\bar{t}}(\bar{x},\bar{t})\Big)^2 d\bar{x}\right)\delta\dot{\bar{y}},\end{aligned} \tag{2.20}$$

and

$$\delta T_e = m\frac{D\bar{y}}{D\bar{t}}\big(\bar{x}=L(\bar{t}),\bar{t}\big)\delta\dot{\bar{y}} + \rho\int_0^{L(\bar{t})}\frac{D\bar{y}}{D\bar{t}}(\bar{x},\bar{t})d\bar{x}\delta\dot{\bar{y}}. \tag{2.21}$$

Finally, the variation of work, using equation (2.11), is

$$\begin{aligned}\delta W_e = \bar{P}(\bar{x},\bar{t})\delta\bar{y}\Big|_{\bar{x}=L(\bar{t})} + \int_0^{L(\bar{t})}\bar{p}(\bar{x},\bar{t})d\bar{x}\delta\bar{y} \\ - c_m\frac{D\bar{y}}{D\bar{t}}\big(\bar{x}=L(\bar{t}),\bar{t}\big)\delta\bar{y} - \int_0^{L(\bar{t})}c_\rho\frac{D\bar{y}}{D\bar{t}}(\bar{x},\bar{t})d\bar{x}\delta\bar{y}.\end{aligned} \tag{2.22}$$

Inserting (2.18), (2.21) and (2.22) into (2.13) gives

$$\begin{aligned}\int_{\bar{t}_1}^{\bar{t}_2}\Bigg(&\underbrace{m\frac{D\bar{y}}{D\bar{t}}\big(\bar{x}=L(\bar{t}),\bar{t}\big)\delta\dot{\bar{y}}}_{\#1} + \underbrace{\rho\int_0^{L(\bar{t})}\frac{D\bar{y}}{D\bar{t}}(\bar{x},\bar{t})d\bar{x}\delta\dot{\bar{y}}}_{\#2} \\ &- F_\tau(\bar{x},\bar{t})\bar{y}_{\bar{x}}\delta\bar{y}\Big|_{\bar{x}=L(\bar{t})} + F_\tau(\bar{x},\bar{t})\bar{y}_{\bar{x}}\delta\bar{y}\Big|_{\bar{x}=0} + \int_0^{L(\bar{t})}\big(F_\tau(\bar{x},\bar{t})\bar{y}_{\bar{x}}\big)_{\bar{x}}\delta\bar{y}d\bar{x} \\ &+ \bar{P}(\bar{x},\bar{t})\delta\bar{y}\Big|_{\bar{x}=L(\bar{t})} + \int_0^{L(\bar{t})}\bar{p}(\bar{x},\bar{t})d\bar{x}\delta\bar{y} \\ &- c_m\frac{D\bar{y}}{D\bar{t}}\big(\bar{x}=L(\bar{t}),\bar{t}\big)\delta\bar{y} - \int_0^{L(\bar{t})}c_\rho\frac{D\bar{y}}{D\bar{t}}(\bar{x},\bar{t})d\bar{x}\delta\bar{y}\Bigg)d\bar{t} = 0.\end{aligned} \tag{2.23}$$

Using integration by parts evaluate the integral of the term labeled #1 as

$$\begin{aligned}\int_{\bar{t}_1}^{\bar{t}_2}m\frac{D\bar{y}}{D\bar{t}}\big(\bar{x}=L(\bar{t}),\bar{t}\big)\delta\dot{\bar{y}}d\bar{t} = m\frac{D\bar{y}}{D\bar{t}}\big(\bar{x}=L(\bar{t}),\bar{t}\big)\delta\bar{y}\Big|_{\bar{t}_1}^{\bar{t}_2} \\ - \int_{\bar{t}_1}^{\bar{t}_2}m\frac{D^2\bar{y}}{D\bar{t}^2}\big(\bar{x}=L(\bar{t}),\bar{t}\big)\delta\bar{y}d\bar{t},\end{aligned} \tag{2.24}$$

and since variation $\delta\bar{y}$ vanishes at initial and terminal points, $\bar{t}_1$ and $\bar{t}_2$, the first term on the right hand side drops out resulting in

$$\int_{\bar{t}_1}^{\bar{t}_2}m\frac{D\bar{y}}{D\bar{t}}\big(\bar{x}=L(\bar{t}),\bar{t}\big)\delta\dot{\bar{y}}d\bar{t} = -\int_{\bar{t}_1}^{\bar{t}_2}m\frac{D^2\bar{y}}{D\bar{t}^2}\big(\bar{x}=L(\bar{t}),\bar{t}\big)\delta\bar{y}d\bar{t}. \tag{2.25}$$

Similarly, using integration by parts, evaluate the term labeled #2 as follows

$$\int_{\bar{t}_1}^{\bar{t}_2}\underbrace{\rho\int_0^{L(\bar{t})}\frac{D\bar{y}}{D\bar{t}}(\bar{x},\bar{t})d\bar{x}}_{u}\underbrace{\delta\dot{\bar{y}}d\bar{t}}_{dv} = uv\Big|_{\bar{t}_1}^{\bar{t}_2} - \int_{\bar{t}_1}^{\bar{t}_2}vdu. \tag{2.26}$$

Evaluating du using the Leibniz's rule (A.10) gives

$$\begin{aligned} du = \frac{d}{d\bar{t}}\Big(\int_0^{L(\bar{t})} \rho \frac{D\bar{y}}{D\bar{t}}(\bar{x},\bar{t})d\bar{x}\Big)d\bar{t} = & \int_0^{L(\bar{t})} \rho \frac{D^2\bar{y}}{D\bar{t}^2}(\bar{x},\bar{t})d\bar{x} \\ & + \rho \frac{D\bar{y}}{D\bar{t}}(\bar{x},\bar{t})\Big|_{\bar{x}=L(\bar{t})} \frac{d}{d\bar{t}}\big(L(\bar{t})\big) \\ & - \rho \frac{D\bar{y}}{D\bar{t}}(\bar{x},\bar{t})\Big|_{\bar{x}=0} \frac{d}{d\bar{t}}\big(0\big). \end{aligned} \tag{2.27}$$

Expression (2.26) then becomes

$$\begin{aligned} \int_{\bar{t}_1}^{\bar{t}_2} \rho \int_0^{L(\bar{t})} \frac{D\bar{y}}{D\bar{t}}(\bar{x},\bar{t})d\bar{x}\delta\dot{\bar{y}}d\bar{t} = & \rho \int_0^{L(\bar{t})} \frac{D\bar{y}}{D\bar{t}}(\bar{x},\bar{t})d\bar{x}\delta\bar{y}\Big|_{\bar{t}_1}^{\bar{t}_2} \\ & - \int_{\bar{t}_1}^{\bar{t}_2} \Big(\int_0^{L(\bar{t})} \rho \frac{D^2\bar{y}}{D\bar{t}^2}(\bar{x},\bar{t})d\bar{x} \\ & + \rho \frac{D\bar{y}}{D\bar{t}}(\bar{x},\bar{t})\bar{v}(\bar{t})\Big|_{\bar{x}=L(\bar{t})}\Big)\delta\bar{y}d\bar{t}. \end{aligned} \tag{2.28}$$

Again, since variation $\delta\bar{y}$ vanishes at $\bar{t}_1$ and $\bar{t}_2$, the first term drops out and one arrives at

$$\begin{aligned} \int_{\bar{t}_1}^{\bar{t}_2} \rho \int_0^{L(\bar{t})} \frac{D\bar{y}}{D\bar{t}}(\bar{x},\bar{t})d\bar{x}\delta\dot{\bar{y}}d\bar{t} = & -\int_{\bar{t}_1}^{\bar{t}_2} \int_0^{L(\bar{t})} \rho \frac{D^2\bar{y}}{D\bar{t}^2}(\bar{x},\bar{t})d\bar{x}\delta\bar{y}d\bar{t} \\ & - \int_{\bar{t}_1}^{\bar{t}_2} \rho \frac{D\bar{y}}{D\bar{t}}(\bar{x},\bar{t})\Big|_{\bar{x}=L(\bar{t})} \bar{v}(\bar{t})\delta\bar{y}d\bar{t}. \end{aligned} \tag{2.29}$$

In light of (2.25) and (2.29), (2.23) becomes

$$\begin{aligned} & \int_{\bar{t}_1}^{\bar{t}_2} \int_0^{L(\bar{t})} \Big(-\rho \frac{D^2\bar{y}}{D\bar{t}^2}(\bar{x},\bar{t}) - c_\rho \frac{D\bar{y}}{D\bar{t}}(\bar{x},\bar{t}) + \Big(F_\tau(\bar{x},\bar{t})\bar{y}_{\bar{x}}\Big)_{\bar{x}} + \bar{p}(\bar{x},\bar{t})\Big)d\bar{x}\delta\bar{y}d\bar{t} \\ & - \int_{\bar{t}_1}^{\bar{t}_2} \Big(m\frac{D^2\bar{y}}{D\bar{t}^2} + \rho\frac{D\bar{y}}{D\bar{t}}\bar{v}(\bar{t}) + c_m\frac{D\bar{y}}{D\bar{t}} + F_\tau(\bar{x},\bar{t})\bar{y}_{\bar{x}} - \bar{P}(\bar{x},\bar{t})\Big)\delta\bar{y}\Big|_{\bar{x}=L(\bar{t})}d\bar{t} \\ & + \int_{\bar{t}_1}^{\bar{t}_2} \Big(F_\tau(\bar{x},\bar{t})\bar{y}_{\bar{x}}\Big)\delta\bar{y}\Big|_{\bar{x}=0}d\bar{t} = 0. \end{aligned} \tag{2.30}$$

The term under the last integral in the above equation is associated with the transverse force acting at $\bar{x} = 0$. The expression is incomplete as the boundary input has not been defined at this point, please see Assumption 2.5. Now, for $\delta S = 0$, individual terms of (2.30) must vanish. By equating to zero inner expressions of the first and second integrals of (2.30) gives the PDE, and the ODE associated with the boundary condition at $\bar{x} = L(\bar{t})$:

$$\rho\frac{D^2\bar{y}}{D\bar{t}^2}(\bar{x},\bar{t}) + c_\rho\frac{D\bar{y}}{D\bar{t}}(\bar{x},\bar{t}) - \Big(F_\tau(\bar{x},\bar{t})\bar{y}_{\bar{x}}(\bar{x},\bar{t})\Big)_{\bar{x}} - \bar{p}(\bar{x},\bar{t}) = 0, \tag{2.31}$$

$$\Big(m\frac{D^2\bar{y}}{D\bar{t}^2}(\bar{x},\bar{t})+\rho\frac{D\bar{y}}{D\bar{t}}(\bar{x},\bar{t})\bar{v}(\bar{t}) + c_m\frac{D\bar{y}}{D\bar{t}}(\bar{x},\bar{t})+F_\tau(\bar{x},\bar{t})\bar{y}_{\bar{x}}(\bar{x},\bar{t})-\bar{P}(\bar{x},\bar{t})\Big)_{\bar{x}=L(\bar{t})}=0. \tag{2.32}$$

Using definition of the total derivative found in (2.9) to rewrite (2.31) and (2.32) as

$$\rho\Big(\bar{y}_{\bar{t}\bar{t}}(\bar{x},\bar{t})+2\bar{v}(\bar{t})\bar{y}_{\bar{x}\bar{t}}(\bar{x},\bar{t})+\dot{\bar{v}}(\bar{t})\bar{y}_{\bar{x}}(\bar{x},\bar{t})+\bar{v}(\bar{t})^2\bar{y}_{\bar{x}\bar{x}}(\bar{x},\bar{t})\Big)-\bar{p}(\bar{x},\bar{t}) + c_\rho\Big(\bar{y}_{\bar{t}}(\bar{x},\bar{t})+\bar{v}(\bar{t})\bar{y}_{\bar{x}}(\bar{x},\bar{t})\Big)-\Big(F_{\tau_{\bar{x}}}(\bar{x},\bar{t})\bar{y}_{\bar{x}}(\bar{x},\bar{t})+F_\tau(\bar{x},\bar{t})\bar{y}_{\bar{x}\bar{x}}(\bar{x},\bar{t})\Big)=0, \tag{2.33}$$

$$\Big(m\Big(\bar{y}_{\bar{t}\bar{t}}(\bar{x},\bar{t})+2\bar{v}(\bar{t})\bar{y}_{\bar{x}\bar{t}}(\bar{x},\bar{t})+\dot{\bar{v}}(\bar{t})\bar{y}_{\bar{x}}(\bar{x},\bar{t})+\bar{v}(\bar{t})^2\bar{y}_{\bar{x}\bar{x}}(\bar{x},\bar{t})\Big) + \rho\Big(\bar{y}_{\bar{t}}(\bar{x},\bar{t})+\bar{v}(\bar{t})\bar{y}_{\bar{x}}(\bar{x},\bar{t})\Big)\bar{v}(\bar{t})+c_m\Big(\bar{y}_{\bar{t}}(\bar{x},\bar{t})+\bar{v}(\bar{t})\bar{y}_{\bar{x}}(\bar{x},\bar{t})\Big) + F_\tau(\bar{x},\bar{t})\bar{y}_{\bar{x}}(\bar{x},\bar{t})-\bar{P}(\bar{x},\bar{t})\Big)_{\bar{x}=L(\bar{t})}=0. \tag{2.34}$$

Please observe that the inertia part of (2.33) contains additional terms. These are associated with the local Coriolis force ($2\bar{v}(\bar{t})$ term), tangential acceleration ($\dot{\bar{v}}(\bar{t})$ term), and centripetal force ($\bar{v}(\bar{t})^2$ term). Finally, introduce control parameters ϵ_a and ϵ_τ, definition of string tension form (2.7), and re-arrange equations (2.33) and (2.34):

$$\bar{y}_{\bar{t}\bar{t}}(\bar{x},\bar{t})+2\bar{v}(\bar{t})\bar{y}_{\bar{x}\bar{t}}(\bar{x},\bar{t})+\Big(\dot{\bar{v}}(\bar{t})+\epsilon_\tau\big(g-\dot{\bar{v}}(\bar{t})\big)+\frac{c_\rho\bar{v}(\bar{t})}{\rho}\Big)\bar{y}_{\bar{x}}(\bar{x},\bar{t})+\frac{c_\rho}{\rho}\bar{y}_{\bar{t}}(\bar{x},\bar{t}) + \Big(\bar{v}(\bar{t})^2-\Big(\frac{m}{\rho}+\epsilon_\tau\big(L(\bar{t})-\bar{x}\big)\Big)\big(g-\epsilon_a\dot{\bar{v}}(\bar{t})\big)\Big)\bar{y}_{\bar{x}\bar{x}}(\bar{x},\bar{t})-\frac{\bar{p}(\bar{x},\bar{t})}{\rho}=0, \tag{2.35}$$

$$\Big(\bar{y}_{\bar{t}\bar{t}}(\bar{x},\bar{t})+2\bar{v}(\bar{t})\bar{y}_{\bar{x}\bar{t}}(\bar{x},\bar{t})+\bar{v}(\bar{t})^2\bar{y}_{\bar{x}\bar{x}}(\bar{x},\bar{t})+\Big(\frac{\rho\bar{v}(\bar{t})}{m}+\frac{c_m}{m}\Big)\bar{y}_{\bar{t}}(\bar{x},\bar{t}) + \Big(\dot{\bar{v}}(\bar{t})+\frac{\rho\bar{v}(\bar{t})^2}{m}+\big(g-\epsilon_a\dot{\bar{v}}(\bar{t})\big)+\frac{c_m\bar{v}(\bar{t})}{m}\Big)\bar{y}_{\bar{x}}(\bar{x},\bar{t})-\frac{\bar{P}(\bar{x},\bar{t})}{m}\Big)_{\bar{x}=L(\bar{t})}=0. \tag{2.36}$$

To complete the system, and per Assumption 2.5, the boundary condition at $x=0$ is

$$\bar{y}_{\bar{t}}(0,\bar{t})=\bar{u}(\bar{t}). \tag{2.37}$$

The binary, 0 or 1, epsilon parameters in (2.35)–(2.36) allow one to turn on or off effects such as:

- Varying string tension due to the weight of the string: ϵ_τ,
- Varying string tension due to the acceleration of the string and the mass: ϵ_a.

Furthermore, by adjusting c_ρ and c_m one can control amount of damping affecting the string and the mass respectively. Finally, using Assumption 2.7 the length of the string becomes

$$L(\bar{t}) = L_0 + \int_0^{\bar{t}} \bar{v}(\bar{t}) d\bar{t}, \tag{2.38}$$

where $L_0 > 0$ is the initial length of the string.

In summary, the equation system (2.35)–(2.37) describes a mass suspended on a one dimensional ideal string whose length changes with the prescribed velocity profile. The string is actuated using transverse velocity input at the boundary $x = 0$. Both the string and the mass are subject to gravity, damping, and external disturbances.

2.3. Dimensionless Analysis

The dimensionless analysis will be used to re-express the equations of motion (2.35)–(2.37). This is done to better understand the behaviour of the dynamical system and not just a particular case that might be obtained by assuming some representative parameter values. The benefits of this approach will be most apparent when comparing results for various control problems to be considered later, as well as when simulating these problems numerically.

Begin by defining dimensionless variables: $x = \frac{\bar{x}}{L_0}, y = \frac{\bar{y}}{L_0}, l(t) = \frac{L(\bar{t})}{L_0}$, and $t = \frac{\bar{t}}{t_c}$ with constant t_c to be specified later. Spatial and temporal derivatives then become $\frac{d^n}{d\bar{x}^n} = \frac{1}{(L_0)^n}\frac{d^n}{dx^n}$ and $\frac{d^n}{d\bar{t}^n} = \frac{1}{(t_c)^n}\frac{d^n}{dt^n}$. Furthermore, $\bar{v}(\bar{t}) = v(t)\frac{L_0}{t_c}$ and $\dot{\bar{v}}(\bar{t}) = \frac{1}{t_c}\frac{d}{dt}\bar{v}(\bar{t}) = \frac{L_0}{t_c^2}\dot{v}(t)$. Insert above definitions in (2.35)–(2.37) and divide all equations by a common term $\frac{L_0}{t_c^2}$ to obtain

$$\begin{aligned} &y_{tt}(x,t) + 2v(t)y_{xt}(x,t) + \Big(\dot{v}(t) + \frac{c_\rho t_c v(t)}{\rho} + \epsilon_\tau\big(\frac{gt_c^2}{L_0} - \dot{v}(t)\big)\Big)y_x(x,t) \\ &\quad + \left(v(t)^2 - \Big(\frac{m}{L_0\rho} + \epsilon_\tau\big(l(t) - x\big)\Big)\big(\frac{gt_c^2}{L_0} - \epsilon_a\dot{v}(t)\big)\right)y_{xx}(x,t) \\ &\quad + \frac{c_\rho t_c}{\rho}y_t(x,t) - \frac{t_c^2}{L_0\rho}\bar{p}(L_0x, tt_c) = 0, \end{aligned} \tag{2.39}$$

$$y_t(0,t) = \frac{t_c}{L_0}\bar{u}(\bar{t}), \tag{2.40}$$

and

$$\begin{aligned}\Big(& y_{tt}(x,t) + 2v(t)y_{xt}(x,t) + v(t)^2 y_{xx}(x,t) \\ & + \Big(\dot{v}(t) + \frac{L_0\rho v(t)^2}{m} + \big(\frac{gt_c^2}{L_0} - \epsilon_a\dot{v}(t)\big) + \frac{c_m t_c v(t)}{m}\Big) y_x(x,t) \\ & + \Big(\frac{L_0\rho v(t)}{m} + \frac{c_m t_c}{m}\Big) y_t(x,t) - \frac{t_c^2}{L_0 m}\bar{P}(L_0 x, tt_c)\Big)_{x=l(t)} = 0.\end{aligned} \tag{2.41}$$

Now, define $t_c = \frac{L_0}{\sqrt{\frac{mg}{\rho}}}$, and set $u(t) = \frac{1}{\sqrt{\frac{mg}{\rho}}}\bar{u}(\bar{t})$, $p(x,t) = \frac{L_0}{mg}\bar{p}(xL_0, tt_c)$, $P(x,t) = \frac{L_0\rho}{m^2 g}\bar{P}(xL_0, tt_c)$. Then, collecting likewise terms gives

$$\begin{aligned} y_{tt}(x,t) = & -2v(t)y_{xt}(x,t) \\ & - \Big(v(t)^2 - \Big(\frac{m}{L_0\rho} + \epsilon_\tau\big(l(t)-x\big)\Big)\Big(\frac{L_0\rho}{m} - \epsilon_a\dot{v}(t)\Big)\Big) y_{xx}(x,t) \\ & - \Big(\dot{v}(t) + \frac{c_\rho L_0 v(t)}{\rho\sqrt{\frac{mg}{\rho}}} + \epsilon_\tau\big(\frac{L_0\rho}{m} - \dot{v}(t)\big)\Big) y_x(x,t) \\ & - \frac{c_\rho L_0}{\rho\sqrt{\frac{mg}{\rho}}} y_t(x,t) + p(x,t), \end{aligned} \tag{2.42}$$

$$y_t(0,t) = u(t), \tag{2.43}$$

$$\begin{aligned}\Big(y_{tt}(x,t) = & -v(t)^2 y_{xx}(x,t) - 2v(t)y_{tx}(x,t) \\ & - \Big(\dot{v}(t) + \frac{L_0\rho v(t)^2}{m} + \frac{c_m L_0 v(t)}{m\sqrt{\frac{mg}{\rho}}} + \Big(\frac{L_0\rho}{m} - \epsilon_a\dot{v}(t)\Big)\Big) y_x(x,t) \\ & - \Big(\frac{L_0\rho v(t)}{m} + \frac{c_m L_0}{m\sqrt{\frac{mg}{\rho}}}\Big) y_t(x,t) + P(x,t)\Big)_{x=l(t)}, \end{aligned} \tag{2.44}$$

where $l(t)$ is the normalized length of the string given by

$$l(t) = 1 + \int_0^t v(t)dt. \tag{2.45}$$

Equations (2.42) and (2.44) are the non-dimensionalized equations of motion. As a quick check let's assume a particular case. Set the non-dimensional velocity $v(t)$, epsilon parameters, and the disturbance $p(x,t)$ to zero in equation (2.42). The PDE then becomes $y_{tt} = y_{xx}$, a simple wave equation with the wave speed of one. While the system (2.42)–(2.44) appears complicated, it can be thought of as a modified wave

equation. When the $v(t) \neq 0$, the string extends or retracts at the given speed. The length of the string starts at the normalized value of one and then increases or decreases as per (2.45). Accordingly, the system (2.42)–(2.44) is characterized by a moving boundary. In the following chapters, this system of equations will provide the basis for the analysis of various boundary control problems.

3. ADAPTIVE BOUNDARY CONTROL FOR A STRING-MASS SYSTEM OF CONSTANT LENGTH AND WITH DISTURBANCES[2]

3.1. Introduction

This chapter considers the first boundary control problem. The equations of motion derived previously will be used as a model for the control of a string of constant length under time-dependent disturbances. Furthermore, additional assumption will be stated do better define the control problem as well as the nature of the required boundary input.

3.2. Problem Statement

Consider (2.42)–(2.44). The following physical assumptions are made about the system:

Assumption 3.1. The velocity of the string is zero, $v(t) = 0$. The string then is of constant length $l(t) = 1$ as per expression (2.45).

Assumption 3.2. There are not any in-domain damping forces affecting the string, $c_\rho = 0$.

Assumption 3.3. Tension in the string is constant and due only to the weight of the mass, $F_\tau(x,t) = mg$. This implies: $\epsilon_\tau = 0$ and $\epsilon_a = 0$.

Assumption 3.4. The string itself is under the influence of temporal disturbances only, which take the form of

$$p(t) = \sum_{i=1}^{n} g_i \sin(\omega_i t + \phi_i). \tag{3.1}$$

[2]This chapter is a modified version of Szczesiak and Basturk (2020) and has been reproduced here with the permission of the copyright holder.

Assumption 3.5. The mass is under the influence of temporal disturbances only, which take the form of

$$P(t) = \sum_{i=1}^{n} h_i \sin(\omega_i t + \varphi_i). \tag{3.2}$$

Assumptions 3.4 and 3.5 can be seen as a simple model for harmonic disturbances, such as waves or wind gusts, that might affect the string and the suspended load. Under Assumptions 3.1–3.5 system (2.42)–(2.44) reduces to

$$y_{tt}(x,t) = y_{xx}(x,t) + \sum_{i=1}^{n} g_i \sin(\omega_i t + \phi_i), \tag{3.3}$$

$$y_t(0,t) = u(t), \tag{3.4}$$

$$y_{tt}(1,t) = -b y_x(1,t) + (a+b) y_t(1,t) + \sum_{i=1}^{n} h_i \sin(\omega_i t + \varphi_i), \tag{3.5}$$

where

$$a = -\Big(\frac{L_0\rho}{m} + \frac{c_m L_0}{m\sqrt{\frac{mg}{\rho}}}\Big), \tag{3.6}$$

$$b = \frac{L_0\rho}{m}, \tag{3.7}$$

and for $x \in [0,1]$. Parameters $g_i \in \mathbb{R}$, $h_i \in \mathbb{R}$, $w_i \in \mathbb{R}$, $\phi_i \in \mathbb{R}$, $\varphi_i \in \mathbb{R}$ are amplitudes, frequencies, and phases of the disturbances respectively. In addition, following control assumptions are stated

Assumption 3.6. Symbol n stands for a known number of distinct but otherwise unknown disturbance frequencies. All frequencies are assumed to have known bounds such that each $\omega_i \in [\underline{\omega}_i, \bar{\omega}_i]$, where from now on the underbar and the overbar symbols will indicate minimum and maximum bounds respectively.

Assumption 3.7. Unknown disturbance amplitudes g_i and h_i are assumed to have known bounds, $|g_i| \leq g_{max}$ and $|h_i| \leq h_{max}$.

Assumption 3.8. Parameters a and b are assumed to be unknown but have known bounds $a \in [\underline{a}, \bar{a}]$ and $b \in [\underline{b}, \bar{b}]$. Moreover, parameter $b \neq 0$ is of a known sign.

Assumption 3.9. Boundary states, $y_t(0,t)$, $y_x(0,t)$, and $y_t(1,t)$, are assumed to be measured. Their present values as well as their histories are available for feedback.

The aim of this chapter is to design boundary control input $u(t)$ at boundary $x = 0$, see (3.4), such that:

$$\lim_{t\to\infty} y_t(1,t) = 0 \tag{3.8}$$

i.e., the velocity of the bottom boundary, or the mass, converges to zero despite presence of unmeasured disturbances and an uncertain boundary dynamics.

In the next section, the problem is reformulated using a set of Riemann variables. This enables one to express bottom boundary condition (3.5) as an LTI system with delayed input.

3.3. Reformulation of the Problem

The outlined problem is reformulated as a stabilization of an LTI system describing dynamics at the bottom boundary, $x = 1$. This is accomplished by following Basturk (2017) and defining two Riemann variables

$$\xi(x,t) = y_t(x,t) + y_x(x,t), \tag{3.9}$$

$$\eta(x,t) = y_t(x,t) - y_x(x,t), \tag{3.10}$$

which transform second order wave PDE (3.3) into two first order equations:

$$\xi_t(x,t) = \xi_x(x,t) + \sum_{i=1}^{n} g_i \sin(\omega_i t + \phi_i), \tag{3.11}$$

$$\eta_t(x,t) = -\eta_x(x,t) + \sum_{i=1}^{n} g_i \sin(\omega_i t + \phi_i). \tag{3.12}$$

Using the Laplace transform method solve equations (3.11) and (3.12), and re-express both $\xi(x,t)$ and $\eta(x,t)$ as

$$\xi(x,t) = \xi(1, t+x-1) + \nu_{\xi_1}(x,t), \tag{3.13}$$

$$\eta(x,t) = \eta(0, t-x) + \nu_{\eta_0}(x,t), \tag{3.14}$$

where

$$\begin{aligned}\nu_{\xi_1}(x,t) = \sum_{i=1}^{n} &\alpha_i^c \big(\cos(\omega_i(t+x-1)) - \cos(\omega_i t)\big) \\ &- \alpha_i^s \big(\sin(\omega_i(t+x-1)) - \sin(\omega_i t)\big),\end{aligned} \tag{3.15}$$

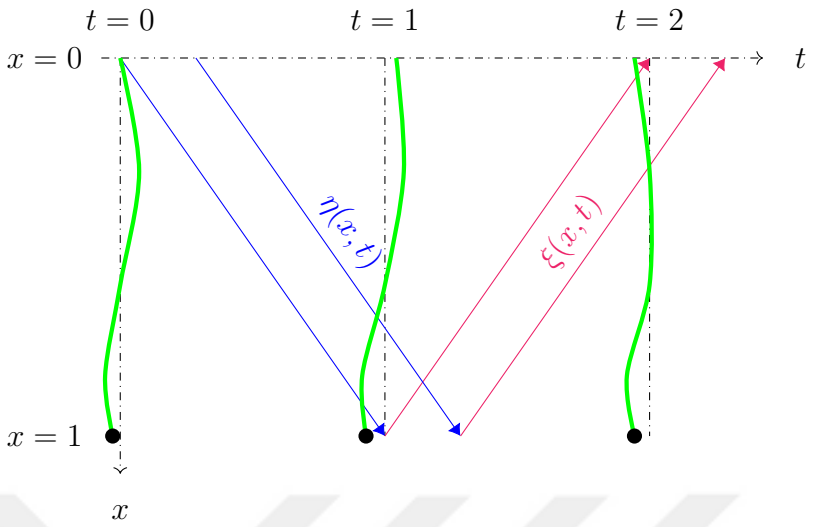

Figure 3.1. Signal flow for Riemann variables $\xi(x,t)$ and $\eta(x,t)$.

and

$$\begin{aligned}\nu_{\eta_0}(x,t) = \sum_{i=1}^{n} &\alpha_i^c\big(\cos(\omega_i(t-x)) - \cos(\omega_i t)\big) \\ &- \alpha_i^s\big(\sin(\omega_i(t-x)) - \sin(\omega_i t)\big),\end{aligned} \tag{3.16}$$

with $\alpha_i^c = \frac{g_i\cos(\phi_i)}{\omega_i}$ and $\alpha_i^s = \frac{g_i\sin(\phi_i)}{\omega_i}$. The signal flow for equations (3.13)–(3.14) is portrayed in Figure 3.1. Evaluating (3.14) at $x = 1$ and with the help of definition (3.10) gives

$$y_x(1,t) = y_t(1,t) - y_t(0,t-1) + y_x(0,t-1) - \nu_{\eta_0}(1,t). \tag{3.17}$$

The boundary condition (3.5) can then be re-expressed, using (3.17), as follows

$$y_{tt}(1,t) = ay_t(1,t) + b\big(u(t-1) - y_x(0,t-1)\big) + \nu(t), \tag{3.18}$$

where

$$\nu(t) = \sum_{i=1}^{n} d_i\sin(\omega_i t + \Psi_i), \tag{3.19}$$

for

$$d_i = \sqrt{h_i^2 + \Big(\frac{2\frac{L_o\rho}{m}g_i\sin(\frac{\omega_i}{2})}{\omega_i}\Big)^2 - \frac{4\frac{L_o\rho}{m}g_ih_i\cos(\phi_i - \varphi_i + \frac{\omega_i}{2})\sin(\frac{\omega_i}{2})}{\omega_i}}, \tag{3.20}$$

$$\Psi_i = \arctan\Big(-\frac{\frac{L_o\rho}{m}g_i\big(\cos(\phi_i+\omega_i) - \cos(\phi_i)\big) - h_i\omega_i\sin(\varphi_i)}{\frac{L_o\rho}{m}g_i\big(\sin(\phi_i+\omega_i) - \sin(\phi_i)\big) + h_i\omega_i\cos(\varphi_i)}\Big). \tag{3.21}$$

The disturbance $\nu(t)$ is the combination of ν_{η_0}(1,t) and $P(t)$. Since both disturbances are defined by the same frequencies, these can be expressed as a series of just sine terms with amplitudes d_i and phases Ψ_i as in (3.19). Please note that the original BC now takes the form of a LTI system (3.18) characterized by two uncertain parameters a and b, a delayed input $u(t-1)$, and an unknown disturbance $\nu(t)$. States $y_t(1,t)$ and $y_x(0,t)$ are both measured and available for feedback. In the next section, observer for the unknown disturbance will be developed and parametrized.

3.4. Disturbance Parametrization and Estimation

Since the disturbance in (3.19) is not known, it needs to be parametrized and phrased in a form suitable for further observer design. Following Nikiforov (2004), the disturbance is then expressed as an output of an unknown LTI exo-system

$$\dot{\mathbf{w}}(t) = \mathbf{S}\mathbf{w}(t), \tag{3.22}$$

$$\nu(t) = \mathbf{h}^T\mathbf{w}(t), \tag{3.23}$$

where $\mathbf{h} \in \mathbb{R}^{2n}$, $\mathbf{S} \in \mathbb{R}^{2n\times 2n}$, and $\mathbf{w}(t) \in \mathbb{R}^{2n}$. By definition, $(\mathbf{h}^T, \mathbf{S})$ is an observable pair. Now, let $\mathbf{G} \in \mathbb{R}^{2n\times 2n}$ be a Hurwitz matrix and $(\mathbf{G}, \mathbf{l})$ be a controllable pair chosen by the designer. Since eigenvalues of matrix $\mathbf{S}$ lie on the imaginary axis, spectra of $\mathbf{G}$ and $\mathbf{S}$ are disjoint. The solution of Sylvester equation

$$\mathbf{MS} - \mathbf{GM} = \mathbf{l}\mathbf{h}^T, \tag{3.24}$$

matrix $\mathbf{M} \in \mathbb{R}^{2n\times 2n}$, is then unique and invertable, please see Nikiforov (2004). Using change of coordinates $\mathbf{z}(t) = \mathbf{M}\mathbf{w}(t)$, together with (3.22)–(3.24), the exo-system becomes

$$\dot{\mathbf{z}}(t) = \mathbf{G}\mathbf{z}(t) + \mathbf{l}\nu(t), \tag{3.25}$$

$$\nu(t) = \boldsymbol{\theta}_s^T\mathbf{z}(t), \tag{3.26}$$

where $\boldsymbol{\theta}_s^T = \mathbf{h}^T\mathbf{M}^{-1}$.

It is desired to express $\nu(t)$ in terms of delayed vector $\mathbf{z}(t-1)$ as to incorporate disturbance estimation and its rejection in the formalism of the subsequent backstep-

ping transformation. This is done with the help of the following lemma.

Lemma 3.10. Disturbance $\nu(t)$ in equation (3.26) can be re-expressed in terms of delayed vector, $\mathbf{z}(t-1)$, as follows

$$\nu(t) = \boldsymbol{\theta}_a^T \mathbf{z}(t-1), \tag{3.27}$$

where $\boldsymbol{\theta}_a^T = \mathbf{h}^T \mathbf{e}^{\mathbf{S}} \mathbf{M}^{-1}$.

Proof of Lemma 3.10. Using explicit solution of the equation (3.22), expression (3.23) is rewritten as

$$\nu(t') = \mathbf{h}^T \mathbf{e}^{\mathbf{S}t'} \mathbf{w}(0). \tag{3.28}$$

Then,

$$\nu(t'+1) = \mathbf{h}^T \mathbf{e}^{\mathbf{S}} \mathbf{M}^{-1} \mathbf{M} \mathbf{W}(t'), \tag{3.29}$$

where identity $\mathbf{M}^{-1}\mathbf{M}$ has been inserted into the expression. Using definition of $\mathbf{z}(t')$, and evaluating (3.29) at $t' = t-1$, gives (3.27). □

State $\mathbf{z}(t)$ found in expression (3.26) cannot be used since the disturbance $\nu(t)$ is not measured. An observer is designed to estimate state $\mathbf{z}(t)$. This is done with the help of the following lemma.

Lemma 3.11. The unknown disturbance $\nu(t)$ can be cast into the form

$$\nu(t) = \boldsymbol{\theta}_a^T \boldsymbol{\tau}(t-1) + \boldsymbol{\beta}_a^T \boldsymbol{\rho}_a(t-1) + \boldsymbol{\beta}_b^T \boldsymbol{\rho}_b(t-1) + \boldsymbol{\beta}_\delta^T \boldsymbol{\delta}(t), \tag{3.30}$$

where $\boldsymbol{\beta}_a^T = a\boldsymbol{\theta}_a^T$, $\boldsymbol{\beta}_b^T = b\boldsymbol{\theta}_a^T$, and $\boldsymbol{\beta}_\delta^T = \boldsymbol{\theta}_a^T \mathbf{e}^{-\mathbf{G}}$ for $\boldsymbol{\theta}_a^T = \mathbf{h}^T \mathbf{e}^{\mathbf{S}} \mathbf{M}^{-1}$. Furthermore, the observer filters are given as

$$\boldsymbol{\tau}(t) = \boldsymbol{\rho}(t) + \mathbf{l} y_t(1,t), \tag{3.31}$$

$$\dot{\boldsymbol{\rho}}(t) = \mathbf{G}\boldsymbol{\tau}(t), \tag{3.32}$$

$$\dot{\boldsymbol{\rho}}_a(t) = \mathbf{G}\boldsymbol{\rho}_a(t) - \mathbf{l} y_t(1,t), \tag{3.33}$$

$$\dot{\boldsymbol{\rho}}_b(t) = \mathbf{G}\boldsymbol{\rho}_b(t) - \mathbf{l} U(t-1), \tag{3.34}$$

where

$$U(t) = u(t) - y_x(0,t), \tag{3.35}$$

and $y_t(1,t)$ act as the filter inputs. Finally, the estimation error, $\boldsymbol{\delta} \in \mathbb{R}^{2n}$, obeys the following dynamics

$$\dot{\boldsymbol{\delta}}(t) = \mathbf{G}\boldsymbol{\delta}(t). \tag{3.36}$$

Proof of Lemma 3.11. Define the estimation error as

$$\boldsymbol{\delta}(t) = \mathbf{z}(t) - \boldsymbol{\tau}(t) - a\boldsymbol{\rho}_a(t) - b\boldsymbol{\rho}_b(t). \tag{3.37}$$

The dynamics (3.36) is obtained by taking the time derivative of $\boldsymbol{\delta}(t)$ in the above expression and by considering (3.18), (3.25), and (3.31)–(3.34). By evaluating (3.37) for $\mathbf{z}(t-1)$ and inserting it into (3.27) one concludes (3.30). □

Finally, using (3.30) and (3.35) the LTI system (3.18), and thus boundary condition (3.5), becomes

$$\begin{aligned} y_{tt}(1,t) = {} & a y_t(1,t) + bU(t-1) \\ & + \boldsymbol{\theta}_a^T \boldsymbol{\tau}(t-1) + \boldsymbol{\beta}_a^T \boldsymbol{\rho}_a(t-1) + \boldsymbol{\beta}_b^T \boldsymbol{\rho}_b(t-1) + \boldsymbol{\beta}_{\boldsymbol{\delta}}^T \boldsymbol{\delta}(t). \end{aligned} \tag{3.38}$$

Consider (3.4), (3.10), and (3.35). It can then be written $\eta(0,t) = U(t)$. Signal η carries signal U down the string toward the bottom boundary where it acts as an delayed input in (3.38). Please also see Figure 3.1.

The unknown disturbance $\nu(t)$ has been parametrized and expressed as a product of an unknown but constant parameter vectors, $\boldsymbol{\theta}_a$, $\boldsymbol{\beta}_a$, and $\boldsymbol{\beta}_b$, with know, time delayed regressors, $\boldsymbol{\tau}(t-1)$, $\boldsymbol{\rho}_a(t-1)$, and $\boldsymbol{\rho}_b(t-1)$, plus an exponentially decaying error term.

Remark 3.12. The implementation of the update laws, to be considered later, requires evaluation of bounds on parameter vector $\boldsymbol{\theta}_a$. This is done as follows. The parametric solution of the Sylvester equation (3.24) gives matrix $\mathbf{M} = \mathbf{M}(\omega_1, ..., \omega_{2n})$. Vector $\boldsymbol{\theta}_a^T = \big(\theta_1(\omega_1, ..., \omega_n), ..., \theta_{2n}(\omega_1, ..., \omega_n)\big)$ is obtained by evaluating expression $\boldsymbol{\theta}_a^T = \mathbf{h}^T \mathbf{e}^{\mathbf{S}} \mathbf{M}^{-1}$. Separate bounds on each element θ_j, designated $[\underline{\theta_j} \bar{\theta_j}]$ for $j = 1, ..., 2n$, are then determined by finding its extrema considering known frequency bounds, $\omega_i \in [\underline{\omega}_i, \bar{\omega}_i]$ for $i = 1, ..., n$, as per Assumption 3.6. Furthermore, bounds on the unknown signal $\mathbf{z}(t)$ can be shown using its definition, $\mathbf{z}(t) = \mathbf{M}\mathbf{w}(t)$, as follows

$$|\mathbf{z}(t)|^2 < \bar{\mathbf{z}}^T \bar{\mathbf{z}} = \max\{\mathbf{w}^T \mathbf{w}\} \max_{\lambda | \omega \in [\underline{\omega}, \bar{\omega}]} \{\mathbf{M}^T \mathbf{M}\}. \tag{3.39}$$

Here, λ stands for eigenvalue and expression $\max\{\mathbf{w}^T\mathbf{w}\}$ can be bounded using known bounds on parameters g_i, h_i, and ω_i, for $i = 1, ..., n$, as per Assumption 3.6 and Assumption 3.7.

Next, the LTI system (3.38) will be transformed into a target system, a system with beneficial control properties.

3.5. Backstepping Transformation

The aim of this section is to transform the LTI system into the target system, a system to be used in the stability analysis. This is done by performing a form of Volterra transformation, or the backstepping transformation. In doing so, approach found in Krstic and Smyshlyaev (2008a) is adopted. Before proceeding however, one needs to prepare the LTI system (3.38) by re-expressing all delayed variables. Transport PDE representation in line with reference Krstic (2009b) is used. For that purpose, a first order hyperbolic PDE together with a separate boundary condition is used for each of the delayed variables

$$\Gamma_z(z,t) = \Gamma_t(z,t), \tag{3.40}$$

$$\Gamma(1,t) = U(t), \tag{3.41}$$

$$\boldsymbol{\gamma}_z^{\tau}(z,t) = \boldsymbol{\gamma}_t^{\tau}(z,t), \tag{3.42}$$

$$\boldsymbol{\gamma}^{\tau}(1,t) = \boldsymbol{\tau}(t), \tag{3.43}$$

$$\boldsymbol{\gamma}_z^{\rho_a}(z,t) = \boldsymbol{\gamma}_t^{\rho_a}(z,t), \tag{3.44}$$

$$\boldsymbol{\gamma}^{\rho_a}(1,t) = \boldsymbol{\rho}_a(t), \tag{3.45}$$

$$\boldsymbol{\gamma}_z^{\rho_b}(z,t) = \boldsymbol{\gamma}_t^{\rho_b}(z,t), \tag{3.46}$$

$$\boldsymbol{\gamma}^{\rho_b}(1,t) = \boldsymbol{\rho}_b(t), \tag{3.47}$$

with explicit solutions given as

$$\Gamma(z,t) = U(t+z-1), \tag{3.48}$$

$$\boldsymbol{\gamma}^{\tau}(z,t) = \boldsymbol{\tau}(t+z-1), \tag{3.49}$$

$$\boldsymbol{\gamma}^{\rho_a}(z,t) = \boldsymbol{\rho}_a(t+z-1), \tag{3.50}$$

$$\boldsymbol{\gamma}^{\rho_b}(z,t) = \boldsymbol{\rho}_b(t+z-1), \tag{3.51}$$

and for $z \in [0,1]$. Please note the difference between scalar domain variable z and vector $\mathbf{z}$ which is the unknown regressor for the parametrized disturbance as found in (3.27). Using (3.48)–(3.51), the LTI system (3.38) is then written as

$$\begin{aligned} y_{tt}(1,t) = {} & a y_t(1,t) + b\Gamma(0,t) \\ & + \boldsymbol{\theta}_a^T \boldsymbol{\gamma}^{\tau}(0,t) + \boldsymbol{\beta}_a^T \boldsymbol{\gamma}^{\rho_a}(0,t) + \boldsymbol{\beta}_b^T \boldsymbol{\gamma}^{\rho_b}(0,t) + \boldsymbol{\beta}_{\boldsymbol{\delta}}^T \boldsymbol{\delta}(t). \end{aligned} \tag{3.52}$$

Now, define the backstepping transformation as

$$\begin{aligned} W(z,t) = {} & \hat{b}\Gamma(z,t) + \hat{\boldsymbol{\theta}}_a^T \boldsymbol{\gamma}^{\tau}(z,t) + \hat{\boldsymbol{\beta}}_a^T \boldsymbol{\gamma}^{\rho_a}(z,t) + \hat{\boldsymbol{\beta}}_b^T \boldsymbol{\gamma}^{\rho_b}(z,t) - (k-\hat{a}) e^{\hat{a}z} y_t(1,t) \\ & - (k-\hat{a}) \int_0^z e^{\hat{a}(z-\zeta)} \Big(\hat{b}\Gamma(\zeta,t) + \hat{\boldsymbol{\theta}}_a^T \boldsymbol{\gamma}^{\tau}(\zeta,t) \\ & \qquad + \hat{\boldsymbol{\beta}}_a^T \boldsymbol{\gamma}^{\rho_a}(\zeta,t) + \hat{\boldsymbol{\beta}}_b^T \boldsymbol{\gamma}^{\rho_b}(\zeta,t) \Big) d\zeta, \end{aligned} \tag{3.53}$$

where $k \in \mathbb{R}$ is the control gain, and where parameter estimation variables, designated by the hat notation $\hat{a} = a - \tilde{a}$, $\hat{b} = b - \tilde{b}$, $\hat{\boldsymbol{\theta}}_a^T = \boldsymbol{\theta}_a^T - \tilde{\boldsymbol{\theta}}_a^T$, $\hat{\boldsymbol{\beta}}_a^T = \boldsymbol{\beta}_a^T - \tilde{\boldsymbol{\beta}}_a^T$, and $\hat{\boldsymbol{\beta}}_b^T = \boldsymbol{\beta}_b^T - \tilde{\boldsymbol{\beta}}_b^T$, are used. Tilde parameters designate error between estimate and the true value. Time dependence of all tilde and hat parameters is assumed without stating it explicitly.

Lower-triangularity of the Volterra operator, see Krstic (2009b), ensures existence of the transformation from $W(z,t)$ to $\Gamma(z,t)$

$$\begin{aligned} \Gamma(z,t) = {} & \frac{1}{\hat{b}} \Big(W(z,t) - \hat{\boldsymbol{\theta}}_a^T \boldsymbol{\gamma}^{\tau}(z,t) - \hat{\boldsymbol{\beta}}_a^T \boldsymbol{\gamma}^{\rho_a}(z,t) - \hat{\boldsymbol{\beta}}_b^T \boldsymbol{\gamma}^{\rho_b}(z,t) \\ & + (k-\hat{a}) e^{kz} y_t(1,t) + (k-\hat{a}) \int_0^z e^{k(z-\zeta)} W(\zeta,t) d\zeta \Big). \end{aligned} \tag{3.54}$$

Remark 3.13. It may not be clear to the reader how the transformation (3.54) is obtained. For the detailed procedure please see Appendix B.

Evaluate (3.54) at $z = 0$ and re-express (3.52) as

$$\begin{aligned} y_{tt}(1,t) = {} & k y_t(1,t) + \tilde{a} y_t(1,t) + \tilde{\boldsymbol{\theta}}_a^T \boldsymbol{\gamma}^{\tau}(0,t) + \tilde{\boldsymbol{\beta}}_a^T \boldsymbol{\gamma}^{\rho_a}(0,t) + \tilde{\boldsymbol{\beta}}_b^T \boldsymbol{\gamma}^{\rho_b}(0,t) \\ & + \frac{\tilde{b}}{\hat{b}} \Big(W(0,t) + (k-\hat{a}) y_t(1,t) \\ & \qquad - \hat{\boldsymbol{\theta}}_a^T \boldsymbol{\gamma}^{\tau}(0,t) - \hat{\boldsymbol{\beta}}_a^T \boldsymbol{\gamma}^{\rho_a}(0,t) - \hat{\boldsymbol{\beta}}_b^T \boldsymbol{\gamma}^{\rho_b}(0,t) \Big) + W(0,t) + \boldsymbol{\beta}_{\boldsymbol{\delta}}^T \boldsymbol{\delta}(t). \end{aligned} \tag{3.55}$$

Expression (3.55), together with PDE governing dynamics of $W(z,t)$ and the boundary condition $W(1,t)$ given as

$$\begin{aligned} W_t(z,t) = & W_z(z,t) + \tilde{a} g_a(z,t) + \tilde{b} g_b(z,t) + \dot{\hat{a}} p_a(z,t) + \dot{\hat{b}} p_b(z,t) \\ & + \tilde{\boldsymbol{\theta}}_a^T \mathbf{g}_\theta(z,t) + \tilde{\boldsymbol{\beta}}_a^T \mathbf{g}_a(z,t) + \tilde{\boldsymbol{\beta}}_b^T \mathbf{g}_b(z,t) + \boldsymbol{\beta}_{\boldsymbol{\delta}}^T \mathbf{g}_\delta(z,t) \\ & + \dot{\hat{\boldsymbol{\theta}}}_a^T \mathbf{p}_\theta(z,t) + \dot{\hat{\boldsymbol{\beta}}}_a^T \mathbf{p}_a(z,t) + \dot{\hat{\boldsymbol{\beta}}}_b^T \mathbf{p}_b(z,t), \end{aligned} \tag{3.56}$$

$$W(1,t) = 0, \tag{3.57}$$

where

$$g_a(z,t) = -(k-\hat{a}) e^{\hat{a}z} y_t(1,t), \tag{3.58}$$

$$\begin{aligned} g_b(z,t) = & -\frac{(k-\hat{a})}{\hat{b}} e^{\hat{a}z} \Big(W(0,t) + (k-\hat{a}) y_t(1,t) \\ & - \hat{\boldsymbol{\theta}}_a^T \boldsymbol{\gamma}^\tau(0,t) - \hat{\boldsymbol{\beta}}_a^T \boldsymbol{\gamma}^{\rho_a}(0,t) - \hat{\boldsymbol{\beta}}_b^T \boldsymbol{\gamma}^{\rho_b}(0,t) \Big), \end{aligned} \tag{3.59}$$

$$\begin{aligned} p_a(z,t) = & \Big(1 - (k-\hat{a})\Big) e^{\hat{a}z} y_t(1,t) + \int_0^z e^{\hat{a}(z-\zeta)} \Big(1 - (k-\hat{a})(z-\zeta)\Big) \\ & \cdot \Big(W(\zeta,t) + (k-\hat{a}) e^{k\zeta} y_t(1,t) + (k-\hat{a}) \int_0^\zeta e^{k(\zeta-\sigma)} W(\sigma,t) d\sigma \Big) d\zeta, \end{aligned} \tag{3.60}$$

$$\begin{aligned} p_b(z,t) = & \frac{1}{\hat{b}} \Big(W(z,t) - \hat{\boldsymbol{\theta}}_a^T \boldsymbol{\gamma}^\tau(z,t) - \hat{\boldsymbol{\beta}}_a^T \boldsymbol{\gamma}^{\rho_a}(z,t) - \hat{\boldsymbol{\beta}}_b^T \boldsymbol{\gamma}^{\rho_b}(z,t) \\ & + (k-\hat{a}) e^{kz} y_t(1,t) + (k-\hat{a}) \int_0^z e^{k(z-\zeta)} W(\zeta,t) d\zeta \Big) \\ & - \frac{(k-\hat{a})}{\hat{b}} \int_0^z e^{\hat{a}(z-\zeta)} \Big(W(\zeta,t) - \hat{\boldsymbol{\theta}}_a^T \boldsymbol{\gamma}^\tau(\zeta,t) - \hat{\boldsymbol{\beta}}_a^T \boldsymbol{\gamma}^{\rho_a}(\zeta,t) \\ & - \hat{\boldsymbol{\beta}}_b^T \boldsymbol{\gamma}^{\rho_b}(\zeta,t) + (k-\hat{a}) e^{k\zeta} y_t(1,t) \\ & + (k-\hat{a}) \int_0^\zeta e^{k(\zeta-\sigma)} W(\sigma,t) d\sigma \Big) d\zeta, \end{aligned} \tag{3.61}$$

$$\mathbf{g}_\theta(z,t) = -(k-\hat{a}) e^{\hat{a}z} \boldsymbol{\gamma}^\tau(0,t), \tag{3.62}$$

$$\mathbf{g}_a(z,t) = -(k-\hat{a}) e^{\hat{a}z} \boldsymbol{\gamma}^{\rho_a}(0,t), \tag{3.63}$$

$$\mathbf{g}_b(z,t) = -(k-\hat{a}) e^{\hat{a}z} \boldsymbol{\gamma}^{\rho_b}(0,t), \tag{3.64}$$

$$\mathbf{g}_\delta(z,t) = -(k-\hat{a}) e^{\hat{a}z} \boldsymbol{\delta}(t), \tag{3.65}$$

$$\mathbf{p}_\theta(z,t) = \boldsymbol{\gamma}^\tau(z,t) - (k-\hat{a}) \int_0^z e^{\hat{a}(z-\zeta)} \boldsymbol{\gamma}^\tau(\zeta,t) d\zeta, \tag{3.66}$$

$$\mathbf{p}_a(z,t) = \boldsymbol{\gamma}^{\rho_a}(z,t) - (k-\hat{a}) \int_0^z e^{\hat{a}(z-\zeta)} \boldsymbol{\gamma}^{\rho_a}(\zeta,t) d\zeta, \tag{3.67}$$

$$\mathbf{p}_b(z,t) = \boldsymbol{\gamma}^{\rho_b}(z,t) - (k-\hat{a}) \int_0^z e^{\hat{a}(z-\zeta)} \boldsymbol{\gamma}^{\rho_b}(\zeta,t) d\zeta, \tag{3.68}$$

constitute the target system. This system is characterized by beneficial stability properties, which will become apparent in the later sections. Before proving the stability of the target system, the main results, including the control law, the update laws, and the stability theorem, are presented next.

3.6. Main Results and Stability Theorem

By evaluating the backstepping transformation (3.53) at $z = 1$, and in light of expressions (3.40)-(3.51), the intermediate input (3.35), and the boundary dynamics (3.57), the controller becomes

$$\begin{aligned} u(t) = y_x(0,t) + \frac{1}{\hat{b}}\Bigg(& - \hat{\boldsymbol{\theta}}_a^T \boldsymbol{\tau}(t) - \hat{\boldsymbol{\beta}}_a^T \boldsymbol{\rho}_a(t) - \hat{\boldsymbol{\beta}}_b^T \boldsymbol{\rho}_b(t) + (k-\hat{a}) e^{\hat{a}} y_t(1,t) \\ & + (k-\hat{a}) \int_{t-1}^{t} e^{\hat{a}(t-\zeta)} \Big(\hat{b}\big(u(\zeta) - y_x(0,\zeta)\big) + \hat{\boldsymbol{\theta}}_a^T \boldsymbol{\tau}(\zeta) \\ & + \hat{\boldsymbol{\beta}}_a^T \boldsymbol{\rho}_a(\zeta) + \hat{\boldsymbol{\beta}}_b^T \boldsymbol{\rho}_b(\zeta) \Big) d\zeta \Bigg). \end{aligned} \tag{3.69}$$

The update laws for the unknown parameters are

$$\dot{\hat{a}}(t) = k_a \mathrm{Proj}_{\Pi_a}\{\tau_c(t) y_t(1,t)\}, \tag{3.70}$$

$$\dot{\hat{b}}(t) = k_b \mathrm{Proj}_{\Pi_a}\{\tau_c(t)\big(u(t-1) - y_x(0,t-1)\big)\}, \tag{3.71}$$

$$\dot{\hat{\boldsymbol{\theta}}}_a(t) = k_\theta \mathrm{Proj}_{\Pi_\theta}\{\tau_c(t) \boldsymbol{\tau}(t-1)\}, \tag{3.72}$$

$$\dot{\hat{\boldsymbol{\beta}}}_a(t) = k_{\beta_a} \mathrm{Proj}_{\Pi_{\beta_a}}\{\tau_c(t) \boldsymbol{\rho}_a(t-1)\}, \tag{3.73}$$

$$\dot{\hat{\boldsymbol{\beta}}}_b(t) = k_{\beta_b} \mathrm{Proj}_{\Pi_{\beta_b}}\{\tau_c(t) \boldsymbol{\rho}_b(t-1)\}, \tag{3.74}$$

where $k_a, k_b, k_\theta, k_{\beta_a}$, and k_{β_b} are all positive definite update gains, and

$$\tau_c(t) = \frac{1}{N(t)}\Big(\frac{p y_t(1,t)}{c_w} - (k-\hat{a}) \int_0^1 (1+z) e^{\hat{a}z} W(z,t) dz\Big), \tag{3.75}$$

where

$$\begin{aligned} N(t) = 1 + & p y_t(1,t)^2 + \boldsymbol{\rho}(t)^T \mathbf{P}_G \boldsymbol{\rho}(t) + \boldsymbol{\rho}_a(t)^T \mathbf{P}_G \boldsymbol{\rho}_a(t) \\ & + c_w \int_0^1 (1+z) W(z,t)^2 dx + c_\tau \int_0^1 (1+z) |\boldsymbol{\tau}(t+z-1)|^2 dz \\ & + c_\xi \int_0^1 e^x R(x,t)^2 dx + c_a \int_0^1 (1+z) |\boldsymbol{\rho}_a(t+z-1)|^2 dz, \end{aligned} \tag{3.76}$$

$$
\begin{aligned}
R(x,t) = 2y_t(1,t+x-1) - \frac{k-\hat{a}(t+x-2)}{\hat{b}(t+x-2)} \\
\cdot \Big(e^{\hat{a}(t+x-2)} y_t(1,t+x-2) + \int_{t+x-3}^{t+x-2} e^{\hat{a}(t+x-2)(t+x-2-\zeta)} \\
\cdot \Big(\hat{\boldsymbol{\theta}}_a^T(t+x-2)\boldsymbol{\tau}(\zeta) + \hat{\boldsymbol{\beta}}_a^T(t+x-2)\boldsymbol{\rho}_a(\zeta) \\
+ \hat{\boldsymbol{\beta}}_b^T(t+x-2)\boldsymbol{\rho}_b(\zeta) \\
+ \hat{b}(t+x-2)\big(u(\zeta) - y_x(0,\zeta)\big)\Big) d\zeta \Big) \\
- \Big(\frac{\hat{\boldsymbol{\theta}}_a^T(t+x-1)}{\hat{b}(t+x-1)} - \frac{\hat{\boldsymbol{\theta}}_a^T(t+x-2)}{\hat{b}(t+x-2)} \Big) \boldsymbol{\tau}(t+x-2) \\
- \Big(\frac{\hat{\boldsymbol{\beta}}_a^T(t+x-1)}{\hat{b}(t+x-1)} - \frac{\hat{\boldsymbol{\beta}}_a^T(t+x-2)}{\hat{b}(t+x-2)} \Big) \boldsymbol{\rho}_a(t+x-2) \\
- \Big(\frac{\hat{\boldsymbol{\beta}}_b^T(t+x-1)}{\hat{b}(t+x-1)} - \frac{\hat{\boldsymbol{\beta}}_b^T(t+x-2)}{\hat{b}(t+x-2)} \Big) \boldsymbol{\rho}_b(t+x-2),
\end{aligned}
\tag{3.77}
$$

for positive definite scalars c_a, c_w, c_τ, and c_ξ. Here, as an exception to the rule, the parameter estimation variables are explicitly evaluated at a particular time. For example, $\hat{a}(t+x-2)$ stands for $\hat{a}$ evaluated at time $(t+x-2)$. Furthermore, positive scalar p and positive definite matrix $\mathbf{P}_G$ are the solutions to the Lyapunov equations

$$2pk = -q, \tag{3.78}$$

$$\mathbf{G}^T\mathbf{P}_G + \mathbf{P}_G\mathbf{G} = -\mathbf{Q}_G, \tag{3.79}$$

where scalar $q > 0$, and positive definite matrix $\mathbf{Q}_G$, or rather minimum eigenvalues, $\min_\lambda\{\mathbf{Q}_G\}$, are to be determined from the stability analysis. The generic projection operator used in the update laws is

$$\text{Proj}_{\Pi_\kappa}\{f_\kappa\tau_c(t)\} = \begin{cases} 0 & \text{if } \hat{\kappa} = \bar{\kappa} \text{ and } f_\kappa\tau_c(t) > 0 \\ 0 & \text{if } \hat{\kappa} = \underline{\kappa} \text{ and } f_\kappa\tau_c(t) < 0 \\ f_\kappa\tau_c(t) & \text{if else} \end{cases} \tag{3.80}$$

for $f_\kappa = y_t(1,t), u(t-1) - y_x(0,t-1), \boldsymbol{\tau}(t-1), \boldsymbol{\rho}_a(t-1), \boldsymbol{\rho}_b(t-1)$, and where $\hat{\kappa}$ stands for estimate of $a, b, \boldsymbol{\theta}_a, \boldsymbol{\beta}_a$ or $\boldsymbol{\beta}_b$ with $\bar{\kappa}$ and $\underline{\kappa}$ representing maxima and minima bounds as per

$$\Pi_a = \{a \in \mathbb{R} | \bar{a} > a > \underline{a}\}, \tag{3.81}$$

$$\Pi_b = \{b \in \mathbb{R} | \bar{b} > b > \underline{b}, \bar{b} \text{ and } \underline{b} \neq 0, \text{sign}(\bar{b}) = \text{sign}(\underline{b})\}, \tag{3.82}$$

$$\Pi_{\theta_a} = \{\boldsymbol{\theta}_a = [\theta_{a_1}...\theta_{a_{2n}}]^T \in \mathbb{R}^{2n} | \bar{\theta}_{a_i} > \theta_{a_i} > \underline{\theta}_{a_i}, i = 1...2n\}, \tag{3.83}$$

$$\Pi_{\beta_a} = \{\boldsymbol{\beta}_a = [\beta_{a_1}...\beta_{a_{2n}}]^T \in \mathbb{R}^{2n} | \bar{\beta}_{a_i} > \beta_{a_i} > \underline{\beta}_{a_i}, i = 1...2n\}, \tag{3.84}$$

$$\Pi_{\beta_b} = \{\boldsymbol{\beta}_b = [\beta_{b_1}...\beta_{b_{2n}}]^T \in \mathbb{R}^{2n} | \bar{\beta}_{b_i} > \beta_{b_i} > \underline{\beta}_{b_i}, i = 1...2n\}. \tag{3.85}$$

The projection operator ensures that the parameter estimates remain within the bounds (3.81)–(3.85) obtained with the help of Assumption 3.6 and Assumption 3.8. Parameter vector $\boldsymbol{\theta}_a$ is bounded using procedure outlined in Section 3.4, Remark 3.12. Bounds on $\boldsymbol{\beta}_a$ and $\boldsymbol{\beta}_b$ come from definitions, $\boldsymbol{\beta}_a = a\boldsymbol{\theta}_a$ and $\boldsymbol{\beta}_b = b\boldsymbol{\theta}_a$.

Remark 3.14. It may not be clear to the reader what is the origin and purpose of variable $R(x,t)$. For more detailed overview please see Appendix C.

Now, the main stability theorem is stated.

Theorem 3.15. Consider closed-loop system comprised of (3.3)–(3.5), control law (3.69), update laws (3.70)–(3.74), and observer filters (3.31)–(3.34) under Assumptions 3.6–3.9. There exists constant $\bar{k} > 0$ such that for any update gain $k_i \in (0, \bar{k}]$ there exists positive constants Λ and $\bar{\Lambda}$ such that the following inequality holds

$$\Upsilon(t) \leq \Lambda\big(e^{\bar{\Lambda}\Upsilon(0)} - 1\big), \quad \forall t > 0, \tag{3.86}$$

where

$$\begin{aligned}\Upsilon(t) = {} & y_t(1,t)^2 + \boldsymbol{\tau}(t)^T\boldsymbol{\tau}(t) + \boldsymbol{\rho}_a(t)^T\boldsymbol{\rho}_a(t) + \tilde{a}(t)^2 + \tilde{b}(t)^2 \\ & + \tilde{\boldsymbol{\theta}}_a(t)^T\tilde{\boldsymbol{\theta}}_a(t) + \tilde{\boldsymbol{\beta}}_a(t)^T\tilde{\boldsymbol{\beta}}_a(t) + \tilde{\boldsymbol{\beta}}_b(t)^T\tilde{\boldsymbol{\beta}}_b(t) + \boldsymbol{\delta}(t)^T\boldsymbol{\delta}(t) \\ & + \int_0^1 \Big(\Big(\hat{\boldsymbol{\beta}}_b(t)^T\boldsymbol{\rho}_b(t+x-1) + \hat{b}\big(u(0,t+x-1) - y_x(0,t+x-1)\big)\Big)^2 \\ & \qquad + |\boldsymbol{\tau}(t+x-1)|^2 + |\boldsymbol{\rho_a}(t+x-1)|^2 + R(x,t)^2 \Big) dx.\end{aligned} \tag{3.87}$$

I.e., the equilibrium of the closed-loop system is stable in the sense of the norm $\Upsilon(t)^{\frac{1}{2}}$. Furthermore,

$$\lim_{t\to\infty} y_t(1,t) = 0, \tag{3.88}$$

$$\lim_{t\to\infty} \Big(\hat{b}(t)\big(u(t) - y_x(0,t)\big) + \hat{\boldsymbol{\beta}}_b(t)^T\boldsymbol{\rho}_b(t)\Big) = 0. \tag{3.89}$$

Remark 3.16. Observe that the closed loop system and Theorem 3.15 call for prior states, states evaluated at $t < 0$. In general, these states are not available. Once these

states become accessible the system achieves closed loop stability as per Theorem 3.15.

3.7. Stability Proof

Before proof of Theorem 3.15 is given, an important inequality required for the proof is first established. The following lemma provides the necessary result.

Lemma 3.17. There exists a suitably large constant $\bar{M} > 0$ such that the following inequality holds

$$\begin{aligned} &2c_w \int_0^1 (1+z)W(z,t)\Big(\dot{\hat{a}}p_a(z,t) + \dot{\hat{b}}p_b(z,t) \\ &\qquad + \dot{\hat{\boldsymbol{\theta}}}_a^T \mathbf{p}_\theta(z,t) + \dot{\hat{\boldsymbol{\beta}}}_a^T \mathbf{p}_a(z,t) + \dot{\hat{\boldsymbol{\beta}}}_b^T \mathbf{p}_b(z,t)\Big)dz \\ &\leq 5c_w \bar{k}\bar{M}\Big(y_t(1,t)^2 + \boldsymbol{\gamma}^\tau(0,t)^T\boldsymbol{\gamma}^\tau(0,t) + ||\boldsymbol{\gamma}^\tau(t)||^2 + \boldsymbol{\delta}(t)^T\boldsymbol{\delta}(t) \\ &\qquad + \boldsymbol{\gamma}^{\rho_a}(0,t)^T\boldsymbol{\gamma}^{\rho_a}(0,t) + ||\boldsymbol{\gamma}^{\rho_a}(t)||^2 + ||W(t)||^2 + W(0,t)^2\Big), \end{aligned} \tag{3.90}$$

where $\bar{k} = \max\{k_a, k_b, k_\theta, k_{\beta_a}, k_{\beta_b}\}$.

Proof of Lemma 3.17. It can be shown, thru lengthy but straightforward calculations, and with the help of Young's and Cauchy-Schwarz Inequalities, together with (3.37) and (3.39), that the inequality (3.90) does indeed hold. □

Proof of Theorem 3.15. Consider the following Lyapunov-Krasovski functional

$$\begin{aligned} V(t) = &\ \ln\big(N(t)\big) + \frac{c_w}{k_a}\tilde{a}^2 + \frac{c_w}{k_b}\tilde{b}^2 \\ &+ \frac{c_w}{k_\theta}\tilde{\boldsymbol{\theta}}_a^T\tilde{\boldsymbol{\theta}}_a + \frac{c_w}{k_{\beta_a}}\tilde{\boldsymbol{\beta}}_a^T\tilde{\boldsymbol{\beta}}_a + \frac{c_w}{k_{\beta_b}}\tilde{\boldsymbol{\beta}}_b^T\tilde{\boldsymbol{\beta}}_b + c_\delta\boldsymbol{\delta}^T\mathbf{P}_G\boldsymbol{\delta} \end{aligned} \tag{3.91}$$

with $N(t)$ defined in (3.76) as per normalized Lyapunow tuning in Bresch-Pietri and Krstic (2009), and for positive constant c_δ. Using Young's and Cauchy-Schwarz' Inequalities, together with results of Lemma 3.17, the time derivative of (3.91) is then

$$\begin{aligned} \dot{V}(t) \leq \frac{1}{N(t)}\Big(&- L_x y_t(1,t)^2 - L_\rho\boldsymbol{\rho}(t)^T\boldsymbol{\rho}(t) - L_{\rho_a}\boldsymbol{\rho_a}(t)^T\boldsymbol{\rho_a}(t) - L_w||W(t)||^2 \\ &- L_{w_0}W(0,t)^2 - L_\tau\big(||\boldsymbol{\gamma}^\tau(t)||^2 + \boldsymbol{\gamma}^\tau(0,t)^T\boldsymbol{\gamma}^\tau(0,t)\big) \\ &- L_{\gamma_a}\big(||\boldsymbol{\gamma}^{\rho_a}(t)||^2 + \boldsymbol{\gamma}^{\rho_a}(0,t)^T\boldsymbol{\gamma}^{\rho_a}(0,t)\big) \\ &- L_\delta\boldsymbol{\delta}(t)^T\boldsymbol{\delta}(t) - L_r\big(||R(t)||^2 + R(0,t)^2\big)\Big), \end{aligned} \tag{3.92}$$

where

$$\begin{aligned} L_x = \; & q - \frac{p^2}{\epsilon_4} - \epsilon_1 p^2 - \epsilon_3 - \epsilon_a - 2c_\tau\big(1 + \mathbf{l}^T\mathbf{l}\big) \\ & - 5c_w\bar{k}\bar{M} - 4ec_\xi\Big(4 + \frac{a_k^2}{b_1^2}\Big), \end{aligned} \tag{3.93}$$

$$\begin{aligned} L_\rho = \; & \min_\lambda\{\mathbf{Q}_G\} - \frac{1}{\epsilon_3}\max_\lambda\big\{\mathbf{P}_G\mathbf{G}\mathbf{l}(\mathbf{G}\mathbf{l})^T\mathbf{P}_G\big\} \\ & - 2c_\tau\Big(1 + \max_\lambda\{\mathbf{l}\mathbf{l}^T\}\Big), \end{aligned} \tag{3.94}$$

$$L_{\rho_a} = \; \min_\lambda\{\mathbf{Q}_G\} - \frac{1}{\epsilon_a}\max_\lambda\{\mathbf{P}_G\mathbf{l}\mathbf{l}^T\mathbf{P}_G\} - 2c_a \tag{3.95}$$

$$L_w = \; c_w - \frac{c_w\epsilon_\delta}{\epsilon_2} - 5c_w\bar{k}\bar{M}, \tag{3.96}$$

$$L_{w_0} = \; c_w - \frac{1}{\epsilon_1} - 5c_w\bar{k}\bar{M} - \frac{2ec_\xi}{b_1^2}, \tag{3.97}$$

$$L_\tau = \; c_\tau - 5c_w\bar{k}\bar{M}, \tag{3.98}$$

$$L_{\gamma_a} = \; c_a - 5c_w\bar{k}\bar{M}, \tag{3.99}$$

$$L_\delta = \; c_\delta\min_\lambda\{\mathbf{Q}_G\} - 5c_w\bar{k}\bar{M} - (\epsilon_4 + c_w\epsilon_2)\max_\lambda\{\boldsymbol{\beta}_\delta\boldsymbol{\beta}_\delta^T\}, \tag{3.100}$$

$$L_r = \; c_\xi, \tag{3.101}$$

where $\epsilon_1, \epsilon_2, \epsilon_3, \epsilon_4$ and ϵ_a, are positive and adjustable, term weight parameters, and $\epsilon_\delta = \max_{\hat{a}\in[\underline{a},\bar{a}]}\big\{(k-\hat{a})^2\int_0^1(1+x)^2e^{2\hat{a}x}dx\big\}$. Furthermore, where $b_1 = \min\{|\underline{b}|, |\bar{b}|\}$ and $a_k = \max\{|k-\underline{a}|, |k-\bar{a}|\}$. By selecting

$$\bar{k} \le \frac{\underline{\mathrm{M}}}{5c_w\bar{M}}, \tag{3.102}$$

where

$$\begin{aligned} \underline{\mathrm{M}} = \min\Bigg\{ & q - \frac{p^2}{\epsilon_4} - \epsilon_1 p^2 - \epsilon_3 - \epsilon_a - 2c_\tau\big(1 + \mathbf{l}^T\mathbf{l}\big) - 4ec_\xi\Big(4 + \frac{a_k^2}{b_1^2}\Big), \\ & c_w - \frac{1}{\epsilon_1} - \frac{2ec_\xi}{b_1^2}, c_w - \frac{c_w\epsilon_\delta}{\epsilon_2}, c_\tau, c_a, \\ & c_\delta\min_\lambda\{\mathbf{Q}_G\} - (\epsilon_4 + c_w\epsilon_2)\max_\lambda\{\boldsymbol{\beta}_\delta\boldsymbol{\beta}_\delta^T\}\Bigg\}, \end{aligned} \tag{3.103}$$

and for $\underline{\mathrm{M}} > 0$, it can be shown that

$$V(t) \le V(0), \;\; \forall t > 0. \tag{3.104}$$

I.e., the equilibrium of the target system is stable and that all signals of (3.91) are uniformly bounded.

Before the main proof is completed, a set of signal inequalities is first derived. Using definition (3.91), and the fact that $(e^x - 1) \geq x$ for $x \geq 0$, results in

$$\begin{aligned}\tilde{a}^2 + \tilde{b}^2 + \tilde{\boldsymbol{\theta}}_a^T \tilde{\boldsymbol{\theta}}_a + \tilde{\boldsymbol{\beta}}_a^T \tilde{\boldsymbol{\beta}}_a + \tilde{\boldsymbol{\beta}}_b^T \tilde{\boldsymbol{\beta}}_b + \boldsymbol{\delta}(t)^T \boldsymbol{\delta}(t) \leq & \Big(\frac{\bar{k}}{c_w} + \frac{1}{c_\delta \min_\lambda\{\mathbf{P}_G\}} \Big) \\ & \cdot \big(e^{V(t)} - 1 \big).\end{aligned} \tag{3.105}$$

Starting form (3.91), and using $e^x \geq 1$ for $x \geq 0$, gives

$$\frac{e^{V(t)} - 1}{p} \geq y_t(1,t)^2, \tag{3.106}$$

$$\frac{e^{V(t)} - 1}{\min_\lambda\{\mathbf{P}_G\}} \geq \boldsymbol{\rho}(t)^T \boldsymbol{\rho}(t), \tag{3.107}$$

$$\frac{e^{V(t)} - 1}{\min_\lambda\{\mathbf{P}_G\}} \geq \boldsymbol{\rho_a}(t)^T \boldsymbol{\rho_a}(t), \tag{3.108}$$

$$\frac{e^{V(t)} - 1}{c_w} \geq ||W(t)||^2, \tag{3.109}$$

$$\frac{e^{V(t)} - 1}{c_\tau} \geq ||\boldsymbol{\gamma}^\tau(t)||^2, \tag{3.110}$$

$$\frac{e^{V(t)} - 1}{c_a} \geq ||\boldsymbol{\gamma}^{\rho_a}(t)||^2, \tag{3.111}$$

$$\frac{e^{V(t)} - 1}{c_\xi} \geq ||R(t)||^2. \tag{3.112}$$

The definition of a norm can be found in Appendix A, expressions (A.1) and (A.2). The upper bound on the norm $||W(t)||^2$, for sufficiently large and positive constants r_1, r_2, r_3, and r_4, can be obtained using transformation (3.53)

$$\begin{aligned}||W(t)||^2 \leq & \, r_1 y_t(1,t)^2 + r_2 ||\boldsymbol{\gamma}^\tau(t)||^2 + r_3 ||\boldsymbol{\gamma}^{\rho_a}(t)||^2 \\ & + r_4 ||\hat{\boldsymbol{\beta}}_b^T \boldsymbol{\gamma}^{\rho_b}(z,t) + \hat{b}\big(y_t(0, t+z-1) - y_x(0, t+z-1) \big)||^2.\end{aligned} \tag{3.113}$$

Using transformation (3.54), together with expressions (3.106) and (3.109)–(3.111), and for sufficiently large and positive constants r_5, r_6, r_7, and r_8, gives bounded norm as follows

$$\begin{aligned}& ||\hat{\boldsymbol{\beta}}_b^T \boldsymbol{\gamma}^{\rho_b}(z,t) + \hat{b}\big(y_t(0, t+z-1) - y_x(0, t+z-1) \big)||^2 \\ & \leq \Big(\frac{r_5}{c_w} + \frac{r_6}{c_\tau} + \frac{r_7}{c_a} + \frac{r_8}{p} \Big) \big(e^{V(t)} - 1 \big).\end{aligned} \tag{3.114}$$

The above inequalities (3.113) and (3.114) are expressed using transformation $\Gamma(x,t)$ as found in equation (3.48), using definition of the intermediate input (3.35), and the actual input (3.4).

Starting from (3.91) once more and using $\ln(1+x) \leq x$ for $x \geq -1$, together with (3.113), it can shown that for a sufficiently large and positive constants s_1, s_2, s_3, s_4, s_5, and s_6, the following inequality holds

$$\begin{aligned} V(t) \leq\ & s_1 y_t(1,t)^2 + s_2 \boldsymbol{\tau}(t)^T \boldsymbol{\tau}(t) + s_3 \boldsymbol{\rho_a}(t)^T \boldsymbol{\rho_a}(t) \\ & + s_4 ||\boldsymbol{\gamma}^{\tau}(t)||^2 + s_5 ||\boldsymbol{\gamma}^{\rho_a}(t)||^2 + e c_\xi ||R(t)||^2 + c_\delta \max_{\lambda}\{\mathbf{P}_G\} \boldsymbol{\delta}(t)^T \boldsymbol{\delta}(t) \\ & + s_6 ||\hat{\boldsymbol{\beta}}_b^T \boldsymbol{\gamma}^{\rho_b}(z,t) + \hat{b}\big(y_t(0,t+z-1) - y_x(0,t+z-1)\big)||^2 \\ & + \frac{c_w}{k_a}\tilde{a}^2 + \frac{c_w}{k_b}\tilde{b}^2 + \frac{c_w}{k_\theta}\tilde{\boldsymbol{\theta}}_a^T \tilde{\boldsymbol{\theta}}_a + \frac{c_w}{k_{\beta_a}}\tilde{\boldsymbol{\beta}}_a^T \tilde{\boldsymbol{\beta}}_a + \frac{c_w}{k_{\beta_b}}\tilde{\boldsymbol{\beta}}_b^T \tilde{\boldsymbol{\beta}}_b. \end{aligned} \tag{3.115}$$

Finally, using error equation (3.37), and for positive constants f_1, f_2 and f_3, bound on norm $||\boldsymbol{\gamma}^{\rho_b}(t)||^2$ becomes

$$||\boldsymbol{\gamma}^{\rho_b}(t)||^2 \leq f_1\big(\bar{\mathbf{z}}^T \bar{\mathbf{z}} + ||\boldsymbol{\gamma}^{\tau}(t)||^2\big) + f_2 ||\boldsymbol{\gamma}^{\rho_a}(t)||^2 + f_3 \boldsymbol{\delta}(t)^T \boldsymbol{\delta}(t). \tag{3.116}$$

Having established the above inequalities, it is now possible to conclude the proof of Theorem 3.15 by proving inequality (3.86) and the convergence of the state. Using definition (3.87), inserting expressions (3.105)–(3.108), (3.110)–(3.112), and (3.114), results in the following

$$\Upsilon(t) \leq \Lambda\big(e^{V(t)} - 1\big), \tag{3.117}$$

where

$$\Lambda = \frac{c_\delta\big(2 + \max_\lambda\{\mathbf{l}\mathbf{l}^T\}\big) + 1}{c_\delta \min_\lambda\{\mathbf{P}_G\}} + \frac{r_5 + \bar{k}}{c_w} + \frac{r_6 + 1}{c_\tau} + \frac{r_7 + 1}{c_a} + \frac{r_8 + 2 + \mathbf{l}^T\mathbf{l}}{p} + \frac{1}{c_\xi}. \tag{3.118}$$

In light of (3.87) and (3.115) one can state

$$V(t) \leq \bar{\Lambda} \Upsilon(t), \tag{3.119}$$

where

$$\bar{\Lambda} = \max\Big\{s_1, s_2, s_3, s_4, s_5, e c_\xi, c_\delta \max_\lambda\{\mathbf{P}_G\}, s_6, \frac{c_w}{k_a}, \frac{c_w}{k_b}, \frac{c_w}{k_\theta}, \frac{c_w}{k_{\beta_a}}, \frac{c_w}{k_{\beta_b}}\Big\}. \tag{3.120}$$

For $t = 0$, the expression (3.119) becomes

$$V(0) \leq \bar{\Lambda} \Upsilon(0). \tag{3.121}$$

Now, using (3.104)

$$V(t) \leq \bar{\Lambda} \Upsilon(0). \tag{3.122}$$

Inserting (3.122) into (3.117) gives (3.86).

From the Lyapunov analysis $|y_t(1,t)|, |\boldsymbol{\rho}(t)|, |\boldsymbol{\rho_a}(t)|,\ ||W(t)||, ||\boldsymbol{\gamma}^{\tau}(t)||, ||\boldsymbol{\gamma}^{\rho_a}(t)||$, $|\hat{a}(t)|, |\hat{b}(t)|, |\hat{\boldsymbol{\theta}}_a(t)|, |\hat{\boldsymbol{\beta}}_a(t)|, |\hat{\boldsymbol{\beta}}_b(t)|, |\boldsymbol{\delta}(t)|$ and $||R(t)||$ are all uniformly bounded. Boundedness of $|\boldsymbol{\rho}(t)|$ and $|y_t(0,t)|$ implies boundedness of $|\boldsymbol{\tau}(t)|$ using (3.31). Furthermore, using (3.37) and boundedness of $|\mathbf{z}(t)|$, one concludes boundedness of $|\boldsymbol{\rho}_b(t)|$. Boundedness of $||\hat{\boldsymbol{\beta}}_b^T\boldsymbol{\gamma}^{\rho_b}(t)+\hat{b}\Gamma(t)||$ and $||\boldsymbol{\gamma}^{\rho_b}(t)||$ comes from inequalities (3.114) and (3.116) respectively. Using inverse transformation (3.54), and having already established boundedness of all other variables, one states boundedness of the norm $||\Gamma(t)||$. Bounded $||\Gamma(t)||$ implies bounded control $|u(t)|$ and $|y_t(0,t)|$. Finally, bounded $|y_{tt}(1,t)|$ is obtained from equation (3.55).

Convergence of the state, $\lim_{t\to\infty} y_t(1,t) = 0$, is proven using the Barbalat's lemma, Farkas and Wegner (2016), and square integrability of $|y_t(1,t)|$ obtained from the Lyapunov analysis.

Consider square integrability of the Lyapunov variables, see (3.92). Square integrability of $\hat{b}\big(u(t) - y_x(0,t)\big) + \hat{\boldsymbol{\beta}}_b^T\boldsymbol{\rho}_b(t)$ can be obtained from (3.54) and (3.48). Now, take $\frac{d}{dt}\Big(\hat{b}\big(u(t) - y_x(0,t)\big) + \hat{\boldsymbol{\beta}}_b^T\boldsymbol{\rho}_b(t)\Big)^2$ or $\frac{d}{dt}\big(\hat{b}\Gamma(1,t) + \hat{\boldsymbol{\beta}}_b^T\boldsymbol{\rho}_b(t)\big)^2$. Use (3.54) once more, and evaluate resulting expression for $W_t(x,t)$ with the help of (3.56)-(3.68). Having already shown boundedness of all other variables, the uniform boundedness of $\frac{d}{dt}\Big(\hat{b}\big(u(t) - y_x(0,t)\big) + \hat{\boldsymbol{\beta}}_b^T\boldsymbol{\rho}_b(t)\Big)^2$ is proven. Using the Barbalat's lemma once again gives (3.89). □

The above stability is extended to the original states, $y_t(x,t)$ and $y_x(x,t)$. First, define auxiliary variable

$$\begin{aligned} T(x,t) = \nu_{\eta_0}(1,t+x-1) - \nu_{\xi_1}(x,t) \\ -\frac{1}{\hat{b}(t+x-1)}\Big(&\hat{\boldsymbol{\theta}}_a^T(t+x-1)\boldsymbol{\gamma}^{\tau}(0,t+x-1) \\ &+ \hat{\boldsymbol{\beta}}_a^T(t+x-1)\boldsymbol{\gamma}^{\rho_a}(0,t+x-1) \\ &+ \hat{\boldsymbol{\beta}}_b^T(t+x-1)\boldsymbol{\gamma}^{\rho_b}(0,t+x-1)\Big). \end{aligned} \tag{3.123}$$

Add the Riemann variable $\eta(x,t)$ on both sides of expression (C.5), and use (3.123), to state

$$R(x,t) + \eta(x,t) = \xi(x,t) + \eta(x,t) + T(x,t). \tag{3.124}$$

Using (3.10), (3.14), (3.48), (3.35), (3.4), and the fact that the relation between domain variable x and z is

$$x = 1 - z, \tag{3.125}$$

gives

$$\eta(x,t) = \Gamma(z,t) + \nu_{\eta_0}(x,t). \tag{3.126}$$

Now, adding (3.9) and (3.10) together allows re-expression of the sum of $\xi(x,t)$ and $\eta(x,t)$ in terms of $y_t(x,t)$ on the right side of (3.124). On the left hand side of (3.124) use (3.126). Re-arrange the resulting equation to get

$$R(x,t) + \Gamma(z,t) = 2y_t(x,t) + T(x,t) - \nu_{\eta_0}(x,t). \tag{3.127}$$

After squaring and integrating both sides, use definition of a norm to obtain the following inequality

$$||2y_t(x,t) + T(x,t) - \nu_{\eta_0}(x,t)||^2 \leq 2||\Gamma(t)||^2 + 2||R(t)||^2. \tag{3.128}$$

Similarly, subtract $\eta(x,t)$ on both sides of (C.5), use definition (3.123), and re-express the difference between $\xi(x,t)$ and $\eta(x,t)$ in terms of $y_x(x,t)$

$$R(x,t) - \Gamma(z,t) = 2y_t(x,t) + T(x,t) + \nu_{\eta_0}(x,t). \tag{3.129}$$

After squaring and integrating both sides, use definition of a norm to obtain the following inequality

$$||2y_x(x,t) + T(x,t) + \nu_{\eta_0}(x,t)||^2 \leq 2||\Gamma(t)||^2 + 2||R(t)||^2. \tag{3.130}$$

The boundedness of the original states, $y_x(x,t)$ and $y_t(x,t)$, is established using inequalities (3.128)–(3.130), and known boundedness of $||R(t)||$ and $||\Gamma(t)||$ obtained previously from the Lyapunov analysis.

3.8. Numerical Results

Closed loop system comprised of (3.3)–(3.5), control law (3.69), update laws (3.70)–(3.74), and observer filters (3.31)–(3.34) is simulated using explicit finite-difference method (FDM) in Matlab (R2020b). The simulation is performed with $\Delta t = 0.005$ and $\Delta x = 0.1$. By setting $L_0 = 50$, $\rho = 0.1$, $m = 50$, $g = 9.81$, and $c_m = -14$ in (3.6)–(3.7) an ODE system describing bottom boundary with $a = 0.1$ and $b = 0.1$ is obtained. Bounds on unknown parameters are assumed to be $a \in [-0.1, 0.1]$ and $b \in [0.05, 0.2]$, with estimates initiated at $\hat{a}(0) = -0.1$ and $\hat{b}(0) = 0.15$. Unknown disturbances, in-domain $p(t)$ and boundary $P(t)$, are

$$p(t) = 0.15\sin(0.3t + \pi) + 0.1\sin(1.7t + 1), \tag{3.131}$$

$$P(t) = 0.1\sin(0.3t + 1.5) + 0.07\sin(1.7t). \tag{3.132}$$

Bounds on the unknown angular frequencies are set as follows: $\omega_1 \in [0.2, 0.5]$ and $\omega_2 \in [1.5, 2]$. Initial conditions are set to $y(x,0) = 0.5x^3 - 0.75x^2$ and $y_t(x,0) = 2\sin(1.5\pi x)$. All Update gains, $k_a, k_b, k_\theta, k_{\beta_a}$, and k_{β_b}, are set to 3.4×10^{-25}, together with $c_w = 0.55$, $c_\tau = 0.1$, $c_a = 0.1$, $c_\xi = 10^{-7}$, $c_\delta = 10^8$ $q = 15.5$, $\mathbf{Q}_G = \mathbf{I}_{4x4}$ and control gain $k = -8$. Controllable pair $(\mathbf{G}, \mathbf{l})$ is as follows: $\mathbf{l} = [0,0,0,1]^T$ and $\mathbf{G} = [0,1,0,0;0,0,1,0;0,0,0,1;-3,-9.5,-11,-5.5]$ with eigenvalues of $-1,-1,-2,-1.5$. Limits on the unknown parameter vector $\boldsymbol{\theta}_a$ are calculated as per Remark 3.12:
$\theta_1 \in [-3.9941, 2.1241]$, $\theta_2 \in [9.3363, 12.0548]$, $\theta_3 \in [-9.2825, -0.4432]$, and $\theta_4 \in [3.6252, 10.3801]$. Figure 3.2 gives extrema of $\theta_1(\omega_1, \omega_2)$ for $\omega_1 \in [\underline{\omega_1}, \bar{\omega_1}]$ and $\omega_2 \in [\underline{\omega_2}, \bar{\omega_2}]$ as well as the true value located at $\omega_1 = 0.3$ and $\omega_2 = 1.7$. Figure 3.3 shows disturbance $\nu(t)$ vs. disturbance estimation defined as $\hat{\nu} = \nu(t) - \boldsymbol{\beta}_{\boldsymbol{\delta}}^T \boldsymbol{\delta}(t)$, please see expression (3.30). Figure 3.4 and Figure 3.5 illustrate the bottom boundary velocity $y_t(1,t)$ and the control input $u(t)$, respectively for: a) proposed boundary controller (3.69), b) free boundary condition $u(t) = y_x(0,t)$. The free boundary condition gives the response of the string to the initial conditions, with the top of the string free to move along the lateral direction. Lastly, Figure 3.6 gives the total string displacement $y(x,t)$ for the proposed controller.

3.9. Discussion

Adaptive boundary control using the delay control method has been successfully applied to a physical system comprised of a mass suspended from an ideal, one-dimensional string of constant length. Disturbance cancellation has been incorporated into the control problem. Unknown but bounded harmonic disturbances affecting the domain as well as the boundary have been parametrized and then canceled out in the controller through the construction of an observer. In theory, the estimation error and the state are guaranteed to converge, but in practice, it may not be possible in a timely manner. Convergence is slow due to low gain values. This can clearly be seen from Figure 3.3 where once the state approaches zero, at $t \approx 40$ in Figure 3.4, the disturbance estimation diminishes considerably and the system oscillates to the tune of the estimation error. By that time, however, the amplitude of the oscillations experienced by the bottom mass is reduced greatly. In the following chapter, the control problem will be expanded to include a domain with a moving boundary, i.e., a string whose length is no longer constant in time.

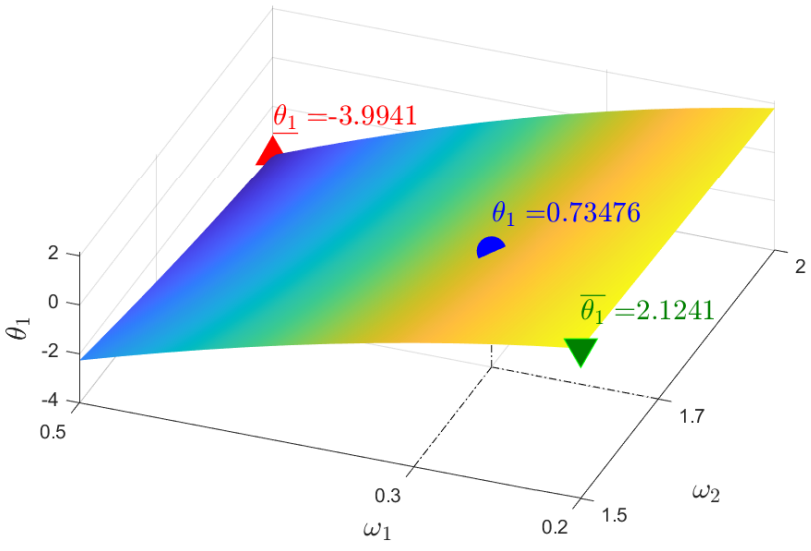

Figure 3.2. $\theta_1(\omega_1, \omega_2) \in [\underline{\theta_1}, \bar{\theta_1}]$.

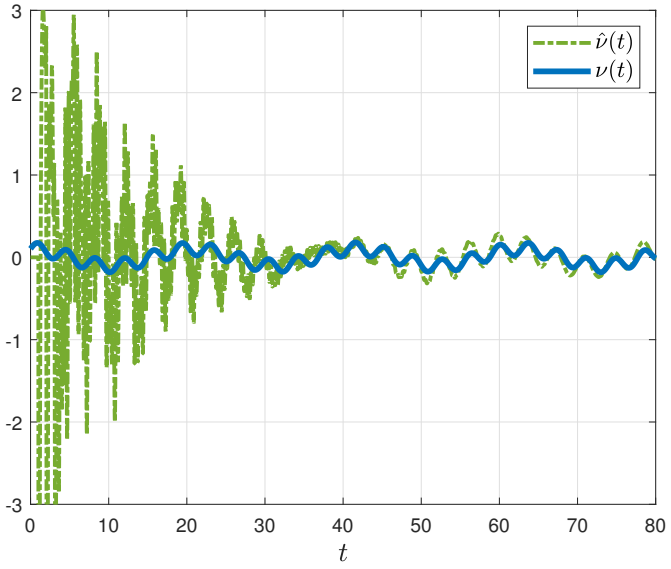

Figure 3.3. Disturbance Estimation $\hat{\nu} = \nu(t) - \boldsymbol{\beta}_{\boldsymbol{\delta}}^T \boldsymbol{\delta}(t)$ vs. Disturbance $\nu(t)$.

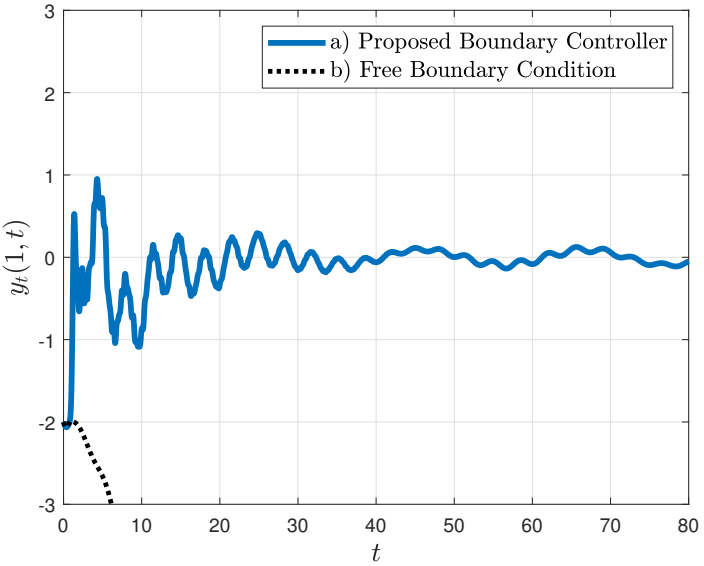

Figure 3.4. Boundary velocity $y_t(1,t)$ for: a) Proposed Boundary Controller (3.69), b) Free Boundary Condition $u(t) = y_x(0,t)$.

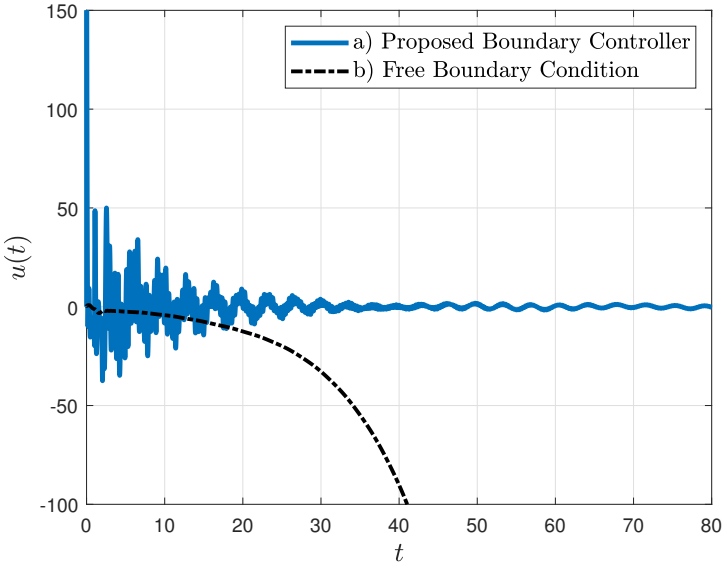

Figure 3.5. Control input $u(t)$ for: a) Proposed Boundary Controller (3.69), b) Free Boundary Condition $u(t) = y_x(0,t)$.

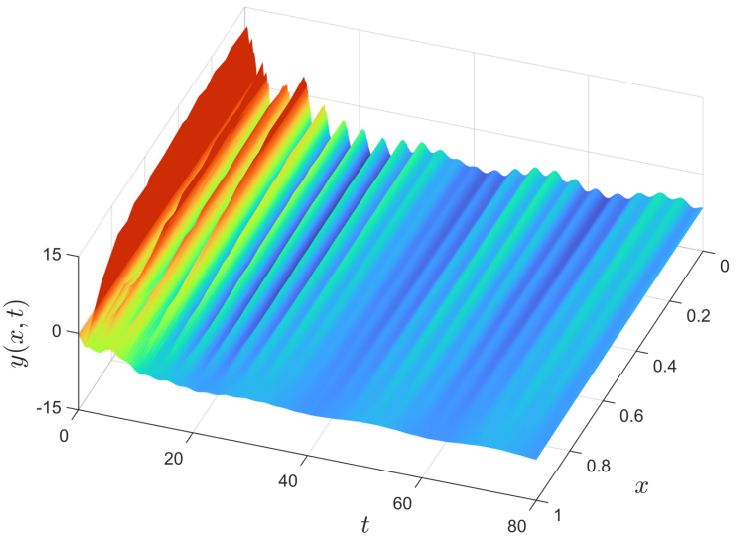

Figure 3.6. Total string displacement $y(x,t)$.

4. ADAPTIVE BOUNDARY CONTROL FOR A STRING-MASS SYSTEM WITH TIME-VARYING LENGTH HAVING CONSTANT VELOCITY [3]

4.1. Introduction

This chapter considers the second boundary control problem. The equations of motion derived in Chapter 2 will be used once again to model an ideal string-mass system with a a non-constant length. The length of the string, or the boundary of the wave PDE, will be assumed to evolve under a constant velocity profile.

4.2. Problem Statement

Consider (2.42)–(2.44). The following physical assumptions are made about the system:

Assumption 4.1. The velocity governing the length of the string is assumed to be constant, $v(t) = v$.

Assumption 4.2. There are not any in-domain damping forces affecting the string, $c_\rho = 0$.

Assumption 4.3. Tension in the string is constant and due only to the weight of the mass, $F_\tau(x,t) = mg$. This implies: $\epsilon_\tau = 0$ and $\epsilon_a = 0$.

Assumption 4.4. The string as well at the mass are not affected by any disturbances, $p(x,t) = P\big(l(t),t\big) = 0$.

Under Assumptions 4.1–4.4 system (2.42)–(2.44) reduces to

$$y_{tt}(x,t) = (1-v^2)y_{xx}(x,t) - 2vy_{tx}(x,t), \tag{4.1}$$

[3]This chapter is a modified version of Szczesiak and Basturk (2021) and has been reproduced here with the permission of the copyright holder.

$$y_t(0,t) = u(t), \tag{4.2}$$

$$\begin{aligned} y_{tt}\big(l(t),t\big) = & -v^2 y_{xx}\big(l(t),t\big) - 2v y_{xt}\big(l(t),t\big) \\ & + \frac{a(1-v)+b}{1-v} y_t\big(l(t),t\big) + (av-b) y_x\big(l(t),t\big), \end{aligned} \tag{4.3}$$

for

$$a = -\frac{\rho L_0\Big(mg(1+v) + c_m\sqrt{\frac{mg}{\rho}}\Big)}{gm^2}, \tag{4.4}$$

$$b = \frac{L_0\rho(1-v)}{m}, \tag{4.5}$$

where $t \in [0,\infty)$, $x \in [0, l(t)]$, and where

$$l(t) = 1 + \int_0^t v dt \tag{4.6}$$

is the normalized string length. Symbol $v \in \mathbb{R}$ stands for the velocity or the rate at which the boundary of the domain x is changing, and $a \in \mathbb{R}$ and $b \in \mathbb{R}$ are constant parameters defined in (4.4)–(4.5).

As in the previous chapter, the delay control methods will be employed in the analysis. Since the velocity of the string is constant, the length will continue to change as $t \to \infty$. To prevent this unrealistic case and to bound the subsequent delay, an additional constraint is placed on the velocity:

Assumption 4.5. Assume the following velocity profile

$$v = \begin{cases} v_c & 0 \le t < T \\ 0 & t \ge T, \end{cases} \tag{4.7}$$

such that the velocity $v_c \neq 0$ and $|v_c| < 1$ is known and constant. Time $T > 0$ is assumed to be known, constant, and finite. Furthermore, if velocity $v_c < 0$, then condition $T|v_c| < 1$ is required.

Under Assumption 4.5, the length of the string (4.6) becomes

$$l_c(t) = \begin{cases} 1 + v_c t & 0 \le t < T \\ 1 + v_c T & t \ge T, \end{cases} \tag{4.8}$$

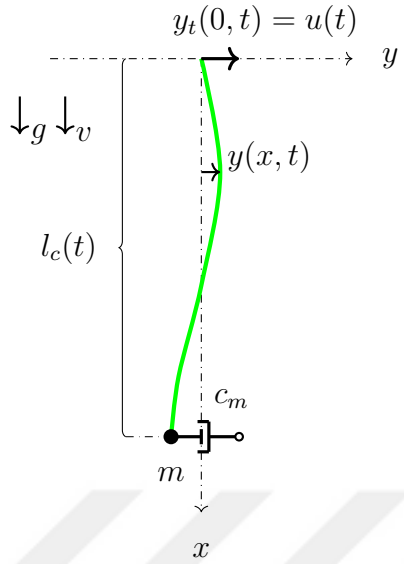

Figure 4.1. String diagram.

resulting in $x \in [0, l_c(t)]$. Condition $|v_c| < 1$ ensures the string remains under tension. In general, $|v_c| \ll 1$. Condition $T|v_c| < 1$ guarantees that the length of the string $l_c(t) > 0$, $\forall t \geq 0$. Please see Figure 4.1.

In addition, the following control assumptions are made for the system (4.1)–(4.3):

Assumption 4.6. Parameters a and b are assumed to be unknown but have known bounds $a \in [\underline{a}, \bar{a}]$ and b belongs to a set Ψ_b such that

$$\Psi_b = \left\{ b \in \mathbb{R} | \bar{b} \geq b \geq \underline{b}, \bar{b} \text{ and } \underline{b} \neq 0, \text{sign}(\bar{b}) = \text{sign}(\underline{b}) \right\}, \tag{4.9}$$

where underbar and overbar symbols indicate the minimum and the maximum bounds, respectively. Under the above definition, the parameter $b \neq 0$ is of a known sign as per Assumption 4.5 and definition (4.5).

The unknown parameters a and b represent limited knowledge of the damping coefficient c_m and/or the other physical properties of the system. Please see (4.4)–(4.5).

Assumption 4.7. Boundary states, $y_t(0,t)$, $y_x(0,t)$, and $y_t\big(l_c(t),t\big)$ are assumed to be measured. Their present values as well as their histories are available for feedback.

The aim of this chapter is to design boundary control input $u(t)$ at boundary $x = 0$, see (4.2), such that $y_t\big(l_c(t), t\big)$ is Lyapunov stable and bounded on the interval $[0, T)$. I.e., it is desired to stabilize the transverse velocity, $y_t\big(l_c(t), t\big)$, of the mass at $x = l_c(t)$ by actuating the transverse velocity, $y_t(0, t)$, of the string at the boundary $x = 0$. Furthermore, the closed-loop stability of the system (4.1)–(4.3), despite presence of an uncertain boundary dynamics, needs to be proven.

The subsequent analysis is applicable on $t \in [0, T)$. The interval $[T, \infty)$, which is not considered thereafter, corresponds to a problem where the length of the string is constant. The study of a wave PDE on a constant domain is a well-researched problem. In particular, the analysis found in Chapter 3 can be readily applied for $t \in [T, \infty)$.

4.3. Reformulation of the Problem

The outlined problem is first reformulated as a stabilization of an LTI system describing dynamics at the bottom boundary, $x = l_c(t)$. This is accomplished by following Cai and Krstic (2016) and Basturk (2017) and defining two Riemann variables as

$$\xi(x, t) = y_t(x, t) + (1 + v)y_x(x, t), \tag{4.10}$$

$$\eta(x, t) = y_t(x, t) - (1 - v)y_x(x, t), \tag{4.11}$$

which transform PDE (4.1) into a 2×2 hyperbolic system

$$\xi_t(x, t) = (1 - v)\xi_x(x, t), \tag{4.12}$$

$$\eta_t(x, t) = -(1 + v)\eta_x(x, t). \tag{4.13}$$

Solving PDEs (4.12) and (4.13) gives

$$\xi(x, t) = \xi\bigg(l_c\Big(t - \big(l_c(t) - x\big)\Big), t - \big(l_c(t) - x\big)\bigg), \tag{4.14}$$

$$\eta(x, t) = \eta\Big(0, t - \frac{x}{1 + v}\Big). \tag{4.15}$$

Solutions (4.14)–(4.15) provide a link between the in-domain states and the boundary states of the PDE system (4.1)–(4.3) as per definitions (4.10)–(4.11). Taking the spatial

derivative of equation (4.15) results in

$$\eta_x(x,t) = \eta_t\Big(0, t - \frac{x}{1+v}\Big)\Big(-\frac{1}{1+v}\Big). \tag{4.16}$$

Now, re-express $y_x\big(l_c(t),t\big)$, $y_{tx}\big(l_c(t),t\big)$, and $y_{xx}\big(l_c(t),t\big)$ in the BC (4.3) in terms of the states at the boundary $x = 0$. Begin by inserting $\eta(x,t)$ from (4.11) into (4.15). Then, evaluate the result at $x = l_c(t)$. Solving for $y_x\big(l_c(t),t\big)$ gives the first expression

$$y_x\big(l_c(t),t\big) = \frac{1}{1-v}\Big(y_t\big(l_c(t),t\big) - y_t\big(0,\phi(t)\big)\Big) + y_x\big(0,\phi(t)\big), \tag{4.17}$$

where

$$\phi(t) = t - g(t) \tag{4.18}$$

is the delay function, and where

$$g(t) = \frac{l_c(t)}{1+v} \tag{4.19}$$

is the time-varying delay. Physically, the delay $g(t)$ is the time required for the signal originating at the top of the string, $x = 0$, to reach the bottom at $x = l_c(t)$.

Continuing, use (4.13) in (4.16). Evaluate both sides of the obtained expression by substituting in the spatial derivative of the Riemann variable (4.11). Evaluate at $x = l_c(t)$, use definitions (4.18)–(4.19), and solve for $y_{tx}\big(l_c(t),t\big)$:

$$y_{tx}\big(l_c(t),t\big) = y_{tx}\big(0,\phi(t)\big) - (1-v)\Big(y_{xx}\big(0,\phi(t)\big) - y_{xx}\big(l_c(t),t\big)\Big). \tag{4.20}$$

Evaluate PDE (4.1) at $x = l_c(t)$ and solve for:

$$y_{xx}\big(l_c(t),t\big) = \frac{1}{1-v^2}\Big(y_{tt}\big(l_c(t),t\big) + 2v y_{tx}\big(l_c(t),t\big)\Big). \tag{4.21}$$

Substitute (4.21) into (4.20) and collect like wise terms to obtain the second expression

$$\begin{aligned} y_{tx}\big(l(t),t\big) = \frac{1}{1-v}\Big(&y_{tt}\big(l(t),t\big) + (1+v)y_{tx}\big(0,\phi(t)\big) \\ &- (1-v^2)y_{xx}\big(0,\phi(t)\big)\Big). \end{aligned} \tag{4.22}$$

Substitute (4.22) into (4.21) to obtain the third

$$\begin{aligned} y_{xx}\big(l_c(t),t\big) = \frac{1}{(1-v)^2}\Big(&y_{tt}\big(l_c(t),t\big) + 2v y_{tx}\big(0,\phi(t)\big) \\ &- 2v(1-v)y_{xx}\big(0,\phi(t)\big)\Big). \end{aligned} \tag{4.23}$$

The boundary condition (4.3) can now be re-expressed as an LTI system. First, insert (4.17), (4.22), and (4.23) into BC (4.3). Multiply the resulting expression by $\big(\frac{1}{1-v}\big)$ and move all second-order derivative terms to the left side to obtain the following

$$\begin{aligned}&\frac{1}{1-v}y_{tt}\big(l_c(t),t\big)+\frac{2v}{1-v}y_{tx}\big(0,\phi(t)\big)-2vy_{xx}\big(0,\phi(t)\big)\\&=a\Big(y_t\big(l_c(t),t\big)-vy_t\big(0,\phi(t)\big)-v(v-1)y_x\big(0,\phi(t)\big)\Big)\\&\quad+b\Big(y_t\big(0,\phi(t)\big)+(v-1)y_x\big(0,\phi(t)\big)\Big).\end{aligned}\tag{4.24}$$

Now, define state $X(t)\in\mathbb{R}$ as

$$X(t)=y_t\big(l_c(t),t\big)-vy_t\big(0,\phi(t)\big)-v(v-1)y_x\big(0,\phi(t)\big).\tag{4.25}$$

Taking the time derivative of $X(t)$ gives

$$\begin{aligned}\dot{X}(t)&=y_{tt}\big(l_c(t),t\big)+vy_{tx}\big(l_c(t),t\big)\\&\quad-\Big(\frac{v}{1+v}\Big)\Big(y_{tt}\big(0,\phi(t)\big)+(v-1)y_{tx}\big(0,\phi(t)\big)\Big),\end{aligned}\tag{4.26}$$

where material derivative: $\frac{D}{Dt}\big(y_t\big(l_c(t),t\big)\big)=\frac{\partial y_t(x,t)}{\partial t}|_{x=l_c(t)}+\dot{l_c}(t)\frac{\partial y_t(x,t)}{\partial x}|_{x=l_c(t)}$, together with expressions (4.7)-(4.8), is used. Using (4.22), and $y_{tt}\big(0,\phi(t)\big)$ from (4.1), in equation (4.26), it can be shown that the left hand side of (4.24) is in fact $\dot{X}(t)$. Furthermore, using definition of the state (4.25) and input (4.2) on the right hand side of (4.24) enables one to re-express (4.24), and thus BC equation (4.3), as

$$\dot{X}(t)=aX(t)+bU\big(\phi(t)\big),\tag{4.27}$$

where intermediate control input $U(t)$ is

$$U(t)=u(t)+(v-1)y_x(0,t).\tag{4.28}$$

Effects of $U(t)$ at $x=0$ show up explicitly in the boundary dynamics at $x=l_c(t)$ as a delayed input $U\big(\phi(t)\big)$. The boundary condition (4.3) is then cast into a form of an LTI system with a non-constant input delay (4.27).

Remark 4.8. Please note that under Assumption 4.5, the delay $g(t)$ given in (4.19) satisfies $g(t)>0$ and $g(t)<\infty$. The first condition guarantees that the LTI system (4.27) is causal, while the second one ensures that all input signals eventually reach the system. Furthermore, $\dot{g}(t)<1$ indicates that the direction of the input signal may never change, and the condition $\dot{g}(t)>-\infty$ guarantees that the delay may only

disappear gradually.

4.4. Backstepping Transformation

The purpose of this section is to transform an input-delayed system (4.27) into the target system, a PDE-ODE cascade characterized by desirable stability properties. This is realized by performing a backstepping transformation following approach found in Krstic and Smyshlyaev (2008a). First however, the transport PDE representation, as per Bekiaris-Liberis and Krstic (2013), is employed to re-express the input. The delayed input is modelled as a first order hyperbolic PDE with a variable propagation speed.

Begin by defining the state of the transport equation as

$$\Pi(z,t) = \eta\Big(0, \phi\Big(t + z\big(\phi^{-1}(t) - t\big)\Big)\Big), \tag{4.29}$$

for $z \in [0,1]$, and where

$$\phi^{-1}(t) = t + l_c(t) \tag{4.30}$$

is the inverse of the delay function $\phi(t)$ such that $\phi^{-1}\big(\phi(t)\big) = t$. Using expressions (4.30), (4.18)–(4.19), (4.11), (4.28), and Assumption 4.5, the definition (4.29) can be rewritten as

$$\Pi(z,t) = U\Big(\frac{t + z l_c(t) - 1}{1+v}\Big). \tag{4.31}$$

Using expression (4.31) the LTI system (4.27) can now be written without explicit delay as

$$\dot{X}(t) = aX(t) + b\Pi(0,t), \tag{4.32}$$

$$\Pi_t(z,t) = \pi(z,t)\Pi_z(z,t), \tag{4.33}$$

$$\Pi(1,t) = U(t), \tag{4.34}$$

where

$$\pi(z,t) = \frac{1 + z\Big(\frac{d}{dt}\big(\phi^{-1}(t)\big) - 1\Big)}{\phi^{-1}(t) - t} = \frac{1+vz}{l_c(t)} \tag{4.35}$$

is the propagation speed of the transport system (4.33)–(4.34). It can be easily verified that (4.29) is the solution to (4.33)–(4.34), and where from (4.31):

$$\Pi(0,t) = U\big(\phi(t)\big). \tag{4.36}$$

System (4.32)–(4.34) constitutes a PDE-ODE cascade system. The output of the transport PDE (4.33) and its boundary input (4.34) acts as a time-varying delay input (4.36) into the ODE (4.32). Following Bekiaris-Liberis and Krstic (2013) define the backstepping transformation as the mapping of the system (4.32)–(4.34) into the target system

$$W(z,t) = \hat{b}\Pi(z,t) - (k-\hat{a})\Big(e^{\hat{a}zl_c(t)}X(t) + l_c(t)\hat{b}\int_0^z e^{\hat{a}(z-\zeta)l_c(t)}\Pi(\zeta,t)d\zeta\Big), \tag{4.37}$$

where $k \in \mathbb{R}$ is the control gain. Since parameters a and b are unknown, utilize estimates defined as $\hat{a} = a - \tilde{a}$ and $\hat{b} = b - \tilde{b}$. Without stating it explicitly, assume time dependence of all tilde and hat parameters.

The inverse transformation, $\big(X, W\big) \to \big(X, \Pi\big)$, is given as

$$\Pi(z,t) = \frac{1}{\hat{b}}\bigg(W(z,t) + (k-\hat{a})\Big(e^{kzl_c(t)}X(t) + l_c(t)\int_0^z e^{k(z-\zeta)l_c(t)}W(\zeta,t)d\zeta\Big)\bigg). \tag{4.38}$$

The existence of the inverse transformation (4.38) can be verified by solving equation (4.37) for $\Pi(z,t)$. The recursive function obtained in this manner can then be expanded thru self-substitution. Using integration by parts and the definition of a power series expansion for an exponential function gives expression (4.38). For details, please see Appendix B.

Evaluating $W_z(z,t)$ and $W_t(z,t)$ using (4.37) gives us the dynamics of $W(z,t)$. This, together with (4.32), evaluated using $\Pi(0,t)$ from (4.38) gives the target system

$$\dot{X}(t) = kX(t) + \tilde{a}X(t) + W(0,t) + \frac{\tilde{b}}{\hat{b}}\Big(W(0,t) + (k-\hat{a})X(t)\Big), \tag{4.39}$$

$$W_t(z,t) = \pi(z,t)W_z(z,t) + \tilde{a}g_1(z,t) + \tilde{b}g_2(z,t) + \dot{\hat{a}}g_3(z,t) + \dot{\hat{b}}g_4(z,t), \tag{4.40}$$

$$W(1,t) = 0, \tag{4.41}$$

$$g_1(z,t) = -(k-\hat{a})e^{\hat{a}zl_c(t)}X(t), \tag{4.42}$$

$$g_2(z,t) = -\frac{1}{\hat{b}}(k-\hat{a})^2 e^{\hat{a}zl_c(t)}\bigg(\frac{W(0,t)}{(k-\hat{a})} + X(t)\bigg), \tag{4.43}$$

$$
\begin{aligned}
g_3(z,t) = {} & \big(1-(k-\hat{a})l_c(t)z\big)e^{\hat{a}zl_c(t)}X(t) \\
& + l_c(t)\int_0^z e^{\hat{a}(z-\zeta)l_c(t)}\big(1-(k-\hat{a})l_c(t)(z-\zeta)\big) \\
& \qquad \cdot \Big(W(\zeta,t)+(k-\hat{a})\big(e^{k\zeta l_c(t)}X(t) \\
& \qquad\quad + l_c(t)\int_0^\zeta e^{k(\zeta-\sigma)l_c(t)}W(\sigma,t)d\sigma\big)\Big)d\zeta,
\end{aligned} \tag{4.44}
$$

$$
\begin{aligned}
g_4(z,t) = {} & \frac{1}{\hat{b}}\Big(W(z,t)+(k-\hat{a})\Big(e^{kzl_c(t)}X(t)+l_c(t)\int_0^z e^{k(z-\zeta)l_c(t)}W(\zeta,t)d\zeta\Big) \\
& - (k-\hat{a})l_c(t)\int_0^z e^{\hat{a}(z-\zeta)l_c(t)}\Big(W(\zeta,t)+(k-\hat{a})\big(e^{k\zeta l_c(t)}X(t) \\
& \qquad\qquad + l_c(t)\int_0^\zeta e^{k(\zeta-\sigma)l_c(t)}W(\sigma,t)d\sigma\big)\Big)d\zeta\Big).
\end{aligned} \tag{4.45}
$$

The PDE–ODE cascade system (4.32)–(4.34) has been successfully transformed into the target system (4.39)–(4.41) using transformation (4.37). Since the backstepping transformation is invertible, please see (4.37)–(4.38), proving stability of the target system in the transformed variables (X,W) implies stability of the system in the variables (X,U). However, before proving stability, important results which include the control law, the update laws, and the stability theorem, are first offered.

4.5. Main Results and Stability Theorem

Evaluating (4.37) at $z=1$, and in light of (4.41), (4.31), (4.34), (4.28), state (4.25), and input (4.2), our controller becomes

$$
\begin{aligned}
u(t) = {} & (1-v)y_x(0,t) \\
& + \frac{(k-\hat{a})}{\hat{b}}e^{\hat{a}l_c(t)}\Big(y_t\big(l_c(t),t\big)-vu\big(\phi(t)\big)-v(v-1)y_x\big(0,\phi(t)\big)\Big) \\
& + (k-\hat{a})l_c(t)\int_0^1 e^{\hat{a}(1-z)l_c(t)}\Big(u\Big(\frac{t+zl_c(t)-1}{1+v}\Big)+(v-1) \\
& \qquad\qquad \cdot y_x\Big(0,\frac{t+zl_c(t)-1}{1+v}\Big)\Big)dz.
\end{aligned} \tag{4.46}
$$

The update laws for the unknown parameters are

$$
\dot{\hat{a}}(t) = k_a\mathrm{Proj}_a\Big\{\tau(t)\Big(y_t\big(l_c(t),t\big)-vu\big(\phi(t)\big)-v(v-1)y_x\big(0,\phi(t)\big)\Big)\Big\}, \tag{4.47}
$$

$$
\dot{\hat{b}}(t) = k_b\mathrm{Proj}_b\Big\{\tau(t)\Big(u\big(\phi(t)\big)+(v-1)y_x\big(0,\phi(t)\big)\Big)\Big\}, \tag{4.48}
$$

for $k_a > 0$ and $k_b > 0$, the update gains, and where

$$\begin{aligned}\tau(t) = \frac{1}{N(t)}\Bigg(\frac{p}{c_w}\Big(y_t\big(l_c(t),t\big) - vu\big(\phi(t)\big) - v(v-1)y_x\big(0,\phi(t)\big)\Big) \\ - (k-\hat{a})\int_0^1 e^{z(h+\hat{a}l_c(t))}W(z,t)dz\Bigg),\end{aligned} \tag{4.49}$$

$$\begin{aligned}N(t) = 1 + p\Big(y_t\big(l_c(t),t\big) - v(v-1)y_x\big(0,\phi(t)\big) - vu\big(\phi(t)\big)\Big)^2 \\ + c_w\int_0^1 e^{hz}W(z,t)^2dz \\ + c_\xi\int_0^{l_c(t)} e^x\Bigg(\frac{2y_t\Big(l_c\big(t-l_c(t)+x\big),t-l_c(t)+x\Big)}{1-v} + (1+v) \\ \cdot y_x\Big(0,\phi\big(t-l_c(t)+x\big)\Big) - \frac{1+v}{1-v}u\Big(\phi\big(t-l_c(t)+x\big)\Big)\Bigg)^2 dx,\end{aligned} \tag{4.50}$$

for scalars $c_w > 0$, $c_\xi > 0$, and with h bounded by

$$h \geq \max\left\{0, -v\max\left\{1, \frac{1}{1+v}\right\}\right\}. \tag{4.51}$$

Please note, the last integral term of (4.50) is equivalent to $c_\xi\int_0^{l_c(t)} e^x\xi(x,t)^2dx$, where (4.14), (4.10), and (4.17) have been used. Expression in (4.50) is then given in terms of the measurable boundary states as per Assumption 4.7. The expression given in terms of $\xi(x,t)$ is used in the later part of this chapter where the stability analysis is discussed.

Furthermore, scalar $p > 0$ satisfies the following equation

$$2pk = -q, \tag{4.52}$$

where $q \in \mathbb{R}$ such that $q > 0$ is to be determined from the stability analysis. Generic projection operator in the update laws is

$$\text{Proj}\{\tau f_\kappa\} = \begin{cases} 0 & \text{if } \hat{\kappa} = \bar{\kappa} \text{ and } \tau f_\kappa \geq 0 \\ 0 & \text{if } \hat{\kappa} = \underline{\kappa} \text{ and } \tau f_\kappa \leq 0 \\ \tau f_\kappa & \text{otherwise} \end{cases} \tag{4.53}$$

for $f_\kappa = X(t)$, $U\big(\phi(t)\big)$, and where $\hat{\kappa}$ stands for estimate of a or b with $\bar{\kappa}$ and $\underline{\kappa}$ representing maxima and minima bounds as per Assumption 4.6. The main stability theorem can now be stated.

Theorem 4.9. Consider a closed-loop system comprised of system (4.1)–(4.3), the control law (4.46), and the update laws (4.47)–(4.48) under Assumptions 4.5–4.7. There exists a constant $\bar{k} > 0$ such that for any update gain $k_i \in (0, \bar{k}]$ there exists a positive constant Λ and $\bar{\Lambda}$ such that the following inequality holds

$$\Upsilon(t) \leq \Lambda\big(e^{\bar{\Lambda}\Upsilon(0)} - 1\big), \quad \forall t \in [0, T), \tag{4.54}$$

where

$$\begin{aligned}\Upsilon(t) = \tilde{a}^2 + \tilde{b}^2 + \Big(y_t\big(l_c(t), t\big) - v(v-1)y_x\big(0, \phi(t)\big) - vu\big(\phi(t)\big)\Big)^2 \\ + \int_0^1 \Big(u\Big(\frac{t + zl_c(t) - 1}{1+v}\Big) + (v-1)y_x\Big(0, \frac{t + zl_c(t) - 1}{1+v}\Big)\Big)^2 dz \\ + \int_0^{l_c(t)} \Big(\frac{2y_t\Big(l_c\big(t - l_c(t) + x\big), t - l_c(t) + x\Big)}{1-v} + (1+v) \\ \cdot y_x\Big(0, \phi\big(t - l_c(t) + x\big)\Big) - \frac{1+v}{1-v}u\Big(\phi\big(t - l_c(t) + x\big)\Big)\Big)^2 dx,\end{aligned} \tag{4.55}$$

i.e., the equilibrium of the closed-loop system is stable in the sense of norm $\Upsilon(t)^{\frac{1}{2}}$.

Remark 4.10. Please observe that the control (4.46), as well as the update laws, (4.47)–(4.48), call for prior states, states evaluated at $t \in [-\frac{2}{1-v_c}, 0)$. In general, these states are not available. Once these states become accessible the system achieves closed-loop stability as per Theorem 4.9.

4.6. Stability Proof

In this section, the proof of stability Theorem 4.9 is presented. First, however, an important inequality required for the proof is given. The following lemma provides the necessary result.

Lemma 4.11. There exists a suitably large constant $\bar{M} > 0$ such that the following inequality holds

$$\begin{aligned}2c_w \int_0^1 e^{hz} W(z,t)\big(\dot{\hat{a}} g_3(z,t) + \dot{\hat{b}} g_4(z,t)\big)dz \\ \leq 2c_w \bar{k}\bar{M}\big(|X(t)|^2 + ||W(t)||^2 + |W(0,t)|^2\big),\end{aligned} \tag{4.56}$$

where $\bar{k} = \max\{k_a, k_b\}$.

Proof of Lemma 4.11. Insert expressions (4.44)-(4.45) and the update laws (4.47)-(4.48) on the left-hand side of inequality (4.56). Use Young's Inequality and expand the resulting expression by multiplying out all the terms. Use Cauchy-Schwarz' Inequality to reduce integral terms. The time-dependent parameters such as $\hat{a}(t), \hat{b}(t)$, and $l_c(t)$, are bounded using Assumptions 4.5–4.6, and expression (4.9). Use the definition of a norm. In particular, for $z \in [0,1]$ and $h \geq 0$ as per (4.51) one can write $\int_0^1 e^{2hz} W(z,t)^2 dz \leq e^h \int_0^1 e^{hz} W(z,t)^2 dz = e^h ||W(t)||^2$. When encountering quartic terms, $X(t)^4, ||W(t)||^2 X(t)^2, ...$, utilize the normalization function (4.50). When written in the denominator as $\min\{1, p, c_w, c_\xi\}\big(1 + X(t)^2 + ||W(t)||^2 + ||\xi(t)||^2\big)$ it allows us to reduce quartic terms to quadratic terms such as $X(t)^2, ||W(t)||^2$, and $||W(0,t)||^2$. Taking maximum and now constant pre-multiplicative coefficient and calling it $\bar{M}$ allows us to then state inequality (4.56). □

Proof of Theorem 4.9. Consider the Lyapunov-Krasovski functional

$$V(t) = \ln\big(N(t)\big) + \frac{c_w}{k_a}\tilde{a}^2 + \frac{c_w}{k_b}\tilde{b}^2 \tag{4.57}$$

with normalization function $N(t)$ defined as in equation (4.50). Using Young's and Cauchy-Schwarz' Inequalities, together with the results of Lemma 4.11, the time derivative of the Lyapunov-Krasovski functional (4.57) is then bounded by the following expression

$$\begin{aligned} \dot{V} \leq \frac{1}{N(t)}\Big(&- L_\xi\big(||\xi(t)||^2 + \xi(0,t)^2\big) - L_X X(t)^2 \\ &- L_W ||W(t)||^2 - L_{W_0} W(0,t)^2\Big) \end{aligned} \tag{4.58}$$

for

$$L_\xi = c_\xi(1-v), \tag{4.59}$$

$$L_X = q - \epsilon_1 - 2c_w \bar{k}\bar{M} - \frac{2c_\xi e^{\bar{l}}}{(b_1)^2(1-v)^2}\big(2b_2 + (1-v)a_k\big)^2, \tag{4.60}$$

$$L_W = c_w\beta - 2c_w\bar{k}\bar{M}, \tag{4.61}$$

$$L_{W_0} = \frac{c_w}{\bar{l}} - \frac{p^2}{\epsilon_1} - \frac{2c_\xi e^{\bar{l}}}{(b_1)^2} - 2c_w\bar{k}\bar{M}, \tag{4.62}$$

where, for bounded $l_c(t)$ under Assumption 4.5, $\bar{l} \geq \max\{l_c(t)\}$. Moreover, where $\epsilon_1 > 0$, $b_1 = \min\{|\underline{b}|, |\bar{b}|\}$, $b_2 = \max\{|\underline{b}|, |\bar{b}|\}$, $a_k = \max\{|k - \underline{a}|, |k - \bar{a}|\}$, and recalling

definition of h in (4.51)

$$\beta = \frac{1}{\bar{l}} \min\Big\{h + v, h + v(h+1)\Big\}. \tag{4.63}$$

By selecting

$$\bar{k} \leq \frac{\underline{\mathrm{M}}}{2c_w \bar{M}}, \tag{4.64}$$

where

$$\underline{\mathrm{M}} = \min\left\{q - \epsilon_1 - \frac{2c_\xi e^{\bar{l}}\big(2b_2 + (1-v)a_k\big)^2}{(b_1)^2(1-v)^2}, c_w\beta, \frac{c_w}{\bar{l}} - \frac{p^2}{\epsilon_1} - \frac{2c_\xi e^{\bar{l}}}{(b_1)^2}\right\}, \tag{4.65}$$

and for $\underline{\mathrm{M}} > 0$, the following inequality is stated

$$V(t) \leq V(0), \quad \forall t \in [0, T). \tag{4.66}$$

I.e., the equilibrium of the target system is stable and all signals of (4.57) are uniformly bounded.

Before the main proof is completed, a set of signal inequalities is first derived. Using definition of the Lyapunov-Krasovski functional (4.57), and the fact that $(e^x - 1) \geq x$ for $x \geq 0$, state

$$\Big(\frac{k_a}{c_w} + \frac{k_b}{c_w}\Big)\Big(e^{V(t)} - 1\Big) \geq \tilde{a}^2 + \tilde{b}^2. \tag{4.67}$$

Starting form functional (4.57) once more, and using $e^x \geq 1$ for $x \geq 0$, write the following set of inequalities

$$\frac{e^{V(t)} - 1}{p} \geq X(t)^2, \tag{4.68}$$

$$\frac{e^{V(t)} - 1}{c_w} \geq ||W(t)||^2, \tag{4.69}$$

$$\frac{e^{V(t)} - 1}{c_\xi} \geq ||\xi(t)||^2. \tag{4.70}$$

From the backstepping transformation (4.37) and the inverse (4.38), bounded $l_c(t)$ from Assumption 4.5–4.6, and for sufficiently large and positive constants r_1, r_2, and s_1, s_2, one can obtain inequalities:

$$||W(t)||^2 \leq r_1 X(t)^2 + r_2 ||\Pi(t)||^2, \tag{4.71}$$

$$||\Pi(t)||^2 \leq s_1 X(t)^2 + s_2 ||W(t)||^2. \tag{4.72}$$

Using (4.68) and (4.69) in (4.72) gives

$$||\Pi(t)||^2 \leq \Big(\frac{s_1}{p} + \frac{s_2}{c_w}\Big)\big(e^{V(t)} - 1\big). \tag{4.73}$$

Furthermore, please notice that (4.55) can be written as

$$\Upsilon(t) = X(t)^2 + \tilde{a}^2 + \tilde{b}^2 + \int_0^{l_c(t)} \xi(x,t)^2 dx + \int_0^1 \Pi(z,t)^2 dz. \tag{4.74}$$

Having obtained the above expressions, it is now possible to prove inequality (4.54). Using inequalities (4.67), (4.68), (4.72), and (4.69) in definition (4.74) results in

$$\Upsilon(t) \leq \Lambda\big(e^{V(t)} - 1\big), \tag{4.75}$$

where

$$\Lambda = \frac{1 + s_1}{p} + \frac{s_2 + k_a + k_b}{c_w} + \frac{1}{c_\xi}. \tag{4.76}$$

Starting from expression (4.57), and using $\ln(1 + x) \leq x$ for $x \geq -1$, together with (4.71), gives the following

$$V(t) \leq \bar{\Lambda}\Upsilon(t), \tag{4.77}$$

where

$$\bar{\Lambda} = \max\left\{(p + c_w r_1), c_w r_2 e^h, c_\xi e^{\bar{l}}, \frac{c_w}{k_a}, \frac{c_w}{k_b}\right\}. \tag{4.78}$$

Evaluating (4.77) at $t = 0$ and together with (4.66) allows one to state

$$V(t) \leq \bar{\Lambda}\Upsilon(0). \tag{4.79}$$

Inserting (4.79) into (4.75) finally gives the main stability statement, the inequality (4.54).

From the Lyapunov analysis $|X(t)|$, $||W(t)||$, and $||\xi(t)||$ are all uniformly bounded. Using inequality (4.72), and having already established the boundedness of all other variables, one concludes boundedness of $||\Pi(t)||$. Bounded $||\Pi(t)||$ implies bounded intermediate control input $|U(t)|$ in accordance with expression (4.31). From the definition of the state (4.25), control (4.2), and (4.28), expressions $|y_t(l_c(t), t)|$, $|y_t(0, t)|$, and $|y_x(0, t)|$ are all bounded. Bounded input $|u(t)|$ follows from (4.28).

The stability will now be extended to that of the in-domain states, $y_t(x,t)$ and $y_x(x,t)$. Considering (4.11), (4.15), and (4.2), write

$$\eta(x,t) = U\big(t - \frac{x}{1+v}\big). \tag{4.80}$$

The relation between $x \in [0, l(t)]$ and $z \in [0,1]$ can be stated as

$$z = \frac{x}{l(t)}. \tag{4.81}$$

Examining (4.80), (4.31), and (4.81) gives

$$\eta(x,t) = \Pi\big(1 - \frac{x}{l(t)}, t\big). \tag{4.82}$$

Since $||\Pi(t)||$ is known to be bounded, $||\eta(t)||$ must be bounded as well. From the definitions of the Riemann variables (4.10) and (4.11), the explicit expressions for $y_t(x,t)$ and $y_x(x,t)$ are obtained

$$\xi(x,t) - \eta(x,t) = 2y_x(x,t), \tag{4.83}$$

$$(1-v)\xi(x,t) + (1+v)\eta(x,t) = 2y_t(x,t). \tag{4.84}$$

Using the definition of a norm, the above expressions can be written as the following inequalities

$$||\xi(t)|| + ||\eta(t)|| \geq 2||y_x(t)||, \tag{4.85}$$

$$(1-v)^2||\xi(t)|| + (1+v)^2||\eta(t)|| \geq 2||y_t(t)||. \tag{4.86}$$

The boundedness of the in-domain states, $y_x(x,t)$ and $y_t(x,t)$, is due to that of $||\xi(t)||$, based on the Lyapunov analysis and the boundedness of $||\eta(t)||$ established from that of $||\Pi(t)||$ and the relation (4.82). □

4.7. Numerical Results

The closed-loop system comprised of (4.1)–(4.3), the control law (4.46), and the update laws (4.47)–(4.48) is simulated using the explicit FDM in Matlab (R2020b) environment. The simulation is performed with $\Delta t = 0.0005$ and $\Delta z = 0.05$ in both the extraction mode, $v_1 = 0.071$, and in the retraction mode where $v_2 = -0.071$. Please see Chapter 6 for a more detailed overview of the numerical analysis employed in the

simulations. The unstable boundary system parameters $a_{v_1} = 0.1$ corresponding to v_1 and $a_{v_2} = 0.1286$ corresponding to v_2 with bounds $a \in [-0.1, 1]$ and parameters $b_{v_1} = 0.1857$ and $b_{v_2} = 0.2143$ with bounds $b \in [0.1, 1]$ are used during the simulation. The initial conditions for $x \in [0, 1]$ at $t = 0$ are set to $y(x, 0) = 0.1\sin(3\pi x)$ and $y_t(x, 0) = -0.3\sin(\pi x)$ with $\hat{a}(0) = \hat{b}(0) = 0.5$. All the update gains, k_a, and k_b, are set to $2.2 \cdot 10^{-14}$, together with $c_w = 0.5$, $c_\xi = 5 \cdot 10^{-8}$, $\epsilon = 0.2$, $q = 0.4$, and the control gain $k = -2$.

Figures 4.2 and Figure 4.3 illustrate the bottom boundary velocity $y_t\big(l_c(t), t\big)$ and the control input $u(t)$ for the extraction mode, $v_1 = 0.071$. Similarly, Figure 4.4 and Figure 4.5 give the bottom boundary velocity $y_t\big(l_c(t), t\big)$ and the control input $u(t)$ for the retraction mode, $v_2 = -0.071$. All the subplots include four separate cases: a) the proposed controller as in (4.46), b) robust proportional controller of the form $u(t) = (1 - v)y_x(0, t) + KX(t)$, where $A + BK < 0$ for A taking values of $\underline{a}$ and $\bar{a}$, and for B taking values of $\underline{b}$ and $\bar{b}$, here, $K = -11$, c) high gain adaptive controller of the form $u(t) = (1 - v)y_x(0, t) + \frac{(k-\hat{a})}{\hat{b}}X(t)$ where $\dot{\hat{a}}(t) = k_a X(t)^2$ and $\dot{\hat{b}}(t) = -k_b \text{sign}(b)(k - \hat{a})X(t)^2$, and d) the free boundary condition where the top of the string is free, $u(t) = (1 - v)y_x(0, t)$. Case b) and c) allow for comparison between the delay-compensated and the closest two uncompensated controllers based on system (4.27) with no delay, $\phi(t) = t$. Case d) is given to illustrate that the simulated systems are unstable and diverge as the mass at the bottom of the string accelerates and pulls the top free end of the string. Table 4.1 summarizes performance of the outlined controllers by providing RMS values over the relevant time periods for the bottom boundary velocity $y_t\big(l_c(t), t\big)$ and the input velocity $u(t) = y_t\big(0, t\big)$. The root mean square (RMS) value is calculated over a time interval as per

$$f_{RMS} = \sqrt{\frac{1}{t_2 - t_1}\int_{t_1}^{t_2} f(t)^2 dt}. \tag{4.87}$$

In the case of $y_t\big(l_c(t), t\big)$, the interval is $t \in [1, 10]$, as it takes signal introduced at $x = 0$ one time unit to reach the bottom of the string. The interval $t \in [0, 1]$ is then fully governed by the response to the initial conditions. For the input, the relevant time interval depends on the mode. In the extraction mode $t \in [0, 8.400]$ and in the

retraction mode $t \in [0, 9.692]$, ie., the last signal to reach the bottom of the string at $t = 10$ is emitted at $t = 8.400$ and $t = 9.692$, respectively. Finally, Figure 4.6 and Figure 4.7 present the total in-domain displacement for the proposed controller in both the extraction and the retraction modes respectively.

Table 4.1. RMS values of $y_t\big(l_c(t), t\big)$ and $u(t) = y_t(0, t)$ for various controllers.

RMS	**Extraction Mode**		**Retraction Mode**	
	$y_t\big(l_c(t), t\big)$	$u(t)$	$y_t\big(l_c(t), t\big)$	$u(t)$
Proposed Controller	0.033	0.173	0.0149	0.2294
Robust Controller	0.822	3.0377	0.1394	1.1143
High Gain Controller	0.0395	0.2584	0.0228	0.2351

4.8. Discussion

This chapter provides an effectual method for boundary control of a string-mass system with a time-varying length. This is achieved by reformulating the original problem as an adaptive control of an uncertain LTI system with a non-constant input delay. The application of the backstepping method enabled the derivation of the control and transformed the problem into a target system whose stability was then proven. The proposed controller clearly outperforms the delay-uncompensated controllers in stabilizing the string-mass system. Even though the analysis guarantees only stability in the Lyapunov sense, the velocity state converges to zero. Furthermore, the convergence of the velocity signal is much faster, and the control effort much smaller for the proposed controller. The extraction where $v > 0$ is a more challenging mode, when compared to the retraction mode, as the delay increases with the length of the string. While the current chapter considered a special case where $v = const.$, in the next one, a more general case where $v = v(t)$ will be investigated.

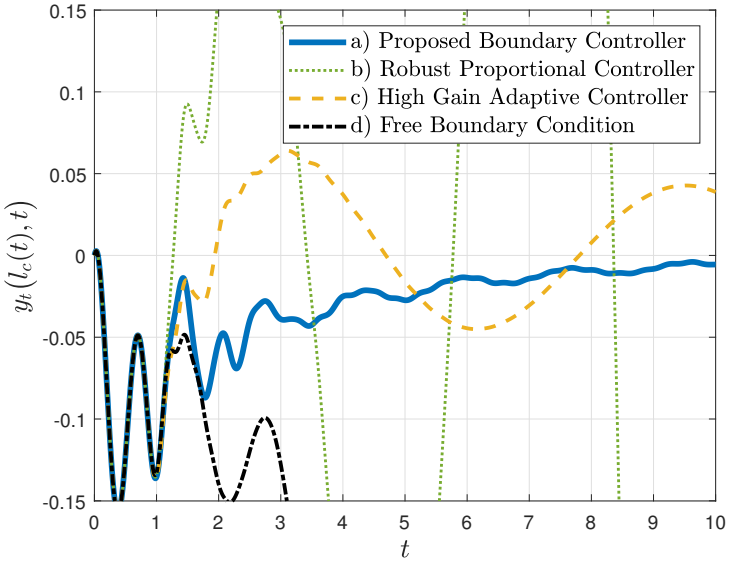

Figure 4.2. Boundary velocity $y_t\big(l_c(t),t\big)$ in the extraction mode $v = 0.071$ for: a) Proposed Controller (4.46), b) Robust Proportional Controller of the form $u(t) = (1-v)y_x(0,t) + KX(t)$, c) High Gain Adaptive Controller of the form $u(t) = (1-v)y_x(0,t) + \frac{(k-\hat{a})}{\hat{b}}X(t)$, d) Free Boundary Condition $u(t) = (1-v)y_x(0,t)$.

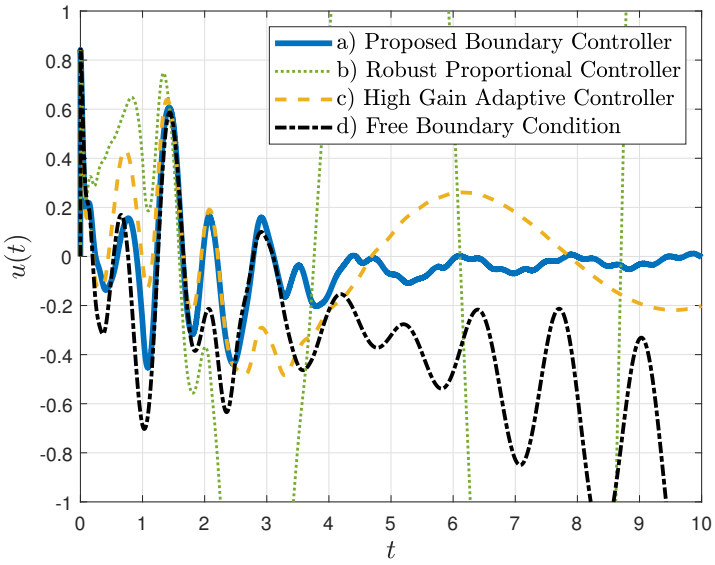

Figure 4.3. Control input $u(t)$ in the extraction mode $v = 0.071$ for: a) Proposed Controller (4.46), b) Robust Proportional Controller of the form $u(t) = (1-v)y_x(0,t) + KX(t)$, c) High Gain Adaptive Controller of the form $u(t) = (1-v)y_x(0,t) + \frac{(k-\hat{a})}{\hat{b}}X(t)$, d) Free Boundary Condition $u(t) = (1-v)y_x(0,t)$.

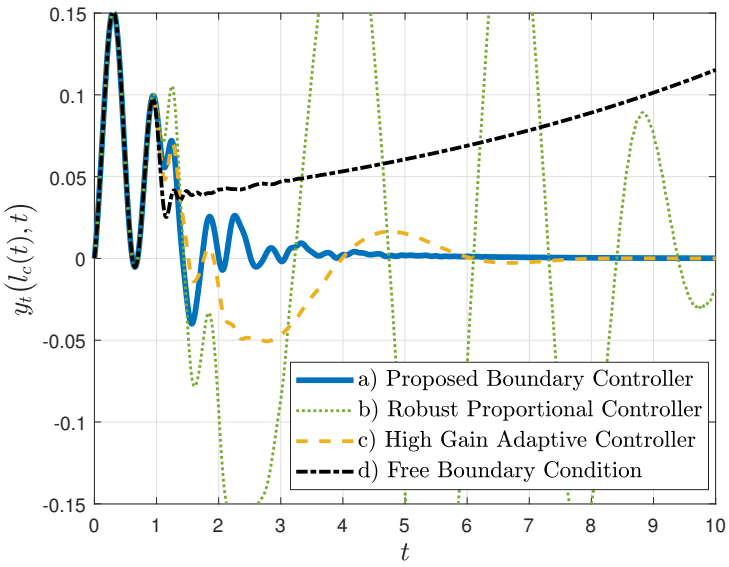

Figure 4.4. Boundary velocity $y_t\big(l_c(t),t\big)$ in the retraction mode $v=-0.071$ for: a) Proposed Controller (4.46), b) Robust Proportional Controller of the form $u(t)=(1-v)y_x(0,t)+KX(t)$, c) High Gain Adaptive Controller of the form $u(t)=(1-v)y_x(0,t)+\frac{(k-\hat{a})}{\hat{b}}X(t)$, d) Free Boundary Condition $u(t)=(1-v)y_x(0,t)$.

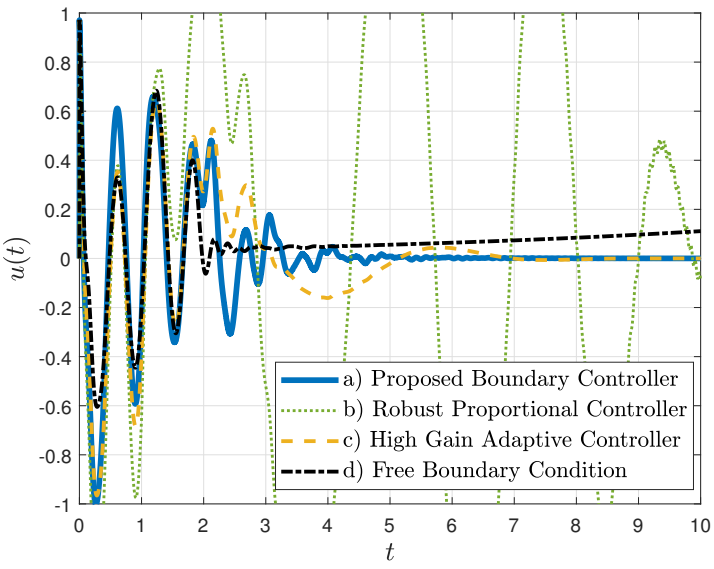

Figure 4.5. Control input $u(t)$ in the retraction mode $v=-0.071$ for: a) Proposed Controller (4.46), b) Robust Proportional Controller of the form $u(t)=(1-v)y_x(0,t)+KX(t)$, c) High Gain Adaptive Controller of the form $u(t)=(1-v)y_x(0,t)+\frac{(k-\hat{a})}{\hat{b}}X(t)$, d) Free Boundary Condition $u(t)=(1-v)y_x(0,t)$.

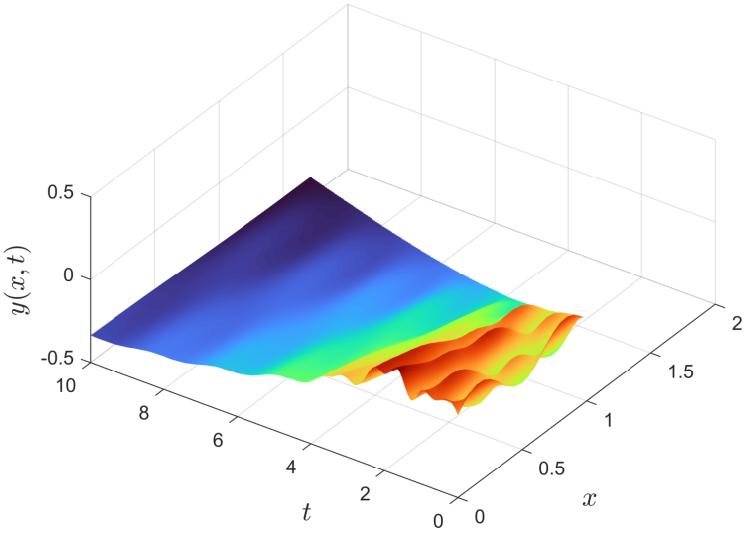

Figure 4.6. Total string displacement $y(x,t)$ in the extraction mode for the proposed controller.

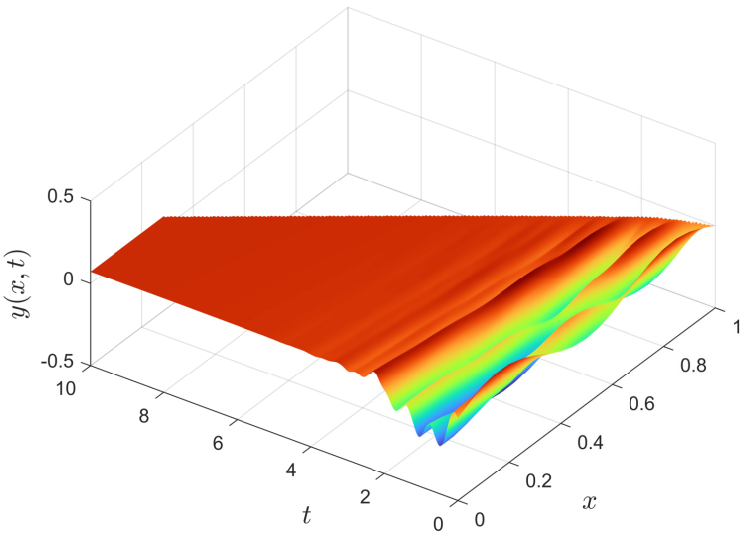

Figure 4.7. Total string displacement $y(x,t)$ in the retraction mode for the proposed controller.

5. BOUNDARY CONTROL FOR A STRING-MASS SYSTEM WITH TIME-VARYING LENGTH HAVING TIME-VARYING VELOCITY

5.1. Introduction

This chapter presents the most general case for the control of a string-mass system as considered in this work. The length of the string will be assumed to change under a time-dependent velocity profile. As in the previous problems, the equations of motion found in Chapter 2 are used to model an ideal string-mass system with a a non-constant length.

5.2. Problem Statement

Consider (2.42)–(2.44). The following physical assumptions are made about the system:

Assumption 5.1. The velocity governing the length of the string is assumed to be a function of time, $v(t)$.

Assumption 5.2. There are not any in-domain damping forces affecting the string, $c_\rho = 0$.

Assumption 5.3. Tension in the string is constant and due only to the weight of the mass, $F_\tau(x,t) = mg$. This implies: $\epsilon_\tau = 0$ and $\epsilon_a = 0$.

Assumption 5.4. The string as well at the mass are not affected by any disturbances, $p(x,t) = P\big(l(t),t\big) = 0$.

Under Assumptions 5.1–5.4 system (2.42)–(2.44) reduces to

$$y_{tt}(x,t) = \big(1 - v(t)^2\big)y_{xx}(x,t) - 2v(t)y_{tx}(x,t) - \dot{v}(t)y_x(x,t), \tag{5.1}$$

$$y_t(0,t) = u(t), \tag{5.2}$$

$$
\begin{aligned}
y_{tt}\big(l(t),t\big) = & -v(t)^2 y_{xx}\big(l(t),t\big) - 2v(t)y_{xt}\big(l(t),t\big) \\
& - \Big(\frac{v(t)L_0\rho}{m} + \frac{c_m L_0}{m\sqrt{\frac{mg}{\rho}}}\Big) y_t\big(l(t),t\big) \\
& - \Big(\frac{v(t)^2 L_0\rho}{m} + \frac{v(t)c_m L_0}{m\sqrt{\frac{mg}{\rho}}} + \frac{L_0\rho}{m} + \dot{v}(t)\Big) y_x\big(l(t),t\big),
\end{aligned} \tag{5.3}
$$

where $t \in [0,\infty)$, $x \in [0, l(t)]$, and where

$$
l(t) = 1 + \int_0^t v(t)dt \tag{5.4}
$$

is the normalized string length. Symbol $v(t) \in \mathbb{R}$ is the velocity or rate at which the boundary of the domain x is changing. Please see Assumption 2.7 and Figure 5.1.

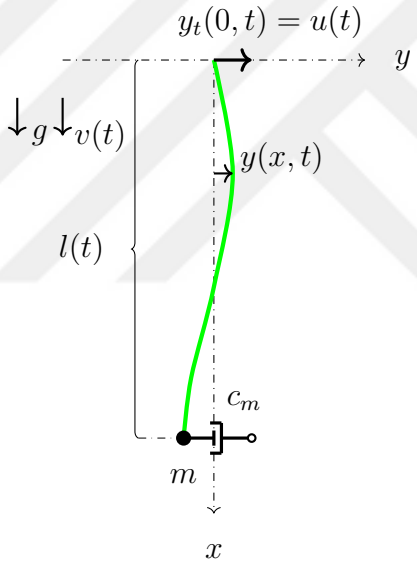

Figure 5.1. String diagram.

As in the previous chapters, the delay control methods will be employed in the analysis. To bound the delay, an additional constraint is placed on the velocity:

Assumption 5.5. The velocity profile $v(t)$ is a known, continuous, and a differentiable, function such that $|v(t)| < 1$. Furthermore, $\int_0^t v(t)dt > -1$, $v(t < 0) = 0$, and $v(t \geq T) = 0$ where time T is known, finite, and constant.

Condition $|v(t)| < 1$ ensures the string remains under tension. In general, $|v(t)| \ll 1$. Condition $\int_0^t v(t)dt > -1$ guarantees that the length of the string $l(t) > 0$, $\forall t \geq 0$. The last condition indicates the length is bounded and becomes constant for $t \geq T$.

Assumption 5.6. All physical parameters: initial length L_0, mass m, linear density ρ, and damping coefficient c_m are assumed to be constant and known.

In addition, the following control assumption is made for the system (5.1)–(5.3):

Assumption 5.7. Boundary states, $y_t(0,t)$, $y_x(0,t)$, and $y_t\big(l(t),t\big)$ are assumed to be measured. Their present values as well as their histories are available for feedback.

The aim of this chapter is to design boundary control input $u(t)$ at boundary $x = 0$, see (5.2), such that

$$\lim_{t\to\infty} y_t\big(l(t),t\big) = 0, \tag{5.5}$$

i.e., it is desired to stabilize the transverse velocity, $y_t\big(l(t),t\big)$, of the mass at $x = l(t)$ by actuating the transverse velocity, $y_t(0,t)$, of the string at the boundary $x = 0$. Furthermore, the closed-loop stability of the system (5.1)–(5.3) needs to be proven.

In the following section system (5.1)-(5.3) is reformulated using a set of Riemann variables. This enables one to express the bottom BC as an LTV system with a non-constant input delay.

5.3. Reformulation of the Problem

The outlined problem is first reformulated as a stabilization of an LTV system describing the dynamics at the bottom boundary, $x = l(t)$. This is accomplished by following Cai and Krstic (2016) and Basturk (2017) and defining two Riemann variables

$$\xi(x,t) = y_t(x,t) + \big(1 + v(t)\big)y_x(x,t), \tag{5.6}$$

$$\eta(x,t) = y_t(x,t) - \big(1 - v(t)\big)y_x(x,t), \tag{5.7}$$

which transform PDE (5.1) into a 2×2 hyperbolic system

$$\xi_t(x,t) = \big(1 - v(t)\big)\xi_x(x,t), \tag{5.8}$$

$$\eta_t(x,t) = -\big(1 + v(t)\big)\eta_x(x,t). \tag{5.9}$$

Solutions to PDEs (5.8) and (5.9) are

$$\xi(x,t) = \Psi\Big(x + \int_0^t \big(1 - v(\tau)\big)d\tau\Big), \tag{5.10}$$

$$\eta(x,t) = \Phi\Big(-x + \int_0^t \big(1 + v(\tau)\big)d\tau\Big), \tag{5.11}$$

which are given for arbitrary functions Ψ and Φ. In light of (5.10)–(5.11) and under Assumption 5.5 the following statements are enforced

$$\xi(x,t) = \xi\Big(l\big(t + f(x,t)\big), t + f(x,t)\Big), \tag{5.12}$$

$$\eta(x,t) = \eta\big(0, t - g(x,t)\big), \tag{5.13}$$

for yet to be determined functions $f(x,t)$ and $g(x,t)$ such that $f\big(l(t),t\big) = 0$ and $g(0,t) = 0$. Substitute (5.10)–(5.11) into (5.12)–(5.13) to obtain

$$l\big(t + f(x,t)\big) - x = \int_{t+f(x,t)}^{t} \big(1 - v(z)\big)dz, \tag{5.14}$$

$$x = \int_{t-g(x,t)}^{t} \big(1 + v(z)\big)dz. \tag{5.15}$$

The functions $f(x,t)$ and $g(x,t)$ are obtained by solving (5.14)–(5.15), respectively. Since $|v(t)| < 1$ from Assumption 5.5 and $x \geq 0$, $t - g(x,t) \leq t$ and $t + f(x,t) \leq t$. Now, define the delay function $\phi(t)$ as

$$\phi(t) = t - g\big(l(t),t\big), \tag{5.16}$$

where $g\big(l(t),t\big)$ is the time-varying delay. It can be shown that for $v(t) = 0$, $g(x,t) = x$, and $\phi(t) = t - 1$ or a constant delay as in the problem in Chapter 3. For $v(t) = v$, $g(x,t) = \frac{x}{1+v}$ and $\phi(t) = t - \frac{1+vt}{1+v}$ or a linearly changing delay as found in the problem in Chapter 4. Moreover, by taking spatial and time derivatives of the expression (5.15) it can shown that

$$g_x\big(l(t),t\big) = \frac{1}{1 + v\big(\phi(t)\big)}, \tag{5.17}$$

$$g_t\big(l(t),t\big) = \frac{v\big(\phi(t)\big) - v(t)}{1 + v\big(\phi(t)\big)}, \tag{5.18}$$

and

$$\dot{\phi}(t) = 1 - g_t\big(l(t),t\big) - v(t)g_x\big(l(t),t\big) = \frac{1}{1 + v\big(\phi(t)\big)}. \tag{5.19}$$

Once more, since $|v(t)| < 1$, $\dot{\phi}(t) > 0$.

Variables $\xi(x,t)$ and $\eta(x,t)$ are continuous and differentiable functions in both $x \in [0, l(t)]$ and $t \in [0, \infty)$ by definitions (5.6)–(5.7) and Assumption 5.5. Since the transport PDEs (5.8)–(5.9) are non-dissipative and decoupled, the signals $\xi(x,t)$ and $\eta(x,t)$ are preserved as they propagate. This allows enforcement of relations (5.12)–(5.13). The existence and the continuity of functions $f(x,t)$ and $g(x,t)$ is then stated. Assuming that there exist a continuous $g\big(l(t),t\big) \in \mathbb{R}$ which is the solution to equation (5.15) at $x = l(t)$, then the delay $g\big(l(t),t\big)$ and the delay function $\phi(t)$ are differentiable as per (5.16)–(5.19), and Assumption 5.5. Since $\phi(t)$ is continuously differentiable and with nonzero derivatives as per (5.19) and Assumption 5.5, by Inverse Function Theorem, $\phi(t)$ is an invertible function and the inverse is continuously differentiable.

Now, take the spatial derivative of (5.13) to obtain

$$\eta_x(x,t) = \eta_t\big(0, t - g(x,t)\big)\big(-g_x(x,t)\big), \tag{5.20}$$

which together with (5.9), and when evaluated at $x = l(t)$, gives

$$\eta_x(l(t),t) = \Big(1 + v\big(\phi(t)\big)\Big) g_x\big(l(t),t\big)\eta_x\big(0,\phi(t)\big). \tag{5.21}$$

Re-express $y_x\big(l(t),t\big)$, $y_{tx}\big(l(t),t\big)$, and $y_{xx}\big(l(t),t\big)$ in the BC (5.3) in terms of the states at $x = 0$. Use (5.7) in (5.13) and evaluate at $x = l(t)$ to obtain the first expression

$$y_x\big(l(t),t\big) = \frac{1}{1 - v(t)}\bigg(y_t\big(l(t),t\big) - y_t\big(0,\phi(t)\big) + \Big(1 - v\big(\phi(t)\big)\Big) y_x\big(0,\phi(t)\big)\bigg). \tag{5.22}$$

Solve (5.1) for $y_{xx}(x,t)$ and evaluate at $x = l(t)$:

$$y_{xx}\big(l(t),t\big) = \frac{1}{1 - v(t)^2}\Big(y_{tt}(l(t),t) + 2v(t)y_{tx}\big(l(t),t\big) + \dot{v}(t)y_x\big(l(t),t\big)\Big). \tag{5.23}$$

For the second expression, take spatial derivative of (5.7), evaluate at $\big(x = l(t), t\big)$, and at $\big(x = 0, t = \phi(t)\big)$, and substitute into (5.21). Use (5.23) together with (5.22) and solve for $y_{tx}\big(l(t),t\big)$:

$$\begin{aligned} y_{tx}\big(l(t),t\big) = {} & \frac{1 + v(t)}{1 - v(t)}\bigg(y_{tx}\big(0,\phi(t)\big) - \Big(1 - v\big(\phi(t)\big)\Big) y_{xx}\big(0,\phi(t)\big)\bigg) \\ & + \frac{\dot{v}(t)}{\big(1 - v(t)\big)^2}\bigg(y_t\big(l(t),t\big) - y_t\big(0,\phi(t)\big) \\ & \qquad + \Big(1 - v\big(\phi(t)\big)\Big) y_x\big(0,\phi(t)\big)\bigg) + \frac{y_{tt}\big(l(t),t\big)}{1 - v(t)}. \end{aligned} \tag{5.24}$$

Substitute (5.24) into (5.23) to obtain the third:

$$\begin{aligned} y_{xx}\big(l(t),t\big) = &\frac{y_{tt}\big(l(t),t\big)}{\big(v(t)-1\big)^2} - \frac{\dot{v}(t)}{\big(v(t)-1\big)^3} \\ &\cdot \bigg(y_t\big(l(t),t\big) - y_t\big(0,\phi(t)\big) + \Big(1-v\big(\phi(t)\big)\Big) y_x\big(0,\phi(t)\big) \bigg) \\ &+ \frac{2v(t)}{\big(v(t)-1\big)^2} \bigg(y_{tx}\big(0,\phi(t)\big) - \Big(1-v\big(\phi(t)\big)\Big) y_{xx}\big(0,\phi(t)\big) \bigg). \end{aligned} \tag{5.25}$$

The boundary condition (5.3) can now be re-express as an LTV system. Substitute (5.22), (5.24), and (5.25) into BC (5.3) and solve for $y_{tt}\big(l(t),t\big)$:

$$\begin{aligned} y_{tt}\big(l(t),t\big) = a(t) y_t\big(l(t),t\big) &+ b(t) \bigg(y_t\big(0,\phi(t)\big) - \Big(1-v\big(\phi(t)\big)\Big) y_x\big(0,\phi(t)\big) \bigg) \\ &+ d(t) \bigg(y_{tx}\big(0,\phi(t)\big) - \Big(1-v\big(\phi(t)\big)\Big) y_{xx}\big(0,\phi(t)\big) \bigg). \end{aligned} \tag{5.26}$$

where

$$a(t) = \big(v(t)-1\big) \bigg(\frac{c_m L_0}{m\sqrt{\frac{mg}{\rho}}} + \frac{L_0 \rho \big(1+v(t)\big)}{m} + \frac{\dot{v}(t)}{\big(v(t)-1\big)^2} \bigg), \tag{5.27}$$

$$b(t) = \frac{\big(v(t)-1\big)^2}{1-v(t)} \bigg(\frac{c_m L_0 v(t)}{m\sqrt{\frac{mg}{\rho}}} + \frac{L_0 \rho \big(1+v(t)^2\big)}{m} + \frac{\dot{v}(t)}{\big(v(t)-1\big)^2} \bigg), \tag{5.28}$$

$$d(t) = -2v(t). \tag{5.29}$$

Now, define state $X(t) \in \mathbb{R}$ as

$$X(t) = y_t\big(l(t),t\big) - v(t) U\big(\phi(t)\big), \tag{5.30}$$

where the intermediate input is

$$U(t) = u(t) - \big(1-v(t)\big) y_x\big(0,t\big). \tag{5.31}$$

Taking the time derivative of $X(t)$ gives

$$\dot{X}(t) = A(t) X(t) + B(t) U\big(\phi(t)\big), \tag{5.32}$$

where

$$A(t) = a(t) + \frac{a(t)v(t)}{1-v(t)} + \frac{v(t)\dot{v}(t)}{\big(1-v(t)\big)^2}, \tag{5.33}$$

$$B(t) = -\dot{v}(t) - \frac{b(t)+a(t)v(t)}{v(t)-1} - \frac{\big(1-v(t)\big)v(t)\dot{v}(t)}{\big(v(t)-1\big)^2}. \tag{5.34}$$

The effects of the input $U(t)$ at the boundary $x = 0$ show up explicitly in the boundary dynamics at $x = l(t)$ as a delayed input $U\big(\phi(t)\big)$. The boundary condition (5.3) is then cast into a form of an LTV system (5.32) with a non-constant input delay.

Remark 5.8. Please note that under Assumption 5.5, the delay $g\big(l(t), t\big) > 0$ and $g\big(l(t), t\big) < \infty$. The first condition guarantees that the LTV system (5.32) is causal, while the second one ensures that all input signals eventually reach the system. Furthermore, $\frac{Dg\left(l(t),t\right)}{Dt} = \frac{v\left(\phi(t)\right)}{1+v\left(\phi(t)\right)} < 1$ indicates that the direction of the input signal may never change, and the condition $\frac{Dg\left(l(t),t\right)}{Dt} > -\infty$ guarantees that the delay may only disappear gradually.

5.4. Feedback Control and Predictor State

The input-delayed LTV system (5.32) will be stabilized using control of the form

$$U(t) = K\big(\phi^{-1}(t)\big)X\big(\phi^{-1}(t)\big) \tag{5.35}$$

where $\phi^{-1}(t)$ is the inverse of the delay function $\phi(t)$ such that $\phi^{-1}\big(\phi(t)\big) = t$, and were

$$K_1(t) = K\big(\phi^{-1}(t)\big) \tag{5.36}$$

is yet to be determined time-varying update gain. Evaluating (5.35) at $t = \phi(t)$ gives the desired feedback control

$$U\big(\phi(t)\big) = K(t)X(t). \tag{5.37}$$

Begin by evaluating (5.32) at $t = \sigma(\theta) = \phi^{-1}(\theta)$ with $dt = \frac{d\sigma(\theta)}{d\theta}d\theta$, resulting in

$$\frac{dX\big(\sigma(\theta)\big)}{\dot{\sigma}d\theta} = A\big(\sigma(\theta)\big)X\big(\sigma(\theta)\big) + B\big(\sigma(\theta)\big)U\Big(\phi\big(\phi^{-1}(\theta)\big)\Big), \tag{5.38}$$

all for $\phi(t) \leq \theta \leq t$. Now, define a predictor state

$$P(t) = X\big(\phi^{-1}(t)\big), \tag{5.39}$$

and two auxiliary variables

$$A_1(\theta) = A\big(\sigma(\theta)\big), \tag{5.40}$$

$$B_1(\theta) = B\big(\sigma(\theta)\big). \tag{5.41}$$

Using the predictor state (5.39) and (5.40)–(5.41) write (5.38) as

$$\dot{P}(\theta) = \dot{\sigma}\Big(A_1(\theta)P(\theta) + B_1(\theta)U(\theta)\Big). \tag{5.42}$$

The solution to (5.42) is given as

$$P(\theta) = e^{\int_{\theta_0}^{\theta} A_1(s)\dot{\sigma}(s)ds}\Big(P(\theta_0) + \int_{\theta_0}^{\theta} e^{-\int_{\theta_0}^{\tau} A_1(s)\dot{\sigma}(s)ds} B_1(\tau)U(\tau)\dot{\sigma}(\tau)d\tau\Big), \tag{5.43}$$

where $\theta_0 = \phi(t)$. Recognizing that $P(\theta_0) = P(\phi(t)) = X(t)$, $\frac{d}{d\theta}\phi^{-1}(\theta) = \dot{\sigma}(\theta) = \frac{1}{\phi'(\phi^{-1}(t))}$ using differentiation rule for the inverse of a function where $\phi'(\cdot)$ denotes the derivative of $\phi(\cdot)$, and finally evaluating the above expression at $\theta = t$ gives the predictor state

$$P(t) = e^{\int_{\phi(t)}^{t} \frac{A_1(s)}{\phi'(\phi^{-1}(s))}ds}\Big(X(t) + \int_{\phi(t)}^{t} e^{-\int_{\phi(t)}^{\tau} \frac{A_1(s)}{\phi'(\phi^{-1}(s))}ds} B_1(\tau)\frac{U(\tau)}{\phi'(\phi^{-1}(\tau))}d\tau\Big). \tag{5.44}$$

The predictor state (5.44), together with the original definition of the state found in (5.39), allows one to obtain control (5.35) necessary to secure the desired feedback law (5.37).

In the next section, the backstepping transformation will be utilized, and the system will be transformed into the target system.

5.5. Infinite-Dimensional States and Backstepping Transformation

The aim of this section is to transform the input-delayed system (5.32) into the target system. This PDE-ODE cascade system will be characterized by desirable stability properties and can be obtained by performing a backstepping transformation. Once again, the analysis follows Krstic and Smyshlyaev (2008a). In preparation for the backstepping transformation, and as per Bekiaris-Liberis and Krstic (2013), variables need to be re-expressed using the transport PDE representation.

Start with the infinite-dimensional version of the predictor state which will be used to define the backstepping transformation. For $\theta = \phi\big(t + z(\sigma(t) - t)\big)$ where the

domain $\{z \in \mathbb{R} | 0 \leq z \leq 1\}$ define

$$p(z,t) = P(\theta) = P\Big(\phi\big(t + z(\sigma(t) - t)\big)\Big). \tag{5.45}$$

Since $\frac{d\theta}{dz} = \phi'\Big(t + z\big(\sigma(t) - t\big)\Big)\big(\sigma(t) - t\big)$ rewrite (5.42) as

$$\frac{dp(z,t)}{dz}\frac{dz}{d\theta} = \frac{d\sigma(\theta)}{dz}\frac{dz}{d\theta}\Big(A_1(\theta)p(z,t) + B_1(\theta)U(\theta)\Big). \tag{5.46}$$

For $\frac{d\sigma(\theta)}{dz} = \frac{d\phi^{-1}(\theta)}{dz} = \frac{d}{dz}\Big(\phi^{-1}\big(\phi(t + z(\sigma(t) - t))\big)\Big) = (\sigma(t) - t)$, (5.46) becomes

$$\frac{dp(z,t)}{dz} = \big(\sigma(t) - t\big)\Big(A_1(\theta)p(z,t) + B_1(\theta)U(\theta)\Big) \tag{5.47}$$

Equation (5.47) is the expression (5.42) written in terms of the infinite-dimensional predictor state (5.45). Similarly, define additional states and their boundary values:

$$\Pi(z,t) = U(\theta) = U\Big(\phi\big(t + z(\sigma(t) - t)\big)\Big), \tag{5.48}$$

$$\Pi(0,t) = U\big(\phi(t)\big), \tag{5.49}$$

$$\alpha(z,t) = A_1(\theta) = A_1\Big(\phi\big(t + z(\sigma(t) - t)\big)\Big), \tag{5.50}$$

$$\alpha(0,t) = A_1\big(\phi(t)\big) = A(t), \tag{5.51}$$

$$\beta(z,t) = B_1(\theta) = B_1\Big(\phi\big(t + z(\sigma(t) - t)\big)\Big), \tag{5.52}$$

$$\beta(0,t) = B_1\big(\phi(t)\big) = B(t), \tag{5.53}$$

$$\kappa(z,t) = K_1(\theta) = K_1\Big(\phi\big(t + z(\sigma(t) - t)\big)\Big), \tag{5.54}$$

$$\kappa(0,t) = K_1\big(\phi(t)\big) = K(t). \tag{5.55}$$

Using the infinite-dimensional states (5.48), (5.50), and (5.52), rewrite (5.47), plus the boundary condition, as

$$\frac{dp(z,t)}{dz} = \big(\sigma(t) - t\big)\big(\alpha(z,t)p(z,t) + \beta(z,t)\Pi(z,t)\big), \tag{5.56}$$

$$p(0,t) = P\big(\phi(t)\big) = X(t). \tag{5.57}$$

Solution to the system (5.56)–(5.57) is then

$$\begin{aligned} p(z,t) = e^{\int_0^z \alpha(s,t)\left(\sigma(t)-t\right)ds}\Big(p(0,t) \\ + \int_0^z e^{-\int_0^\tau \alpha(s,t)\left(\sigma(t)-t\right)ds}\beta(\tau,t)\Pi(\tau,t)\big(\sigma(t) - t\big)d\tau\Big). \end{aligned} \tag{5.58}$$

Now, define the backstepping transformation

$$W(z,t) = \Pi(z,t) - \kappa(z,t)p(z,t), \tag{5.59}$$

which, using expression (5.58), is

$$W(z,t) = \Pi(z,t) - \kappa(z,t)e^{\int_0^z \alpha(s,t)\left(\phi^{-1}(t)-t\right)ds} \cdot \Big(X(t) + \left(\phi^{-1}(t)-t\right)\int_0^z e^{-\int_0^\tau \alpha(s,t)\left(\phi^{-1}(t)-t\right)ds}\beta(\tau,t)\Pi(\tau,t)d\tau\Big). \tag{5.60}$$

Inverse transformation, $\left(X,W\right) \to \left(X,\Pi\right)$, is given as

$$\Pi(z,t) = W(z,t) + \kappa(z,t)e^{\int_0^z \left(\alpha(s,t)+\beta(s,t)\kappa(s,t)\right)\left(\phi^{-1}(t)-t\right)ds}X(t) + \left(\phi^{-1}(t)-t\right) \cdot \kappa(z,t)\int_0^z \Big(e^{\left(\phi^{-1}(t)-t\right)\left(\int_0^z \left(\alpha(s,t)+\beta(s,t)\kappa(s,t)\right)ds - \int_0^\tau \left(\alpha(s,t)+\beta(s,t)\kappa(s,t)\right)ds\right)} \cdot \beta(\tau,t)W(\tau,t)\Big)d\tau. \tag{5.61}$$

The procedure for the derivation of the inverse transformation (5.61) is given in Appendix B. Now, using expression (5.49), (5.51), and (5.53), the LTV system (5.32) is written as

$$\dot{X}(t) = \alpha(0,t)X(t) + \beta(0,t)\Pi(0,t). \tag{5.62}$$

Transport equations for the infinite-dimensional variables are:

$$\Pi_t(z,t) = \pi(z,t)\Pi_z(z,t), \tag{5.63}$$

$$\Pi(1,t) = U(t), \tag{5.64}$$

$$\alpha_t(z,t) = \pi(z,t)\alpha_z(z,t), \tag{5.65}$$

$$\alpha(1,t) = A(\phi^{-1}(t)), \tag{5.66}$$

$$\beta_t(z,t) = \pi(z,t)\beta_z(z,t), \tag{5.67}$$

$$\beta(1,t) = B(\phi^{-1}(t)), \tag{5.68}$$

$$\kappa_t(z,t) = \pi(z,t)\kappa_z(z,t), \tag{5.69}$$

$$\kappa(1,t) = K(\phi^{-1}(t)), \tag{5.70}$$

where propagation speed of the transport equations is

$$\pi(z,t) = \frac{1 + z\left(\frac{d(\phi^{-1}(t))}{dt} - 1\right)}{\phi^{-1}(t) - t}. \tag{5.71}$$

System (5.62)–(5.64) constitutes a PDE-ODE cascade system. The output of the transport PDE (5.63) and its boundary input (5.64) acts as a time-varying delay input (5.49) into the ODE (5.62).

Evaluating $W_z(z,t)$ and $W_t(z,t)$ using (5.60) gives the dynamics of $W(z,t)$. This, together with (5.62), evaluated using $\Pi(0,t)$ from (5.61) and inserting (5.51), (5.53), and (5.55), gives the target system:

$$\dot{X}(t) = \big(A(t) + B(t)K(t)\big)X(t) + B(t)W(0,t), \tag{5.72}$$

$$W_t(z,t) = \pi(z,t)W_z(z,t), \tag{5.73}$$

$$W(1,t) = 0. \tag{5.74}$$

To obtain the BC (5.74), evaluate (5.60) at $z = 1$ and use expression (5.64) to obtain $U(t)$ on the right hand side. Evaluate the same $U(t)$ using (5.35), (5.39), and (5.44).

The PDE–ODE cascade system (5.62)–(5.64) is transformed into the target system (5.72)–(5.74) using transformation (5.60). Since the backstepping transformation is invertible, please see expressions (5.60)–(5.61), proving stability of the target system in the transformed variables (X, W) implies stability of the system in the variables (X, U). Important results, such as the control law and the stability theorem, are now stated.

5.6. Main Results and Stability Theorem

Evaluate the backstepping transformation (5.60) at $z = 1$. In light of (5.74), and using the definition of the infinite-dimensional states (5.50)–(5.55), the intermediate control becomes

$$\begin{aligned} U(t) = {} & K\big(\phi^{-1}(t)\big)e^{\int_{\phi(t)}^{t} \frac{A(\phi^{-1}(\tau))}{\phi'(\phi^{-1}(\tau))}d\tau} \\ & \cdot \Big(X(t) + \int_{\phi(t)}^{t} e^{-\int_{\phi(t)}^{\tau} \frac{A(\phi^{-1}(s))}{\phi'(\phi^{-1}(s))}ds} \frac{B(\phi^{-1}(\tau))U(\tau)}{\phi'\big(\phi^{-1}(\tau)\big)}d\tau\Big). \end{aligned} \tag{5.75}$$

Using definitions (5.30) and (5.31), the boundary controller can be written as

$$\begin{aligned} u(t) = {} & \big(1 - v(t)\big)y_x(0,t) + K\big(\phi^{-1}(t)\big)e^{\int_{\phi(t)}^{t} \frac{A(\phi^{-1}(\tau))}{\phi'(\phi^{-1}(\tau))}d\tau} \\ & \cdot \Bigg(\Big[y_t\big(l(t),t\big) - v(t)\Big(u\big(\phi(t)\big) - \Big(1 - v\big(\phi(t)\big)\Big)y_x\big(0,\phi(t)\big)\Big)\Big] \\ & + \int_{\phi(t)}^{t} e^{-\int_{\phi(t)}^{\tau} \frac{A(\phi^{-1}(s))}{\phi'(\phi^{-1}(s))}ds} \frac{B(\phi^{-1}(\tau))\Big(u\big(\tau\big) - \big(1 - v(\tau)\big)y_x(0,\tau)\Big)}{\phi'\big(\phi^{-1}(\tau)\big)}d\tau\Bigg), \end{aligned} \tag{5.76}$$

where $A(t)$ and $B(t)$ can be obtained from (5.33)–(5.34) for $a(t)$ and $b(t)$ as per (5.27)–(5.28). The update gain in (5.75) and (5.76) is

$$K(t) = -\frac{1}{2}B(t)\Big(R(t) + 1\Big), \tag{5.77}$$

where $R(t) \in \mathbb{R}$ is a solution to the Riccati differential equation (RDE):

$$\dot{R}(t) + 2R(t)A(t) - R^2(t)B^2(t) + Q(t) = 0, \tag{5.78}$$

and where $Q(t) \in \mathbb{R}$ is to be determined from the stability analysis.

Two important prepositions concerning system $\big(A(t), B(t)\big)$ are further stated.

Preposition 5.9. Since $A(t)$ and $B(t)$ are differentiable on $\mathbb{R}_+$, please see Assumption 5.5, definitions (5.33)–(5.34) and (5.27)–(5.27), and $B(t) \neq 0$, then system $\big(A(t), B(t)\big)$ is Globally-Null Controllable (GNC) in finite time Phat (2006).

Preposition 5.10. Since system $\big(A(t), B(t)\big)$ is GNC in finite time, for any $Q(t) \in \mathbb{R}_{\geq 0}$ the associated RDE (5.78) has a solution $R(t) \in \mathbb{R}_{\geq 0}$ Phat (2006). Furthermore, $R(t)$ is bounded:

$$\sup_{t \in \mathbb{R}_+} ||R(t)||_\infty = \overline{R} < +\infty, \tag{5.79}$$

where the over-bar $\overline{(\cdot)}$ and the underline $\underline{(\cdot)}$ denote the maximum and the minimum bounds, respectively.

Remark 5.11. Please notice that control law (5.75) calls for the future values of $K\big(\phi^{-1}(t)\big)$, $A\big(\phi^{-1}(t)\big)$, and $B\big(\phi^{-1}(t)\big)$. These values are available as per Assumption 5.5–5.6. In practice, the RDE (5.78) is to be solved on a time interval $t_f = \phi^{-1}(t) \to 0$ for a terminal value $R(t_f) = R_f$ which can be obtained by solving Riccati Algebraic Equation (ARE), RDE (5.78) with $\dot{R}(t) = 0$ and $t = t_f$.

The main stability theorem is now stated.

Theorem 5.12. Consider a closed-loop system comprised of system (5.1)–(5.3), the control law (5.75) under Assumptions 5.5–5.7. There exist constants $\lambda > 0$ and $\Lambda_0 > 0$

such that the following inequality holds

$$\Upsilon(t) \leq \Lambda_0 e^{-\lambda t}\Upsilon(0), \quad \forall t > 0, \tag{5.80}$$

for

$$\begin{aligned}
\Upsilon(t) = &\Big(y_t\big[l(t),t\big] - v(t)\Big(u\big[\phi(t)\big] - \Big(1 - v\big[\phi(t)\big]\Big)y_x\big[0,\phi(t)\big]\Big)\Big)^2 \\
&+ \int_0^1 \Bigg(u\Big[\phi\big(\varrho(z,t)\big)\Big] - \Big(1 - v\Big[\phi\big(\varrho(z,t)\big)\Big]\Big)y_x\Big[0,\phi\big(\varrho(z,t)\big)\Big] \\
&\qquad - K\big[\varrho(z,t)\big]e^{\int_0^z A[\varrho(s,t)]\left(\phi^{-1}(t)-t\right)ds} \\
&\qquad \cdot \Big(y_t\big[l(t),t\big] - v(t)\Big(u\big[\phi(t)\big] - \Big(1 - v\big[\phi(t)\big]\Big)y_x\big[0,\phi(t)\big]\Big) \\
&\qquad + \big(\phi^{-1}(t) - t\big)\int_0^z e^{-\int_0^\tau A[\varrho(s,t)]\left(\phi^{-1}(t)-t\right)ds} B\big[\varrho(\tau,t)\big] \\
&\qquad \cdot \Big(u\big[\phi(\varrho(\tau,t))\big] - \big(1 - v\big[\phi(\varrho(\tau,t))\big]\big)y_x\big[0,\phi(\varrho(\tau,t))\big]\Big)d\tau\Bigg)\Bigg)^2 dz \\
&+ \int_0^{l(t)} \Bigg(\frac{2}{1 - v\big[t + f(x,t)\big]}y_x\big[l\big(t + f(x,t)\big), t + f(x,t)\big] \\
&\qquad - \frac{1 + v\big[t + f(x,t)\big]}{1 - v\big[t + f(x,t)\big]}\Big(u\big[\phi\big(t + f(x,t)\big)\big] \\
&\qquad - \big(1 - v\big[\phi\big(t + f(x,t)\big)\big]\big)y_x\big[0,\phi\big(t + f(x,t)\big)\big]\Big)\Bigg)^2 dx,
\end{aligned} \tag{5.81}$$

and where for conciseness $\varrho(z,t) = t + z\big(\phi^{-1}(t) - t\big)$.

I.e., the equilibrium of the closed-loop system is exponentially stable in the sense of the norm $\Upsilon(t)^{\frac{1}{2}}$. Furthermore,

$$\lim_{t\to\infty} y_t\big(l(t),t\big) = 0, \tag{5.82}$$

$$\lim_{t\to\infty} u(t) = 0. \tag{5.83}$$

Remark 5.13. Please observe that the control (5.75) calls for prior states, states evaluated at $t \in [\phi\big(t + f(0,t),t\big),0)$. In general, these states are not available. Once these states become accessible the system achieves closed-loop stability in accordance with Theorem 5.12.

5.7. Stability Proof

This section presents the proof of Theorem 5.12.

Proof of Theorem 5.12. Consider the Lyapunov-Krasovski functional

$$V(t) = \underbrace{\big(R(t)+1\big)X(t)^2}_{V_X(t)} + \underbrace{c_w \int_0^1 e^{hz} W(z,t)^2 dz}_{V_W(t)} + \underbrace{c_\xi \int_0^{l(t)} e^x \xi(x,t)^2 dx}_{V_\xi(t)}. \tag{5.84}$$

where $c_w > 0$, $c_\xi > 0$, and for

$$h \geq \Big(1 - \big(\dot{\phi^{-1}}(t)\big)\Big) \max\{1, \frac{1}{\big(\dot{\phi^{-1}}(t)\big)}\}. \tag{5.85}$$

Furthermore, for $h \geq 0$

$$\begin{aligned} &X(t)^2 + c_w \int_0^1 W(z,t)^2 dz + c_\xi \int_0^{l(t)} \xi(x,t)^2 dx \leq V(t) \\ &\leq \big(\overline{R}+1\big)X(t)^2 + c_w \int_0^1 e^h W(z.t)^2 dz + c_\xi \int_0^{l(t)} e^{\bar{l}} \xi(x,t)^2 dx. \end{aligned} \tag{5.86}$$

The functional $V(t)$ is positive definite, radially unbounded and decrescent. Using (5.77), (5.78), and Young's Inequality (A.3), the time derivative of $V_X(t)$ in (5.84) is

$$\dot{V}_X(t) \leq \big(Q(t) + 2A(t) - \epsilon_X\big)X(t)^2 + \Big(\frac{B(t)^2 R(t)^2}{\epsilon_X} + 1\Big)W(0,t)^2, \tag{5.87}$$

for $\epsilon_X > 0$. In a similar fashion, take the time derivative of $V_W(t)$ term in functional (5.84). Using the dynamics of the target system (5.73)–(5.74), and applying the Cauchy-Schwarz' Inequality (A.5), the derivative becomes

$$\dot{V}_W(t) \leq -c_w \pi_0 \beta_0 ||W(t)||^2 - c_w \pi_0 W(0,t)^2, \tag{5.88}$$

where

$$\beta(t) = \min\{h - 1 + \big(\dot{\phi^{-1}}(t)\big), (h+1)\big(\dot{\phi^{-1}}(t)\big) - 1\}, \tag{5.89}$$

and $\beta_0 = \underline{\beta(t)}$, and $\pi_0 = \underline{\pi(0,t)}$ as per (5.71). The derivation of the time derivative of $V_\xi(t)$ term of functional (5.84) can be found in Appendix D. The result is given as

$$\begin{aligned} \dot{V}_\xi(t) \leq &- c_\xi\big(1 - v(t)\big)||\xi(t)||^2 - c_\xi\big(1 - v(t)\big)\xi(0,t)^2 \\ &+ \frac{2c_\xi e^{l(t)}}{\big(1 - v(t)\big)^2}\Big(2 + \frac{1}{2}B(t)\big(R(t)+1\big)\big(1 - v(t)\big)\Big)^2 X(t)^2 \\ &+ 2c_\xi e^{l(t)} W(0,t)^2, \end{aligned} \tag{5.90}$$

Collecting individual terms of (5.84), as found in expressions (5.87), (5.88), and (5.90), the time derivative of the Lyapunov-Krasovski functional $V(t)$ can be written as

$$\begin{aligned}\dot{V}(t) \leq & \left(-\underline{Q} + 2\overline{|A|} + \epsilon_X + 4c_\xi e^{\bar{l}} \left(\frac{4}{\left(1-\overline{|v|}\right)^2} + 0.25\overline{|B|}^2(\overline{R}+1)^2 \right) \right) X(t)^2 \\ & + \left(-c_w\pi_0 + \frac{\overline{|B|}^2(\overline{R}+1)^2}{\epsilon_X} + 1 + 2c_\xi e^{\bar{l}} \right) W(0,t)^2 \\ & - c_w\pi_0\beta_0||W(t)||^2 - c_\xi\big(1-v(t)\big)||\xi(t)||^2 - c_\xi\big(1-v(t)\big)\xi(0,t)^2.\end{aligned} \tag{5.91}$$

Now set

$$\epsilon_X = \frac{\overline{|B|}^2(\overline{R}+1)^2}{c_w\pi_0 - 1 - 2c_\xi e^{\bar{l}}}, \tag{5.92}$$

and collect likewise terms

$$\begin{aligned}\dot{V}(t) \leq & \left(-\underline{Q} + 2\overline{|A|} + \frac{16c_\xi e^{\bar{l}}}{\left(1-\overline{|v|}\right)^2} \right. \\ & \left. + \overline{|B|}^2(\overline{R}+1)^2 \left(\frac{1}{c_w\pi_0 - 1 - 2c_\xi e^{\bar{l}}} + c_\xi e^{\bar{l}} \right) \right) X(t)^2 \\ & - c_w\pi_0\beta_0||W(t)||^2 - c_\xi\big(1-v(t)\big)||\xi(t)||^2 - c_\xi\big(1-v(t)\big)\xi(0,t)^2.\end{aligned} \tag{5.93}$$

Set

$$c_w = \frac{1 + 2c_\xi e^{\bar{l}} + \frac{1}{c_\xi e^{\bar{l}}}}{\pi_0}, \tag{5.94}$$

such that

$$\begin{aligned}\dot{V}(t) \leq & \left(-\underline{Q} + 2\overline{|A|} + c_\xi e^{\bar{l}} \left(\frac{16}{\left(1-\overline{|v|}\right)^2} + 2\overline{|B|}^2(\overline{R}+1)^2 \right) \right) X(t)^2 \\ & - c_w\pi_0\beta_0||W(t)||^2 - c_\xi\big(1-v(t)\big)||\xi(t)||^2 - c_\xi\big(1-v(t)\big)\xi(0,t)^2.\end{aligned} \tag{5.95}$$

The above expression can be written as

$$\dot{V}(t) \leq -L_X\big(R(t)+1\big)X(t)^2 - \pi_0\beta_0c_w||W(t)||^2 - \big(1-\overline{|v|}\big)c_\xi||\xi(t)||^2, \tag{5.96}$$

where

$$L_X = \frac{1}{(\overline{R}+1)} \left(\underline{Q} - 2\overline{|A|} - c_\xi e^{\bar{l}} \left(\frac{16}{\left(1-\overline{|v|}\right)^2} + 2\overline{|B|}^2(\overline{R}+1)^2 \right) \right). \tag{5.97}$$

Setting $\underline{Q} > 2\overline{|A|}$, and since c_ξ is a free parameter, $L_X > 0$. Using the functional (5.84), now state

$$\dot{V}(t) \leq -\lambda V(t), \tag{5.98}$$

where

$$\lambda = \min\left\{L_X, \pi_0\beta_0, \left(1 - \overline{|v|}\right)\right\}. \tag{5.99}$$

Recall that by Assumption 5.5, $|v(t)| < 1$. Finally,

$$V(t) \leq e^{-\lambda t}V(0), \tag{5.100}$$

Assuming finite prior and initial conditions, and using definitions (5.2), (5.30), (5.31), (5.6), (5.48), and (5.60), results in $V(0)$ being finite and bounded.

The definition (5.84) allows one to write further

$$V(t) \geq X(t)^2, \tag{5.101}$$

$$\frac{V(t)}{c_w} \geq ||W(t)||^2, \tag{5.102}$$

$$\frac{V(t)}{c_\xi} \geq ||\xi(t)||^2. \tag{5.103}$$

Assumptions 5.5–5.6 and definitions (5.27)–(5.28) guarantee boundedness of $a(t)$ and $b(t)$. This in turn gives us boundedness of $A(t)$ and $B(t)$ using (5.33)–(5.34). Bounded $R(t)$ gives bounded $K(t)$ as per (5.77). In light of the above, the definitions (5.50), (5.52), and (5.54), together with (5.36), (5.40), and (5.41), the boundedness of $||\alpha(t)||$, $||\beta(t)||$, and $||\kappa(t)||$ is stated.

From the transformation (5.60) and the inverse (5.61), bounded $l(t)$ from Assumption 5.5, and for sufficiently large and positive constants r_1, r_2, and s_1, s_2, it can be shown that

$$||W(t)||^2 \leq r_1 X(t)^2 + r_2||\Pi(t)||^2, \tag{5.104}$$

$$||\Pi(t)||^2 \leq s_1 X(t)^2 + s_2||W(t)||^2. \tag{5.105}$$

Bounded $||\Pi(t)||$ implies bounded control $|U(t)|$ in accordance with expression (5.48). From the definition of the state (5.30), control (5.2), and (5.31) one obtains bounded $|y_t\big(l(t), t\big)|$, $|y_t(0,t)|$, and $|y_x(0,t)|$. Bounded $|\dot{X}(t)|$ comes from (5.32). Using (5.101) and (5.102) in the expression (5.105) gives

$$||\Pi(t)||^2 \leq \left(s_1 + \frac{s_2}{c_w}\right)V(t). \tag{5.106}$$

The inequality (5.80) can now be proven. Please notice that (5.81) can be written as

$$\Upsilon(t) = X(t)^2 + \int_0^1 \Pi(z,t)^2 dz + \int_0^{l(t)} \xi(x,t)^2 dx. \tag{5.107}$$

Using expressions (5.101), (5.103), and (5.106), in (5.107) gives

$$\Upsilon(t) \leq \Lambda V(t), \tag{5.108}$$

where

$$\Lambda = 1 + s_1 + \frac{1}{c_\xi} + \frac{s_2}{c_w}. \tag{5.109}$$

Starting from functional (5.84), together with (5.104), results in

$$V(t) \leq \bar{\Lambda} \Upsilon(t), \tag{5.110}$$

where

$$\bar{\Lambda} = \max\Big\{(\overline{R} + 1 + c_w r_1), c_w r_2 e^h, c_\xi e^{\bar{l}}\Big\}. \tag{5.111}$$

Evaluate (5.110) at $t = 0$, and together with (5.100) state

$$V(t) \leq \bar{\Lambda} \Upsilon(0). \tag{5.112}$$

Inserting (5.112) into (5.108) finally gives the inequality (5.80) for $\Lambda_0 = \Lambda\bar{\Lambda}$. □

The stability analysis can now be extended to the in-domain states, $y_t(x,t)$ and $y_x(x,t)$. Considering (5.13), (5.7), (5.31), and boundary input (5.2), write

$$\eta(x,t) = U\big(t - g(x,t)\big). \tag{5.113}$$

Evaluate (5.64) at $t = t'$ and then at $t' = t - g(x,t)$ to get

$$\Pi\big(1, t - g(x,t)\big) = U\big(t - g(x,t)\big). \tag{5.114}$$

Comparing expressions (5.113) and (5.114) allows one to state a relation between Riemann variable η and the state Π as:

$$\eta(x,t) = \Pi\big(1, t - g(x,t)\big). \tag{5.115}$$

Since $||\Pi(t)||$ is known to be bounded by (5.105), so must be its boundary state at an earlier time, see right hand side of (5.115). This implies boundedness of $||\eta(t)||$. From

(5.6) and (5.7), an explicit expressions for $y_t(x,t)$ and $y_x(x,t)$ can be obtained as

$$\xi(x,t) - \eta(x,t) = 2y_x(x,t), \tag{5.116}$$

$$\big(1 - v(t)\big)\xi(x,t) + \big(1 + v(t)\big)\eta(x,t) = 2y_t(x,t). \tag{5.117}$$

Using the definition of a norm finally gives

$$||\xi(t)|| + ||\eta(t)|| \geq 2||y_x(t)||, \tag{5.118}$$

$$\big(1 - v(t)\big)^2||\xi(t)|| + \big(1 + v(t)\big)^2||\eta(t)|| \geq 2||y_t(t)||. \tag{5.119}$$

The boundedness of the in-domain states, $y_x(x,t)$ and $y_t(x,t)$, is due to that of $||\xi(t)||$, based on the Lyapunov analysis and the boundedness of $||\eta(t)||$ established from that of $||\Pi(t)||$ and the relation (5.115).

5.8. Numerical Results

The explicit FDM is used to simulate the closed loop system comprised of (5.1)–(5.3) and the control law (5.75). The simulation utilizes $\Delta t = 0.005$ and $\Delta z = 0.1$. Please see Chapter 6 for a more detailed overview of the numerical analysis employed in the simulations. In accordance with Assumption 5.5 the velocity profile is set to

$$v(t) = \begin{cases} -1.40030 \cdot 10^{-5}\, t^6 + 4.20076 \cdot 10^{-4}\, t^5 \\ -4.20063 \cdot 10^{-3}\, t^4 + 1.40017 \cdot 10^{-2}\, t^3 & 0 \leq t \leq 10 \\ 0 & t > 10. \end{cases} \tag{5.120}$$

The length of the string, its velocity, and the acceleration are given in Figure 5.2. The time-varying coefficients $A(t)$ and $B(t)$ are shown in Figure 5.3. Figure 5.4 illustrates the delay function $\phi(t)$, its inverse $\phi^{-1}(t)$, and the delay $g\big(l(t),t\big)$. The RDE input, set to $Q(t) = 2|A(t)| + 50$, and the resulting solution $R(t)$ can bee seen in Figure 5.5. Finally, the initial conditions for $x \in [0,1]$ at $t = 0$ are set to $y(x,0) = -0.25\sin(3\pi x)$ and $y_t(x,0) = 0.5\sin(4.5\pi x)$.

Figure 5.6 gives the resultant bottom boundary velocity $y_t\big(l(t),t\big)$ for: a) proposed boundary controller (5.76), b) free boundary condition $u(t) = \big(1 - v(t)\big)y_x(0,t)$.

In Figure 5.7 the required control input $u(t)$ as per (5.75) is shown for both cases. Finally, Figure 5.8 and Figure 5.9 illustrate the motion of the string-mass system for the proposed controller. The total string displacement is given as a 3D plot in Figure 5.8. The profile motion of the system is shown in Figure 5.9 for $t = 0 : 0.5 : 10$.

5.9. Discussion

The boundary control of a string-mass system with a time-variable length has been successfully illustrated using the most general case where the string velocity is a function of time. The restrictions placed on the velocity profile are minimal and lend themselves to a reasonable simulation of a problem where the string is extended or retracted in any practical applications. The delay control method for an LTI system with a variable input delay has been extended to an LTV system describing the dynamics of the mass. However, the stability of the system depends on the validity of the Prepositions (5.9)–(5.10). The numerical simulations appear to support the analysis. While the analytic derivation of the delay function may not in general be possible, one can rely on the numerical methods to solve equation (5.15). While the derived controller requires future values of parameters $A(t)$ and $B(t)$, these, under Assumptions 5.5–5.6, are available and can be computed offline. The control gain $K(t)$ can then be obtained from (5.77) where, for sufficiently large $Q(t)$, $R(t)$ is a positive solution of the RDE (5.78).

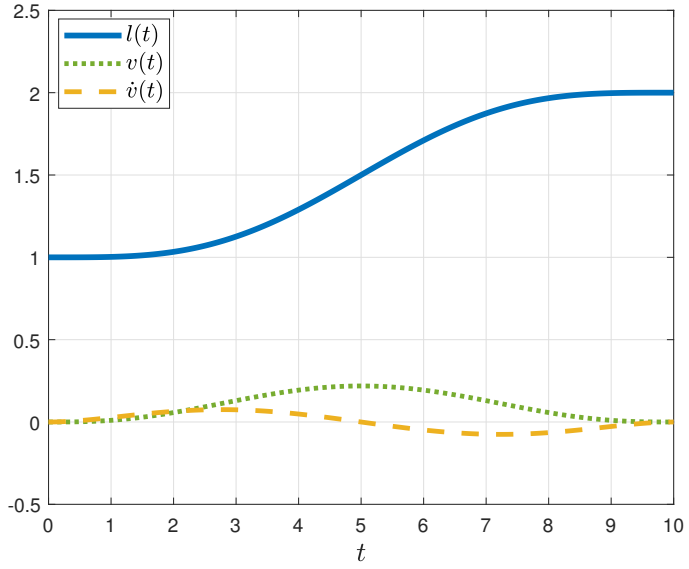

Figure 5.2. String length $l(t)$, velocity $v(t)$, and acceleration $\dot{v}(t)$.

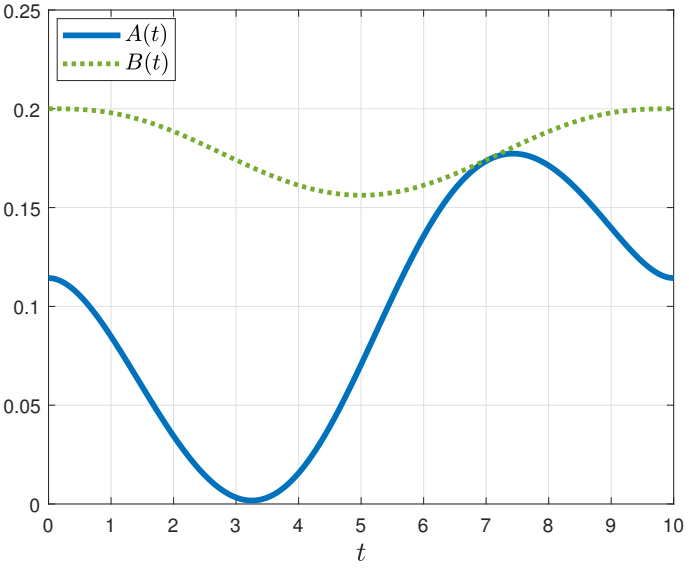

Figure 5.3. Time-varying parameters $A(t)$ and $B(t)$.

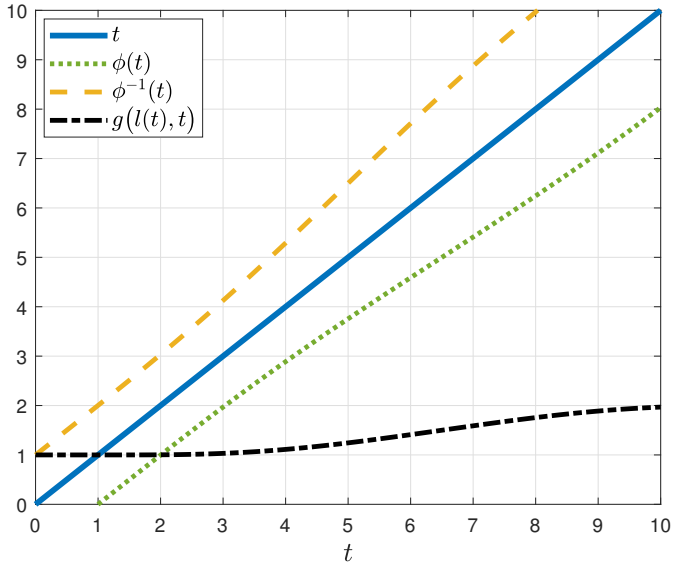

Figure 5.4. Delay function $\phi(t)$, its inverse $\phi^{-1}(t)$, and the delay $g\big(l(t),t\big)$.

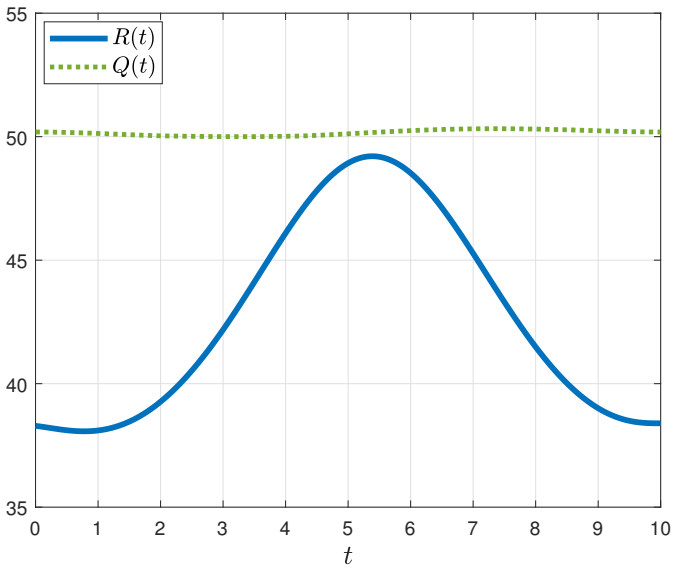

Figure 5.5. Riccati differential equation solution $R(t)$ and input $Q(t)$.

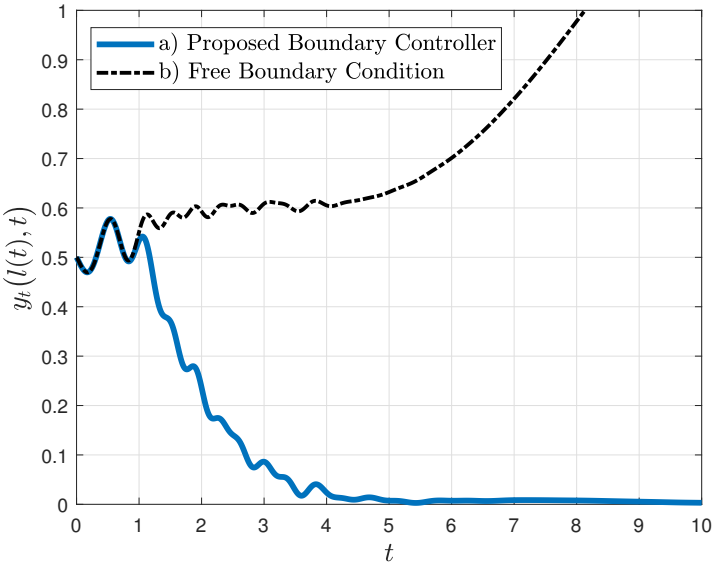

Figure 5.6. Boundary velocity $y_t\big(l(t),t\big)$ for: a) Proposed Boundary Controller (5.76), b) Free Boundary Condition $u(t) = \big(1 - v(t)\big)y_x(0,t)$.

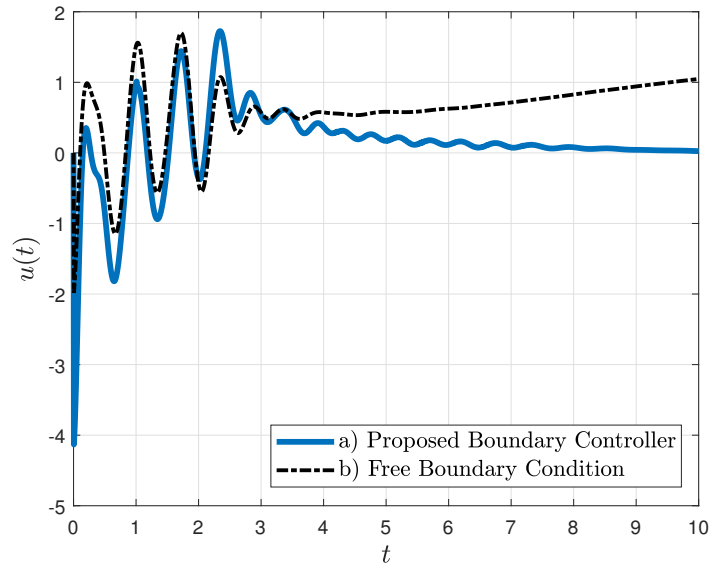

Figure 5.7. Control input $u(t)$ for: a) Proposed Boundary Controller (5.76), b) Free Boundary Condition $u(t) = \big(1 - v(t)\big)y_x(0,t)$.

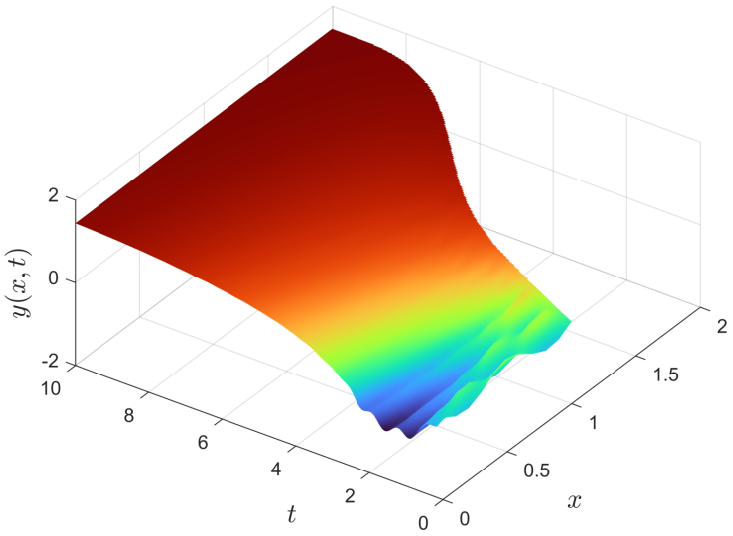

Figure 5.8. Total string displacement $y(x,t)$.

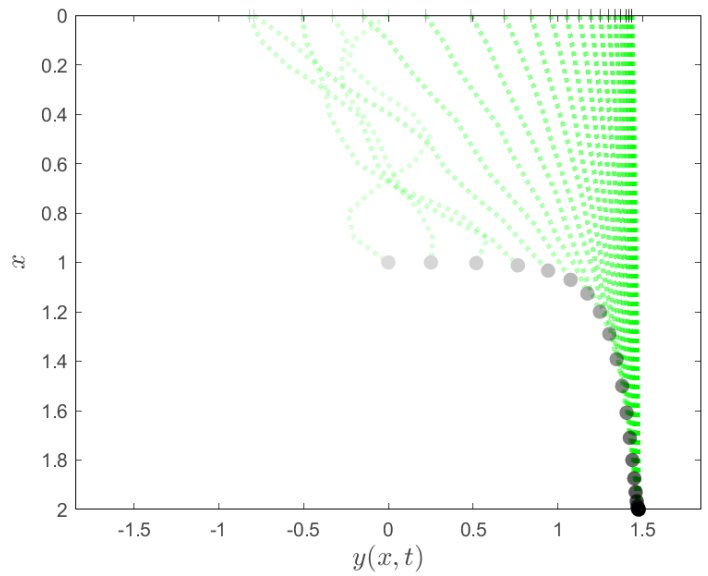

Figure 5.9. String motion, $t = 0 : 0.5 : 10$. Lighter lines correspond to earlier time frames.

6. NUMERICAL ANALYSIS

6.1. Introduction

The numerical methods have been successfully applied to solve PDEs in various scientific fields. Here, the finite-difference method has been used to simulate the string-mass system on a domain with a constant as well as a moving boundary.

The FDM uses finite differences to approximate the derivatives of a continuous PDE. When the spatial and temporal domains are discretized, the values at the nearby points are used to calculate the derivatives. As such, a continuous PDE is transformed into a system of linear equations. This system is then solved giving the value of the function at each discrete point. In the explicit FDM, one derives an explicit formula for a value of a function at a particular point in terms of the earlier values. This formula is then applied at each spatial point to obtain the solution. The implicit FDM solves a system of equations for all points at a particular time. While the explicit method is simpler to implement than the implicit one, it is also prone to numerical instabilities due to a potential build-up of the round-off error. The numerical results given previously are all based on the explicit FDM. A more comprehensive overview of the method will be presented in this chapter. First however, the nature of the variable domain associated with a moving boundary has to be addressed.

6.2. Domain Transformation

Since the domain of the problem (2.42)–(2.44) for $v(t) \neq 0$ is not constant but varies with time, it is convenient to transform the problem into a one on a constant domain. This is achieved by introducing a new function $Z(z,t)$ and a domain variable $z \in [0,1]$ such that

$$y(x,t) = Z(z,t), \tag{6.1}$$

$$z = \frac{x}{l(t)}. \tag{6.2}$$

Taking the partial derivative of $Z(z,t)$ with respect to z gives

$$\frac{\partial Z(z,t)}{\partial z} = \frac{\partial y(x,t)}{\partial z} = \frac{\partial y}{\partial x}\frac{\partial x}{\partial z} + \frac{\partial y}{\partial t}\frac{\partial t}{\partial z}. \tag{6.3}$$

Since $\frac{\partial t}{\partial z} = 0$ and $\frac{\partial x}{\partial z} = l(t)$, the above expression gives the partial derivative of $y(x,t)$ with respect to spatial variable x as follows

$$y_x(x,t) = \frac{1}{l(t)} Z_z(z,t). \tag{6.4}$$

Using the same procedure, and by taking the partial derivative with respect to z of the expression (6.3), results in

$$y_{xx}(x,t) = \frac{1}{l(t)^2} Z_{zz}(z,t). \tag{6.5}$$

By taking the partial derivative of $Z(z,t)$ with respect to time, and in light of $\frac{\partial x}{\partial t} = zv(t)$, one obtains

$$y_t(x,t) = Z_t(z,t) - \frac{zv(t)}{l(t)} Z_z(z,t). \tag{6.6}$$

In the same manner, and using expressions (6.4)–(6.5), it can be shown that

$$y_{tx} = \frac{1}{l(t)} Z_{zt}(z,t) - \frac{zv(t)}{l(t)^2} Z_{zz}(z,t) - \frac{v(t)}{l(t)^2} Z_z(z,t). \tag{6.7}$$

Finally, taking the partial derivative with respect to time of equation (6.6) and using the definition of the total derivative and expression (6.7) gives

$$\begin{aligned} y_{tt} = Z_{tt}(z,t) &- \frac{z\big(\dot{v}(t)l(t) - 2v(t)^2\big)}{l(t)^2} Z_z(z,t) \\ &- \frac{2zv(t)}{l(t)} Z_{zt}(z,t) + \frac{z^2 v(t)^2}{l(t)^2} Z_{zz}(z,t). \end{aligned} \tag{6.8}$$

Expressions (6.4)-(6.8) and (6.2) can be used to rewrite original equations of motion (2.42)-(2.44), including the input BC (3.4), (4.2), or (5.2), such that the domain of the transformed system is now constant. The transformed equations of motion are

$$\begin{aligned} &Z_{tt}(z,t) + \frac{2v(t)}{l(t)}(1-z)Z_{zt}(z,t) + \frac{c_\rho L_0}{\rho\sqrt{\frac{mg}{\rho}}} Z_t(z,t) - p\big(zl(t),t\big) \\ &+ \frac{1}{l(t)^2}\Big(v(t)^2(1-z)^2 - \big(\frac{m}{\rho} + \epsilon_\tau L_0 l(t)(1-z)\big)\big(\frac{\rho}{m} - \frac{\epsilon_a \dot{v}(t)}{L_0}\big)\Big) Z_{zz}(z,t) \\ &+ \frac{1}{l(t)^2}\Big(- 2v(t)^2(1-z) \\ &\qquad + l(t)\Big(\epsilon_\tau\big(\frac{L_0\rho}{m} - \dot{v}(t)\big) + (1-z)\big(\frac{c_\rho L_0 v(t)}{\rho\sqrt{\frac{mg}{\rho}}} + \dot{v}(t)\big)\Big)\Big) Z_z(z,t) = 0, \end{aligned} \tag{6.9}$$

$$Z_t(0,t) = u(t), \tag{6.10}$$

$$\begin{aligned} Z_{tt}(1,t) = &- \frac{L_0\rho}{m}\Big(\frac{c_m}{\rho\sqrt{\frac{mg}{\rho}}} + v(t)\Big)Z_t(1,t) \\ &- \frac{1}{l(t)}\Big(\frac{L_0\rho}{m} - \epsilon_a\dot{v}(t)\Big)Z_z(1,t) + P(1,t). \end{aligned} \tag{6.11}$$

The initial conditions, given $y(x,0)$ and $y_t(x,0)$, are as follows

$$Z(z,0) = y(x,0), \tag{6.12}$$

$$Z_t(z,0) = y_t(x,0) + zv(0)Z_z(z,0). \tag{6.13}$$

The above equations are valid on a domain $z \in [0,1]$. As such, these are now ready for discretization using finite-difference approximations of individual derivative terms.

6.3. Finite-Difference Approximation

The finite-difference approximation is an approximation of a derivative using values at a discrete set of points. This numerical technique allows one to write the governing equations (6.9)–(6.13) in terms of discrete formulas, which are then used in the numerical simulation of the string-mass system.

Using Taylor series expansion of a function, see (A.11), one can write

$$Z(z+\Delta z,t) = Z(z,t) + \Delta z Z_z(z,t) + \frac{1}{2!}(\Delta z)^2 Z_{zz}(z,t) + ... \tag{6.14}$$

and

$$Z(z-\Delta z,t) = Z(z,t) - \Delta z Z_z(z,t) + \frac{1}{2!}(\Delta z)^2 Z_{zz}(z,t) + ... \tag{6.15}$$

where Δz and Δt are space and time increments, respectively. Retaining only the linear terms in (6.14) and solving for the $Z_z(z,t)$ gives the forward-difference (FD) approximation of the first-order spatial derivative

$$Z_z(z,t) \approx \frac{Z(z+\Delta,t) - Z(z,t)}{\Delta z}. \tag{6.16}$$

The approximation is due to an omission of the higher order terms from the infinite Taylor expansion. Similarly, retaining only the linear terms and solving (6.15) for $Z_z(z,t)$ gives the backward-difference (BD) approximation of the first-order spatial

derivative

$$Z_z(z,t) \approx \frac{Z(z,t) - Z(z-\Delta,t)}{\Delta z}. \tag{6.17}$$

Taking average of the two gives the central-difference (CD) formula

$$Z_z(z,t) \approx \frac{Z(z+\Delta z,t) - Z(z-\Delta z,t)}{2\Delta t}. \tag{6.18}$$

The second time derivative approximation is obtained by adding (6.14) and (6.15) together, retaining only linear and quadratic terms, and solving for $Z_{zz}(z,t)$

$$Z_{zz}(z,t) \approx \frac{Z(z+\Delta z,t) - 2Z(z,t) + Z(z-\Delta z,t)}{(\Delta z)^2}. \tag{6.19}$$

The temporal derivatives are obtained in the same manner. The first-order derivative expressed using the central-difference, and the second-order time derivative are

$$Z_t(z,t) \approx \frac{Z(z,t+\Delta t) - Z(z,t-\Delta t)}{2\Delta t}, \tag{6.20}$$

$$Z_{tt}(z,t) \approx \frac{Z(z,t+\Delta t) - 2Z(z,t) + Z(z,t-\Delta t)}{(\Delta t)^2}. \tag{6.21}$$

The mixed derivative $Z_{zt}(z,t)$ can be expressed in various ways. Using central-difference approximation for both the space and the time, the derivative becomes

$$\begin{aligned} Z_{zt}(z,t) \approx \frac{1}{4\Delta t \Delta z}\Big(&Z(z+\Delta z,t+\Delta t) - Z(z-\Delta z,t+\Delta t) \\ &- Z(z+\Delta z,t-\Delta t) + Z(z-\Delta z,t-\Delta t)\Big). \end{aligned} \tag{6.22}$$

The domain of the problem is discretized by dividing the $z-t$ plane into a rectangular grid using assumed increments Δz and Δt. The coordinates of a function at a particular node within the domain can then be written as

$$z = (i-1)\Delta z, \qquad i = 1, 2, ..., N_z, \tag{6.23}$$

$$t = (n-1)\Delta t, \qquad n = 1, 2, ..., N_t. \tag{6.24}$$

Since the domain in z is already bounded, $z \in [0,1]$, $N_z = \frac{1}{\Delta z} + 1$. The temporal domain is bounded by assuming the maximum and finite time T. As such, $N_t = \frac{T}{\Delta t} + 1$.

Once the equations of motion are written in terms of the finite-difference approximations, an iterative process is used to solve for the value of the function at the next

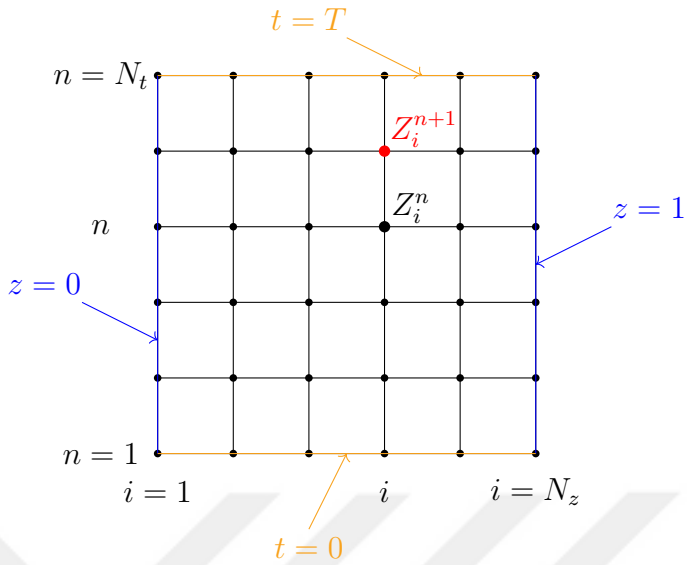

Figure 6.1. Discretized domain, current node Z_i^n, and the target node Z_i^{n+1}.

point in the domain, the target node. The target node will be denoted as Z_i^{n+1}. The index notation will be used from now on. Furthermore, the approximation sign, $\approx$, will be replaced with equality.

The range of the indices i and n represents the physical domain both in z and t as per Figure 6.1. The analysis, however, extends the range of the indices to include ghost nodes beyond the physical domain. Ghost nodes at $i = 0, i = N_z + 1$, as well as $n = 0$, corresponding to a prior state $t = -\Delta t$, are used. Ghost nodes allow one to use the central-difference approximation for the first derivative at the boundary. Two equations, the PDE and the BC, are solved for the two unknowns, the ghost node, and the target node. Given initial conditions $y(x, 0)$ and $y_t(z, 0)$ the prior state $Z_i^{n=0}$ can be obtained from (6.12)–(6.13) using BD approximation.

Two different discretization schemes are presented. The choice of the finite-difference formulas for each scheme is outlined in Table 6.1. For all schemes, the finite-difference formulas (6.18)–(6.21) are used. The major difference comes about in the choice of the finite-difference for the mixed derivative Z_{zt}. The first scheme utilizes CD for z and the BD in t for the mixed derivative, both for the in-domain and the boundary nodes at $n > 1$. This in turn requires one to solve and then store data for

the ghost nodes. For $n = 1$ the boundary node at $i = 1$ calls for BD in time and FD in space. Again at $n = 1$, the boundary node at $i = N_z$ uses BD in both space and time. The marching process in the first scheme is from $i = 1$ to $i = N_z$. The second scheme has two separate cases, one for $v \geq 0$ where the marching process is from $i = 1$ to $i = N_z$ and another one for velocity $v < 0$ where the marching process is from $i = N_z$ to $i = 1$.

The first case uses CD in t and BD in z in the PDE for $1 < i \leq N_z$. At $i = 1$, the mixed derivative has FD in space and BD in time. The second case uses CD in t and FD in z in the PDE for $1 \leq i < N_z$. At $i = N_z$, the mixed derivative has BD in both space and time. In general, for $N_z > i > 1$, the PDE needs to be solved for one unknown, the target node Z_i^{n+1}. At the boundary nodes, two equations, the PDE and the corresponding boundary conditions have to be solved for two unknowns, the target node, and the ghost node. However, only in two instances are the ghost nodes required for subsequent iterations. Please see the table note in Table 6.1. The last column of Table 6.1 gives the resultant stencil for the target node.

Finally, the equations of motion expressed using the finite-difference formulas are given in Appendix E. Furthermore, the same appendix provides the explicit formulas for the target nodes.

6.4. Finite-Difference Scheme Comparison and Instability

In the previous section, two finite-difference schemes were presented. The first one is a standard explicit scheme where the target node is calculated based on the values at the earlier time. In the second scheme, the formula for the target node includes a node located at the same temporal level, the same time. This is readily illustrated by the stencil for the target node, as seen in Table 6.1.

A comparison of the two schemes is given below. Unless noted otherwise, the parameters given in the numerical results of Chapter 5 are used throughout this anal-

ysis. Figure 6.2 gives the bottom boundary string velocity $y_t\big(l(t),t\big)$ for both schemes evaluated at $\Delta t = 0.005$ and $\Delta z = 0.1$. Since $v \geq 0$, scheme two defaults to case 1, where $i = 1:1:N_z$. Figure 6.3 gives the same data for increments $\Delta t = 0.001$ and $\Delta z = 0.05$.

Table 6.1. Finite-difference schemes.

Scheme	**March Direction**	**n**	**i**	$\mathbf{Z_{zt}}$	**Equations**	**Ghost Node**	**Stencil, for Z_i^{n+1}**
1	$i = 1:1:N_z$	$n = 1$	$i = 1$	BD in t, FD in z	PDE +BC($z = 0$)	Z_0^{1*}	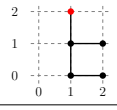
			$N_z > i > 1$	BD in t, CD in z	PDE	—	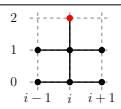
			$i = N_z$	BD in t, BD in z	PDE +BC($z = 1$)	$Z_{N_z+1}^1$	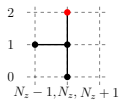
		$n > 1$	$i = 1$	BD in t, CD in z	PDE +BC($z = 0$)	Z_0^{n*}	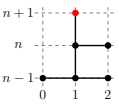
			$N_z > i > 1$		PDE	—	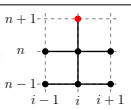
			$i = N_z$		PDE +BC($z = 1$)	$Z_{N_z+1}^n$	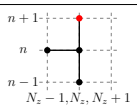
2	$v \geq 0$, $i = 1:1:N_z$	$n \geq 1$	$i = 1$	BD in t, FD in z	PDE +BC($z = 0$)	Z_0^n	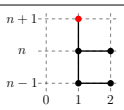
			$N_z > i > 1$	CD in t, BD in z	PDE	—	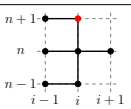
			$i = N_z$		PDE +BC($z = 1$)	$Z_{N_z+1}^n$	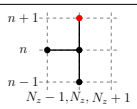
	$v < 0$, $i = N_z:-1:1$	$n \geq 1$	$i = 1$	CD in t, FD in z	PDE +BC($z = 0$)	Z_0^n	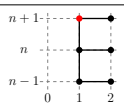
			$N_z > i > 1$		PDE	—	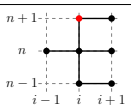
			$i = N_z$	BD in t, BD in z	PDE +BC($z = 1$)	$Z_{N_z+1}^n$	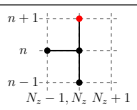

* These ghost nodes require storage for subsequent iterations.

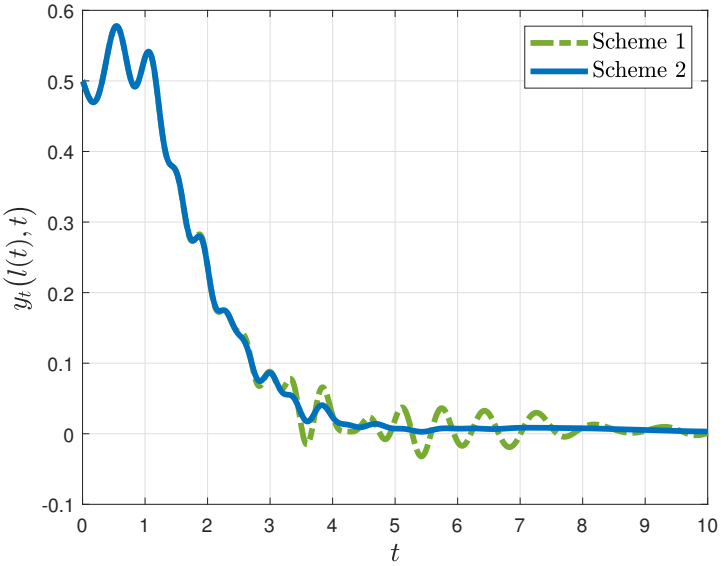

Figure 6.2. Boundary velocity $y_t\big(l(t),t\big)$ for schemes 1 and 2 at $\Delta t = 0.005$ and $\Delta z = 0.1$.

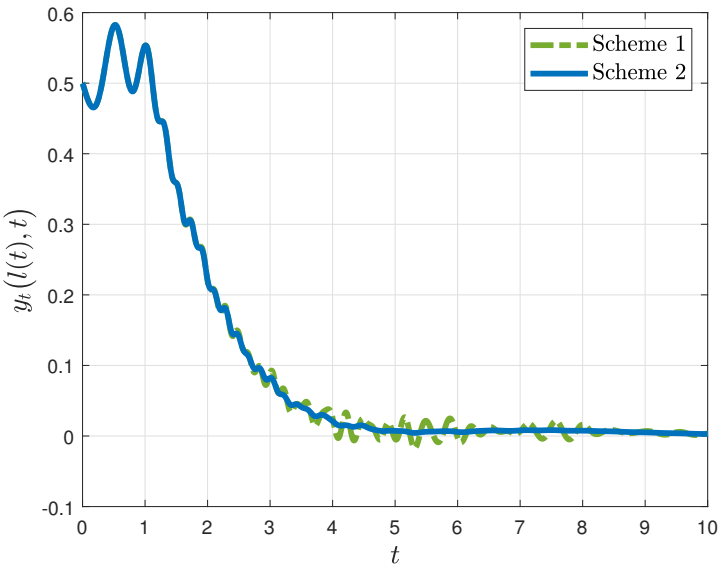

Figure 6.3. Boundary velocity $y_t\big(l(t),t\big)$ for schemes 1 and 2 at $\Delta t = 0.001$ and $\Delta z = 0.05$.

The convergence of the solution is much faster when scheme 2 is utilized. This is true in both cases. Please see Figure 6.2 and Figure 6.3. Furthermore, scheme 1 at $\Delta t = 0.001$ and $\Delta z = 0.05$ under-performs the output of scheme 2 at $\Delta t = 0.005$ and $\Delta z = 0.1$. This behavior can be glanced at when comparing both figures. The

superior performance of scheme 2 extends to all simulations where $v \neq 0$. It is not just the feature of this particular example. Please notice that scheme 2 comes with two separate cases differentiated by the direction of the marching process. For the string velocity $v \geq 0$, the marching process is from $i = 1$ to $i = N_z$. For the string velocity $v < 0$, an opposite marching process is used. Figure 6.4 illustrates the output of the simulation using scheme 2 for case $v \geq 0$ but with a reversed marching direction $i = N_z : -1 : 1$. Plot for the forward-marching direction, $i = 1 : 1 : N_z$, is given for reference. The bottom boundary velocity appears to oscillate about the zero value with increasing amplitude. The oscillations appear to be unrelated to the size of the increments Δt and Δz. Moreover, Figure 6.5, where the total string displacement is given, shows the same behavior taking place not only at $i = N_z$ associated with $y\big(l(t), t\big)$ and $y_t\big(l(t), t\big)$, but at each spatial node.

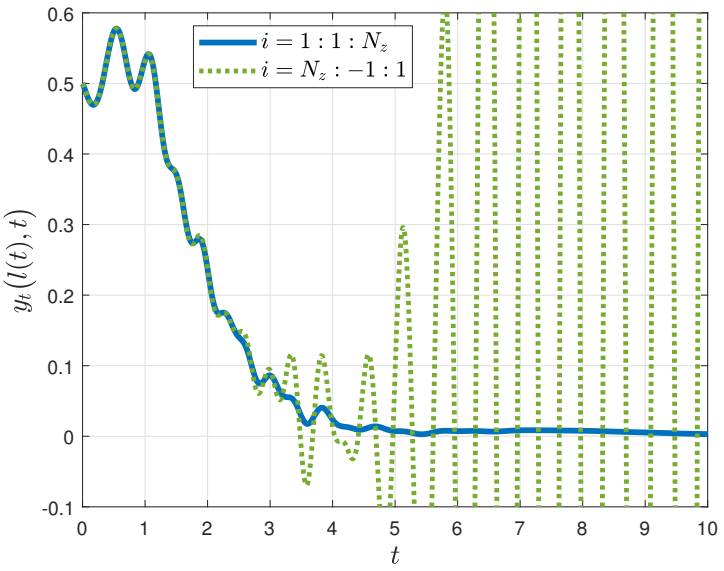

Figure 6.4. Boundary velocity $y_t\big(l(t), t\big)$ as per scheme 2, where $v \geq 0$, $\Delta t = 0.001$, and $\Delta z = 0.1$, for the forward-marching direction $i = 1 : 1 : N_z$ and for the backward-marching direction $i = N_z : -1 : 1$.

Observe that the oscillations are independent of the nature of the control. Figure 6.6 and Figure 6.7 give the output for a stable boundary dynamics with $c_m = 0$, where the top of the string is free to move: $U = 0$ and fixed: $y_t(0, t) = 0$, respectively. When

backward-marching direction is used for $v \geq 0$, the osculations inevitably appear. Identical behavior shows up for $v < 0$ case where forward-marching direction is used.

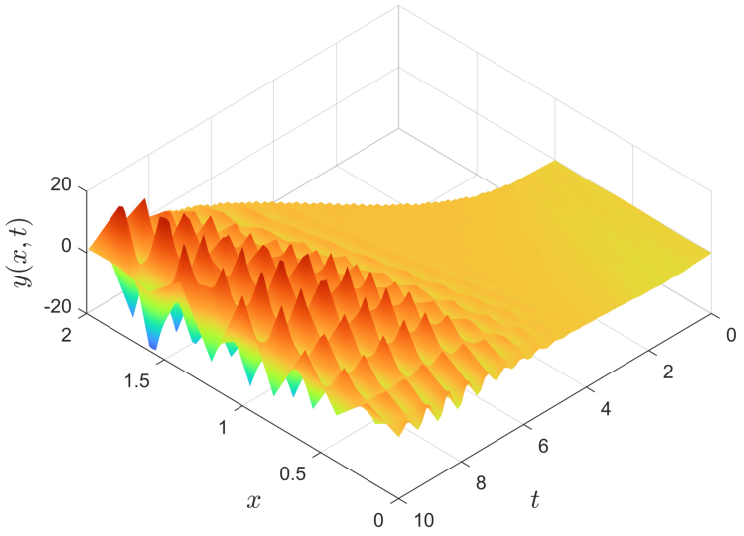

Figure 6.5. Total string displacement $y(x,t)$ as per scheme 2, where $v \geq 0$, $\Delta t = 0.005$, and $\Delta z = 0.1$, for the backward-marching direction $i = N_z : -1 : 1$.

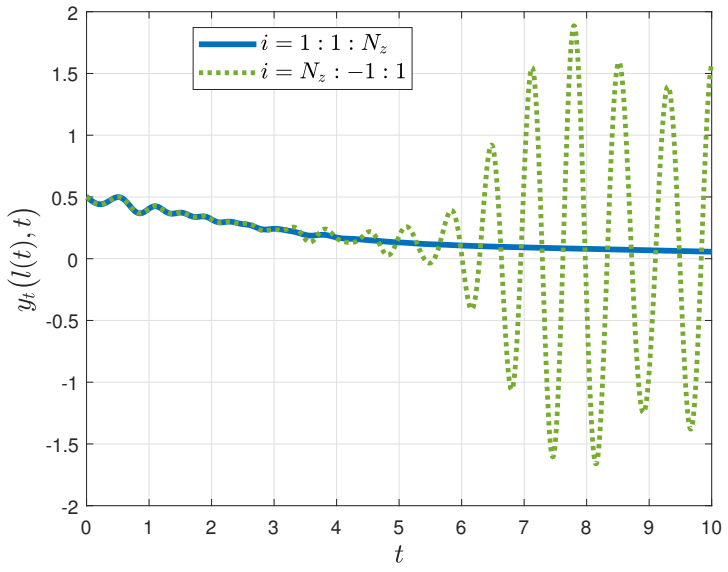

Figure 6.6. Boundary velocity $y_t\big(l(t),t\big)$ as per scheme 2, where $v \geq 0$, $\Delta t = 0.005$, $\Delta z = 0.1$, $c_m = 0$, and free top BC: $U = 0$, for the forward-marching direction $i = 1:1:N_z$ and for the backward-marching direction $i = N_z : -1 : 1$.

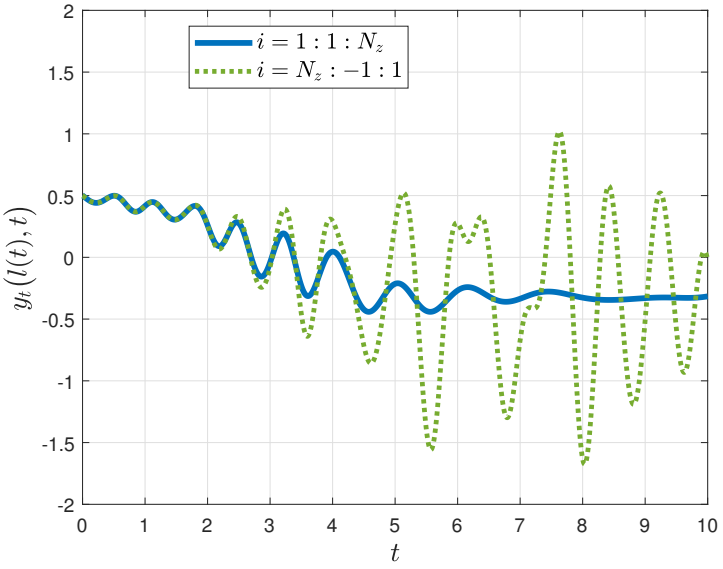

Figure 6.7. Boundary velocity $y_t\big(l(t),t\big)$ as per scheme 2, where $v \geq 0$, $\Delta t = 0.005$, $\Delta z = 0.1$, $c_m = 0$, and fixed top BC: $y_t(0,t) = 0$, for the forward-marching direction $i = 1:1:N_z$ and for the backward-marching direction $i = N_z:-1:1$.

6.5. Discussion

The examination indicates a numerical instability associated with scheme 2 when the marching direction opposes the string's axial velocity. This pairing is an example of a downwind scheme. The downwind scheme is characterized by the usage of the larger number of downstream nodes than the upstream nodes in the calculation of the flow field. In general, the downwind schemes are numerically unstable. As an illustrative example, please see Figure 6.5. When the marching direction matches the velocity of the string, more upstream nodes are used, and the scheme is called an upwind scheme. Please see the stencils for the target nodes associated with scheme 2 for $N_z > i > 1$ as per Table 6.1. The upwind schemes for hyperbolic equations are only conditionally stable. For a simple, first order upwind scheme describing a 1D linear advection equation

$$\frac{\partial f}{\partial t} + v\frac{\partial f}{\partial x} = 0, \tag{6.25}$$

represented by either

$$\frac{n_i^{n+1} - n_i^n}{\Delta t} + v\frac{u_i^n - u_{i-1}^n}{\Delta x} = 0 \quad for \quad v > 0, \tag{6.26}$$

or

$$\frac{n_i^{n+1} - n_i^n}{\Delta t} + v\frac{u_{i+1}^n - u_i^n}{\Delta x} = 0 \quad for \quad v < 0, \tag{6.27}$$

the stability is conditioned upon the CFL (Courant-Friedrichs-Lewy) number defined by

$$\sigma = \left|\frac{v\Delta t}{\Delta x}\right|. \tag{6.28}$$

The CFL stability criterion then becomes

$$0 \leq \sigma \leq 1. \tag{6.29}$$

The above CFL stability can be readily verified using the Von Neumann method for stability analysis. More detailed overview of the subject can be found in Hirsch (2007). Clearly, in the above example, the differentiation of the schemes based on the direction of propagation matches the prescription found in Table 6.1 for scheme 2. However, stability analysis for initial, boundary value problem with complex boundary conditions can be quite complicated. No attempt is made here to derive the stability condition. The numerical results presented in this work are verified to converge by running successive simulations with different increment values.

7. CASE STUDY

7.1. Introduction

This chapter contains a numerical simulation. Previously derived controllers are used to control a load in the presence of the water waves. Unlike the preceding results, where the parameters were chosen to stress the pedagogy, this simulation is more comprehensive and based on a "realistic" disturbance model that utilizes parameters obtained from the experimental data. The analysis and the results in this chapter are presented using the original "bar" coordinates. The outcomes of the simulation, and the discussion that follows, should give the reader a better insight into a practical application of the research presented in this work.

7.2. Problem Statement

Consider an underwater sensor deployed into the sea from a surface vessel. The load is submerged up to a designated depth where it then loiters until stabilized to perform the desired sensing operation. The effect of sea waves on the sensor should be eliminated, as it represents an undesired disturbance. The deployment is then comprised of two stages. During the first extraction stage, the load is extended following a prescribed velocity profile $\bar{v}(\bar{t})$ up to time $\bar{t}_1$. It then remains at the desired depth until its lateral velocity falls below a specific limit at $\bar{t}_2$. Once the deployment is complete, the sensing operation can commence, $\bar{t} > \bar{t}_2$. Please see Figure 7.1 for a general overview.

The above system is considered under previously stated Assumptions: 2.1–2.3, 2.5–2.7, 3.6, 3.7, 3.9, and 5.1. As per Assumption 2.5 the power required for the actuation of the system is neglected in the analysis. Furthermore, the dynamics of the vessel and the effect of the water disturbances on the vessel itself are not considered, i.e., it is assumed that the vessel has the power to track required input velocity $\bar{y}_{\bar{t}}(0, \bar{t})$.

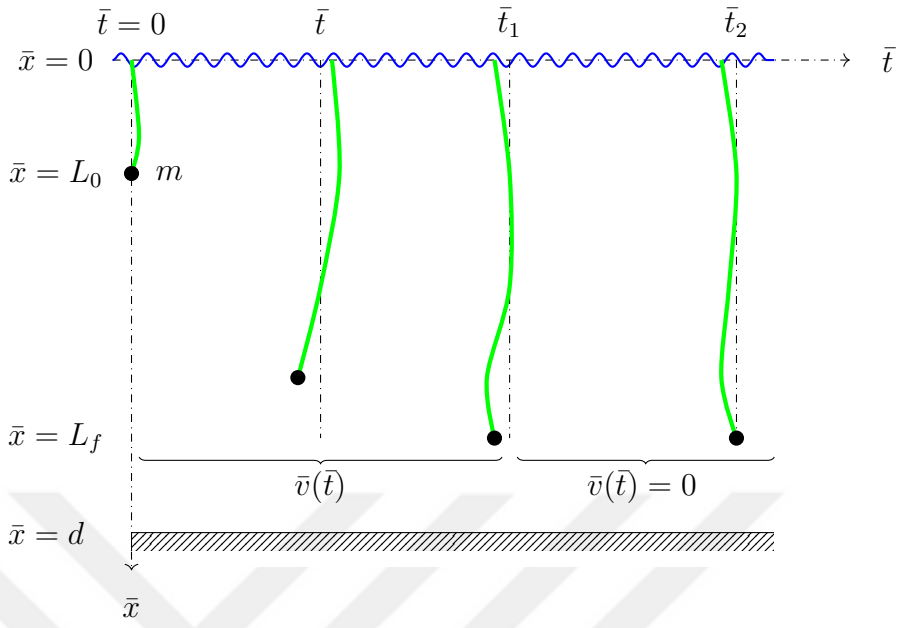

Figure 7.1. Underwater deployment and operation.

In addition, the following assumptions are stated:

Assumption 7.1. For the purpose of calculating the drag coefficient, the underwater sensor is assumed to be a smooth sphere of radius r_s. Similarly, the cable is a smooth cylinder of diameter d_c, Figure 7.2.

Assumption 7.2. The disturbance force F_d acting on a sphere and force per unit length f_d acting on a cylinder are due to the water flow/drag and are proportional to velocity square as per

$$F_d = \begin{cases} 0 & if\ v_r = 0, \\ -\frac{\bar{v}_r}{2|\bar{v}_r|}\rho_w(\pi r_s^2)c_{d_s}\bar{v}_r^2 & else, \end{cases} \tag{7.1}$$

$$f_d = \begin{cases} 0 & if\ v_r = 0, \\ -\frac{\bar{v}_r}{2|\bar{v}_r|}\rho_w d_c c_{d_c}\bar{v}_r^2 & else, \end{cases} \tag{7.2}$$

for the relative velocity $\bar{v}_r = \bar{y}_{\bar{t}} - \bar{v}_{\bar{y}}$, horizontal flow velocity $\bar{v}_{\bar{y}}$, water density ρ_w, and drag coefficients c_{d_s} and c_{d_c} for the sphere and the cylinder respectively. The damping parameters c_ρ and c_m are assumed to be zero and the the effect of damping/drag are incorporated into the definition of the disturbance.

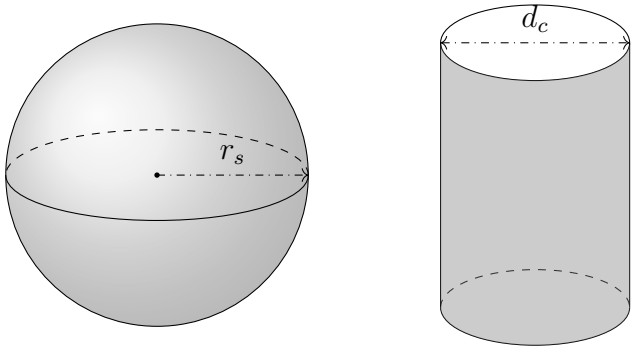

Figure 7.2. Geometry of the sensor, a sphere, and the cable, a cylinder.

Since the relative velocity v_r is anticipated to be around 10^0, together with typical values for the density and the dynamic viscosity of water, the resulting Reynolds's number ($Re \gg 1$). As such, the drag equation in Assumption 7.2 is that of square-law, and not the Stoke's drag which is linear in nature, Fox and McDonald (1999).

Under the above assumptions, it is desired to stabilize the lateral velocity $\bar{y}_{\bar{t}}(L_f, \bar{t})$ of the sensor m, below given threshold $\bar{y}_{\bar{t}_{max.}}$. This is done using the actuation input $\bar{u}(\bar{t}) = \bar{y}_{\bar{t}}(0, \bar{t})$.

7.3. Disturbance Modeling

The disturbance affecting the underwater sensor and the cable is modeled as water waves. The following assumptions are made about the problem:

Assumption 7.3. The fluid motion is assumed to be irrotational and the fluid to be incompressible. The effects of viscosity, surface tension, turbulence, or sea bed are neglected. Stoke's drift and water currents are not considered.

Assumption 7.4. The water waves are progressive and periodic in nature. Wave parameters such as the wave period T, the wavelength λ and the wave height h are assumed to be known. The depth of the sea bed d is known.

Assumption 7.5. The waves will be analyzed using the linear wave theory. It is assumed that $h \ll \lambda$ and $h \ll d$.

The analysis presented below mirrors the one found in Dean and Dalrymple (1991). Given the velocity vector $\mathbf{u} = \bar{v}_{\bar{x}}\,\mathbf{i} + \bar{v}_{\bar{y}}\,\mathbf{j}$, the periodic water waves under the Assumption 7.3 can be modeled using the continuity equation

$$\nabla \cdot \mathbf{u} = 0, \tag{7.3}$$

which under the definition of a potential function, $\mathbf{u} = -\nabla\phi$, such that $\bar{v}_{\bar{y}} = -\frac{\partial\phi}{\partial\bar{y}}$ and $\bar{v}_{\bar{x}} = -\frac{\partial\phi}{\partial\bar{x}}$, leads to the Laplace's equation

$$\nabla^2\phi = \frac{\partial^2\phi}{\partial\bar{x}^2} + \frac{\partial^2\phi}{\partial\bar{y}^2} = 0. \tag{7.4}$$

The equation (7.4) is the PDE describing the fluid. The boundary value problem is illustrated by Figure 7.3. The boundary conditions are stated as follows. At the sea bed, where $\bar{x} = d$, the flow is assumed to be along the horizontal direction only. This is then the bottom boundary condition (BBC) which can be expressed as

$$\frac{\partial\phi}{\partial\bar{x}}\Big|_{\bar{x}=d} = 0. \tag{7.5}$$

Since the problem is periodic in nature, please see Assumption 7.4, periodic lateral boundary conditions (PLBC) in space and time are used:

$$\phi(\bar{y},\bar{t}) = \phi(\bar{y}+\lambda,\bar{t}), \tag{7.6}$$

$$\phi(\bar{y},\bar{t}) = \phi(\bar{y},\bar{t}+T), \tag{7.7}$$

Finally, the boundary conditions describing the free wave surface are required. The kinematic free surface boundary condition (KFSBC) describing no flow across the surface, $\mathbf{u}\cdot\mathbf{n} = 0$ where $\mathbf{n}$ is the unit vector normal to the free surface, is stated as

$$\Big(\frac{\partial\phi}{\partial\bar{x}} = -\frac{\partial\eta}{\partial\bar{t}} + \frac{\partial\phi}{\partial\bar{y}}\frac{\partial\eta}{\partial\bar{y}}\Big)_{\bar{x}=\eta(\bar{y},\bar{t})}, \tag{7.8}$$

where $\eta(\bar{y},\bar{t})$ is the displacement of the free surface about the horizontal plane $\bar{x} = 0$. For reference, see Figure 7.3. The second surface BC is called the dynamic free surface boundary condition (DFSBC). It is a statement of a uniform pressure on the free surface along the wave form, which can be expressed using Bernoulli's equation

$$\Big(-\frac{\partial\phi}{\partial\bar{t}} + \frac{1}{2}\Big(\big(\frac{\partial\phi}{\partial\bar{y}}\big)^2 + \big(\frac{\partial\phi}{\partial\bar{x}}\big)^2\Big) - g\eta = C(\bar{t})\Big)_{\bar{x}=\eta(\bar{y},\bar{t})}, \tag{7.9}$$

where g is the gravitational acceleration constant, $C(\bar{t})$ is an integration "constant", and where the gauge pressure is assumed to be zero.

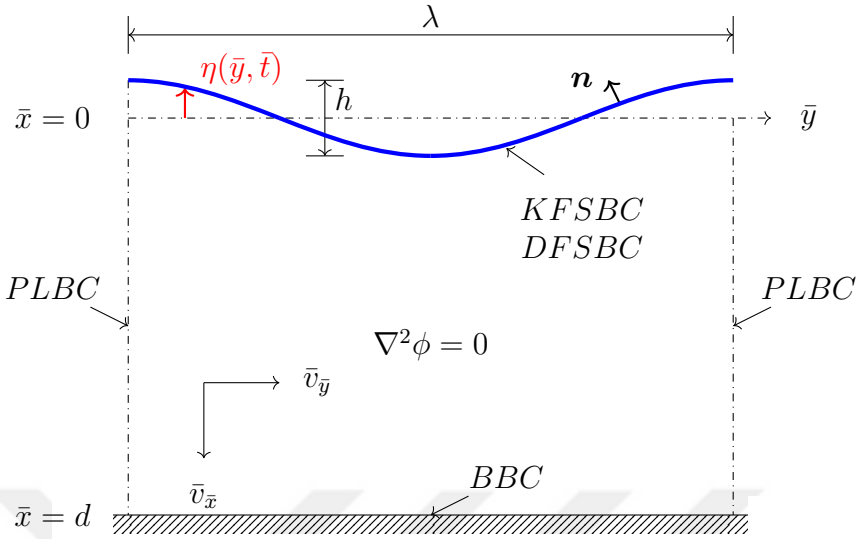

Figure 7.3. Boundary value problem for periodic water waves.

As per Assumption 7.5 the Taylor series expansion (A.11) can be used to linearize the KFSBC and the DFSBC. The solution is then obtained by utilizing the method of separation of variables. For a step by step derivation procedure the reader is referred to Dean and Dalrymple (1991). As per Assumption 7.4, the progressive solution to the boundary value system (7.4)–(7.9) is

$$\phi = -\frac{ghT}{4\pi}\frac{\cosh\left(\frac{2\pi}{\lambda}(-\bar{x}+d)\right)}{\cosh\left(\frac{2\pi}{\lambda}d\right)}\sin\left(\frac{2\pi\bar{y}}{\lambda}-\frac{2\pi\bar{t}}{T}\right). \tag{7.10}$$

The displacement of the free surface is

$$\eta = -\frac{h}{2}\cos\left(\frac{2\pi\bar{y}}{\lambda}-\frac{2\pi\bar{t}}{T}\right). \tag{7.11}$$

Lastly, the dispersion equation which describes dependence of the wave angular frequency on the wavelength is given by

$$\bar{\omega}^2 = \frac{4\pi^2}{T^2} = g\frac{2\pi}{\lambda}\tanh\left(\frac{2\pi}{\lambda}d\right). \tag{7.12}$$

The flow velocities can be obtained from the solution (7.10) and the definition of a potential function as

$$\bar{v}_{\bar{y}} = \frac{ghT}{2\lambda}\frac{\cosh\left(\frac{2\pi}{\lambda}(-\bar{x}+d)\right)}{\cosh\left(\frac{2\pi}{\lambda}d\right)}\cos\left(\frac{2\pi\bar{t}}{T}-\frac{2\pi\bar{y}}{\lambda}\right), \tag{7.13}$$

$$\bar{v}_{\bar{x}} = \frac{ghT}{2\lambda}\frac{\sinh\left(\frac{2\pi}{\lambda}(-\bar{x}+d)\right)}{\cosh\left(\frac{2\pi}{\lambda}d\right)}\sin\left(\frac{2\pi\bar{t}}{T}-\frac{2\pi\bar{y}}{\lambda}\right). \tag{7.14}$$

In addition to being periodic in space and time, the flow velocity functions are exponentially decaying in $\bar{x}$. Assuming the sensor reached the final depth $\bar{x} = L_f$ and the controller stabilized the lateral velocity $\bar{y}_{\bar{t}}(L_f, \bar{t}) \approx 0$ such that $\bar{y}$ is constant, then the velocity function is periodic in time only and resembles the type of disturbances assumed in Chapter 3. The in-domain disturbance however, would still be a function of depth $\bar{x}$.

Now, using definitions (7.1)–(7.2) the disturbances, please recall Figure 2.4, can be written as

$$\bar{P}\big(\bar{x} = L(\bar{t}), \bar{y}, \bar{y}_{\bar{t}}, \bar{t}\big) = \begin{cases} 0 & if\ \bar{v}_r = 0, \\ -\frac{\bar{v}_r}{2|\bar{v}_r|}(\pi r_s^2)\rho_w c_{d_s}\bar{v}_r^2 & else, \end{cases} \tag{7.15}$$

$$\bar{p}(\bar{x}, \bar{y}, \bar{y}_{\bar{t}}, \bar{t}) = \begin{cases} 0 & if\ v_r = 0, \\ -\frac{\bar{v}_r}{2|\bar{v}_r|}d_c\rho_w c_{d_c}\bar{v}_r^2 & else. \end{cases} \tag{7.16}$$

The relative velocity $\bar{v}_r$, using (7.13), becomes

$$\bar{v}_r(\bar{x}, \bar{y}, \bar{y}_{\bar{t}}, \bar{t}) = \bar{y}_{\bar{t}}(\bar{x}, \bar{t}) - \frac{ghT}{2\lambda}\frac{\cosh\left(\frac{2\pi}{\lambda}(-\bar{x}+d)\right)}{\cosh\left(\frac{2\pi}{\lambda}d\right)}\cos\Big(\frac{2\pi\bar{t}}{T} - \frac{2\pi\bar{y}(\bar{x}, \bar{t})}{\lambda}\Big). \tag{7.17}$$

Please observe that (7.15)–(7.16) are functions of the depth $\bar{x}$, string displacement $\bar{y}(\bar{x}, \bar{t})$, time $\bar{t}$, and the lateral string velocity $\bar{y}_{\bar{t}}(\bar{x}, \bar{t})$. The equations (7.15)–(7.16) are the disturbances affecting the cable and the sensor and together with the definition (7.17) will be used in the forthcoming numerical simulation.

7.4. Parameter Data

The disturbance model given in the previous section calls for parameters such as wave height, wave period, wavelength, sea bed depth, etc. These parameters are taken from the experimental as well as analytical data obtained from the relevant publications. Table 7.1 gives typical data for a sea swell which is the best physical match for the type of waves considered by the linear wave theory. The wave parameters for the Black Sea are from Divinsky and Kosyan (2018), which in turn relies on the experimental data collected by the Datawell Waverider instrument Kos' yan *et al.*

(1998). The wavelength has been calculated on the assumption that $\lambda = \frac{gT^2}{2\pi}$ as per Hastie (1985). The sea water properties, at the temperature of 10°C and salinity of 20 ppt, are taken from Nayar *et al.* (2016b). Please also see Sharqawy *et al.* (2010) and Nayar *et al.* (2016a).

Table 7.1. Wave parameter data and sea water properties.

Parameter	**Parameter Name**	**Value**	**Reference**
T	Wave period	7 s	Divinsky and Kosyan (2018)
h	Wave height	0.5 m	Divinsky and Kosyan (2018)
λ	Wavelength	76.5 m	Hastie (1985)
d	Sea bed depth	85 m	Divinsky and Kosyan (2018)
ρ_w	Sea water density	1015.2 $\frac{\text{kg}}{\text{m}^3}$	Nayar *et al.* (2016b)
μ_w	Sea water dynamic viscosity	0.001355 $\frac{\text{kg}}{\text{m s}}$	Nayar *et al.* (2016b)

The physical parameters of the sensor, a sphere, and the steel cable, a cylinder, were selected judiciously and are given in Table 7.2. The drag coefficients are taken as typical values for Reynolds's number in the range between $10^4 - 10^5$. The velocity at which the surface waves propagate is $c = \frac{\lambda}{T}$ or, as per data in Table 7.1, equal to 10.928 $\frac{\text{m}}{\text{s}}$. The IC are assumed to be $\bar{y}(\bar{x}, 0) = \bar{y}_{\bar{t}}(\bar{x}, 0) = 0$. The velocity profile is:

$$\bar{v}(\bar{t}) = \begin{cases} -\frac{140}{\bar{t}_1^7}(L_f - L_0)\bar{t}^6 + \frac{420}{\bar{t}_1^6}(L_f - L_0)\bar{t}^5 \\ -\frac{420}{\bar{t}_1^5}(L_f - L_0)\bar{t}^4 + \frac{140}{\bar{t}_1^4}(L_f - L_0)\bar{t}^3 & 0 \leq \bar{t} \leq \bar{t}_1 \\ 0 & \bar{t} > \bar{t}_1. \end{cases} \tag{7.18}$$

Table 7.2. Physical parameter data.

Parameter	**Parameter Name**	**Parameter Value**
m	Sensor mass	60 kg
r_s	Sensor radius	0.2 m
ρ	Cable linear density	0.36 $\frac{\text{kg}}{\text{m}}$
d_c	Cable diameter	0.0095 m
L_0	Initial depth	2 m
L_f	Desired depth	40 m
$\bar{t}_1$	Time to depth	40 s
c_{d_s}	Drag coefficient of a sphere	0.5*
c_{d_c}	Drag coefficient of a cylinder	1.1**

* Bailey and Hiatt (1972).
** Heddleson *et al.* (1957).

The string velocity $\bar{v}(\bar{t})$ should not exceed the maximum velocity of an object falling thru the fluid under the influence of gravity, buoyancy, and the fluid drag. For the sensor sphere, and neglecting the effect of the cable, the falling velocity $\bar{v}_f(\bar{t})$ can be obtained by solving

$$\dot{\bar{v}}_f(\bar{t}) = g - \frac{1}{2m}(\pi r_s^2)\rho_w c_{d_s}\big(\bar{v}_f(\bar{t}) - \bar{v}_{\bar{x}}(\bar{t})\big)^2 - \frac{g\rho_w}{m}(\frac{4}{3}\pi r_s^3), \tag{7.19}$$

for $\bar{v}_{\bar{x}}(\bar{t})$ as per (7.14) with $\bar{x} = L(\bar{t})$ and $\bar{y} = \bar{y}\big(L(\bar{t}), \bar{t}\big)$.

7.5. Conventional Control and Tuning

The proposed controllers will be compared with standard control methods. The forthcoming numerical results include data for the conventional controllers such as Proportional-Integral-Derivative (PID) and Proportional-Derivative (PD) + lead compensator. Here, a short overview is given. Furthermore, tuning and the final control parameters are provided at the end of this section.

The PID control is an industry-standard feedback control that applies correction input based on the error between the setpoint and the output. The controller utilizes a sum of proportional, integral, and derivative terms to construct a corrective input

$$u(t) = k_p e(t) + k_i \int_0^t e(t)dt + k_d \dot{e}(t), \tag{7.20}$$

where k_p, k_i, k_d are the proportional, integral, and the derivative gain constants, respectively, and where $e(t)$ is the difference between feedback and the desired setpoint. Please see Figure 7.4 for the block diagram. The PD + lead/lag controller is a series connection between the PD controller and a compensator. In the frequency domain, the compensator is usually given in terms of the transfer function

$$TF = k_l \frac{s - z_l}{s - p_l}, \tag{7.21}$$

where zero: $z_l = \frac{1}{T_l}$, and pole: $p_l = \frac{1}{\beta T_l}$. For $\beta < 1$, the compensator is the lead compensator. For $\beta > 1$, the lag compensator is obtained. In general, the lead compensator is used to improve stability and to increase the response time. The lag compensator rectifies the steady-state error. The compensator's transfer function (7.21) can be

transformed into a time-domain state-space filter

$$\dot{X}_l(t) = -\frac{1}{\beta T_l} X_l(t) + k_l\big(\frac{1}{T_l} - \frac{1}{\beta T_l}\big) u_e(t), \tag{7.22}$$

$$u(t) = X_l(t) + k_l u_e(t), \tag{7.23}$$

where $u_e(t)$ is the compensator's input as per Figure 7.5.

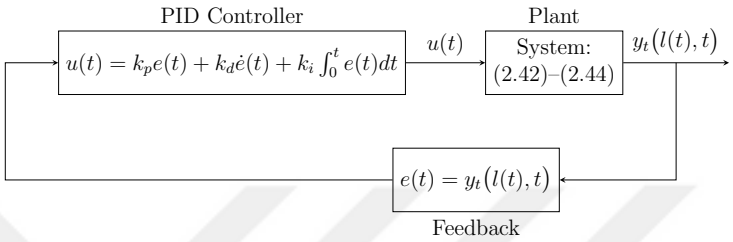

Figure 7.4. PID controller.

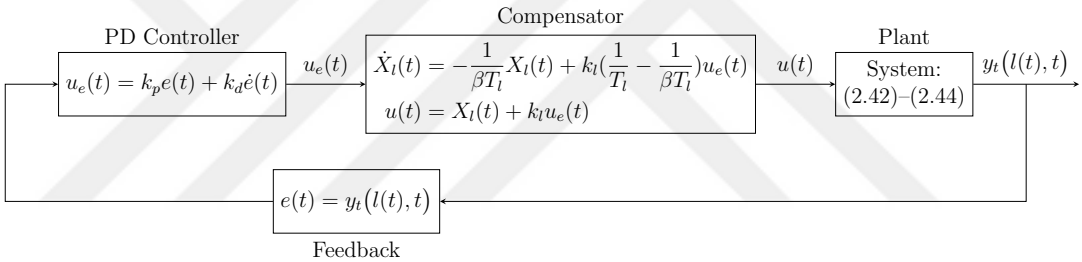

Figure 7.5. PD controller with compensator.

For optimal performance, the constant parameters are tuned. A manual method is used to arrive at the final values. The tuning takes place on the actual system (2.42)–(2.44) with previously described disturbance model as per (7.15)–(7.17), and Tables 7.1 and 7.2. It is assumed that the string is of constant length and at the desired depth. For the PID controller, the k_p gain is set first. The $k_p = -32$ gives the most stable performance with the lowest amplitude of oscillations, Figure 7.6. Afterward, the integral gain k_i is found. Here, the value of $k_i = -2$ lowers the steady-state error without significantly affecting the amplitude of the oscillations, see Figure 7.7. The derivative gain $k_d = -10$ provides stability over the undamped case, Figure 7.8.

Adding a lead compensator to the PID controller did not provide the expected improvements in the performance. Ultimately, it was found that a single lead compensator coupled with a PD controller or the PD + lead control provides the best results.

While various PID control and lead/lag compensator combinations were attempted, it was learned that this particular cascade is the most effective in terms of controlling the amplitude of the oscillations. A similar tuning procedure is used for the PD + compensator controller to obtain $k_d = -120$, $k_l = 1$, $T_l = 5$, and $\beta = 0.05$. The data for the parameter β in the lead configuration is shown in Figure 7.9. In Figure 7.10, the PD + lag compensator is compared to the previously obtained PID control. As mentioned earlier and viewed from the figure, the lag compensator lowers the steady-state error. The performance of the PD + lag control is inferior to that of the PID controller. As it is possible to use multiple compensators, Figure 7.11 gives the results for a series connection PD + lag + lead. The proportional constant for the extraction stage, $\bar{t} \in [0, \bar{t}_1]$, is set to $k_p = -5.7$, the equivalent gain used in the delay-compensated controller. The final control parameters are summarized in Table 7.3.

Table 7.3. Final control parameters for PID and PD + Lead Controllers.

	Control Parameters					
	k_p	k_d	k_i	k_l	T_l	β
PID Controller	$-5.7\,/\,-32^*$	-10	-2	–	–	–
PD + Lead Controller	$-5.7\,/\,-32^*$	-120	–	1	5	0.05

* Left value of the proportional gain k_p is for the extraction $\bar{t} \in [0, \bar{t}_1]$. Value on the right is for $\bar{t} > \bar{t}_1$.

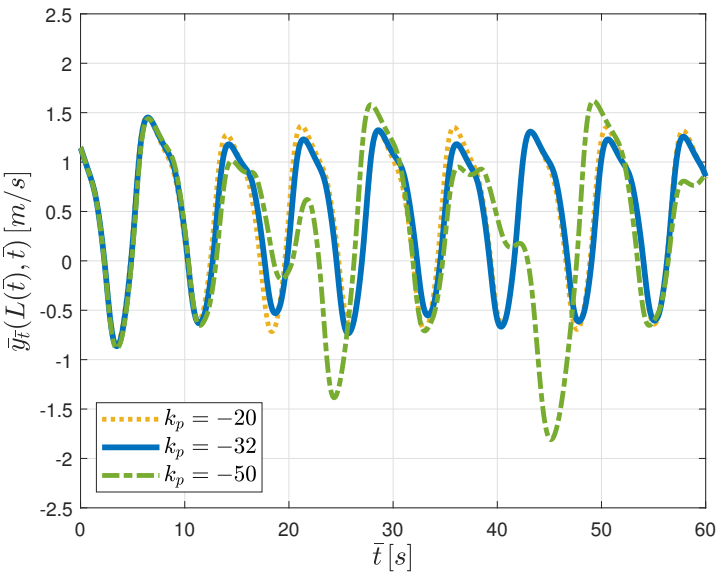

Figure 7.6. PID parameter tuning for proportional gain k_p.

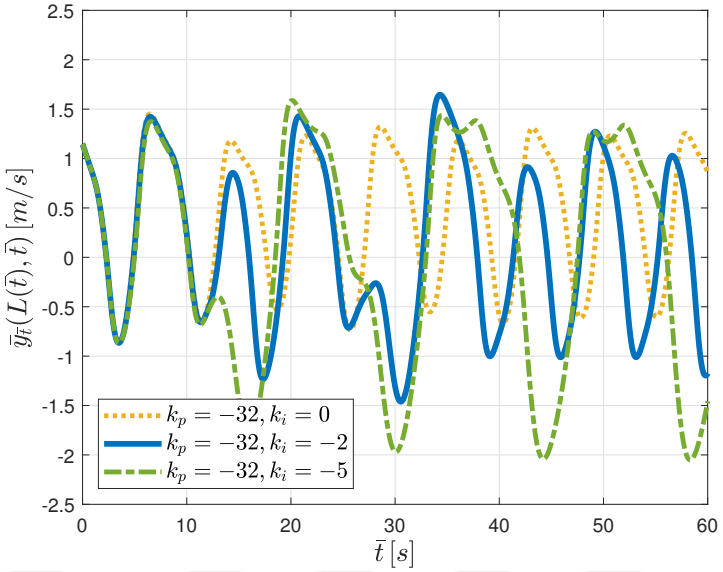

Figure 7.7. PID parameter tuning for integral gain k_i.

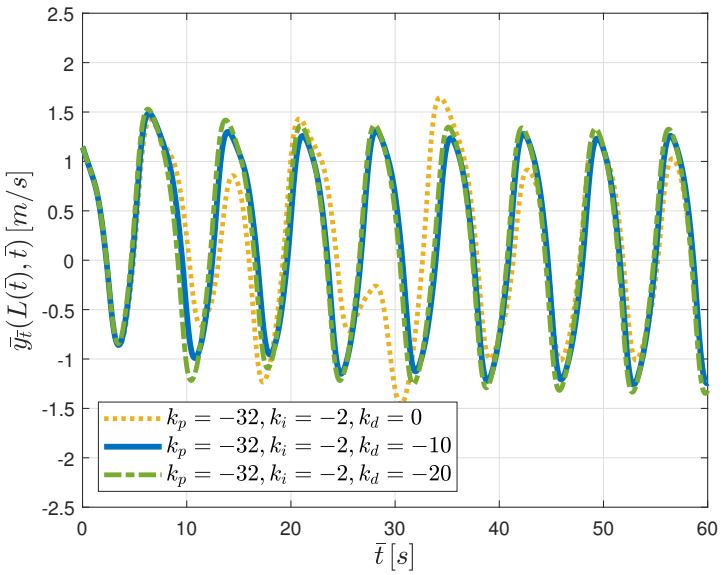

Figure 7.8. PID parameter tuning for derivative gain k_d.

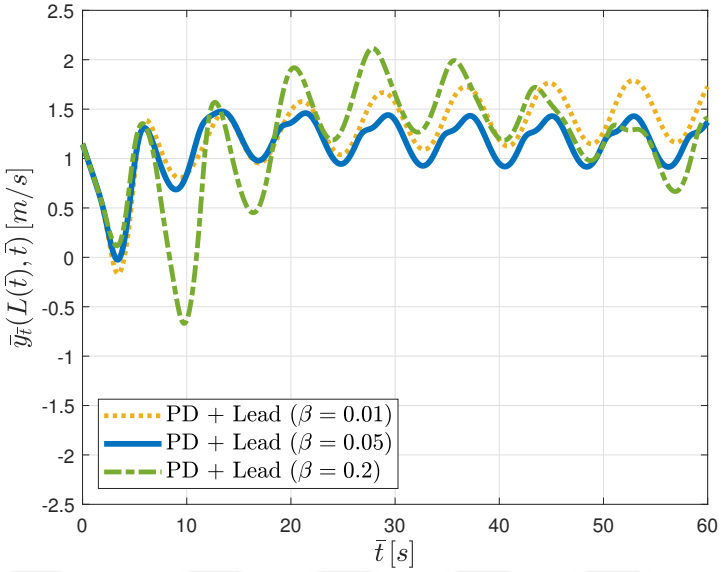

Figure 7.9. PD + Lead compensator parameter tuning for β with all other parameters as per Table 7.3.

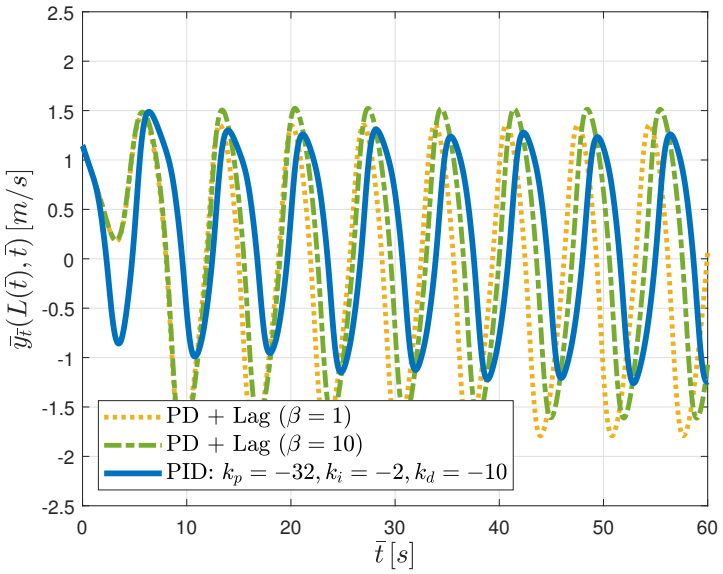

Figure 7.10. PD + Lag compensator at different β with all other parameters as per Table 7.3 vs. PID.

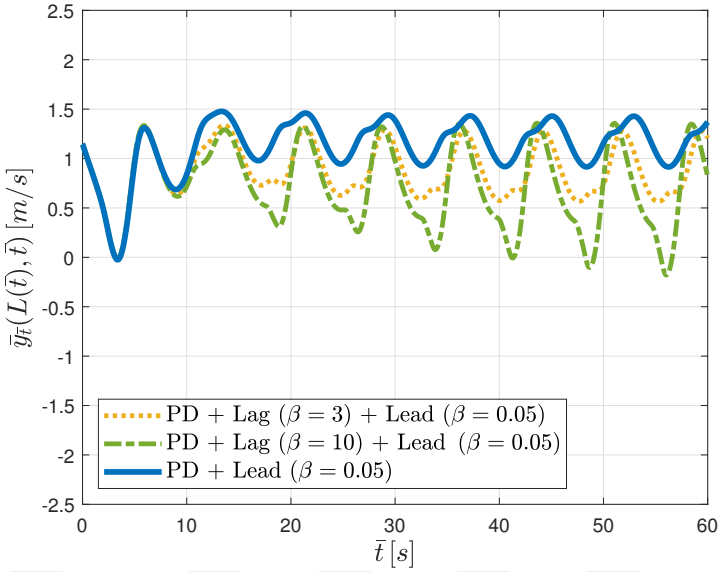

Figure 7.11. PD + Lag + Lead cascade at different β vs. PD + Lead compensator. All other parameters as per Table 7.3.

7.6. Numerical Results

The numerical simulation includes four separate control cases. Please see Table 7.4 for the complete listing. Case 1 gives the response for the free boundary condition where the top of the string is free to move along the horizontal direction. Physically, this can be interpreted as a string-mass system suspended on a free-to-move floating buoy. This case constitutes the baseline for the comparison between various control methods. Next, a standard PID controller is used in Case 2, where feedback $e(t) = y_t\big(l(t),t\big)$. Case 3 gives results for a PD controller cascaded with a lead compensator. Finally, Case 4 shows the response for the proposed, delay-compensated boundary controllers derived in Chapters 3 and 5.

Table 7.4. Controller specifications.

Case	**Controller**
Free Boundary Condition	$u(t) = \big(1 - v(t)\big)y_x(0,t)\ \forall\ \bar{t}$
PID Controller	$u(t) = k_p e(t) + k_d \dot{e}(t) + k_i \int_0^t e(t)dt$
PD + Lead Controller	See Figure 7.5
Proposed Controllers	(5.76) for $\bar{t} \in [0, \bar{t}_1]$ and (3.69) for $\bar{t} > \bar{t}_1$

The problem is simulated over two separate rounds. After the initial extraction stage $\bar{t} \in [0, \bar{t}_1]$, the final conditions of the string, such as the string displacement and transverse velocity, are used as the IC in the second simulation round $\bar{t} \in (\bar{t}_1, \bar{t}_2]$ where $\bar{v}(\bar{t}) = 0$. The data is combined to give the total simulation results. The simulation parameters for both stages are as follows: $\Delta t = 0.025$ and $\Delta z = 0.1$ for stage 1, and $\Delta t = 0.0025$ and $\Delta z = 0.1$ for stage 2. The relatively large time increment for stage 1 is due to a low value of the normalization constant $tc = 0.0495$, which in turn gives a large normalized time of 808.08. This corresponds to an actual stage time of only 40 s. Control parameters for Case 2 and Case 3 are summarized in Table 7.3.

The control parameters for the delay-compensated controllers (3.69) and (5.76) are as follows. The RDE input is set to $Q(t) = 2|A(t)| + 150$. Larger values of $Q(t)$ provide marginal improvement but lead to oscillations in the input at the predefined time increment. Since controller (5.76) is employed, it is assumed that all system parameters are known. The problem at hand is still adaptive in the sense that controller (3.69) employs an observer for the estimation and rejection of the unknown disturbance. All Update gains, k_θ, k_{β_a}, and k_{β_b}, are set at $1.9 \cdot 10^{-21}$, together with $c_w = 0.55$, $c_\tau = 0.1$, $c_a = 0.1$, $c_\xi = 10^{-7}$, $c_\delta = 10^8$ $q = 15.5$, $\mathbf{Q}_G = \mathbf{I}_{2x2}$, and control gain $k = -8$. Controllable pair $(\mathbf{G}, \mathbf{l})$ is given as $\mathbf{l} = [0, 1]^T$ and $\mathbf{G} = [0, 1; -3, -3.5]$ with eigenvalues of -2 and -1.5. Bounds on the unknown angular frequency $\omega = \frac{2\pi}{T} = 0.8976 \, \frac{\text{rad}}{\text{s}}$ are set as $\omega \in [0.5, 1]$. Furthermore, the second delay-compensated controller does have access to prior states; states generated during the first stage.

The length of the string $L(\bar{t})$, its axial velocity $\bar{v}(\bar{t})$, and acceleration $\dot{\bar{v}}(\bar{t})$ are given in Figure 7.12. The maximum permissible velocity $\bar{v}_f(\bar{t})$ of a sphere falling thru fluid is plotted here as well. Please observe that the falling, "terminal", velocity is not constant. It varies because of the fluid flow and the motion of the sensor. The delay function $\bar{\phi}(\bar{t})$, its inverse $\bar{\phi}^{-1}(\bar{t})$, time $\bar{t}$, and the delay $\bar{g}\big(L(\bar{t}), \bar{t}\big)$ are shown in Figure 7.13 for $\bar{t} \in [0, 40]$ s. The transverse velocity of the sensor $\bar{y}_{\bar{t}}\big(L(\bar{t}), \bar{t}\big)$ for all cases is given in Figure 7.14. Finally, the total displacement for the delay-compensated control can be seen in Figure 7.15.

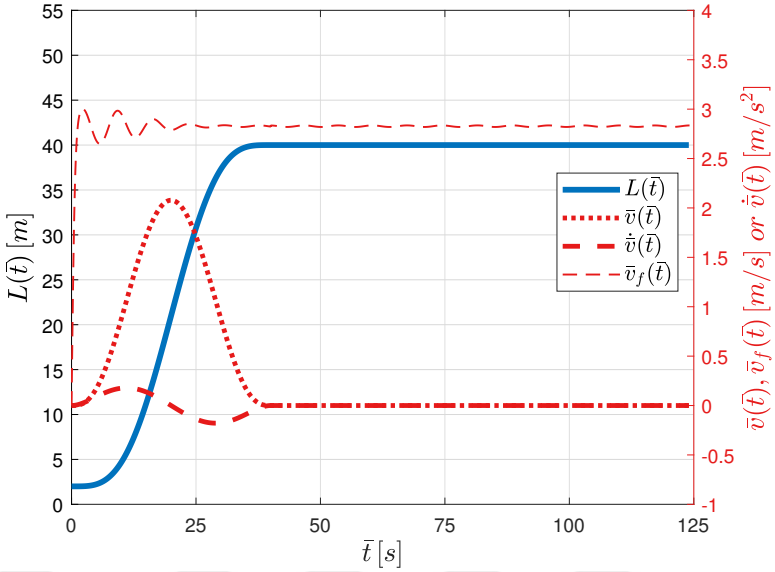

Figure 7.12. String length $L(\bar{t})$, left axis, and axial velocity $\bar{v}(\bar{t})$, acceleration $\dot{\bar{v}}(\bar{t})$, and terminal velocity $\bar{v}_f(\bar{t})$, right axis.

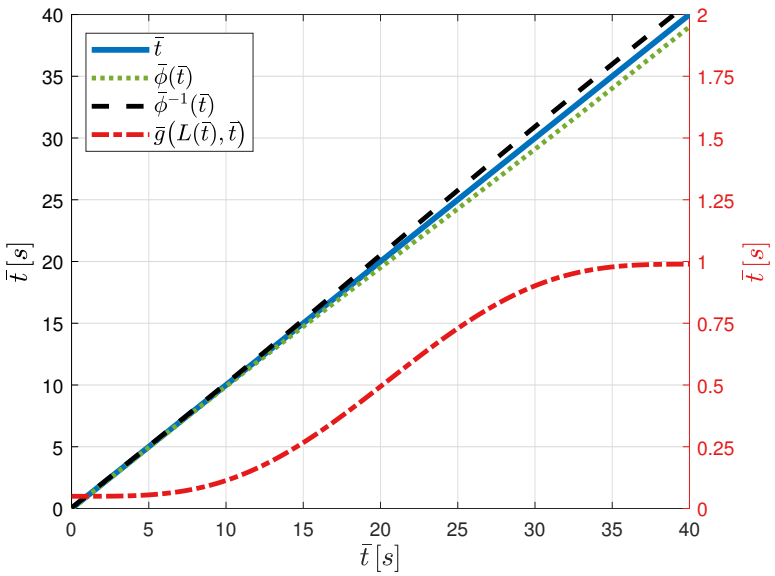

Figure 7.13. The delay function $\bar{\phi}(\bar{t})$, its inverse $\bar{\phi}^{-1}(\bar{t})$, and time $\bar{t}$, left axis. The delay $\bar{g}\big(L(\bar{t}),\bar{t}\big)$, right axis. All on $\bar{t} \in [0, \bar{t}_1]$.

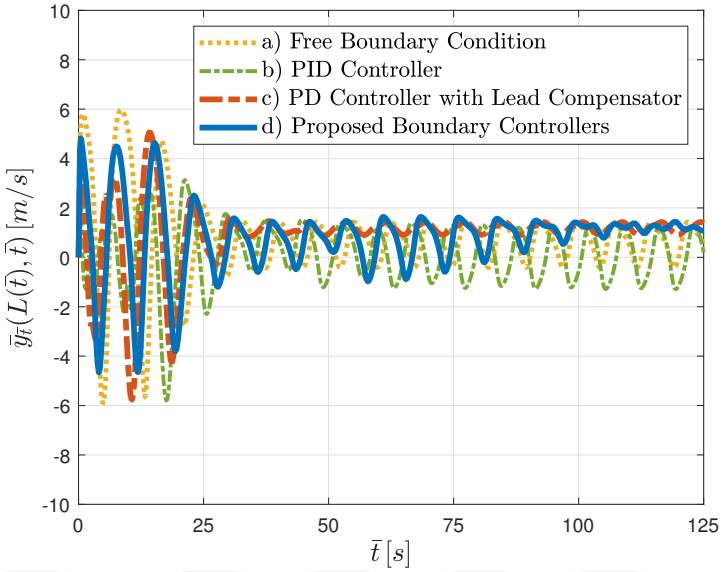

Figure 7.14. Bottom velocity $\bar{y}_{\bar{t}}\big(L(\bar{t}),\bar{t}\big)$ for: a) PD Controller with Lead Compensator, b) Proposed Boundary Controllers (5.76) and (3.69).

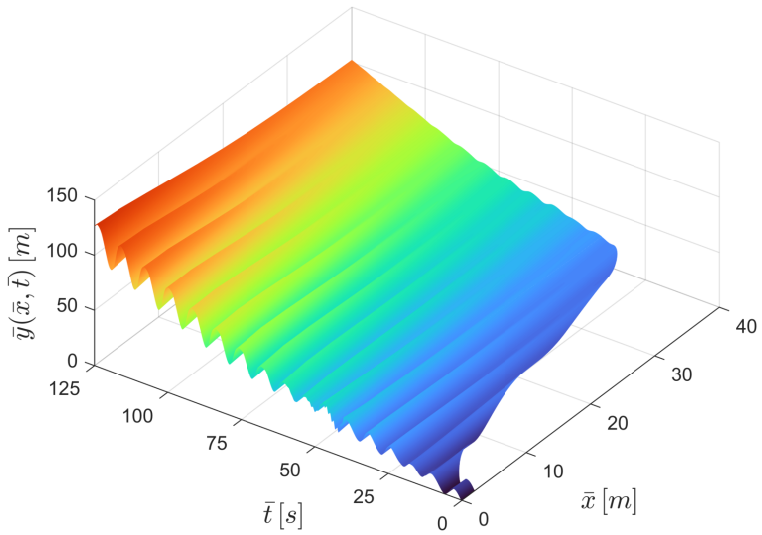

Figure 7.15. Total string displacement $\bar{y}(\bar{x},\bar{t})$ for the proposed controllers.

The performance of each control strategy is evaluated in terms of the RMS values as per Table 7.5. The extraction column gives the RMS values for $\bar{t} \in [0, 40]$ s when the string is extending as per velocity profile (7.18). The steady-state column shows values for a portion of the holding stage, a string of constant length, for $\bar{t} \in [100, 125]$ s. This time period corresponds to stable harmonic oscillations for all cases. Since every

response exhibits a drift, the DC offset has been removed from the data samples before calculating the RMS values in Table 7.5. The DC offset in $(\frac{\mathrm{m}}{\mathrm{s}})$ for $\bar{y}_{\bar{t}}\big(L(\bar{t}),\bar{t}\big)$ and over the steady-state period is given explicitly in the last column.

Table 7.5. RMS values of $\bar{y}_{\bar{t}}\big(L(\bar{t}),\bar{t}\big)$ and $\bar{u}(\bar{t})$.

RMS* in [m/s]	**Extraction:** $\bar{t}\in[0,40]\,\mathrm{s}$		**Steady State:** $\bar{t}\in[100,125]\,\mathrm{s}$		
	$\bar{y}_{\bar{t}}\big(L(\bar{t}),\bar{t}\big)$	$\bar{u}(\bar{t})$	$\bar{y}_{\bar{t}}\big(L(\bar{t}),\bar{t}\big)$	$\bar{u}(\bar{t})$	DC offset
Free Boundary Condition	2.82	3.71	0.60	4.01	0.66
PID Controller	1.90	4.15	0.88	9.35	0.12
PD + Lead Controller	2.34	3.08	0.17	5.09	1.20
Proposed Controllers	2.33	3.07	0.13	8.26	1.20

* DC offset over the relevant time period was subtracted from the signal before calculating the RMS values.

The robustness of the proposed control strategy is tested by adjusting the wave height h of the disturbance. The parameter is changed from the original value of 0.5 m to 0.75 m. The comparison between the PD + lead controller and the proposed boundary control is shown in Figure 7.16. The simulation is performed using original control parameters and runs up to 250 s. The RMS values are given in Table 7.6.

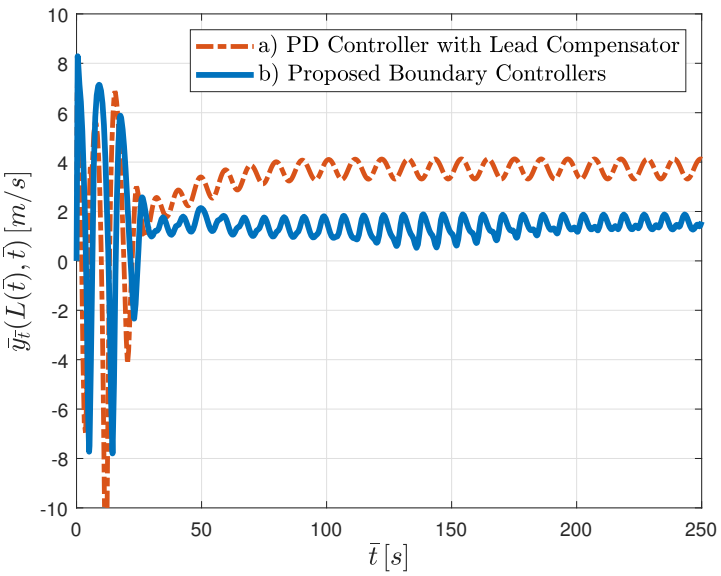

Figure 7.16. Bottom velocity $\bar{y}_{\bar{t}}\big(L(\bar{t}),\bar{t}\big)$ at $h = 0.75\,m$ for: a) PD Controller with Lead Compensator, b) Proposed Boundary Controllers (5.76) and (3.69).

Table 7.6. RMS values of $\bar{y}_{\bar{t}}\big(L(\bar{t}),\bar{t}\big)$ and $\bar{u}(\bar{t})$ for wave height: $h = 0.75\,\mathrm{m}$.

RMS* in [m/s]	**Extraction:** $\bar{t} \in [0, 40]\,\mathrm{s}$		**Steady State:** $\bar{t} \in [200, 250]\,\mathrm{s}$		
	$\bar{y}_{\bar{t}}\big(L(\bar{t}),\bar{t}\big)$	$\bar{u}(\bar{t})$	$\bar{y}_{\bar{t}}\big(L(\bar{t}),\bar{t}\big)$	$\bar{u}(\bar{t})$	DC offset
PD + Lead Controller	3.90	5.05	0.29	5.66	3.72
Proposed Controllers	3.44	5.48	0.21	5.45	1.51

* DC offset over the relevant time period was subtracted from the signal before calculating the RMS values.

7.7. Discussion

The simulated system is stable but follows the trajectory dictated by the presence of wave disturbances. This can be discerned from Table 7.5, where the DC offset for the free boundary condition case is given. Here, the string is free to move, and no external actuation occurs. As the string oscillates under the influence of the waves, it also drifts away. Similar behavior takes place for all other cases. Please see Figure 7.14. Even the PID controller with the smallest DC offset value of 0.12 $\frac{\mathrm{m}}{\mathrm{s}}$ cannot firmly anchor the string at one location. Further, the PID controller fairs worst in terms of the RMS values for the bottom boundary velocity and the input. The observed steady-state error is even more pronounced for Case 3 and Case 4 with a value for the DC offset of 1.20 $\frac{\mathrm{m}}{\mathrm{s}}$. However, the amplitude of oscillations decreases substantially over those in Case 1 and Case 2. Clearly, the two control strategies are best in terms of limiting the oscillations. The delay-compensated controller edges the results for the PD + lead controller, 0.13 $\frac{\mathrm{m}}{\mathrm{s}}$ versus 0.17 $\frac{\mathrm{m}}{\mathrm{s}}$, at an expense of higher input and longer time required to achieve this result. The proposed control is successful in limiting the effects of the delay and the wave disturbances on the system. The delay at the depth of 40 m is approximately 1 s, Figure 7.13. In the extraction stage, $\bar{t} \in [0, 40]\,\mathrm{s}$, the differences between Case 3 and Case 4 are relatively small, both in terms of the state $\bar{y}_{\bar{t}}\big(L(\bar{t}),\bar{t}\big)$ and the input $\bar{u}(\bar{t})$.

The results for Case 2 and Case 3 are for controllers tuned for the system described by the particular plant parameters and the specific disturbance. The robustness of the control can then be tested by changing the system while retaining previously obtained control parameters. This is done by adjusting the disturbance parameter h describing

the wave height as per Figure 7.3. Here, the value increases from 0.5 m to 0.75 m. The resulting performance for the PD + lead controller and the proposed delay-compensated controllers can be seen in Figure 7.16. The RMS values for the comparison are found in Table 7.6. The proposed boundary controller outperforms the standard controller $0.21\,\frac{\mathrm{m}}{\mathrm{s}}$ versus $0.29\,\frac{\mathrm{m}}{\mathrm{s}}$ in terms of the RMS values. Furthermore, the DC offset is also smaller. As the parameter h is increased by 50%, the DC offset for the proposed controller only goes from $1.20\,\frac{\mathrm{m}}{\mathrm{s}}$ to $1.51\,\frac{\mathrm{m}}{\mathrm{s}}$. The same change results in a DC offset for the PD + lead controller to go from $1.20\,\frac{\mathrm{m}}{\mathrm{s}}$ to a staggering value of $3.7\,\frac{\mathrm{m}}{\mathrm{s}}$.

The proposed boundary control is more robust in handling the change in the disturbance. While the PD + lead control would require a new round of tuning of the control parameters, the delay-compensated control derived in this thesis adapts and is more capable of dealing with variations in the system parameters and the disturbances.

None of the control methods is capable of eliminating the steady-state error. The omnipresence of the DC offset results from the complex nature of the disturbance affecting the system, which goes beyond the observer design presented in this work. Simply increasing the number of observer frequencies did not produce the desired results. Incorporating a constant term into the observer by increasing dimensionality from $2n$ to $2n + 1$ failed to compensate the bias. Please see Section 3.4. It may then be necessary to fully integrate an integral control into the delay design utilized in this thesis. Doing this would greatly extend the performance of the proposed control.

The case study simulates the deployment of an underwater sensor. The performance of the previously derived controllers has been tested under conditions mimicking those found in the field operations. The wave disturbance affecting the cable-sensor system is based on actual experimental data. Since the nature of the problem goes far beyond the applicability of the analysis, any statement concerning stability can only be made on a case-by-case basis. It has been observed that the delay-compensated controllers perform well, decreasing the effects of the disturbance on the velocity of the sensor. The proposed control outperforms open-loop control, synonymous with the

free boundary condition. It also fairs better than the industry standard PID and PD + lead controllers in limiting the amplitude of the oscillations. Finally, the proposed boundary control proves to be more robust in handling potential changes in the system or the disturbance.

8. CONCLUSIONS

This thesis provides boundary control strategies for a 1D string-mass system. Variations on the problem include variable string length, adaptivity, and the presence of the disturbances. Under a set of assumptions, this rather difficult problem can be transformed into a more familiar one. Here, it becomes the control of a linear ODE with an input delay. Furthermore, the transformation offers a good insight into the nature of the system itself. The flow of the input signal from one end of the string to the other is explicitly illustrated. The time required for the signal to reach the bottom boundary is the delay. As the length of the string changes, the delay becomes time-varying. Consequently, the controller at the top of the string needs to predict the required input at the bottom some time in the future. It is an intuitive understanding of the problem at hand. Mathematically, it is modelled by decomposing the governing wave equation into two decoupled first-order transport PDEs. The solutions to these equations give the relationships between the states at the two boundaries. By re-expressing the BBC in terms of the states at the top, the delay naturally appears in the dynamics describing the mass. Once a linear system with an input delay is obtained, the machinery of the delay and adaptive controls is applied. Using the backstepping method, the control is derived. The control laws are guaranteed to stabilize the system and in certain instances ensure convergence of the velocity state. Finally, the boundedness of the in-domain states is proven as well.

In summary, an analytically derived boundary input based on the delay control that can guarantee the stability of the string-mass system exists. Furthermore, by utilizing the adaptive strategies, the uncertainties in the boundary dynamics and the presence of disturbances can be overcome with the proposed boundary control.

Within limits imposed by the set of stated assumptions, the analysis guarantees stability and, in some cases, convergence. When one moves beyond the limits, the claims can no longer be substantiated. It is often the case when applying theoretical

results to a practical problem. Revisiting the initial assumptions and discussing their merits in light of a practical application is a worthwhile endeavor.

First, an ideal string does not possess the stiffness of an actual cable. The wave speed is non-dispersive. The lack of material properties beyond the linear density leads to more a predictive response and a better overall performance. Realistically, it would be more difficult to actuate a cable. While stability would most likely not be affected, the ability of the controller in suppressing the effects of disturbances might be. Second, a 1D problem is examined. In practice, the mass would move in two lateral directions. This case is discussed in more detail further down in this section. Whenever the geometry of the load is to be considered, the dynamic on the bottom boundary will be affected. In the case of a sphere, as in Chapter 7, this leads to a drag disturbance force.

The presence of a velocity-proportional damping is used to make systems unstable in the theoretical work. In the case study, the damping is due to the drag force. Here, the velocity-proportional term appears in the disturbance, which is highly nonlinear due to a square drag law. The obtained simulation results indicate a sensitivity of the proposed design to the form of disturbances affecting the system. While the stability is achieved, the performance suffers. The mathematical model introduced in Chapter 2 assumes position and time-dependent disturbances. Controllers derived in the subsequent chapters further limit admissible forms of the disturbances or exclude them entirely. The case study proves that the presence of more complex disturbances significantly reduces the ability of the controller to restrain the oscillations. Please see the upcoming discussion about the possibility of handling spatially dependent disturbances.

Next, by assuming a constant string tension, the equations of motion can be greatly simplified. The wave speed becomes constant along the length of the string. This then allows for the derivation of the delay and the control laws. It is a reasonable assumption whenever the mass of the load is much greater than the mass of the cable.

When that is no longer true, additional effects show up in the actual response of the system. Indeed, this happens in the case study where the mass of the sensor is 60 kg and the total mass of the cable is 14.4 kg. As a result, the performance degrades in terms of controlling the amplitude of the oscillations. Furthermore, while still offering the best performance among tested control strategies, the proposed control cannot eliminate the DC offset. Once again, please see a list of suggestions for a potential solution to this problem.

The reliance on the boundary feedback is a strong point of the design. As only the boundary measurements are required, there is no need for an infinite-dimensional observer, which would be difficult to achieve in field applications. For certain problem configurations, it is further possible to integrate a boundary observer as in Yilmaz and Basturk (2020). The only feedback required in this case would come from the actuated boundary. Please observe that the present design is for velocity stabilization. The regulation of displacement $\bar{y}$ is not currently possible under the measurement assumptions and the boundary conditions. Position regulation could be achieved, at least for the string with a constant length, if a direct measurement of the displacement is available.

Another critical feature of the proposed design is the adaptivity of the controller in overcoming parameter uncertainties. It is of high value as the determination of the parameters might be difficult in practice. Furthermore, the adaptive controllers should handle slow variations in the parameters that might, for example, show up in the physical systems affected by the thermal cycles of night and day. Moreover, the observer estimates and cancels out the unknown harmonic disturbances. Even in the presence of more complex scenarios, as in the case study, the controller does reasonably well. Furthermore, the controller is more reliable as it can adapt to the changing nature of the disturbances as portrayed in the numerical results of Chapter 7.

The analysis presented in the thesis can be extended further. The following list contains some of the most compelling and practical paths for potential future research:

- Inclusion of the spatially-dependent disturbances as in Basturk and Ayberk (2018) should be a natural step forward. In the paper, the in-domain spatial disturbance is first projected onto the dynamics of the bottom boundary. Here, the dimensionality of the boundary system is increased by incorporating the known dynamics of the disturbance. Then, a full state observer is designed leading to an appropriate update law. The stability analysis is finally performed using the error system. A similar analysis can potentially be applied to the problem given in Chapter 3 as long as the system parameters a and b are known. This approach might result in a better control performance for the type of problem presented in Chapter 7. Furthermore, given the results of the case study, an integral control should be examined to alleviate the steady-state error. This option is considered in the discussion at the end of Chapter 7.
- Increasing the dimensionality of the problem might be another worthwhile opportunity. At present, the analysis is limited to a 1D problem. However, it might be possible to apply the proposed controller design to a 2D problem where each independent axis is handled separately and in a discrete sequence. A full 2D motion of the mass would result in a coupled dynamics, Xing *et al.* (2020), that might be challenging to handle with the current methods. If the system could be decoupled under a strict set of assumptions or the coupling were ignored for the feedback design as in Böhm *et al.* (2014), each direction could be handled by a separate controller. Finally, the effects of coupling could also be considered as a disturbance into each independent controller and could potentially be canceled out using the observer.
- Since the reduction model used in the analysis for a string with a moving boundary precluded the inclusion of the disturbances, it would be imperative to look for another method to alleviate this limitation. In Chapter 3, the projection of the in-domain disturbance onto the dynamics of the bottom boundary is equivalent to a change in amplitude and a phase shift. In the case of the dynamic domain, the projection also results in a shift of the angular frequencies. This prevents one from leveraging the same adaptive techniques in dealing with the disturbance. More work in this direction would make the proposed design more practical.

- More research is necessary to see if it is possible to extend the analysis to systems characterized by internal stiffness such as cables and beams. The backstepping control has been successfully applied in the stabilization of beams described by the Euler–Bernoulli or the Timoshenko beam models. Please see Krstic and Smyshlyaev (2008a) for a brief overview. However, the literature is limited to a narrow range of applicable boundary conditions, disturbances, length constraints, and a requirement for an infinite-dimensional state observer. With regard to the research presented in this thesis, the difficulty arises in projecting the controlled boundary states onto the dynamics describing the opposite boundary and expressing control in terms of a system with an explicit delay.

Identification of the challenges in the application of the presented research goes a long way in establishing future efforts. The implementation of the above suggestions would be a great way of extending the applicability of this work.

REFERENCES

Bailey, A. and J. Hiatt, 1972, "Sphere Drag Coefficients for a Broad Range of Mach and Reynolds Numbers", *AIAA Journal*, 10(11), pp. 1436–1440.

Basturk, H. I., 2017, "Observer-Based Boundary Control Design for the Suppression of Stick–Slip Oscillations in Drilling Systems With Only Surface Measurements", *Journal of Dynamic Systems, Measurement, and Control*, 139(10), p. 104501.

Basturk, H. I. and I. U. Ayberk, 2018, "Backstepping Boundary Control of a Wave PDE with Spatially Distributed Time Invariant Unknown Disturbances", *Transactions on Automatic Control*, 64(8), pp. 3469–3475.

Basturk, H. I. and M. Krstic, 2015, "Adaptive Sinusoidal Disturbance Cancellation for Unknown LTI Systems Despite Input Delay", *Automatica*, 58, pp. 131–138.

Bekiaris-Liberis, N. and M. Krstic, editors, 2013, *Nonlinear Control Under Nonconstant Delays*, Society for Industrial and Applied Mathematics, Philadelphia.

Böhm, M., M. Krstic, S. Küchler, and O. Sawodny, 2014, "Modeling and Boundary Control of a Hanging Cable Immersed in Water", *Journal of Dynamic Systems, Measurement, and Control*, 136(1), p. 011006.

Bresch-Pietri, D. and M. Krstic, 2009, "Adaptive Trajectory Tracking Despite Unknown Input Delay and Plant Parameters", *Automatica*, 45(9), pp. 2074–2081.

Bresch-Pietri, D. and M. Krstic, 2014a, "Adaptive Output Feedback for Oil Drilling Stick-Slip Instability Modeled by Wave PDE with Anti-damped Dynamic Boundary", in *American Control Conference*, pp. 386–391.

Bresch-Pietri, D. and M. Krstic, 2014b, "Output-Feedback Adaptive Control of a Wave PDE with Boundary Anti-damping", *Automatica*, 50(5), pp. 1407–1415.

Cai, X., N. Bekiaris-Liberis, and M. Krstic, 2017, "Input-to-State Stability and Inverse Optimality of Linear Time-Varying-Delay Predictor Feedbacks", *Transactions on Automatic Control*, 63(1), pp. 233–240.

Cai, X. and M. Diagne, 2020, "Boundary Control of Nonlinear ODE/Wave PDE Systems with Spatially-Varying Propagation Speed", *Transactions on Automatic Control*, 66(9), pp. 4401–4408.

Cai, X. and M. Krstic, 2016, "Nonlinear Stabilization through Wave PDE Dynamics with a Moving Uncontrolled Boundary", *Automatica*, 68, pp. 27–38.

Carrier, G., 1949, "The Spaghetti Problem", *The American Mathematical Monthly*, 56(10P1), pp. 669–672.

Cooper, J., 1993, "Asymptotic Behavior for the Vibrating String with a Moving Boundary", *Journal of Mathematical Analysis and Applications*, 174(1), pp. 67–87.

D'Andréa-Novel, B. and J.-M. Coron, 2000, "Exponential Stabilization of an Overhead Crane with Flexible Cable via a Backstepping Approach", *Automatica*, 36(4), pp. 587–593.

Dean, R. G. and R. A. Dalrymple, 1991, *Water Wave Mechanics for Engineers and Scientists*, vol. 2, World Scientific Publishing Company, New Jersey.

Diagne, M., N. Bekiaris-Liberis, A. Otto, and M. Krstic, 2016, "Control of Transport PDE/Nonlinear ODE Cascades with State-Dependent Propagation Speed", *55th Conference on Decision and Control (CDC)*, pp. 3125–3130.

Divinsky, B. and R. Kosyan, 2018, "Parameters of Wind Seas and Swell in the Black Sea Based on Numerical Modeling", *Oceanologia*, 60(3), pp. 277–287.

Farkas, B. and S.-A. Wegner, 2016, "Variations on Barbălat's Lemma", *The American Mathematical Monthly*, 123(8), pp. 825–830.

Fox, R. W. and A. T. McDonald, 1999, *Introduction to Fluid Mechanics*, 5th edn., John Wiley & Sons, New York.

Goldstein, H., C. Poole, and J. Safko, 2002, *Classical Mechanics*, 3rd edn., Pearson, San Francisco.

Guo, W. and B.-Z. Guo, 2013, "Parameter Estimation and Non-collocated Adaptive Stabilization for a Wave Equation Subject to General Boundary Harmonic Disturbance", *Transactions on Automatic Control*, 58(7), pp. 1631–1643.

Guo, W., Z.-C. Shao, and M. Krstic, 2017, "Adaptive Rejection of Harmonic Disturbance Anticollocated with Control in 1D Wave Equation", *Automatica*, 79, pp. 17–26.

Hasselmann, W., n.d., *Helicopter Transport Load in the Swiss Mountain*, `https://unsplash.com/photos/pKcN6Sx_ERo`, accessed in March 2021.

Hastie, W., 1985, "Wave Height and Period at Timaru, New Zealand", *New Zealand Journal of Marine and Freshwater Research*, 19(4), pp. 507–515.

He, X., J. Shi, W. He, and C. Sun, 2017, "Boundary Vibration Control of a Variable Length Crane System in Two Dimensional Space with Output Constraints", *IFAC-PapersOnLine*, 50(1), pp. 11996–12001.

Heddleson, C., D. Brown, and R. Cliffe, 1957, "Summary of Drag Coefficients of Various Shaped Cylinders", Technical Report, General Electric Corporation, Cincinnati.

Hirsch, C., 2007, *Numerical Computation of Internal and External Flows: The Fundamentals of Computational Fluid Dynamics*, 2nd edn., Butterworth-Heinemann, Elsevier, Amsterdam.

Izadi, M., J. Abdollahi, and S. S. Dubljevic, 2015, "PDE Backstepping Control of One-Dimensional Heat Equation with Time-Varying Domain", *Automatica*, 54, pp. 41–48.

Kim, C.-S. and K.-S. Hong, 2009, "Boundary Control of Container Cranes from the Perspective of Controlling an Axially Moving String System", *International Journal of Control, Automation and Systems*, 7(3), pp. 437–445.

Kos' yan, R., B. Divinsky, and O. Pushkarev, 1998, "Measurements of Parameters of Wave Processes in the Open Sea Near Gelendzhik", in *The Eight Workshop of NATO TU-WAVES/Black Sea*, Middle East Technical University, pp. 5–6.

Krstic, M., 2009a, "Adaptive Control of an Anti-stable Wave PDE", in *American Control Conference, 2009 (ACC'09)*, pp. 1505–1510.

Krstic, M., 2009b, *Delay Compensation for Nonlinear, Adaptive, and PDE Systems*, Springer, Boston.

Krstic, M., 2010, "Lyapunov Stability of Linear Predictor Feedback for Time-Varying Input Delay", *Transactions on Automatic Control*, 55(2), pp. 554–559.

Krstic, M., I. Kanellakopoulos, P. V. Kokotovic *et al.*, 1995, *Nonlinear and Adaptive Control Design*, vol. 222, Wiley, New York.

Krstic, M. and A. Smyshlyaev, 2008a, "Backstepping Boundary Control for First-Order Hyperbolic PDEs and Application to Systems with Actuator and Sensor Delays", *Systems & Control Letters*, 57(9), pp. 750–758.

Krstic, M. and A. Smyshlyaev, 2008b, *Boundary Control of PDEs: A Course on Backstepping Designs*, vol. 16, Siam, Philadelphia.

Liu, Z., J. Liu, and W. He, 2017, "Modeling and Vibration Control of a Flexible Aerial Refueling Hose with Variable Lengths and Input Constraint", *Automatica*, 77, pp. 302–310.

Miranker, W. L., 1960, "The Wave Equation in a Medium in Motion", *IBM Journal of Research and Development*, 4(1), pp. 36–42.

Nayar, K. G., M. H. Sharqawy, L. D. Banchik *et al.*, 2016a, "Thermophysical Properties of Seawater: A Review and New Correlations that Include Pressure Dependence", *Desalination*, 390, pp. 1–24.

Nayar, K. G., M. H. Sharqawy, and J. H. Lienhard V, 2016b, *Sea Water Thermophysical Properties Lirary*, `http://web.mit.edu/seawater/2017_MIT_Seawater_Property_Tables_r2b.pdf`, accessed in October 2021.

Nihtila, M., 1991, "Finite Pole Assignment for Systems with Time-Varying Input Delays", *Proceedings of the 30th Conference on Decision and Control*, pp. 927–928.

Nikiforov, V. O., 2004, "Observers of External Deterministic Disturbances. II. Objects with Unknown Parameters", *Automation and Remote Control*, 65(11), pp. 1724–1732.

Pham, P. T. and K. S. Hong, 2019, "Vibration Control of a Flexible Marine Riser with Time-Varying Length", *12th Asian Control Conference (ASCC)*, pp. 778–783.

Phat, V. N., 2006, "Global Stabilization for Linear Continuous Time-Varying Systems", *Applied Mathematics and Computation*, 175(2), pp. 1730–1743.

Rübig, J., 2011, *Construction crane*, `https://pixabay.com/photos/site-crane-construction-machinery-285645/`, accessed in July 2021.

Roman, C., D. Bresch-Pietri, C. Prieur, and O. Sename, 2019, "Robustness to In-domain Viscous Damping of a Collocated Boundary Adaptive Feedback Law for an Antidamped Boundary Wave PDE", *Transactions on Automatic Control*, 64(8), pp. 3284–3299.

Sagert, C., F. Di Meglio, M. Krstic, and P. Rouchon, 2013, "Backstepping and Flatness Approaches for Stabilization of the Stick-Slip Phenomenon for Drilling", *IFAC Proceedings Volumes*, 46(2), pp. 779–784.

Sharqawy, M. H., J. H. Lienhard, and S. M. Zubair, 2010, "Thermophysical properties of seawater: a review of existing correlations and data", *Desalination and Water Treatment*, 16(1-3), pp. 354–380.

Smith, O. J. M., 1959, "A Controller to Overcome Dead Time", *ISA Journal*, 6, pp. 28–33.

Smyshlyaev, A., E. Cerpa, and M. Krstic, 2010, "Boundary Stabilization of a 1-D Wave Equation with In-domain Antidamping", *Journal on Control and Optimization*, 48(6), pp. 4014–4031.

Smyshlyaev, A. and M. Krstic, 2004, "Closed-Form Boundary State Feedbacks for a Class of 1-D Partial Integro-Differential Equations", *Transactions on Automatic Control*, 49(12), pp. 2185–2202.

Szczesiak, M. and H. I. Basturk, 2020, "Adaptive Boundary Control for Wave PDEs with Unknown In-domain/Boundary Disturbances and System Parameter", *Automatica*, 120, p. 109115.

Szczesiak, M. and H. I. Basturk, 2021, "Adaptive Boundary Control for Wave PDE on a Domain with Moving Boundary and with Unknown System Parameters in the Boundary Dynamics", *Submitted to Automatica*.

Terumichi, Y., M. Ohtsuka, M. Yoshizawa, Y. Fukawa, and Y. Tsujioka, 1997, "Non-stationary Vibrations of a String with Time-Varying Length and a Mass-Spring Attached at the Lower End", *Nonlinear Dynamics*, 12(1), pp. 39–55.

Wang, J., S. Koga, Y. Pi, and M. Krstic, 2018a, "Axial Vibration Suppression in a Partial Differential Equation Model of Ascending Mining Cable Elevator", *Journal of Dynamic Systems, Measurement, and Control*, 140(11), p. 111003.

Wang, J., Y. Pi, Y. Hu, and Z. Zhu, 2019, "State-observer design of a PDE-modeled mining cable elevator with time-varying sensor delays", *Transactions on Control Systems Technology*, 28(3), pp. 1149–1157.

Wang, J., S.-X. Tang, Y. Pi, and M. Krstic, 2018b, "Exponential Regulation of the Anti-collocatedly Disturbed Cage in a Wave PDE-Modeled Ascending Cable Elevator", *Automatica*, 95, pp. 122–136.

Wolfram Research Inc., 2021, *Mathematica Online, Free Trial*, Champaign, IL.

Xing, X., H. Yang, J. Liu, and S. Wang, 2020, "Vibration Control of Nonlinear Three-Dimensional Length-Varying Sstring with Input Quantization", *Journal of Vibration and Control*, 26(19-20), pp. 1835–1847.

Yilmaz, C. T. and H. I. Basturk, 2020, "Adaptive Output Regulator for Wave PDEs with Unknown Harmonic Disturbance", *Automatica*, 113, p. 108808.

Zhang, X., H. Feng, and S. Chai, 2016, "Performance Output Exponential Tracking for a Wave Equation with a General Boundary Disturbance", *Systems & Control Letters*, 98, pp. 79–85.

Zhao, Z., Y. Liu, W. He, and F. Luo, 2016, "Adaptive Boundary Control of an Axially Moving Belt System with High Acceleration/Deceleration", *IET Control Theory & Applications*, 10(11), pp. 1299–1306.

Zhou, B., Z. Lin, and G.-R. Duan, 2012, "Truncated Predictor Feedback for Linear Systems with Long Time-Varying Input Delays", *Automatica*, 48(10), pp. 2387–2399.

Zhou, H.-C. and B.-Z. Guo, 2018, "Performance Output Tracking for One-Dimensional Wave Equation Subject to Unmatched General Disturbance and Non-collocated Control", *European Journal of Control*, 39, pp. 39–52.

Zhu, W., J. Ni, and J. Huang, 2001, "Active Control of Translating Media with Arbitrarily Varying Length", *Journal of Vibration and Acoustics*, 123(3), pp. 347–358.

APPENDIX A: USEFUL FORMULAS AND IDENTITIES

L2 norm (Scalar)

$$||w(t)||^2 = \int_0^1 w(x,t)^2 dx \tag{A.1}$$

L2 norm (Vector)

$$||\mathbf{w}(t)||^2 = \int_0^1 \mathbf{w}(x,t)^T \mathbf{w}(x,t) dx \tag{A.2}$$

Young's Inequality (Scalar)

$$ab \leq \frac{a^2\epsilon}{2} + \frac{b^2}{2\epsilon} \quad \forall \epsilon > 0 \tag{A.3}$$

Young's Inequality (Vector)

$$\mathbf{a}^T\mathbf{b} \leq \frac{\mathbf{a}^T\mathbf{a}\epsilon}{2} + \frac{\mathbf{b}^T\mathbf{b}}{2\epsilon} \quad \forall \epsilon > 0 \tag{A.4}$$

Cauchy-Schwarz' Inequality (Scalar)

$$\int_0^1 f(x,t)g(x,t)dx \leq \sqrt{\int_0^1 f(x,t)^2 dx \int_0^1 g(x,t)^2 dx} = ||f(t)||\,||g(t)|| \tag{A.5}$$

Cauchy-Schwarz' Inequality (Vector)

$$\int_0^1 \mathbf{a}(x,t)^T \mathbf{b}(x,t) dx \leq \sqrt{\int_0^1 \mathbf{a}^T(x,t)\mathbf{a}(x,t)dx \int_0^1 \mathbf{b}^T(x,t)\mathbf{b}(x,t)dx} = ||\mathbf{a}(t)||\,||\mathbf{b}(t)|| \tag{A.6}$$

Square Norm Inequality (Scalar)

$$||u \pm v||^2 \leq 2\Big(||u||^2 + ||v||^2\Big) \tag{A.7}$$

Triangle Inequality (Vector)

$$||\mathbf{u} + \mathbf{v}|| \leq ||\mathbf{u}|| + ||\mathbf{b}|| \tag{A.8}$$

Other inequalities, assuming $a_i \in \mathbb{R}$ for $i = 1, 2, ..., n$

$$(a_1 + a_2 + ... + a_n)^2 \leq n(a_1^2 + a_2^2 + ... + a_n^2) \tag{A.9}$$

Leibniz's rule

$$\frac{d}{dx}\int_{a(x)}^{b(x)} f(x,y)dy = \int_{a(x)}^{b(x)} \frac{df(x,y)}{dx}dy + f\big(x,b(x)\big)\frac{db(x)}{dx} - f\big(x,a(x)\big)\frac{da(x)}{dx} \tag{A.10}$$

Taylor series expansion of a function $f(x)$

$$f(x+h) = f(x) + f'(x)h + \frac{f''(x)}{2!}h^2 + ... \tag{A.11}$$

APPENDIX B: INVERSE TRANSFORMATIONS

The procedure for obtaining the inverse transformation $\Gamma(z,t)$ is illustrated on the problem from Chapter 3. Without any loss in generality, the same procedure is applicable to the problem found in Chapter 4. The inverse transformation for the problem in Chapter 5 is given later in this appendix. First, solve (3.53) for $\Gamma(z,t)$

$$\begin{aligned}\Gamma(z,t) = \frac{1}{\hat{b}}\Big(&- \hat{\boldsymbol{\theta}}_a^T\boldsymbol{\gamma}^\tau(z,t) - \hat{\boldsymbol{\beta}}_a^T\boldsymbol{\gamma}^{\rho_a}(z,t) - \hat{\boldsymbol{\beta}}_b^T\boldsymbol{\gamma}^{\rho_b}(z,t) + (k-\hat{a})e^{\hat{a}z}y_t(1,t) \\ &+W(z,t) + (k-\hat{a})\int_0^z e^{\hat{a}(z-\zeta)}\Big(\hat{b}\Gamma(\zeta,t) + \hat{\boldsymbol{\theta}}_a^T\boldsymbol{\gamma}^\tau(\zeta,t) \\ &+ \hat{\boldsymbol{\beta}}_a^T\boldsymbol{\gamma}^{\rho_a}(\zeta,t) + \hat{\boldsymbol{\beta}}_b^T\boldsymbol{\gamma}^{\rho_b}(\zeta,t)\Big)d\zeta\Big).\end{aligned} \tag{B.1}$$

Now substitute this expression into itself for $\Gamma(\zeta,t)$ found under the integral on the right hand side of the equation. Do this a number of times

$$\begin{aligned}\Gamma(z,t) = \frac{1}{\hat{b}}\Big(&- \hat{\boldsymbol{\theta}}_a^T\boldsymbol{\gamma}^\tau(z,t) - \hat{\boldsymbol{\beta}}_a^T\boldsymbol{\gamma}^{\rho_a}(z,t) - \hat{\boldsymbol{\beta}}_b^T\boldsymbol{\gamma}^{\rho_b}(z,t) + (k-\hat{a})e^{\hat{a}z}y_t(1,t) \\ &+ W(z,t) + (k-\hat{a})\int_0^z e^{\hat{a}(z-\zeta)}\Big((k-\hat{a})e^{\hat{a}\zeta}y_t(1,t) \\ &+ W(\zeta,t) + (k-\hat{a})\int_0^\zeta e^{\hat{a}(\zeta-\sigma)}\big((k-\hat{a})e^{\hat{a}\sigma}y_t(1,t) \\ &+ W(\sigma,t) + (k-\hat{a})\int_0^\sigma e^{\hat{a}(\sigma-\varrho)}(...)d\varrho\big)d\sigma\Big)d\zeta\Big).\end{aligned} \tag{B.2}$$

Collect likewise terms

$$\begin{aligned}\Gamma(z,t) = \frac{1}{\hat{b}}\Big(&W(z,t) - \hat{\boldsymbol{\theta}}_a^T\boldsymbol{\gamma}^\tau(z,t) - \hat{\boldsymbol{\beta}}_a^T\boldsymbol{\gamma}^{\rho_a}(z,t) - \hat{\boldsymbol{\beta}}_b^T\boldsymbol{\gamma}^{\rho_b}(z,t) \\ &+ (k-\hat{a})e^{\hat{a}z}y_t(1,t) \\ &+ (k-\hat{a})^2\int_0^z e^{\hat{a}z}y_t(1,t)d\zeta \\ &+ (k-\hat{a})^3\int_0^z e^{\hat{a}(z-\zeta)}\int_0^\zeta e^{\hat{a}\zeta}y_t(1,t)d\sigma d\zeta + ... \\ &+ (k-\hat{a})\int_0^z e^{\hat{a}(z-\zeta)}W(\zeta,t)d\zeta \\ &+ (k-\hat{a})^2\int_0^z e^{\hat{a}(z-\zeta)}\int_0^\zeta e^{\hat{a}(\zeta-\sigma)}W(\sigma,t)d\sigma d\zeta \\ &+ (k-\hat{a})^3\int_0^z e^{\hat{a}(z-\zeta)}\int_0^\zeta e^{\hat{a}(\zeta-\sigma)}\int_0^\sigma e^{\hat{a}(\sigma-\varrho)}W(\varrho,t)d\varrho d\sigma d\zeta + ...\Big).\end{aligned} \tag{B.3}$$

Consider terms which include $y_t(1,t)$. After performing integration and simplifying one obtains

$$(k-\hat{a})e^{\hat{a}z}y_t(1,t)\Big(1+(k-\hat{a})z+(k-\hat{a})^2\frac{z^2}{2}+...\Big). \tag{B.4}$$

With just three terms it is easy to see clear progression of the exponential series: $e^x=\sum_{n=0}^{\infty}\frac{x^n}{n!}$ where $x=(k-\hat{a})z$. Then,

$$(k-\hat{a})e^{\hat{a}z}y_t(1,t)\Big(1+(k-\hat{a})z+(k-\hat{a})^2\frac{z^2}{2}+...\Big)=(k-\hat{a})e^{kz}y_t(1,t). \tag{B.5}$$

Now consider all terms of (B.3) which contain W under the integral sign. Simplifying gives

$$\begin{aligned}&(k-\hat{a})\int_0^z e^{\hat{a}(z-\zeta)}W(\zeta,t)d\zeta+(k-\hat{a})^2\int_0^z\int_0^\zeta e^{\hat{a}(z-\sigma)}W(\sigma,t)d\sigma d\zeta\\&+(k-\hat{a})^3\int_0^z\int_0^\zeta\int_0^\sigma e^{\hat{a}(z-\varrho)}W(\varrho,t)d\varrho d\sigma d\zeta+... .\end{aligned} \tag{B.6}$$

Starting with the second term of (B.6) and using integration by parts results in the following

$$(k-\hat{a})^2\int_0^z\underbrace{\int_0^\zeta e^{\hat{a}(z-\sigma)}W(\sigma,t)d\sigma}_{=P(\zeta)}d\zeta=(k-\hat{a})^2\bigg(P(\zeta)\zeta\Big|_0^z-\int_0^z\zeta P'(\zeta)d\zeta\bigg), \tag{B.7}$$

where derivative $P'(\zeta)$ can be evaluated using Leibniz's rule (A.10). Now,

$$\begin{aligned}(k-\hat{a})^2\int_0^z\int_0^\zeta e^{\hat{a}(z-\sigma)}W(\sigma,t)d\sigma d\zeta=(k-\hat{a})^2\bigg(&\zeta\int_0^\zeta e^{\hat{a}(z-\sigma)}W(\sigma,t)d\sigma\Big|_0^z\\&-\int_0^z\zeta e^{\hat{a}(z-\zeta)}W(\zeta,t)d\zeta\bigg).\end{aligned} \tag{B.8}$$

Evaluate the limits, and since σ is the dummy variable rename it to ζ. Simplifying further gives

$$(k-\hat{a})^2\int_0^z\int_0^\zeta e^{\hat{a}(z-\sigma)}W(\sigma,t)d\sigma d\zeta=(k-\hat{a})^2\int_0^z e^{\hat{a}(z-\zeta)}(z-\zeta)W(\zeta,t)d\zeta. \tag{B.9}$$

Turn your attention to the third term of (B.6). Write

$$\begin{aligned}(k-\hat{a})^3\int_0^z\int_0^\zeta\int_0^\sigma e^{\hat{a}(z-\varrho)}W(\varrho,t)d\varrho d\sigma d\zeta=&\\(k-\hat{a})^3e^{\hat{a}z}\int_0^z\int_0^\zeta\underbrace{\int_0^\sigma e^{-\hat{a}\varrho}W(\varrho,t)d\varrho}_{=P(\sigma)}d\sigma d\zeta,&\end{aligned} \tag{B.10}$$

which using integration by parts on term $\int_0^\zeta P(\sigma)d\sigma$ reduces to

$$(k-\hat{a})^3\int_0^z\int_0^\zeta\int_0^\sigma e^{\hat{a}(z-\varrho)}W(\varrho,t)d\varrho d\sigma d\zeta = (k-\hat{a})^3e^{\hat{a}z}\int_0^z(z-\zeta)\underbrace{\int_0^\zeta e^{-\hat{a}\sigma}W(\sigma,t)d\sigma}_{=R(\zeta)}d\zeta. \tag{B.11}$$

Again, using integration by parts on $\int_0^z(z-\zeta)R(\zeta)d\zeta$ results in

$$(k-\hat{a})^3\int_0^z\int_0^\zeta\int_0^\sigma e^{\hat{a}(z-\varrho)}W(\varrho,t)d\varrho d\sigma d\zeta = \frac{1}{2}(k-\hat{a})^3\int_0^z e^{\hat{a}(z-\zeta)}(z-\zeta)^2W(\zeta,t)d\zeta. \tag{B.12}$$

Re-express (B.6) using (B.9) and (B.12)

$$\begin{aligned}&(k-\hat{a})\int_0^z e^{\hat{a}(z-\zeta)}W(\zeta,t)d\zeta+(k-\hat{a})^2\int_0^z e^{\hat{a}(z-\zeta)}(z-\zeta)W(\zeta,t)d\zeta\\&+\frac{1}{2}(k-\hat{a})^3\int_0^z e^{\hat{a}(z-\zeta)}(z-\zeta)^2W(\zeta,t)d\zeta+...,\end{aligned} \tag{B.13}$$

which can be written as

$$(k-\hat{a})\int_0^z e^{\hat{a}(z-\zeta)}W(\zeta,t)\Big(1+(k-\hat{a})(z-\zeta)+\frac{1}{2}(k-\hat{a})^2(z-\zeta)^2+...\Big)d\zeta. \tag{B.14}$$

Using exponential series expansion, (B.14) reduces to

$$(k-\hat{a})\int_0^z e^{k(z-\zeta)}W(\zeta,t)d\zeta. \tag{B.15}$$

Finally, replacing all terms containing $y_t(1,t)$ in (B.3) with right hand side of (B.5), and all terms of (B.3) which contain W under the integral sign with (B.15), gives the inverse transformation (3.54).

The procedure for obtaining the inverse transformation in Chapter 5 is presented below. The existence of the inverse transformation (5.61) can be verified by solving (5.60) for $\Pi(z,t)$. The recursive function obtained in this manner can then be expanded thru self-substitution. The two series expansions, one in X and one in W, need to be proven to converge to the corresponding terms in the transformation (5.61), i.e., are equal to each other. As an example, let's examine the expansion in terms of $X(t)$:

$$\begin{aligned}\Theta_1(z,t)=\kappa(z,t)e^{\int_0^z\alpha(s,t)\left(\phi^{-1}(t)-t\right)ds}\Bigg(&1+\left(\phi^{-1}(t)-t\right)\int_0^z\beta(\tau,t)\kappa(\tau,t)d\tau\\&+\left(\phi^{-1}(t)-t\right)^2\int_0^z\beta(\tau,t)\kappa(\tau,t)\int_0^\tau\beta(\psi,t)\kappa(\psi,t)d\psi d\tau+...\Bigg)X(t).\end{aligned} \tag{B.16}$$

The corresponding term in (5.61) is

$$\Theta_2(z,t) = \kappa(z,t)e^{\int_0^z \left(\alpha(s,t)+\beta(s,t)\kappa(s,t)\right)\left(\phi^{-1}(t)-t\right)ds} X(t). \tag{B.17}$$

It can be shown that both $\Theta_1(z,t)$ and $\Theta_2(z,t)$ obey

$$\Theta_z(z,t) = \left(\phi^{-1}(t) - t\right)\beta(z,t)\kappa(z,t)\Theta(z,t), \tag{B.18}$$

$$\Theta(0,t) = 1. \tag{B.19}$$

Since both (B.16) and (B.17) obey the same ODE (B.18)–(B.19), and the solution to (B.18)–(B.19) is unique by Picard–Lindelöf Theorem, expansion (B.16) converges to (B.17). The same procedure applies in the case of the W terms, thus giving us the inverse transformation (5.61).

APPENDIX C: DISCUSSION ON $R(x,t)$

While $R(x,t)$ in Chapter 3 is given in terms of the measurable signals, such as the boundary feedback, the disturbance filter states, and the parameter estimates, it may not be clear why it is used and what it represents. Start with derivation of (3.77). Add expressions (3.9) and (3.10) together at $t = t'$ and then evaluate the outcome at $x = 1$ and at $t' = t + x - 1$. Use resulting expression for $\xi(1, t + x - 1)$ found in (3.13),

$$\xi(x,t) = 2y_t(1, t + x - 1) - \eta(1, t + x - 1) - \nu_{\xi_1}(x,t). \tag{C.1}$$

Now, evaluate (3.14) at $t = t'$, $x = 1$, and then at $t' = t + x - 1$. Substitute resulting expression for $\eta(1, t + x - 1)$ in (C.1)

$$\xi(x,t) = 2y_t(1, t + x - 1) - \eta(0, t + x - 2) + \nu_{\eta_0}(1, t + x - 1) - \nu_{\xi_1}(x,t). \tag{C.2}$$

Using definition of $\eta(x,t)$ in (3.10), first evaluate at $t = t'$, at $x = 0$, then at $t' = t+x-2$, and finally use expressions (3.4), (3.35), and (3.48), to state

$$\eta(0, t + x - 2) = \Gamma(0, t + x - 1). \tag{C.3}$$

Substitute (C.3) into (C.2) and use definition (3.54) to evaluate $\Gamma(0, t + x - 1)$. This, after rearranging, gives

$$\begin{aligned} &\xi(x,t) - \frac{1}{\hat{b}(t + x - 1)}\Big(\hat{\boldsymbol{\theta}}_a^T(t + x - 1)\boldsymbol{\gamma}^\tau(0, t + x - 1) \\ &+ \hat{\boldsymbol{\beta}}_a^T(t + x - 1)\boldsymbol{\gamma}^{\rho_a}(0, t + x - 1) \\ &+ \hat{\boldsymbol{\beta}}_b^T(t + x - 1)\boldsymbol{\gamma}^{\rho_b}(0, t + x - 1)\Big) + \nu_{\eta_0}(1, t + x - 1) - \nu_{\xi_1}(x,t) = \\ &\Big(2 - \frac{k - \hat{a}(t + x - 1)}{\hat{b}(t + x - 1)}\Big)y_t(1, t + x - 1) - \frac{1}{\hat{b}(t + x - 1)}W(0, t + x - 1). \end{aligned} \tag{C.4}$$

Define $R(x,t)$ as left hand side of (C.4)

$$\begin{aligned} R(x,t) = \xi(x,t) &+ \nu_{\eta_0}(1, t + x - 1) - \nu_{\xi_1}(x,t) \\ &- \frac{1}{\hat{b}(t + x - 1)}\Big(\hat{\boldsymbol{\theta}}_a^T(t + x - 1)\boldsymbol{\gamma}^\tau(0, t + x - 1) \\ &\quad + \hat{\boldsymbol{\beta}}_a^T(t + x - 1)\boldsymbol{\gamma}^{\rho_a}(0, t + x - 1) \\ &\quad + \hat{\boldsymbol{\beta}}_b^T(t + x - 1)\boldsymbol{\gamma}^{\rho_b}(0, t + x - 1)\Big). \end{aligned} \tag{C.5}$$

Alternatively, $R(x,t)$ is equal to the right hand side of (C.4)

$$\begin{aligned} R(x,t) = &\Big(2 - \frac{k - \hat{a}(t+x-1)}{\hat{b}(t+x-1)}\Big) y_t(1, t+x-1) \\ &- \frac{1}{\hat{b}(t+x-1)} W(0, t+x-1). \end{aligned} \tag{C.6}$$

At $x = 1$ the above definition becomes

$$R(1,t) = \Big(2 - \frac{k - \hat{a}(t)}{\hat{b}(t)}\Big) y_t(1,t) - \frac{1}{\hat{b}(t)} W(0,t), \tag{C.7}$$

an expression required when evaluating $\dot{V}(t)$ in (3.92).

By using definitions (3.53), (3.40)–(3.47) and control (3.69) in (C.6) one finally obtains (3.77). By looking at the definition (C.6) it is clear that $R(x,t)$ is directly related to the control signals used in the stability analysis. Examining (C.5) indicates link between $R(x,t)$ and $\xi(x,t)$ or through its definition to $y_x(x,t)$ and $y_t(x,t)$. As a result, $R(x,t)$ plays an important role in extending stability from the control variables bounded by the Lyapunov analysis to the original in-domain states of the PDE.

Since no disturbances are present in the analysis found in Chapter 4 and Chapter 5, no explicit definition of the variable $R(x,t)$ is given. Instead, boundary states are used directly in the definition of the normalization function (4.50), which in turn is included in the Lyapunov function (4.57). Since problem in Chapter 5 is non-adaptive, the normalization function is not used.

APPENDIX D: TIME DERIVATIVE OF $V_\xi(t)$.

The derivation of the expression (5.90) is given in this appendix. Subtract (5.7) from (5.6) with $t = t'$, evaluate at $x = l(t')$ and then at $t' = t + f(x,t)$, to get

$$\begin{aligned}&\xi\Big(l\big(t+f(x,t)\big),t+f(x,t)\Big)-\eta\Big(l\big(t+f(x,t)\big),t+f(x,t)\Big)\\&=2y_x\Big(l\big(t+f(x,t)\big),t+f(x,t)\Big).\end{aligned}\tag{D.1}$$

Using definition of $\eta(x,t)$ in (5.7) and expression (5.12) write (D.1) as

$$\begin{aligned}\xi(x,t)=\;&y_t\Big(l\big(t+f(x,t)\big),t+f(x,t)\Big)\\&+\Big(1+v\big(t+f(x,t)\big)\Big)y_x\Big(l\big(t+f(x,t)\big),t+f(x,t)\Big).\end{aligned}\tag{D.2}$$

Using (5.22), one gets

$$\begin{aligned}\xi(x,t)=\;&\Big(\frac{2}{1-v\big(t+f(x,t)\big)}\Big)y_t\Big(l\big(t+f(x,t)\big),t+f(x,t)\Big)\\&-\Big(\frac{1+v\big(t+f(x,t)\big)}{1-v\big(t+f(x,t)\big)}\Big)\\&\cdot\Big(y_t\Big(0,t+f(x,t)-g\big(l(t+f(x,t)),t+f(x,t)\big)\Big)\\&\quad-\Big(1-v\big(t+f(x,t)-g\big(l(t+f(x,t)),t+f(x,t)\big)\big)\Big)\\&\quad\cdot y_x\Big(0,t+f(x,t)-g\big(l(t+f(x,t)),t+f(x,t)\big)\Big)\Big).\end{aligned}\tag{D.3}$$

Using (5.30) and (5.32) gives

$$\begin{aligned}\xi(x,t)=\;&\Big(\frac{2}{1-v\big(t+f(x,t)\big)}\Big)\\&\cdot\Big(X\big(t+f(x,t)\big)+v\big(t+f(x,t)\big)U\Big(\phi\big(t+f(x,t)\big)\Big)\Big)\\&-\Big(\frac{1+v\big(t+f(x,t)\big)}{1-v\big(t+f(x,t)\big)}\Big)U\Big(\phi\big(t+f(x,t)\big)\Big).\end{aligned}\tag{D.4}$$

Evaluate the above expression at $x = l(t)$. Using $f\big(l(t),t\big) = 0$ results in

$$\xi\big(l(t),t\big)=\Big(\frac{1}{1-v(t)}\Big)\Big(2X(t)-\big(1-v(t)\big)U\big(\phi(t)\big)\Big).\tag{D.5}$$

Using (5.49), (5.55), (5.57), and (5.59) gives

$$\xi\big(l(t),t\big)=\Big(\frac{2-K(t)\big(1-v(t)\big)}{1-v(t)}\Big)X(t)-W(0,t).\tag{D.6}$$

Squaring left side the above expression allows one to write the following inequality

$$\xi\big(l(t),t\big)^2 \leq 2\Big(\frac{2-K(t)\big(1-v(t)\big)}{1-v(t)}\Big)^2 X(t)^2 + 2W(0,t)^2. \tag{D.7}$$

Now, take derivative of V_ξ as found in (5.84):

$$\frac{DV_\xi(t)}{Dt} = c_\xi\Big(\frac{d}{dt}\int_0^{l(t)} e^x \xi(x,t)^2 dx + v(t)\underbrace{\frac{d}{dx}\int_0^{l(t)} e^x \xi(x,t)^2 dx}_{=0}\Big), \tag{D.8}$$

$$\dot{V}_\xi(t) = c_\xi\Big(2\int_0^{l(t)} e^x \xi(x,t)\xi_t(x,t)dx + e^{l(t)}v(t)\xi\big(l(t),t\big)^2\Big). \tag{D.9}$$

The Leibniz's differentiation rule (A.10) has been used to obtain the above expression. Recalling (5.8)

$$\dot{V}_\xi(t) = 2c_r\big(1-v(t)\big)\int_0^{l(t)} e^x \xi(x,t)\xi_x(x,t)dx + c_\xi e^{l(t)}v(t)\xi\big(l(t),t\big)^2. \tag{D.10}$$

Applying integration by parts

$$\dot{V}_\xi(t) = c_\xi\big(1-v(t)\big)\Big(e^x\xi(x,t)^2\Big|_0^{l(t)} - \int_0^{l(t)} e^x\xi(x,t)^2dx\Big) + c_\xi e^{l(t)}v(t)\xi\big(l(t),t\big)^2, \tag{D.11}$$

finally gives

$$\dot{V}_\xi(t) = -c_\xi\big(1-v(t)\big)\xi(0,t)^2 - c_\xi\big(1-v(t)\big)||\xi(t)||^2 + c_\xi e^{l(t)}\xi\big(l(t),t\big)^2. \tag{D.12}$$

Lastly, insert (D.5) and control gain (5.77) to obtain the final expression as in (5.90):

$$\begin{aligned}\dot{V}_\xi(t) \leq & -c_\xi\big(1-v(t)\big)||\xi(t)||^2 - c_\xi\big(1-v(t)\big)\xi(0,t)^2 \\ & + \frac{2c_\xi e^{l(t)}}{\big(1-v(t)\big)^2}\Big(2+\frac{1}{2}B(t)\big(R(t)+1\big)\big(1-v(t)\big)\Big)^2 X(t)^2 \\ & + 2c_\xi e^{l(t)}W(0,t)^2.\end{aligned} \tag{D.13}$$

APPENDIX E: FINITE-DIFFERENCE APPROXIMATION OF THE EQUATIONS OF MOTION.

The following pages contain the equations of motion and the expressions for the target and the ghost nodes written using the finite-difference formulas. The expressions have been generated using Wolfram Research Inc. (2021).

Scheme 1 - Discretization of the equations of motion:

In[1]:=
```
Clear["Global`*"]
```

In[2]:=
```
y_x = Z_z / l[t];
y_t = Z_t - (γ v[t]) / l[t] Z_z;
y_xx = 1 / (l[t])^2 Z_zz;
y_xt = 1 / l[t] Z_zt - v[t] / (l[t])^2 Z_z - (v[t] γ) / (l[t])^2 Z_zz;
y_tt = Z_tt - (2 v[t] γ) / l[t] Z_zt - (γ (v'[t] * l[t] - 2 v[t]^2)) / (l[t])^2 Z_z + ((v[t] γ)^2) / (l[t])^2 Z_zz;
```

PDE (where γ = z)

In[7]:=
```
PDE = Collect[((v[t]^2 - (m/ρ + ϵ_τ * L_0 (l[t] - γ * l[t])))(ρ/m - ϵ_a / L_0 v'[t])) * y_xx + 2 * v[t] * y_xt + c_ρ L_0 / (ρ Sqrt[m g / ρ]) y_t +
  (v'[t] + c_ρ Sqrt[m g / ρ] * L_0 * v[t] / (m g) + ϵ_τ (L_0 * ρ / m - v'[t])) y_x - L_0 / (m g) (p[γ l[t], t]) + y_tt, {Z_tt, Z_zz / l[t]^2, Z_t, Z_z, Z_zt}]
```

Out[7]=
$$-\frac{p[\gamma\, l[t],\, t]\, L_0}{g\, m}+\frac{c_\rho\, L_0\, Z_t}{\sqrt{\frac{g\, m}{\rho}}\,\rho}+Z_{tt}+Z_{zt}\left(\frac{2\, v[t]}{l[t]}-\frac{2\,\gamma\, v[t]}{l[t]}\right)+$$

$$Z_z\left(-\frac{\gamma\, c_\rho\, L_0\, v[t]}{\sqrt{\frac{g\, m}{\rho}}\,\rho\, l[t]}-\frac{2\, v[t]^2}{l[t]^2}+\frac{\frac{\sqrt{\frac{g\, m}{\rho}}\, c_\rho\, L_0\, v[t]}{g\, m}+\epsilon_\tau\left(\frac{\rho\, L_0}{m}-v'[t]\right)+v'[t]}{l[t]}-\frac{\gamma\left(-2\, v[t]^2+l[t]\, v'[t]\right)}{l[t]^2}\right)+$$

$$\frac{Z_{zz}\left(v[t]^2-2\,\gamma\, v[t]^2+\gamma^2\, v[t]^2-\left(\frac{m}{\rho}+(l[t]-\gamma\, l[t])\, L_0\,\epsilon_\tau\right)\left(\frac{\rho}{m}-\frac{\epsilon_a\, v'[t]}{L_0}\right)\right)}{l[t]^2}$$

B.C.2

In[8]:=
```
Clear[γ, t, i, n];
```

In[9]:=
```
γ = 1;
```

In[10]:=
$$BC2 = \text{Collect}\left[\text{Simplify}\left[v[t]^2 * y_{xx} + 2 * v[t] * y_{xt} + \left(\frac{\rho * L_0 * v[t]}{m} + \frac{c_m * L_0}{m * \sqrt{\frac{m g}{\rho}}}\right) y_t + \left(v'[t] + \frac{\rho * L_0 * v[t]^2}{m} + \frac{c_m * L_0 * \rho * v[t] * \sqrt{\frac{m g}{\rho}}}{m^2 * g} + \left(1 + \frac{\rho * L_0 * \epsilon_\tau}{m} (l[t] - \gamma * l[t])\right)\left(\frac{L_0 * \rho}{m} - \epsilon_a * v'[t]\right)\right) y_x - \frac{L_0 * \rho}{m^2 * g} (P[1, t]) + y_{tt}\right], \{Z_{tt}, Z_{zt}, Z_{zz}, Z_t, Z_z\}\right]$$

Out[10]=
$$-\frac{\rho\, P[1, t]\, L_0}{g\, m^2} + Z_{tt} + \frac{Z_t\left(\frac{m\, c_m\, L_0}{\sqrt{\frac{g\, m}{\rho}}} + m\, \rho\, L_0\, v[t]\right)}{m^2} + \frac{Z_z\,(\rho\, L_0 - m\, \epsilon_a\, v'[t])}{m\, l[t]}$$

B.C.1

In[11]:=
```
Clear [γ, t, i, n];
```

In[12]:=
```
γ = 0;
```

In[13]:=
$$BC1 = Z_t - \epsilon_u * \frac{1 - v[t]}{l[t]} Z_z - u[t]$$

Out[13]=
$$Z_t - u[t] - \frac{Z_z\, \epsilon_u\, (1 - v[t])}{l[t]}$$

Discretization for i>1 and n>1

PDE

In[14]:=
$$Z_z = \frac{Z_{i+1}^{n} - Z_{i-1}^{n}}{2\,\Delta z};$$

$$Z_{zz} = \frac{Z_{i+1}^{n} - 2\,Z_i^{n} + Z_{i-1}^{n}}{(\Delta z)^2};$$

$$Z_{tt} = \frac{Z_i^{n+1} - 2\,Z_i^{n} + Z_i^{n-1}}{(\Delta t)^2};$$

$$Z_{zt} = \frac{Z_{i+1}^{n} - Z_{i-1}^{n} - Z_{i+1}^{n-1} + Z_{i-1}^{n-1}}{2\,\Delta t\,\Delta z};$$

$$Z_t = \frac{Z_i^{n+1} - Z_i^{n-1}}{2\,\Delta t};$$

In[15]:=
```
Clear [γ, t, i, n];
```

In[16]:=
```
γ = z;
```

In[17]:=
```
FullSimplify [Solve[PDE == 0, Z_i^(n+1)]]
```

Out[17]=
$$\left\{\left\{Z_i^{1+n} \to \frac{1}{2\sqrt{\frac{g\,m}{\rho}}\,\rho + \Delta t\, c_\rho\, L_0}\, 2\,\Delta t^2 \sqrt{\frac{g\,m}{\rho}}\,\rho\left(-\frac{Z_i^{-1+n}}{\Delta t^2} + \frac{2\,Z_i^{n}}{\Delta t^2} + \frac{p[z\,l[t],\,t]\,L_0}{g\,m} + \frac{Z_i^{-1+n}\,c_\rho\,L_0}{2\,\Delta t\sqrt{\frac{g\,m}{\rho}}\,\rho} + \right.\right.$$

$$\frac{(-1+z)\left(Z_{-1+i}^{-1+n} - Z_{-1+i}^{n} - Z_{1+i}^{-1+n} + Z_{1+i}^{n}\right) v[t]}{\Delta t\,\Delta z\,l[t]} + \frac{1}{m\,\Delta z^2\,\rho\,l[t]^2\,L_0}\left(Z_{-1+i}^{n} - 2\,Z_i^{n} + Z_{1+i}^{n}\right)$$

$$\left(\rho\,L_0\left(m - (-1+z)\,\rho\,l[t]\,L_0\,\epsilon_\tau - m\,(-1+z)^2\,v[t]^2\right) - m\,\epsilon_a\,(m - (-1+z)\,\rho\,l[t]\,L_0\,\epsilon_\tau)\,v'[t]\right) -$$

$$\frac{1}{2\,\Delta z\left(\frac{g\,m}{\rho}\right)^{3/2}\rho^2\,l[t]^2}\,g\left(Z_{-1+i}^{n} - Z_{1+i}^{n}\right)\left(-2\,m\,(-1+z)\sqrt{\frac{g\,m}{\rho}}\,\rho\,v[t]^2 + \right.$$

$$\left.\left.\left.\left.l[t]\left(L_0\left(-\sqrt{\frac{g\,m}{\rho}}\,\rho^2\,\epsilon_\tau + m\,(-1+z)\,c_\rho\,v[t]\right) + m\sqrt{\frac{g\,m}{\rho}}\,\rho\,(-1+z+\epsilon_\tau)\,v'[t]\right)\right)\right)\right\}\right\}$$

PDE + BC1

In[18]:=
```
Clear [γ, t, i, n];
```

In[19]:=
```
γ = 0; i = 1;
```

In[20]:=
```
FullSimplify [Solve[{PDE == 0, BC1 == 0}, {Z_i^(n+1), Z_(i-1)^n}]]
```

Out[20]=
$$\left\{\left\{Z_1^{1+n} \to -\left(\left(-\sqrt{\frac{g\,m}{\rho}}\left(\Delta z\,l[t]\left(Z_1^{-1+n} + 2\,\Delta t\,u[t]\right) - \Delta t\,Z_2^{n}\,\epsilon_u\,(-1+v[t])\right)\right.\right.\right.$$

$$\left(\Delta t\,\rho\,l[t]\,L_0^2\left(g\,(2+\Delta z)\,\rho\,\epsilon_\tau + \Delta z\sqrt{\frac{g\,m}{\rho}}\,c_\rho\,v[t]\right) - 2\,g\,m^2\,\Delta t\,\epsilon_a\,v'[t] + \right.$$

$$\left.\left.\left.g\,m\,\rho\,L_0\left(2\,\Delta t - 2\,\Delta t\,(1+\Delta z)\,v[t]^2 + l[t]\,(2\,\Delta z\,v[t] + \Delta t\,(\Delta z - (\Delta z + 2\,\epsilon_a)\,\epsilon_\tau)\,v'[t])\right)\right) +\right.$$

$$\epsilon_u\,(1-v[t])\left(g\,m\,\Delta z^2\,l[t]^2\,Z_1^{-1+n}\,L_0\left(2\sqrt{\frac{g\,m}{\rho}}\,\rho - \Delta t\,c_\rho\,L_0\right) + \right.$$

$$\sqrt{\frac{g\,m}{\rho}}\left(-2\,\Delta t\,\Delta z\,\rho\,l[t]\,L_0\left(\Delta t\,\Delta z\,l[t] \times p[0,\,t]\,L_0 + g\,m\left(-Z_0^{-1+n} + Z_2^{-1+n}\right)v[t]\right) - 4\,g\,Z_1^{n}\right.$$

$$\left(\rho\,L_0\left(m\,\Delta z^2\,l[t]^2 - \Delta t^2\,\rho\,l[t]\,L_0\,\epsilon_\tau + m\,\Delta t^2\,(-1+v[t]^2)\right) + m\,\Delta t^2\,\epsilon_a\,(m + \rho\,l[t]\,L_0\,\epsilon_\tau)\,v'[t]\right) +$$

$$\Delta t\,Z_2^{n}\left(\Delta t\,\rho\,l[t]\,L_0^2\left(g\,(-2+\Delta z)\,\rho\,\epsilon_\tau + \Delta z\sqrt{\frac{g\,m}{\rho}}\,c_\rho\,v[t]\right) + 2\,g\,m^2\,\Delta t\,\epsilon_a\,v'[t] + g\,m\right.$$

$$\left.\left.\left.\left.\left.\rho\,L_0\left(-2\,\Delta t\left(1 + (-1+\Delta z)\,v[t]^2\right) + l[t]\,(2\,\Delta z\,v[t] + \Delta t\,(\Delta z - (\Delta z - 2\,\epsilon_a)\,\epsilon_\tau)\,v'[t])\right)\right)\right)\right)\right)\Big/$$

$$\left(\Delta z \left(\frac{g\,m}{\rho}\right)^{3/2} \rho^2\, l[t]\, L_0 \left(2\,\Delta t + \frac{\Delta t\,(2+\Delta z)\,\rho\, l[t]\, L_0\, \epsilon_\tau}{m} - 2\,\Delta z\, l[t]\, \epsilon_u\,(-1+v[t]) + 2\,\Delta z\, l[t] \times v[t] - 2\,\Delta t\,(1+\Delta z)\, v[t]^2 + \frac{\Delta t\,\Delta z\, l[t]\, c_\rho\, L_0\,(-\epsilon_u\,(-1+v[t])+v[t])}{\sqrt{\frac{g\,m}{\rho}}\,\rho} - \frac{2\,m\,\Delta t\,\epsilon_a\, v'[t]}{\rho\, L_0} + \Delta t\, l[t]\,(\Delta z - (\Delta z + 2\,\epsilon_a)\,\epsilon_\tau)\, v'[t]\right)\right),$$

$$\overset{n}{Z}_0 \to \left(2\,\Delta z^2\, l[t]^2\, L_0 \left(-2\,g\,m\,\sqrt{\frac{g\,m}{\rho}}\,\rho\,\overset{-1+n}{Z}_1 + 2\,g\,m\,\sqrt{\frac{g\,m}{\rho}}\,\rho\,\overset{n}{Z}_1 + \Delta t\left(\Delta t\,\sqrt{\frac{g\,m}{\rho}}\,\rho\,p[0,t]\,L_0 - g\,m\left(2\,\sqrt{\frac{g\,m}{\rho}}\,\rho + \Delta t\, c_\rho\, L_0\right) u[t]\right) + 2\,\Delta t^2\left(\frac{g\,m}{\rho}\right)^{3/2}\rho\left(\overset{n}{Z}_2\,(\rho\, L_0\,(1+(-1+\Delta z)\,v[t]^2) - m\,\epsilon_a\, v'[t]) + 2\,\overset{n}{Z}_1\,(\rho\, L_0\,(-1+v[t]^2) + m\,\epsilon_a\, v'[t])\right) - g\,\Delta t\, l[t]\, L_0\left(2\,\sqrt{\frac{g\,m}{\rho}}\,\rho\left(m\,\Delta z\left(\overset{-1+n}{Z}_0 - \overset{-1+n}{Z}_2\right) v[t] + 2\,\Delta t\,\overset{n}{Z}_1\,\epsilon_\tau\,(\rho\, L_0 - m\,\epsilon_a\, v'[t])\right) + \overset{n}{Z}_2\left(-m\,\Delta z\left(2\,\sqrt{\frac{g\,m}{\rho}}\,\rho + \Delta t\, c_\rho\, L_0\right)\epsilon_u\,(-1+v[t]) + \Delta t\, L_0\left((-2+\Delta z)\,\sqrt{\frac{g\,m}{\rho}}\,\rho^2\,\epsilon_\tau + m\,\Delta z\, c_\rho\, v[t]\right) + m\,\sqrt{\frac{g\,m}{\rho}}\,\rho\,(2\,\Delta z\, v[t] + \Delta t\,(\Delta z - (\Delta z - 2\,\epsilon_a)\,\epsilon_\tau)\, v'[t])\right)\right)\Big/ \left(g\,\Delta t\left(\Delta t\, l[t]\, L_0^2\left(-\left((2+\Delta z)\,\sqrt{\frac{g\,m}{\rho}}\,\rho^2\,\epsilon_\tau\right) + m\,\Delta z\, c_\rho\,(\epsilon_u\,(-1+v[t]) - v[t])\right) + 2\,m^2\,\Delta t\,\sqrt{\frac{g\,m}{\rho}}\,\epsilon_a\, v'[t] + m\,\sqrt{\frac{g\,m}{\rho}}\,\rho\, L_0\,(-2\,\Delta t + 2\,\Delta t\,(1+\Delta z)\, v[t]^2 + l[t]\,(2\,\Delta z\,\epsilon_u\,(-1+v[t]) - 2\,\Delta z\, v[t] + \Delta t\,(-\Delta z + (\Delta z + 2\,\epsilon_a)\,\epsilon_\tau)\, v'[t])\right)\right)\right)\right\}\right\}$$

PDE + BC2

In[21]:=
```
Clear [γ, t, i, n];
```

In[22]:=
```
γ = 1; i = Nz;
```

In[23]:=
```
FullSimplify [Solve[{PDE == 0, BC2 == 0}, {Z_i^(n+1), Z_(i+1)^n}]]
```

Out[23]=
$$\left\{\left\{\overset{1+n}{Z}_{Nz} \to \left(-4\,g\,m^2\,\Delta t^2\left(\overset{n}{Z}_{-1+Nz} - \overset{n}{Z}_{Nz}\right)(\rho\, L_0 - m\,\epsilon_a\, v'[t])^2 -\right.\right.\right.$$

$$2\,m\,\Delta z\,l[t]\left(-4\,g\,m^2\,Z_{Nz}^{n}-2\,\Delta t^2\,\rho\,P[1,\,t]\,L_0+\bar{Z}_{Nz}^{-1+n}\left(2\,g\,m^2-\Delta t\,\rho\,L_0\left(\sqrt{\frac{g\,m}{\rho}}\;c_m+g\,m\,v[t]\right)\right)\right)$$

$$(-\rho\,L_0+m\,\epsilon_a\,v'[t])+\Delta z^2\,\rho\,l[t]^2\,L_0\left(4\,g\,m^2\,Z_{Nz}^{n}\,(\rho\,L_0\,(-1+\epsilon_\tau)+m\,(\epsilon_a-\epsilon_\tau)\,v'[t])+\right.$$

$$2\,\Delta t^2\,L_0\,(\rho\,P[1,\,t]\,\epsilon_\tau\,(\rho\,L_0-m\,v'[t])+m\,p[l[t],\,t]\,(-\rho\,L_0+m\,\epsilon_a\,v'[t]))+$$

$$\bar{Z}_{Nz}^{-1+n}\left(\Delta t\,\rho\,L_0^2\left(-m\,\sqrt{\frac{g\,m}{\rho}}\;c_\rho+\rho\,\epsilon_\tau\left(\sqrt{\frac{g\,m}{\rho}}\;c_m+g\,m\,v[t]\right)\right)+2\,g\,m^3\,(-\epsilon_a+\epsilon_\tau)\,v'[t]-\right.$$

$$\left.\left.\left.m\,L_0\left(-m\left(2\,g\,\rho+\Delta t\,\sqrt{\frac{g\,m}{\rho}}\;c_\rho\,\epsilon_a\,v'[t]\right)+\rho\,\epsilon_\tau\left(2\,g\,m+\Delta t\left(\sqrt{\frac{g\,m}{\rho}}\;c_m+g\,m\,v[t]\right)v'[t]\right)\right)\right)\right)\Big/$$

$$\left(\Delta z\,l[t]\left(\Delta t\,\Delta z\,\rho^2\,l[t]\,L_0^3\left(-m\,\sqrt{\frac{g\,m}{\rho}}\;c_\rho+\rho\,\epsilon_\tau\left(\sqrt{\frac{g\,m}{\rho}}\;c_m+g\,m\,v[t]\right)\right)+4\,g\,m^4\,\epsilon_a\,v'[t]+\right.\right.$$

$$2\,m^2\,\rho\,L_0\left(-2\,g\,m+\left(g\,m\,\Delta z\,l[t]\,(\epsilon_a-\epsilon_\tau)+\Delta t\,\epsilon_a\left(\sqrt{\frac{g\,m}{\rho}}\;c_m+g\,m\,v[t]\right)\right)v'[t]\right)-$$

$$m\,\rho\,L_0^2\left(2\,\Delta t\,\rho\left(\sqrt{\frac{g\,m}{\rho}}\;c_m+g\,m\,v[t]\right)+\right.$$

$$\left.\left.\left.\Delta z\,l[t]\left(2\,g\,m\,\rho-m\,\Delta t\,\sqrt{\frac{g\,m}{\rho}}\;c_\rho\,\epsilon_a\,v'[t]+\rho\,\epsilon_\tau\left(-2\,g\,m+\Delta t\left(\sqrt{\frac{g\,m}{\rho}}\;c_m+g\,m\,v[t]\right)v'[t]\right)\right)\right)\right)\right),$$

$$Z_{1+Nz}^{n}\to\left(2\,\Delta z^2\,\rho\,l[t]^2\,L_0^2\left(-\Delta t\,\rho\,P[1,\,t]\left(2\,g\,m+\Delta t\,\sqrt{\frac{g\,m}{\rho}}\;c_\rho\,L_0\right)-2\,g\,m\,\bar{Z}_{Nz}^{-1+n}\left(\sqrt{\frac{g\,m}{\rho}}\;\rho\,c_m-\right.\right.\right.$$

$$\left.\left.\left.m\,\sqrt{\frac{g\,m}{\rho}}\;c_\rho+g\,m\,\rho\,v[t]\right)+\Delta t\,p[l[t],\,t]\left(2\,g\,m^2+\Delta t\,\rho\,L_0\left(\sqrt{\frac{g\,m}{\rho}}\;c_m+g\,m\,v[t]\right)\right)\right)+\right.$$

$$4\,g\,m\,Z_{Nz}^{n}\left(-\rho\,L_0^2\left(\sqrt{\frac{g\,m}{\rho}}\;\rho\,(\Delta t^2-\Delta z^2\,l[t]^2)\,c_m+g\,m\,\Delta t^2\,\rho\,v[t]+m\,\Delta z^2\,l[t]^2\left(\sqrt{\frac{g\,m}{\rho}}\;c_\rho-g\,\rho\,v[t]\right)\right)+\right.$$

$$2\,g\,m^3\,\Delta t\,\epsilon_a\,v'[t]+m\,\Delta t\,\rho\,L_0\left(-2\,g\,m+\Delta t\,\epsilon_a\left(\sqrt{\frac{g\,m}{\rho}}\;c_m+g\,m\,v[t]\right)v'[t]\right)+$$

$$g\,\Delta t\,Z_{-1+Nz}^{n}\left(\Delta t\,\Delta z\,\rho^2\,l[t]\,L_0^3\left(-m\,\sqrt{\frac{g\,m}{\rho}}\;c_\rho+\rho\,\epsilon_\tau\left(\sqrt{\frac{g\,m}{\rho}}\;c_m+g\,m\,v[t]\right)\right)-4\,g\,m^4\,\epsilon_a\,v'[t]+\right.$$

$$2\,m^2\,\rho\,L_0\left(2\,g\,m+\left(g\,m\,\Delta z\,l[t]\,(\epsilon_a-\epsilon_\tau)-\Delta t\,\epsilon_a\left(\sqrt{\frac{g\,m}{\rho}}\;c_m+g\,m\,v[t]\right)\right)v'[t]\right)+$$

$$m\,\rho\,L_0^2\left(2\,\Delta t\,\rho\left(\sqrt{\frac{g\,m}{\rho}}\;c_m+g\,m\,v[t]\right)-\right.$$

$$\left.\left.\left.\Delta z\,l[t]\left(2\,g\,m\,\rho-m\,\Delta t\,\sqrt{\frac{g\,m}{\rho}}\;c_\rho\,\epsilon_a\,v'[t]+\rho\,\epsilon_\tau\left(-2\,g\,m+\Delta t\left(\sqrt{\frac{g\,m}{\rho}}\;c_m+g\,m\,v[t]\right)v'[t]\right)\right)\right)\right)\Big/$$

$$\left(g\,\Delta t\left(\Delta t\,\Delta z\,\rho^2\,l[t]\,L_0^3\left(-m\sqrt{\frac{g\,m}{\rho}}\;c_\rho+\rho\,\epsilon_\tau\left(\sqrt{\frac{g\,m}{\rho}}\;c_m+g\,m\,v[t]\right)\right)+4\,g\,m^4\,\epsilon_a\,v'[t]+\right.\right.$$
$$2\,m^2\,\rho\,L_0\left(-2\,g\,m+\left(g\,m\,\Delta z\,l[t]\,(\epsilon_a-\epsilon_\tau)+\Delta t\,\epsilon_a\left(\sqrt{\frac{g\,m}{\rho}}\;c_m+g\,m\,v[t]\right)\right)v'[t]\right)-$$
$$m\,\rho\,L_0^2\left(2\,\Delta t\,\rho\left(\sqrt{\frac{g\,m}{\rho}}\;c_m+g\,m\,v[t]\right)+\right.$$
$$\left.\left.\left.\left.\Delta z\,l[t]\left(2\,g\,m\,\rho-m\,\Delta t\sqrt{\frac{g\,m}{\rho}}\;c_\rho\,\epsilon_a\,v'[t]+\rho\,\epsilon_\tau\left(-2\,g\,m+\Delta t\left(\sqrt{\frac{g\,m}{\rho}}\;c_m+g\,m\,v[t]\right)v'[t]\right)\right)\right)\right)\right)\right\}\}$$

Discretization for n=1 and i=1

PDE+BC1

In[24]:=
```
Clear [γ, t, i, n];
```

In[25]:=
```
γ = 0; i = 1; n = 1;
```

In[26]:=
```
Ztz = (Z[i+1, n] - Z[i, n] - Z[i+1, n-1] + Z[i, n-1]) / (Δt Δz);
```

In[27]:=
```
FullSimplify [Solve[{PDE == 0, BC1 == 0}, {Z[i, n+1], Z[i-1, n]}]]
```

Out[27]=
$$\left\{\left\{Z_1^2\to-\left(\left(-\sqrt{\frac{g\,m}{\rho}}\left(\Delta z\,l[t]\left(Z_1^0+2\,\Delta t\,u[t]\right)-\Delta t\,Z_2^1\,\epsilon_u\,(-1+v[t])\right)\right.\right.\right.$$
$$\left(\Delta t\,\rho\,l[t]\,L_0^2\left(g\,(2+\Delta z)\,\rho\,\epsilon_\tau+\Delta z\sqrt{\frac{g\,m}{\rho}}\;c_\rho\,v[t]\right)-2\,g\,m^2\,\Delta t\,\epsilon_a\,v'[t]+\right.$$
$$\left.g\,m\,\rho\,L_0\left(2\,\Delta t-2\,\Delta t\,(1+\Delta z)\,v[t]^2+l[t]\left(2\,\Delta z\,v[t]+\Delta t\,(\Delta z-(\Delta z+2\,\epsilon_a)\,\epsilon_\tau)\,v'[t]\right)\right)\right)+$$
$$\epsilon_u\,(1-v[t])\left(g\,m\,\Delta z^2\,l[t]^2\,Z_1^0\,L_0\left(2\sqrt{\frac{g\,m}{\rho}}\;\rho-\Delta t\,c_\rho\,L_0\right)+\right.$$
$$\sqrt{\frac{g\,m}{\rho}}\left(-2\,\Delta t\,\Delta z\,\rho\,l[t]\,L_0\left(\Delta t\,\Delta z\,l[t]\times p[0,t]\,L_0+g\,m\left(-Z_0^0+Z_2^0\right)v[t]\right)-4\,g\,Z_1^1\right.$$
$$\left(\rho\,L_0\left(m\,\Delta z^2\,l[t]^2-\Delta t^2\,\rho\,l[t]\,L_0\,\epsilon_\tau+m\,\Delta t^2\left(-1+v[t]^2\right)\right)+m\,\Delta t^2\,\epsilon_a\,(m+\rho\,l[t]\,L_0\,\epsilon_\tau)\,v'[t]\right)+$$
$$\Delta t\,Z_2^1\left(\Delta t\,\rho\,l[t]\,L_0^2\left(g\,(-2+\Delta z)\,\rho\,\epsilon_\tau+\Delta z\sqrt{\frac{g\,m}{\rho}}\;c_\rho\,v[t]\right)+2\,g\,m^2\,\Delta t\,\epsilon_a\,v'[t]+g\,m\right.$$
$$\left.\left.\left.\left.\rho\,L_0\left(-2\,\Delta t\left(1+(-1+\Delta z)\,v[t]^2\right)+l[t]\left(2\,\Delta z\,v[t]+\Delta t\,(\Delta z-(\Delta z-2\,\epsilon_a)\,\epsilon_\tau)\,v'[t]\right)\right)\right)\right)\right)\Big/$$

$$\left(\Delta z \left(\frac{g\,m}{\rho}\right)^{3/2} \rho^2\, l[t]\, L_0 \left(2\,\Delta t + \frac{\Delta t\,(2+\Delta z)\,\rho\, l[t]\, L_0\, \epsilon_\tau}{m} - 2\,\Delta z\, l[t]\, \epsilon_u\,(-1+v[t]) + 2\,\Delta z\, l[t] \times v[t] - 2\,\Delta t\,(1+\Delta z)\, v[t]^2 + \frac{\Delta t\,\Delta z\, l[t]\, c_\rho\, L_0\,(-\epsilon_u\,(-1+v[t])+v[t])}{\sqrt{\frac{g\,m}{\rho}}\,\rho} - \frac{2\,m\,\Delta t\,\epsilon_a\, v'[t]}{\rho\, L_0} + \Delta t\, l[t]\,(\Delta z - (\Delta z + 2\,\epsilon_a)\,\epsilon_\tau)\, v'[t]\right)\right),$$

$$\overset{1}{Z}_0 \to \left(2\,\Delta z^2\, l[t]^2\, L_0 \left(-2\,g\,m\,\sqrt{\frac{g\,m}{\rho}}\,\rho\,\overset{0}{Z}_1 + 2\,g\,m\,\sqrt{\frac{g\,m}{\rho}}\,\rho\,\overset{1}{Z}_1 + \Delta t\left(\Delta t\,\sqrt{\frac{g\,m}{\rho}}\,\rho\,p[0,t]\,L_0 - g\,m\left(2\,\sqrt{\frac{g\,m}{\rho}}\,\rho + \Delta t\, c_\rho\, L_0\right) u[t]\right) + 2\,\Delta t^2\left(\frac{g\,m}{\rho}\right)^{3/2}\rho\left(\overset{1}{Z}_2\,(\rho\, L_0\,(1+(-1+\Delta z)\,v[t]^2) - m\,\epsilon_a\, v'[t]) + 2\,\overset{1}{Z}_1\,(\rho\, L_0\,(-1+v[t]^2) + m\,\epsilon_a\, v'[t])\right) - g\,\Delta t\, l[t]\, L_0\left(2\,\sqrt{\frac{g\,m}{\rho}}\,\rho\left(m\,\Delta z\left(\overset{0}{Z}_0 - \overset{0}{Z}_2\right) v[t] + 2\,\Delta t\,\overset{1}{Z}_1\,\epsilon_\tau\,(\rho\, L_0 - m\,\epsilon_a\, v'[t])\right) + \overset{1}{Z}_2\left(-m\,\Delta z\left(2\,\sqrt{\frac{g\,m}{\rho}}\,\rho + \Delta t\, c_\rho\, L_0\right)\epsilon_u\,(-1+v[t]) + \Delta t\, L_0\left((-2+\Delta z)\,\sqrt{\frac{g\,m}{\rho}}\,\rho^2\,\epsilon_\tau + m\,\Delta z\, c_\rho\, v[t]\right) + m\,\sqrt{\frac{g\,m}{\rho}}\,\rho\,(2\,\Delta z\, v[t] + \Delta t\,(\Delta z - (\Delta z - 2\,\epsilon_a)\,\epsilon_\tau)\, v'[t])\right)\right)\Big/ \left(g\,\Delta t\left(\Delta t\, l[t]\, L_0^2\left(-\left((2+\Delta z)\,\sqrt{\frac{g\,m}{\rho}}\,\rho^2\,\epsilon_\tau\right) + m\,\Delta z\, c_\rho\,(\epsilon_u\,(-1+v[t]) - v[t])\right) + 2\,m^2\,\Delta t\,\sqrt{\frac{g\,m}{\rho}}\,\epsilon_a\, v'[t] + m\,\sqrt{\frac{g\,m}{\rho}}\,\rho\, L_0\,(-2\,\Delta t + 2\,\Delta t\,(1+\Delta z)\, v[t]^2 + l[t]\,(2\,\Delta z\,\epsilon_u\,(-1+v[t]) - 2\,\Delta z\, v[t] + \Delta t\,(-\Delta z + (\Delta z + 2\,\epsilon_a)\,\epsilon_\tau)\, v'[t])\right)\right)\right)\right)$$

Discretization for n=1 and i=Nz

PDE + BC2

In[28]:=
```
Clear [γ, t, i, n];
```

In[29]:=
```
γ = 1; i = Nz; n = 1;
```

In[30]:=
```
Z_tz = (Z_i^n - Z_(i-1)^n - Z_i^(n-1) + Z_(i-1)^(n-1)) / (Δt Δγ);
```

In[31]:=
```
FullSimplify [Solve[{PDE == 0, BC2 == 0}, {Z_i^(n+1), Z_(i+1)^n}]]
```

Out[31]=

$$\left\{\left\{Z_{Nz}^{2} \to \left(-4\, g\, m^2\, \Delta t^2 \left(Z_{-1+Nz}^{1} - Z_{Nz}^{1}\right)(\rho\, L_0 - m\, \epsilon_a\, v'[t])^2 - \right.\right.\right.$$

$$2\, m\, \Delta z\, l[t]\left(-4\, g\, m^2\, Z_{Nz}^{1} - 2\, \Delta t^2\, \rho\, P[1,\, t]\, L_0 + Z_{Nz}^{0}\left(2\, g\, m^2 - \Delta t\, \rho\, L_0\left(\sqrt{\frac{g\, m}{\rho}}\; c_m + g\, m\, v[t]\right)\right)\right)$$

$$(-\rho\, L_0 + m\, \epsilon_a\, v'[t]) + \Delta z^2\, \rho\, l[t]^2\, L_0\left(4\, g\, m^2\, Z_{Nz}^{1}\,(\rho\, L_0\,(-1 + \epsilon_\tau) + m\,(\epsilon_a - \epsilon_\tau)\, v'[t]) + \right.$$

$$2\, \Delta t^2\, L_0\,(\rho\, P[1,\, t]\, \epsilon_\tau\,(\rho\, L_0 - m\, v'[t]) + m\, p[l[t],\, t]\,(-\rho\, L_0 + m\, \epsilon_a\, v'[t])) +$$

$$Z_{Nz}^{0}\left(\Delta t\, \rho\, L_0^2\left(-m\,\sqrt{\frac{g\, m}{\rho}}\; c_\rho + \rho\, \epsilon_\tau\left(\sqrt{\frac{g\, m}{\rho}}\; c_m + g\, m\, v[t]\right)\right) + 2\, g\, m^3\,(-\epsilon_a + \epsilon_\tau)\, v'[t] - \right.$$

$$\left.\left.\left.\left.\left.\left.m\, L_0\left(-m\left(2\, g\, \rho + \Delta t\,\sqrt{\frac{g\, m}{\rho}}\; c_\rho\, \epsilon_a\, v'[t]\right) + \rho\, \epsilon_\tau\left(2\, g\, m + \Delta t\left(\sqrt{\frac{g\, m}{\rho}}\; c_m + g\, m\, v[t]\right) v'[t]\right)\right)\right)\right)\right)\right)\Big/$$

$$\left(\Delta z\, l[t]\left(\Delta t\, \Delta z\, \rho^2\, l[t]\, L_0^3\left(-m\,\sqrt{\frac{g\, m}{\rho}}\; c_\rho + \rho\, \epsilon_\tau\left(\sqrt{\frac{g\, m}{\rho}}\; c_m + g\, m\, v[t]\right)\right) + 4\, g\, m^4\, \epsilon_a\, v'[t] + \right.\right.$$

$$2\, m^2\, \rho\, L_0\left(-2\, g\, m + \left(g\, m\, \Delta z\, l[t]\,(\epsilon_a - \epsilon_\tau) + \Delta t\, \epsilon_a\left(\sqrt{\frac{g\, m}{\rho}}\; c_m + g\, m\, v[t]\right)\right) v'[t]\right) -$$

$$m\, \rho\, L_0^2\left(2\, \Delta t\, \rho\left(\sqrt{\frac{g\, m}{\rho}}\; c_m + g\, m\, v[t]\right) + \right.$$

$$\left.\left.\left.\left.\Delta z\, l[t]\left(2\, g\, m\, \rho - m\, \Delta t\,\sqrt{\frac{g\, m}{\rho}}\; c_\rho\, \epsilon_a\, v'[t] + \rho\, \epsilon_\tau\left(-2\, g\, m + \Delta t\left(\sqrt{\frac{g\, m}{\rho}}\; c_m + g\, m\, v[t]\right) v'[t]\right)\right)\right)\right)\right),$$

$$Z_{1+Nz}^{1} \to \left(2\, \Delta z^2\, \rho\, l[t]^2\, L_0^2\left(-\Delta t\, \rho\, P[1,\, t]\left(2\, g\, m + \Delta t\,\sqrt{\frac{g\, m}{\rho}}\; c_\rho\, L_0\right) - 2\, g\, m\, Z_{Nz}^{0}\left(\sqrt{\frac{g\, m}{\rho}}\; \rho\, c_m - \right.\right.\right.$$

$$\left.\left.\left.m\,\sqrt{\frac{g\, m}{\rho}}\; c_\rho + g\, m\, \rho\, v[t]\right) + \Delta t\, p[l[t],\, t]\left(2\, g\, m^2 + \Delta t\, \rho\, L_0\left(\sqrt{\frac{g\, m}{\rho}}\; c_m + g\, m\, v[t]\right)\right)\right) +$$

$$4\, g\, m\, Z_{Nz}^{1}\left(-\rho\, L_0^2\left(\sqrt{\frac{g\, m}{\rho}}\; \rho\left(\Delta t^2 - \Delta z^2\, l[t]^2\right) c_m + g\, m\, \Delta t^2\, \rho\, v[t] + m\, \Delta z^2\, l[t]^2\left(\sqrt{\frac{g\, m}{\rho}}\; c_\rho - g\, \rho\, v[t]\right)\right) + \right.$$

$$2\, g\, m^3\, \Delta t\, \epsilon_a\, v'[t] + m\, \Delta t\, \rho\, L_0\left(-2\, g\, m + \Delta t\, \epsilon_a\left(\sqrt{\frac{g\, m}{\rho}}\; c_m + g\, m\, v[t]\right) v'[t]\right)\Big) +$$

$$g\, \Delta t\, Z_{-1+Nz}^{1}\left(\Delta t\, \Delta z\, \rho^2\, l[t]\, L_0^3\left(-m\,\sqrt{\frac{g\, m}{\rho}}\; c_\rho + \rho\, \epsilon_\tau\left(\sqrt{\frac{g\, m}{\rho}}\; c_m + g\, m\, v[t]\right)\right) - 4\, g\, m^4\, \epsilon_a\, v'[t] + \right.$$

$$\left.2\, m^2\, \rho\, L_0\left(2\, g\, m + \left(g\, m\, \Delta z\, l[t]\,(\epsilon_a - \epsilon_\tau) - \Delta t\, \epsilon_a\left(\sqrt{\frac{g\, m}{\rho}}\; c_m + g\, m\, v[t]\right)\right) v'[t]\right) +$$

$$m\,\rho\,L_0^2\left(2\,\Delta t\,\rho\left(\sqrt{\frac{g\,m}{\rho}}\;c_m+g\,m\,v[t]\right)-\right.$$

$$\left.\Delta z\;l[t]\left(2\,g\,m\,\rho-m\,\Delta t\,\sqrt{\frac{g\,m}{\rho}}\;c_\rho\,\epsilon_a\,v'[t]+\rho\,\epsilon_\tau\left(-2\,g\,m+\Delta t\left(\sqrt{\frac{g\,m}{\rho}}\;c_m+g\,m\,v[t]\right)v'[t]\right)\right)\right)\Big/$$

$$\left(g\,\Delta t\left(\Delta t\,\Delta z\,\rho^2\,l[t]\,L_0^3\left(-m\,\sqrt{\frac{g\,m}{\rho}}\;c_\rho+\rho\,\epsilon_\tau\left(\sqrt{\frac{g\,m}{\rho}}\;c_m+g\,m\,v[t]\right)\right)+4\,g\,m^4\,\epsilon_a\,v'[t]+\right.\right.$$

$$2\,m^2\,\rho\,L_0\left(-2\,g\,m+\left(g\,m\,\Delta z\;l[t]\,(\epsilon_a-\epsilon_\tau)+\Delta t\,\epsilon_a\left(\sqrt{\frac{g\,m}{\rho}}\;c_m+g\,m\,v[t]\right)\right)v'[t]\right)-$$

$$m\,\rho\,L_0^2\left(2\,\Delta t\,\rho\left(\sqrt{\frac{g\,m}{\rho}}\;c_m+g\,m\,v[t]\right)+\right.$$

$$\left.\left.\left.\Delta z\;l[t]\left(2\,g\,m\,\rho-m\,\Delta t\,\sqrt{\frac{g\,m}{\rho}}\;c_\rho\,\epsilon_a\,v'[t]+\rho\,\epsilon_\tau\left(-2\,g\,m+\Delta t\left(\sqrt{\frac{g\,m}{\rho}}\;c_m+g\,m\,v[t]\right)v'[t]\right)\right)\right)\right)\right\}\right\}$$

Scheme 2 - Discretization of the equations of motion:

In[1]:=
```
Clear["Global`*"]
```

In[2]:=
$$y_x = \frac{Z_z}{l[t]};$$

$$y_t = Z_t - \frac{\gamma\, v[t]}{l[t]}\, Z_z;$$

$$y_{xx} = \frac{1}{(l[t])^2}\, Z_{zz};$$

$$y_{xt} = \frac{1}{l[t]}\, Z_{zt} - \frac{v[t]}{(l[t])^2}\, Z_z - \frac{v[t]\,\gamma}{(l[t])^2}\, Z_{zz};$$

$$y_{tt} = Z_{tt} - \frac{2\, v[t]\,\gamma}{l[t]}\, Z_{zt} - \frac{\gamma\,(v'[t] * l[t] - 2\, v[t]^2)}{(l[t])^2}\, Z_z + \frac{(v[t]\,\gamma)^2}{(l[t])^2}\, Z_{zz};$$

PDE (where γ = z)

In[7]:=
```
PDE = Collect[(v[t]^2 - (m/ρ + ϵτ * L0 (l[t] - γ * l[t])) (ρ/m - ϵa/L0 v'[t])) * yxx + 2 * v[t] * yxt + (cρ L0)/(ρ Sqrt[(m g)/ρ]) yt +
  (v'[t] + (cρ Sqrt[(m g)/ρ] * L0 * v[t])/(m g) + ϵτ (L0 * ρ/m - v'[t])) yx - L0/(m g) (p[γ l[t], t]) + ytt, {Ztt, Zzz/l[t]^2, Zt, Zz, Zzt}]
```

Out[7]=
$$-\frac{p[\gamma\, l[t],\, t]\, L_0}{g\, m} + \frac{c_\rho\, L_0\, Z_t}{\sqrt{\frac{g\, m}{\rho}}\ \rho} + Z_{tt} + Z_{zt}\left(\frac{2\, v[t]}{l[t]} - \frac{2\,\gamma\, v[t]}{l[t]}\right) +$$

$$Z_z\left(-\frac{\gamma\, c_\rho\, L_0\, v[t]}{\sqrt{\frac{g\, m}{\rho}}\ \rho\, l[t]} - \frac{2\, v[t]^2}{l[t]^2} + \frac{\frac{\sqrt{\frac{g\, m}{\rho}}\ c_\rho\, L_0\, v[t]}{g\, m} + \epsilon_\tau\left(\frac{\rho\, L_0}{m} - v'[t]\right) + v'[t]}{l[t]} - \frac{\gamma\,(-2\, v[t]^2 + l[t]\, v'[t])}{l[t]^2}\right) +$$

$$\frac{Z_{zz}\left(v[t]^2 - 2\,\gamma\, v[t]^2 + \gamma^2\, v[t]^2 - \left(\frac{m}{\rho} + (l[t] - \gamma\, l[t])\, L_0\, \epsilon_\tau\right)\left(\frac{\rho}{m} - \frac{\epsilon_a\, v'[t]}{L_0}\right)\right)}{l[t]^2}$$

B.C.2

In[8]:=
```
Clear[γ, t, i, n];
```

In[9]:=
```
γ = 1;
```

In[10]:=
$$BC2 = \text{Collect}\left[\text{Simplify}\left[v[t]^2 * y_{xx} + 2 * v[t] * y_{xt} + \left(\frac{\rho * L_0 * v[t]}{m} + \frac{c_m * L_0}{m * \sqrt{\frac{m g}{\rho}}}\right) y_t + \left(v'[t] + \frac{\rho * L_0 * v[t]^2}{m} + \frac{c_m * L_0 * \rho * v[t] * \sqrt{\frac{m g}{\rho}}}{m^2 * g} + \left(1 + \frac{\rho * L_0 * \epsilon_\tau}{m} (l[t] - \gamma * l[t])\right)\left(\frac{L_0 * \rho}{m} - \epsilon_a * v'[t]\right)\right) y_x - \frac{L_0 * \rho}{m^2 * g} (P[1, t]) + y_{tt}\right], \{Z_{tt}, Z_{zt}, Z_{zz}, Z_t, Z_z\}\right]$$

Out[10]=
$$-\frac{\rho\, P[1, t]\, L_0}{g\, m^2} + Z_{tt} + \frac{Z_t\left(\frac{m\, c_m\, L_0}{\sqrt{\frac{g\, m}{\rho}}} + m\, \rho\, L_0\, v[t]\right)}{m^2} + \frac{Z_z\,(\rho\, L_0 - m\, \epsilon_a\, v'[t])}{m\, l[t]}$$

B.C.1

In[11]:=
```
Clear [γ, t, i, n];
```

In[12]:=
```
γ = 0;
```

In[13]:=
$$BC1 = Z_t - \epsilon_u * \frac{1 - v[t]}{l[t]} Z_z - u[t]$$

Out[13]=
$$Z_t - u[t] - \frac{Z_z\, \epsilon_u\, (1 - v[t])}{l[t]}$$

Discretization for V>0, i=1:1:Nz

PDE

In[14]:=
$$Z_z = \frac{Z_{i+1}^n - Z_{i-1}^n}{2\,\Delta z};$$

$$Z_{zz} = \frac{Z_{i+1}^n - 2\,Z_i^n + Z_{i-1}^n}{(\Delta z)^2};$$

$$Z_{tt} = \frac{Z_i^{n+1} - 2\,Z_i^n + Z_i^{n-1}}{(\Delta t)^2};$$

$$Z_{zt} = \frac{Z_i^{n+1} - Z_{i-1}^{n+1} - Z_i^{n-1} + Z_{i-1}^{n-1}}{2\,\Delta t\,\Delta z};$$

$$Z_t = \frac{Z_i^{n+1} - Z_i^{n-1}}{2\,\Delta t};$$

In[15]:=
```
Clear [γ, t, i, n];
```

In[16]:=
```
γ = z;
```

In[17]:=
```
FullSimplify [Solve[PDE == 0, Z_i^(n+1)]]
```

Out[17]=
$$\left\{\left\{Z_i^{1+n} \to \left(2\,\Delta t^2\,\Delta z\,\sqrt{\frac{g\,m}{\rho}}\;\rho\,l[t]\left(-\frac{Z_i^{-1+n}}{\Delta t^2}+\frac{2\,Z_i^{n}}{\Delta t^2}+\frac{p[z\,l[t],\,t]\,L_0}{g\,m}+\frac{Z_i^{-1+n}\,c_\rho\,L_0}{2\,\Delta t\,\sqrt{\frac{g\,m}{\rho}}\;\rho}+\frac{(-1+z)\,Z_{-1+i}^{-1+n}\,v[t]}{\Delta t\,\Delta z\,l[t]}-\right.\right.\right.$$

$$\frac{(-1+z)\,Z_{-1+i}^{1+n}\,v[t]}{\Delta t\,\Delta z\,l[t]}-\frac{(-1+z)\,Z_i^{-1+n}\,v[t]}{\Delta t\,\Delta z\,l[t]}+\frac{1}{m\,\Delta z^2\,\rho\,l[t]^2\,L_0}\left(Z_{-1+i}^{n}-2\,Z_i^{n}+Z_{1+i}^{n}\right)$$

$$(\rho\,L_0\,(m-(-1+z)\,\rho\,l[t]\,L_0\,\epsilon_\tau-m\,(-1+z)^2\,v[t]^2)-m\,\epsilon_a\,(m-(-1+z)\,\rho\,l[t]\,L_0\,\epsilon_\tau)\,v'[t])-$$

$$\frac{1}{2\,\Delta z\left(\frac{g\,m}{\rho}\right)^{3/2}\rho^2\,l[t]^2}g\left(Z_{-1+i}^{n}-Z_{1+i}^{n}\right)\left(-2\,m\,(-1+z)\,\sqrt{\frac{g\,m}{\rho}}\;\rho\,v[t]^2+\right.$$

$$\left.\left.\left.l[t]\left(L_0\left(-\sqrt{\frac{g\,m}{\rho}}\;\rho^2\,\epsilon_\tau+m\,(-1+z)\,c_\rho\,v[t]\right)+m\,\sqrt{\frac{g\,m}{\rho}}\;\rho\,(-1+z+\epsilon_\tau)\,v'[t]\right)\right)\right)\Big/$$

$$\left.\left.\left(\Delta z\,l[t]\left(2\,\sqrt{\frac{g\,m}{\rho}}\;\rho+\Delta t\,c_\rho\,L_0\right)-2\times(-1+z)\,\Delta t\,\sqrt{\frac{g\,m}{\rho}}\;\rho\,v[t]\right)\right\}\right\}$$

PDE + BC1

In[18]:=
```
Clear [γ, t, i, n];
```

In[19]:=
```
γ = 0; i = 1;
```

In[20]:=
$$Z_{zt} = \frac{Z_{i+1}^{n}-Z_i^{n}-Z_{i+1}^{n-1}+Z_i^{n-1}}{\Delta t\,\Delta z};$$

In[21]:=
```
FullSimplify [Solve[{PDE == 0, BC1 == 0}, {Z_i^(n+1), Z_(i-1)^n}]]
```

Out[21]=
$$\left\{\left\{Z_1^{1+n} \to\right.\right.$$

$$-\left(\left(-\frac{1}{g\,m\,\rho\,L_0}\Delta t\left(\Delta z\,l[t]\left(Z_1^{-1+n}+2\,\Delta t\,u[t]\right)-\Delta t\,Z_2^{n}\,\epsilon_u\,(-1+v[t])\right)\left(\rho\,l[t]\,L_0^2\left(g\,(2+\Delta z)\,\rho\,\epsilon_\tau+\Delta z\,\sqrt{\frac{g\,m}{\rho}}\;c_\rho\right.\right.\right.\right.$$

$$\left.\left.\left.\left.v[t]\right)-2\,g\,m^2\,\epsilon_a\,v'[t]+g\,m\,\rho\,L_0\,(2-2\times(1+\Delta z)\,v[t]^2+l[t]\,(\Delta z-(\Delta z+2\,\epsilon_a)\,\epsilon_\tau)\,v'[t])\right)+\right.\right.$$

$$\Delta z^2\,l[t]^2\,\epsilon_u\,(1-v[t])\left(Z_1^{-1+n}\left(2-\frac{\Delta t\,c_\rho\,L_0}{\sqrt{\frac{g\,m}{\rho}}\;\rho}+\frac{4\,\Delta t\,v[t]}{\Delta z\,l[t]}\right)+\frac{1}{g\,m\,\Delta z^2\,\rho\,l[t]^2\,L_0}\right.$$

$$\left.\left.\left.\left.\left(4\,g\,Z_1^{n}\,(\rho\,L_0\,(-m\,\Delta z^2\,l[t]^2+\Delta t\,l[t]\,(\Delta t\,\rho\,L_0\,\epsilon_\tau-m\,\Delta z\,v[t])-m\,\Delta t^2\,(-1+v[t]^2))-\right.\right.\right.\right.\right.$$

$$
\begin{aligned}
&m\,\Delta t^2\,\epsilon_a\,(m+\rho\,l[t]\,L_0\,\epsilon_\tau)\,v'[t]\Big)+\\
&\Delta t\left(-2\,\Delta z\,\rho\,l[t]\,L_0\left(\Delta t\,\Delta z\,l[t]\times p[0,t]\,L_0+2\,g\,m\,\overset{-1+n}{Z_2}\,v[t]\right)+\overset{n}{Z_2}\left(\Delta t\,\rho\,l[t]\,L_0^2\right.\right.\\
&\left.\left(g\,(-2+\Delta z)\,\rho\,\epsilon_\tau+\Delta z\,\sqrt{\frac{g\,m}{\rho}}\,c_\rho\,v[t]\right)+2\,g\,m^2\,\Delta t\,\epsilon_a\,v'[t]+g\,m\,\rho\,L_0\,(-2\,\Delta t+\right.\\
&\left.\left.\left.4\,\Delta z\,l[t]\times v[t]-2\,\Delta t\,(-1+\Delta z)\,v[t]^2+\Delta t\,l[t]\,(\Delta z-(\Delta z-2\,\epsilon_a)\,\epsilon_\tau)\,v'[t]\right)\right)\right)\Big/\\
&\left(\Delta z\,l[t]\left(2\,\Delta t+\frac{\Delta t\,(2+\Delta z)\,\rho\,l[t]\,L_0\,\epsilon_\tau}{m}-2\,\Delta z\,l[t]\,\epsilon_u\,(-1+v[t])-2\,\Delta t\,(1+\Delta z)\,v[t]^2+\right.\right.\\
&\left.\left.\frac{\Delta t\,\Delta z\,l[t]\,c_\rho\,L_0\,(-\epsilon_u\,(-1+v[t])+v[t])}{\sqrt{\frac{g\,m}{\rho}}\,\rho}-\frac{2\,m\,\Delta t\,\epsilon_a\,v'[t]}{\rho\,L_0}-\Delta t\,l[t]\,(-\Delta z+(\Delta z+2\,\epsilon_a)\,\epsilon_\tau)\,v'[t]\right)\right),\\
&\overset{n}{Z_0}\to\left(2\,\Delta z^2\,l[t]^2\,L_0\left(-2\,g\,m\,\sqrt{\frac{g\,m}{\rho}}\,\rho\,\overset{-1+n}{Z_1}+2\,g\,m\,\sqrt{\frac{g\,m}{\rho}}\,\rho\,\overset{n}{Z_1}+\right.\right.\\
&\Delta t\left(\Delta t\,\sqrt{\frac{g\,m}{\rho}}\,\rho\,p[0,t]\,L_0-g\,m\left(2\,\sqrt{\frac{g\,m}{\rho}}\,\rho+\Delta t\,c_\rho\,L_0\right)u[t]\right)+\\
&2\,\Delta t^2\left(\frac{g\,m}{\rho}\right)^{3/2}\rho\left(\overset{n}{Z_2}\left(\rho\,L_0\left(1+(-1+\Delta z)\,v[t]^2\right)-m\,\epsilon_a\,v'[t]\right)+2\,\overset{n}{Z_1}\left(\rho\,L_0\left(-1+v[t]^2\right)+m\,\epsilon_a\,v'[t]\right)\right)-\\
&g\,\Delta t\,l[t]\,L_0\\
&\left(\overset{n}{Z_2}\left(-m\,\Delta z\left(2\,\sqrt{\frac{g\,m}{\rho}}\,\rho+\Delta t\,c_\rho\,L_0\right)\epsilon_u\,(-1+v[t])+\Delta t\,L_0\left((-2+\Delta z)\,\sqrt{\frac{g\,m}{\rho}}\,\rho^2\,\epsilon_\tau+m\,\Delta z\,c_\rho\,v[t]\right)+\right.\right.\\
&\left.m\,\sqrt{\frac{g\,m}{\rho}}\,\rho\,(4\,\Delta z\,v[t]+\Delta t\,(\Delta z-(\Delta z-2\,\epsilon_a)\,\epsilon_\tau)\,v'[t])\right)-\\
&\left.4\,\sqrt{\frac{g\,m}{\rho}}\,\rho\left(m\,\Delta z\left(-\overset{-1+n}{Z_1}+\overset{-1+n}{Z_2}\right)v[t]+\overset{n}{Z_1}\,(m\,\Delta z\,v[t]+\Delta t\,\epsilon_\tau\,(-\rho\,L_0+m\,\epsilon_a\,v'[t]))\right)\right)\Big/\\
&\left(g\,\Delta t\left(\Delta t\,l[t]\,L_0^2\left(-\left((2+\Delta z)\,\sqrt{\frac{g\,m}{\rho}}\,\rho^2\,\epsilon_\tau\right)+m\,\Delta z\,c_\rho\,(\epsilon_u\,(-1+v[t])-v[t])\right)+\right.\right.\\
&2\,m^2\,\Delta t\,\sqrt{\frac{g\,m}{\rho}}\,\epsilon_a\,v'[t]+m\,\sqrt{\frac{g\,m}{\rho}}\,\rho\,L_0\\
&\left.\left.\left.(2\,\Delta t\,(-1+(1+\Delta z)\,v[t]^2)+l[t]\,(2\,\Delta z\,\epsilon_u\,(-1+v[t])+\Delta t\,(-\Delta z+(\Delta z+2\,\epsilon_a)\,\epsilon_\tau)\,v'[t]))\right)\right)\right\}\Big\}
\end{aligned}
$$

PDE + BC2

In[22]:=
```
Clear [γ, t, i, n];
```

In[23]:=
```
γ = 1; i = Nz;
```

In[24]:=
$$Z_{zt} = \frac{Z_i^{n+1} - Z_{i-1}^{n+1} - Z_i^{n-1} + Z_{i-1}^{n-1}}{2\,\Delta t\,\Delta z};$$

In[25]:=
```
FullSimplify [Solve[{PDE == 0, BC2 == 0}, {Z_i^(n+1), Z_(i+1)^n}]]
```

Out[25]=
$$\left\{\left\{Z_{Nz}^{1+n} \to \left(-4\,g\,m^2\,\Delta t^2\left(Z_{-1+Nz}^{n} - Z_{Nz}^{n}\right)(\rho\,L_0 - m\,\epsilon_a\,v'[t])^2 - \right.\right.\right.$$
$$2\,m\,\Delta z\,l[t]\left(-4\,g\,m^2\,Z_{Nz}^{n} - 2\,\Delta t^2\,\rho\,P[1,\,t]\,L_0 + Z_{Nz}^{-1+n}\left(2\,g\,m^2 - \Delta t\,\rho\,L_0\left(\sqrt{\frac{g\,m}{\rho}}\;c_m + g\,m\,v[t]\right)\right)\right)$$
$$(-\rho\,L_0 + m\,\epsilon_a\,v'[t]) + \Delta z^2\,\rho\,l[t]^2\,L_0\left(4\,g\,m^2\,Z_{Nz}^{n}\,(\rho\,L_0\,(-1+\epsilon_\tau) + m\,(\epsilon_a - \epsilon_\tau)\,v'[t]) + \right.$$
$$2\,\Delta t^2\,L_0\,(\rho\,P[1,\,t]\,\epsilon_\tau\,(\rho\,L_0 - m\,v'[t]) + m\,p[l[t],\,t]\,(-\rho\,L_0 + m\,\epsilon_a\,v'[t])) +$$
$$Z_{Nz}^{-1+n}\left(\Delta t\,\rho\,L_0^2\left(-m\,\sqrt{\frac{g\,m}{\rho}}\;c_\rho + \rho\,\epsilon_\tau\left(\sqrt{\frac{g\,m}{\rho}}\;c_m + g\,m\,v[t]\right)\right) + 2\,g\,m^3\,(-\epsilon_a + \epsilon_\tau)\,v'[t] - \right.$$
$$\left.\left.\left.\left.\left.m\,L_0\left(-m\left(2\,g\,\rho + \Delta t\,\sqrt{\frac{g\,m}{\rho}}\;c_\rho\,\epsilon_a\,v'[t]\right) + \rho\,\epsilon_\tau\left(2\,g\,m + \Delta t\left(\sqrt{\frac{g\,m}{\rho}}\;c_m + g\,m\,v[t]\right)v'[t]\right)\right)\right)\right)\right)\Big/$$
$$\left(\Delta z\,l[t]\left(\Delta t\,\Delta z\,\rho^2\,l[t]\,L_0^3\left(-m\,\sqrt{\frac{g\,m}{\rho}}\;c_\rho + \rho\,\epsilon_\tau\left(\sqrt{\frac{g\,m}{\rho}}\;c_m + g\,m\,v[t]\right)\right) + 4\,g\,m^4\,\epsilon_a\,v'[t] + \right.\right.$$
$$2\,m^2\,\rho\,L_0\left(-2\,g\,m + \left(g\,m\,\Delta z\,l[t]\,(\epsilon_a - \epsilon_\tau) + \Delta t\,\epsilon_a\left(\sqrt{\frac{g\,m}{\rho}}\;c_m + g\,m\,v[t]\right)\right)v'[t]\right) -$$
$$m\,\rho\,L_0^2\left(2\,\Delta t\,\rho\left(\sqrt{\frac{g\,m}{\rho}}\;c_m + g\,m\,v[t]\right) + \right.$$
$$\left.\left.\left.\left.\Delta z\,l[t]\left(2\,g\,m\,\rho - m\,\Delta t\,\sqrt{\frac{g\,m}{\rho}}\;c_\rho\,\epsilon_a\,v'[t] + \rho\,\epsilon_\tau\left(-2\,g\,m + \Delta t\left(\sqrt{\frac{g\,m}{\rho}}\;c_m + g\,m\,v[t]\right)v'[t]\right)\right)\right)\right)\right),$$
$$Z_{1+Nz}^{n} \to \left(2\,\Delta z^2\,\rho\,l[t]^2\,L_0^2\left(-\Delta t\,\rho\,P[1,\,t]\left(2\,g\,m + \Delta t\,\sqrt{\frac{g\,m}{\rho}}\;c_\rho\,L_0\right) - 2\,g\,m\,Z_{Nz}^{-1+n}\left(\sqrt{\frac{g\,m}{\rho}}\;\rho\,c_m - \right.\right.\right.$$
$$\left.\left.\left.m\,\sqrt{\frac{g\,m}{\rho}}\;c_\rho + g\,m\,\rho\,v[t]\right) + \Delta t\,p[l[t],\,t]\left(2\,g\,m^2 + \Delta t\,\rho\,L_0\left(\sqrt{\frac{g\,m}{\rho}}\;c_m + g\,m\,v[t]\right)\right)\right) +$$
$$4\,g\,m\,Z_{Nz}^{n}\left(-\rho\,L_0^2\left(\sqrt{\frac{g\,m}{\rho}}\;\rho\,(\Delta t^2 - \Delta z^2\,l[t]^2)\,c_m + g\,m\,\Delta t^2\,\rho\,v[t] + m\,\Delta z^2\,l[t]^2\left(\sqrt{\frac{g\,m}{\rho}}\;c_\rho - g\,\rho\,v[t]\right)\right) + \right.$$
$$\left.\left.2\,g\,m^3\,\Delta t\,\epsilon_a\,v'[t] + m\,\Delta t\,\rho\,L_0\left(-2\,g\,m + \Delta t\,\epsilon_a\left(\sqrt{\frac{g\,m}{\rho}}\;c_m + g\,m\,v[t]\right)v'[t]\right)\right) +$$

$$g\,\Delta t\,Z_{-1+Nz}^{n}\left(\Delta t\,\Delta z\,\rho^2\,l[t]\,L_0^3\left(-m\sqrt{\frac{g\,m}{\rho}}\,c_\rho+\rho\,\epsilon_\tau\left(\sqrt{\frac{g\,m}{\rho}}\,c_m+g\,m\,v[t]\right)\right)-4\,g\,m^4\,\epsilon_a\,v'[t]+\right.$$
$$2\,m^2\,\rho\,L_0\left(2\,g\,m+\left(g\,m\,\Delta z\,l[t]\,(\epsilon_a-\epsilon_\tau)-\Delta t\,\epsilon_a\left(\sqrt{\frac{g\,m}{\rho}}\,c_m+g\,m\,v[t]\right)\right)v'[t]\right)+$$
$$m\,\rho\,L_0^2\left(2\,\Delta t\,\rho\left(\sqrt{\frac{g\,m}{\rho}}\,c_m+g\,m\,v[t]\right)-\right.$$
$$\left.\left.\left.\left.\left.\Delta z\,l[t]\left(2\,g\,m\,\rho-m\,\Delta t\sqrt{\frac{g\,m}{\rho}}\,c_\rho\,\epsilon_a\,v'[t]+\rho\,\epsilon_\tau\left(-2\,g\,m+\Delta t\left(\sqrt{\frac{g\,m}{\rho}}\,c_m+g\,m\,v[t]\right)v'[t]\right)\right)\right)\right)\right)\right)\Big/$$
$$\left(g\,\Delta t\left(\Delta t\,\Delta z\,\rho^2\,l[t]\,L_0^3\left(-m\sqrt{\frac{g\,m}{\rho}}\,c_\rho+\rho\,\epsilon_\tau\left(\sqrt{\frac{g\,m}{\rho}}\,c_m+g\,m\,v[t]\right)\right)+4\,g\,m^4\,\epsilon_a\,v'[t]+\right.\right.$$
$$2\,m^2\,\rho\,L_0\left(-2\,g\,m+\left(g\,m\,\Delta z\,l[t]\,(\epsilon_a-\epsilon_\tau)+\Delta t\,\epsilon_a\left(\sqrt{\frac{g\,m}{\rho}}\,c_m+g\,m\,v[t]\right)\right)v'[t]\right)-$$
$$m\,\rho\,L_0^2\left(2\,\Delta t\,\rho\left(\sqrt{\frac{g\,m}{\rho}}\,c_m+g\,m\,v[t]\right)+\right.$$
$$\left.\left.\left.\left.\left.\left.\Delta z\,l[t]\left(2\,g\,m\,\rho-m\,\Delta t\sqrt{\frac{g\,m}{\rho}}\,c_\rho\,\epsilon_a\,v'[t]+\rho\,\epsilon_\tau\left(-2\,g\,m+\Delta t\left(\sqrt{\frac{g\,m}{\rho}}\,c_m+g\,m\,v[t]\right)v'[t]\right)\right)\right)\right)\right)\right)\right\}\right\}$$

Discretization for V<0, i=Nz:-1:1

PDE

In[26]:=
```
Clear[γ, t, i, n];
```

In[27]:=
```
γ = z;
```

In[28]:=
$$Z_{zt} = \frac{Z_{i+1}^{n+1} - Z_i^{n+1} - Z_{i+1}^{n-1} + Z_i^{n-1}}{2\,\Delta t\,\Delta z};$$

In[29]:=
```
FullSimplify [Solve[PDE == 0, Z_i^(n+1)]]
```

Out[29]=
$$\left\{\left\{Z_i^{1+n} \to \left(2\,\Delta t^2\,\Delta z\,\sqrt{\frac{g\,m}{\rho}}\;\rho\,l[t]\left(-\frac{Z_i^{-1+n}}{\Delta t^2}+\frac{2\,Z_i^{n}}{\Delta t^2}+\frac{p[z\,l[t],\,t]\,L_0}{g\,m}+\frac{Z_i^{-1+n}\,c_\rho\,L_0}{2\,\Delta t\,\sqrt{\frac{g\,m}{\rho}}\;\rho}+\frac{(-1+z)\,Z_i^{-1+n}\,v[t]}{\Delta t\,\Delta z\,l[t]}-\right.\right.\right.$$

$$\frac{(-1+z)\,Z_{1+i}^{-1+n}\,v[t]}{\Delta t\,\Delta z\,l[t]}+\frac{(-1+z)\,Z_{1+i}^{1+n}\,v[t]}{\Delta t\,\Delta z\,l[t]}+\frac{1}{m\,\Delta z^2\,\rho\,l[t]^2\,L_0}\left(Z_{-1+i}^{n}-2\,Z_i^{n}+Z_{1+i}^{n}\right)$$

$$\left(\rho\,L_0\left(m-(-1+z)\,\rho\,l[t]\,L_0\,\epsilon_\tau-m\,(-1+z)^2\,v[t]^2\right)-m\,\epsilon_a\left(m-(-1+z)\,\rho\,l[t]\,L_0\,\epsilon_\tau\right)v'[t]\right)-$$

$$\frac{1}{2\,\Delta z\left(\frac{g\,m}{\rho}\right)^{3/2}\rho^2\,l[t]^2}g\left(Z_{-1+i}^{n}-Z_{1+i}^{n}\right)\left(-2\,m\,(-1+z)\,\sqrt{\frac{g\,m}{\rho}}\;\rho\,v[t]^2+\right.$$

$$\left.\left.\left.l[t]\left(L_0\left(-\sqrt{\frac{g\,m}{\rho}}\;\rho^2\,\epsilon_\tau+m\,(-1+z)\,c_\rho\,v[t]\right)+m\,\sqrt{\frac{g\,m}{\rho}}\;\rho\,(-1+z+\epsilon_\tau)\,v'[t]\right)\right)\right)\Big/$$

$$\left.\left.\left(\Delta z\,l[t]\left(2\,\sqrt{\frac{g\,m}{\rho}}\;\rho+\Delta t\,c_\rho\,L_0\right)+2\times(-1+z)\,\Delta t\,\sqrt{\frac{g\,m}{\rho}}\;\rho\,v[t]\right)\right\}\right\}$$

PDE + BC1

In[30]:=
```
Clear [γ, t, i, n];
```

In[31]:=
```
γ = 0; i = 1;
```

In[32]:=
```
Z_zt = (Z_(i+1)^(n+1) - Z_i^(n+1) - Z_(i+1)^(n-1) + Z_i^(n-1))/(2 Δt Δz);
```

In[33]:=
```
FullSimplify [Solve[{PDE == 0, BC1 == 0}, {Z_i^(n+1), Z_(i-1)^n}]]
```

Out[33]=
$$\left\{\left\{Z_1^{1+n} \to -\left(\left(-\frac{1}{g\,m\,\rho\,L_0}\Delta t\left(\Delta z\,l[t]\left(Z_1^{-1+n}+2\,\Delta t\,u[t]\right)-\Delta t\,Z_2^{n}\,\epsilon_u\,(-1+v[t])\right)\left(\rho\,l[t]\,L_0^2\left(g\,(2+\Delta z)\,\rho\,\epsilon_\tau+\Delta z\,\sqrt{\frac{g\,m}{\rho}}\;c_\rho\right.\right.\right.\right.\right.$$

$$\left.\left.\left.\left.\left.v[t]\right)-2\,g\,m^2\,\epsilon_a\,v'[t]+g\,m\,\rho\,L_0\left(2-2\times(1+\Delta z)\,v[t]^2+l[t]\,(\Delta z-(\Delta z+2\,\epsilon_a)\,\epsilon_\tau)\,v'[t]\right)\right)+\right.\right.\right.$$

$$\Delta z^2\,l[t]^2\,\epsilon_u\,(1-v[t])\left(Z_1^{-1+n}\left(2-\frac{\Delta t\,c_\rho\,L_0}{\sqrt{\frac{g\,m}{\rho}}\;\rho}+\frac{2\,\Delta t\,v[t]}{\Delta z\,l[t]}\right)+\frac{1}{g\,m\,\Delta z^2\,\rho\,l[t]^2\,L_0}\right.$$

$$\left.\left(4\,g\,Z_1^{n}\left(\rho\,L_0\left(-m\,\Delta z^2\,l[t]^2+\Delta t^2\,\rho\,l[t]\,L_0\,\epsilon_\tau-m\,\Delta t^2\left(-1+v[t]^2\right)\right)-m\,\Delta t^2\,\epsilon_a\left(m+\rho\,l[t]\,L_0\,\epsilon_\tau\right)\right.\right.\right.$$

$$v'[t]) + \Delta t \left(-2\,\Delta z\,\rho\,l[t]\,L_0\left(\Delta t\,\Delta z\,l[t]\times p[0,\,t]\,L_0 + g\,m\left(\overset{-1+n}{Z_2} - \overset{1+n}{Z_2}\right)v[t]\right) + \right.$$

$$\Delta t\,\overset{n}{Z_2}\left(\rho\,l[t]\,L_0^2\left(g\,(-2+\Delta z)\,\rho\,\epsilon_\tau + \Delta z\,\sqrt{\frac{g\,m}{\rho}}\;c_\rho\,v[t]\right) + 2\,g\,m^2\,\epsilon_a\,v'[t] + \right.$$

$$\left.\left.\left.\left.\left.g\,m\,\rho\,L_0\left(-2-2\times(-1+\Delta z)\,v[t]^2 + l[t]\,(\Delta z - (\Delta z - 2\,\epsilon_a)\,\epsilon_\tau)\,v'[t]\right)\right)\right)\right)\right)\Bigg/$$

$$\left(\Delta z\,l[t]\left(2\,\Delta t + \frac{\Delta t\,(2+\Delta z)\,\rho\,l[t]\,L_0\,\epsilon_\tau}{m} - 2\,\Delta z\,l[t]\,\epsilon_u\,(-1+v[t]) + 2\,\Delta t\,\epsilon_u\,(-1+v[t])\,v[t] - \right.\right.$$

$$2\,\Delta t\,(1+\Delta z)\,v[t]^2 + \frac{\Delta t\,\Delta z\,l[t]\,c_\rho\,L_0\,(-\epsilon_u\,(-1+v[t]) + v[t])}{\sqrt{\frac{g\,m}{\rho}}\;\rho} -$$

$$\left.\left.\frac{2\,m\,\Delta t\,\epsilon_a\,v'[t]}{\rho\,L_0} - \Delta t\,l[t]\,(-\Delta z + (\Delta z + 2\,\epsilon_a)\,\epsilon_\tau)\,v'[t]\right)\right),$$

$$\overset{n}{Z_0} \to \left(2\,\Delta z^2\,l[t]^2\,L_0\left(-2\,g\,m\,\sqrt{\frac{g\,m}{\rho}}\;\rho\,\overset{-1+n}{Z_1} + 2\,g\,m\,\sqrt{\frac{g\,m}{\rho}}\;\rho\,\overset{n}{Z_1} + \right.\right.$$

$$\Delta t\left(\Delta t\,\sqrt{\frac{g\,m}{\rho}}\;\rho\,p[0,\,t]\,L_0 - g\,m\left(2\,\sqrt{\frac{g\,m}{\rho}}\;\rho + \Delta t\,c_\rho\,L_0\right)u[t]\right) + 2\,\Delta t^2\left(\frac{g\,m}{\rho}\right)^{3/2}\rho$$

$$\left(\overset{n}{Z_2}\,(\rho\,L_0\,(1+v[t]\,(\epsilon_u + (-1+\Delta z-\epsilon_u)\,v[t])) - m\,\epsilon_a\,v'[t]) + 2\,\overset{n}{Z_1}\left(\rho\,L_0\left(-1+v[t]^2\right) + m\,\epsilon_a\,v'[t]\right)\right) -$$

$$g\,\Delta t\,l[t]\,L_0\left(\overset{n}{Z_2}\left(-m\,\Delta z\left(2\,\sqrt{\frac{g\,m}{\rho}}\;\rho + \Delta t\,c_\rho\,L_0\right)\epsilon_u\,(-1+v[t]) + \right.\right.$$

$$\Delta t\,L_0\left((-2+\Delta z)\,\sqrt{\frac{g\,m}{\rho}}\;\rho^2\,\epsilon_\tau + m\,\Delta z\,c_\rho\,v[t]\right) + m\,\Delta t\,\sqrt{\frac{g\,m}{\rho}}\;\rho\,(\Delta z - (\Delta z - 2\,\epsilon_a)\,\epsilon_\tau)\,v'[t]\Big) -$$

$$\left.\left.2\,\sqrt{\frac{g\,m}{\rho}}\;\rho\left(m\,\Delta z\left(\overset{-1+n}{Z_2} - \overset{1+n}{Z_2} + 2\,\Delta t\,u[t]\right)v[t] + 2\,\Delta t\,\overset{n}{Z_1}\,\epsilon_\tau\,(-\rho\,L_0 + m\,\epsilon_a\,v'[t])\right)\right)\right)\Bigg/$$

$$\left(g\,\Delta t\left(\Delta t\,l[t]\,L_0^2\left(-\left((2+\Delta z)\,\sqrt{\frac{g\,m}{\rho}}\;\rho^2\,\epsilon_\tau\right) + m\,\Delta z\,c_\rho\,(\epsilon_u\,(-1+v[t]) - v[t])\right) + \right.\right.$$

$$2\,m^2\,\Delta t\,\sqrt{\frac{g\,m}{\rho}}\;\epsilon_a\,v'[t] + m\,\sqrt{\frac{g\,m}{\rho}}\;\rho\,L_0\left(2\,\Delta t\left(-1+\epsilon_u\,v[t] + (1+\Delta z-\epsilon_u)\,v[t]^2\right) + \right.$$

$$\left.\left.\left.l[t]\,(2\,\Delta z\,\epsilon_u\,(-1+v[t]) + \Delta t\,(-\Delta z + (\Delta z + 2\,\epsilon_a)\,\epsilon_\tau)\,v'[t])\right)\right)\right\}\Big\}$$

PDE + BC2

In[34]:=
```
Clear [γ, t, i, n];
```

In[35]:=
```
γ = 1; i = Nz;
```

In[36]:=
$$Z_{zt} = \frac{Z_i^n - Z_{i-1}^n - Z_i^{n-1} + Z_{i-1}^{n-1}}{\Delta t\, \Delta z};$$

In[37]:=
```
FullSimplify [Solve[{PDE == 0, BC2 == 0}, {Z_i^(n+1), Z_(i+1)^n}]]
```

Out[37]=
$$\left\{\left\{Z_{Nz}^{1+n} \to \left(-4\, g\, m^2\, \Delta t^2 \left(Z_{-1+Nz}^{n} - Z_{Nz}^{n}\right)(\rho\, L_0 - m\, \epsilon_a\, v'[t])^2 - \right.\right.\right.$$

$$2\, m\, \Delta z\, l[t]\left(-4\, g\, m^2\, Z_{Nz}^{n} - 2\, \Delta t^2\, \rho\, P[1, t]\, L_0 + Z_{Nz}^{-1+n}\left(2\, g\, m^2 - \Delta t\, \rho\, L_0\left(\sqrt{\frac{g\, m}{\rho}}\, c_m + g\, m\, v[t]\right)\right)\right)$$

$$(-\rho\, L_0 + m\, \epsilon_a\, v'[t]) + \Delta z^2\, \rho\, l[t]^2\, L_0\left(4\, g\, m^2\, Z_{Nz}^{n}\,(\rho\, L_0\,(-1 + \epsilon_\tau) + m\,(\epsilon_a - \epsilon_\tau)\, v'[t]) + \right.$$

$$2\, \Delta t^2\, L_0\,(\rho\, P[1, t]\, \epsilon_\tau\,(\rho\, L_0 - m\, v'[t]) + m\, p[l[t], t]\,(-\rho\, L_0 + m\, \epsilon_a\, v'[t])) +$$

$$Z_{Nz}^{-1+n}\left(\Delta t\, \rho\, L_0^2\left(-m\sqrt{\frac{g\, m}{\rho}}\, c_\rho + \rho\, \epsilon_\tau\left(\sqrt{\frac{g\, m}{\rho}}\, c_m + g\, m\, v[t]\right)\right) + 2\, g\, m^3\,(-\epsilon_a + \epsilon_\tau)\, v'[t] - \right.$$

$$\left.\left.\left.\left.\left.m\, L_0\left(-m\left(2\, g\, \rho + \Delta t\sqrt{\frac{g\, m}{\rho}}\, c_\rho\, \epsilon_a\, v'[t]\right) + \rho\, \epsilon_\tau\left(2\, g\, m + \Delta t\left(\sqrt{\frac{g\, m}{\rho}}\, c_m + g\, m\, v[t]\right) v'[t]\right)\right)\right)\right)\right)\right) \Big/$$

$$\left(\Delta z\, l[t]\left(\Delta t\, \Delta z\, \rho^2\, l[t]\, L_0^3\left(-m\sqrt{\frac{g\, m}{\rho}}\, c_\rho + \rho\, \epsilon_\tau\left(\sqrt{\frac{g\, m}{\rho}}\, c_m + g\, m\, v[t]\right)\right) + 4\, g\, m^4\, \epsilon_a\, v'[t] + \right.\right.$$

$$2\, m^2\, \rho\, L_0\left(-2\, g\, m + \left(g\, m\, \Delta z\, l[t]\,(\epsilon_a - \epsilon_\tau) + \Delta t\, \epsilon_a\left(\sqrt{\frac{g\, m}{\rho}}\, c_m + g\, m\, v[t]\right)\right) v'[t]\right) -$$

$$m\, \rho\, L_0^2\left(2\, \Delta t\, \rho\left(\sqrt{\frac{g\, m}{\rho}}\, c_m + g\, m\, v[t]\right) + \right.$$

$$\left.\left.\left.\left.\Delta z\, l[t]\left(2\, g\, m\, \rho - m\, \Delta t\sqrt{\frac{g\, m}{\rho}}\, c_\rho\, \epsilon_a\, v'[t] + \rho\, \epsilon_\tau\left(-2\, g\, m + \Delta t\left(\sqrt{\frac{g\, m}{\rho}}\, c_m + g\, m\, v[t]\right) v'[t]\right)\right)\right)\right)\right),$$

$$Z_{1+Nz}^{n} \to \left(2\, \Delta z^2\, \rho\, l[t]^2\, L_0^2\left(-\Delta t\, \rho\, P[1, t]\left(2\, g\, m + \Delta t\sqrt{\frac{g\, m}{\rho}}\, c_\rho\, L_0\right) - 2\, g\, m\, Z_{Nz}^{-1+n}\left(\sqrt{\frac{g\, m}{\rho}}\, \rho\, c_m - \right.\right.\right.$$

$$\left.\left.\left.m\sqrt{\frac{g\, m}{\rho}}\, c_\rho + g\, m\, \rho\, v[t]\right) + \Delta t\, p[l[t], t]\left(2\, g\, m^2 + \Delta t\, \rho\, L_0\left(\sqrt{\frac{g\, m}{\rho}}\, c_m + g\, m\, v[t]\right)\right)\right) +$$

$$4\, g\, m\, Z_{Nz}^{n}\left(-\rho\, L_0^2\left(\sqrt{\frac{g\, m}{\rho}}\, \rho\,(\Delta t^2 - \Delta z^2\, l[t]^2)\, c_m + g\, m\, \Delta t^2\, \rho\, v[t] + m\, \Delta z^2\, l[t]^2\left(\sqrt{\frac{g\, m}{\rho}}\, c_\rho - g\, \rho\, v[t]\right)\right) + \right.$$

$$\left.2\, g\, m^3\, \Delta t\, \epsilon_a\, v'[t] + m\, \Delta t\, \rho\, L_0\left(-2\, g\, m + \Delta t\, \epsilon_a\left(\sqrt{\frac{g\, m}{\rho}}\, c_m + g\, m\, v[t]\right) v'[t]\right)\right) +$$

$$g\,\Delta t\,Z_{-1+Nz}^{n}\left(\Delta t\,\Delta z\,\rho^2\,l[t]\,L_0^3\left(-m\,\sqrt{\frac{g\,m}{\rho}}\;c_\rho+\rho\,\epsilon_\tau\left(\sqrt{\frac{g\,m}{\rho}}\;c_m+g\,m\,v[t]\right)\right)-4\,g\,m^4\,\epsilon_a\,v'[t]+\right.$$
$$2\,m^2\,\rho\,L_0\left(2\,g\,m+\left(g\,m\,\Delta z\,l[t]\,(\epsilon_a-\epsilon_\tau)-\Delta t\,\epsilon_a\left(\sqrt{\frac{g\,m}{\rho}}\;c_m+g\,m\,v[t]\right)\right)v'[t]\right)+$$
$$m\,\rho\,L_0^2\left(2\,\Delta t\,\rho\left(\sqrt{\frac{g\,m}{\rho}}\;c_m+g\,m\,v[t]\right)-\right.$$
$$\left.\left.\left.\left.\left.\Delta z\,l[t]\left(2\,g\,m\,\rho-m\,\Delta t\,\sqrt{\frac{g\,m}{\rho}}\;c_\rho\,\epsilon_a\,v'[t]+\rho\,\epsilon_\tau\left(-2\,g\,m+\Delta t\left(\sqrt{\frac{g\,m}{\rho}}\;c_m+g\,m\,v[t]\right)v'[t]\right)\right)\right)\right)\right)\right)\Big/$$
$$\left(g\,\Delta t\left(\Delta t\,\Delta z\,\rho^2\,l[t]\,L_0^3\left(-m\,\sqrt{\frac{g\,m}{\rho}}\;c_\rho+\rho\,\epsilon_\tau\left(\sqrt{\frac{g\,m}{\rho}}\;c_m+g\,m\,v[t]\right)\right)+4\,g\,m^4\,\epsilon_a\,v'[t]+\right.\right.$$
$$2\,m^2\,\rho\,L_0\left(-2\,g\,m+\left(g\,m\,\Delta z\,l[t]\,(\epsilon_a-\epsilon_\tau)+\Delta t\,\epsilon_a\left(\sqrt{\frac{g\,m}{\rho}}\;c_m+g\,m\,v[t]\right)\right)v'[t]\right)-$$
$$m\,\rho\,L_0^2\left(2\,\Delta t\,\rho\left(\sqrt{\frac{g\,m}{\rho}}\;c_m+g\,m\,v[t]\right)+\right.$$
$$\left.\left.\left.\left.\left.\left.\Delta z\,l[t]\left(2\,g\,m\,\rho-m\,\Delta t\,\sqrt{\frac{g\,m}{\rho}}\;c_\rho\,\epsilon_a\,v'[t]+\rho\,\epsilon_\tau\left(-2\,g\,m+\Delta t\left(\sqrt{\frac{g\,m}{\rho}}\;c_m+g\,m\,v[t]\right)v'[t]\right)\right)\right)\right)\right)\right)\right\}\right\}$$